

July 2015

Revision 7

# MAGNASTOR®

(Modular Advanced Generation  
Nuclear All-purpose STORage)

---

10 CFR 72.248 and  
10 CFR 72.48(d)(2)  
Partial  
24-Month Updates

**NON-PROPRIETARY VERSION**

**Docket No. 72-1031**



---

Atlanta Corporate Headquarters: 3930 East Jones Bridge Road, Norcross, Georgia 30092 USA  
Phone 770-447-1144, Fax 770-447-1797, [www.nacintl.com](http://www.nacintl.com)

Attachment 1  
Proprietary Affidavit



**NAC INTERNATIONAL  
AFFIDAVIT PURSUANT TO 10 CFR 2.390**

---

George Carver (Affiant), Vice President, Engineering and Licensing, of NAC International, hereinafter referred to as NAC, at 3930 East Jones Bridge Road, Norcross, Georgia 30092, being duly sworn, deposes and says that:

1. Affiant has reviewed the information described in Item 2 and is personally familiar with the trade secrets and privileged information contained therein, and is authorized to request its withholding.
2. The information to be withheld includes the following NAC Proprietary Information that is being provided in a submittal containing the NAC MAGNASTOR FSAR, Revision 7 update.

- NAC MAGNASTOR FSAR Rev. 7, Proprietary Version

NAC is the owner of the information contained in the aforementioned pages/document, so they are considered NAC Proprietary Information.

3. NAC makes this application for withholding of proprietary information based upon the exemption from disclosure set forth in: the Freedom of Information Act ("FOIA"); 5 USC Sec. 552(b)(4) and the Trade Secrets Act; 18 USC Sec. 1905; and NRC Regulations 10 CFR Part 9.17(a)(4), 2.390(a)(4), and 2.390(b)(1) for "trade secrets and commercial financial information obtained from a person, and privileged or confidential" (Exemption 4). The information for which exemption from disclosure is herein sought is all "confidential commercial information," and some portions may also qualify under the narrower definition of "trade secret," within the meanings assigned to those terms for purposes of FOIA Exemption 4.
4. Examples of categories of information that fit into the definition of proprietary information are:
  - a. Information that discloses a process, method, or apparatus, including supporting data and analyses, where prevention of its use by competitors of NAC, without license from NAC, constitutes a competitive economic advantage over other companies.
  - b. Information that, if used by a competitor, would reduce their expenditure of resources or improve their competitive position in the design, manufacture, shipment, installation, assurance of quality or licensing of a similar product.
  - c. Information that reveals cost or price information, production capacities, budget levels or commercial strategies of NAC, its customers, or its suppliers.
  - d. Information that reveals aspects of past, present or future NAC customer-funded development plans and programs of potential commercial value to NAC.

**NAC INTERNATIONAL  
AFFIDAVIT PURSUANT TO 10 CFR 2.390 (continued)**

---

- e. Information that discloses patentable subject matter for which it may be desirable to obtain patent protection.

The information that is sought to be withheld is considered to be proprietary for the reasons set forth in Items 4.a, 4.b, and 4.d.

5. The information to be withheld is being transmitted to the NRC in confidence.
6. The information sought to be withheld, including that compiled from many sources, is of a sort customarily held in confidence by NAC, and is, in fact, so held. This information has, to the best of my knowledge and belief, consistently been held in confidence by NAC. No public disclosure has been made, and it is not available in public sources. All disclosures to third parties, including any required transmittals to the NRC, have been made, or must be made, pursuant to regulatory provisions or proprietary agreements, which provide for maintenance of the information in confidence. Its initial designation as proprietary information and the subsequent steps taken to prevent its unauthorized disclosure are as set forth in Items 7 and 8 following.
7. Initial approval of proprietary treatment of a document/information is made by the Vice President, Engineering, the Project Manager, the Licensing Engineer, or the Director, Licensing – the persons most likely to know the value and sensitivity of the information in relation to industry knowledge. Access to proprietary documents within NAC is limited via “controlled distribution” to individuals on a “need to know” basis. The procedure for external release of NAC proprietary documents typically requires the approval of the Project Manager based on a review of the documents for technical content, competitive effect and accuracy of the proprietary designation. Disclosures of proprietary documents outside of NAC are limited to regulatory agencies, customers and potential customers and their agents, suppliers, licensees and contractors with a legitimate need for the information, and then only in accordance with appropriate regulatory provisions or proprietary agreements.
8. NAC has invested a significant amount of time and money in the research, development, engineering and analytical costs to develop the information that is sought to be withheld as proprietary. This information is considered to be proprietary because it contains detailed descriptions of analytical approaches, methodologies, technical data and/or evaluation results not available elsewhere. The precise value of the expertise required to develop the proprietary information is difficult to quantify, but it is clearly substantial.

Public disclosure of the information to be withheld is likely to cause substantial harm to the competitive position of NAC, as the owner of the information, and reduce or eliminate the availability of profit-making opportunities. The proprietary information is part of NAC’s comprehensive spent fuel storage and transport technology base, and its commercial value extends beyond the original development cost to include the development of the expertise to determine and apply the appropriate evaluation process. The value of this proprietary information and the competitive advantage that it provides to NAC would be lost if the information were disclosed to the public. Making such information available to other parties, including competitors, without their having to make similar investments of time, labor and money would provide competitors with an unfair advantage and deprive NAC of the opportunity to seek an adequate return on its large investment.



NAC INTERNATIONAL  
AFFIDAVIT PURSUANT TO 10 CFR 2.390 (continued)


---

STATE OF GEORGIA, COUNTY OF GWINNETT


Mr. George Carver, being duly sworn, deposes and says:

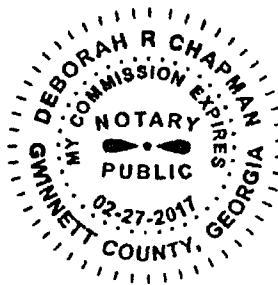
That he has read the foregoing affidavit and the matters stated herein are true and correct to the best of his knowledge, information and belief.

Executed at Norcross, Georgia, this 11<sup>th</sup> day of September, 2015.

  
\_\_\_\_\_  
George Carver  
Vice President, Engineering and Licensing  
NAC International

Subscribed and sworn before me this 11<sup>th</sup> day of September, 2015.

  
\_\_\_\_\_  
Notary Public



**Enclosure 1**

**10 CFR 72.48 Determination Summary Report**

**for the**

**MAGNASTOR<sup>®</sup> FSAR, Revision 7  
(Docket No 72-1031)**

**Period Covered: February 2015 thru July 2015**

**NAC International**

**July 2015**

**72.48 Determination ID #NAC-15-MAG-003**

**Change Description**

Updated MAGNASTOR FSAR Chapter 4 to incorporate the updated thermal analysis results for the MAGNASTOR BWR configuration due to the reduced thermal conductivities for the neutron absorber sheets and the fuel assemblies (UO<sub>2</sub>). FSAR Chapters 8 and 10 were updated with the lower thermal conductivities for the BWR neutron absorber material, which relaxes the requirement for the as fabricated sheets and makes it consistent with the values for the PWR configuration. A 40% reduction in the UO<sub>2</sub> thermal conductivities is used for the fuel assemblies based on NRC Information Notice 2009-23 for the consideration of thermal conductivity degradation for high burnup fuel.

Chapter 4, pages 4-ii, 4-iv, 4.4-30, 4.4-55 thru 4.4-56, 4.4-60 thru 4.4-68, 4.5-2, and 4.6-1;  
Chapter 8, page 8.3-15; and Chapter 10, page 10.1-14.

---

Source of Change: 72.48 Determination ID #NAC-15-MAG-003

Originating Document: DCR(L) 71160-FSAR-6B

This DCR(L) updated MAGNASTOR FSAR Chapter 4 to incorporate the updated thermal analysis results for the MAGNASTOR BWR configuration due to the reduced thermal conductivities for the neutron absorber sheets and the fuel assemblies (UO<sub>2</sub>). FSAR Chapters 8 and 10 were updated with the lower thermal conductivities for the BWR neutron absorber material, which relaxes the requirement for the as fabricated sheets and makes it consistent with the values for the PWR configuration. A 40% reduction in the UO<sub>2</sub> thermal conductivities is used for the fuel assemblies based on NRC Information Notice 2009-23 for the consideration of thermal conductivity degradation for high burnup fuel. The changes include revising general discussions and evaluation details for the following:

1. Revised text in the fourth paragraph on page 4.4-30.
2. Revised Figures 4.4-18 and 4.4-19 on pages 4.4-55 and 4.4-56.
3. Revised Tables 4.4-2, 4.4-3, 4.4-6, 4.4-8, 4.4-10, 4.4-12 thru 4.4-16 on pages 4.4-60 thru 4.4-68.
4. Revised the last embedded table on page 4.5-2.
5. Revised the embedded table on page 4.6-1.
6. Revised Table 8.3-27 on page 8.3-15.
7. Revised the embedded table on page 10.1-14.



**72.48 Determination ID #NAC-15-MAG-004**

Change Description

Updated MAGNASTOR Chapter 7 TSC shell composite closure lid assembly helium testing; elimination of mention to evacuate envelope test method. Editorial changes to Chapter 10 to update a typographical error found within MAGNASTOR FSAR Revision 6.

Chapter 7, page 7.1-3; and Chapter 10, page 10.1-6

---

Source of Change: 72.48 Determination ID #NAC-15-MAG-004

Originating Document: DCR(L) 71160-FSAR-6C

This DCR(L) updated MAGNASTOR Chapter 7 TSC shell composite closure lid assembly helium testing; elimination of mention to evacuate envelope test method. Editorial changes to Chapter 10 to update a typographical error found within MAGNASTOR FSAR Revision 6.

1. Revised the second paragraph on page 7.1-3.
2. Corrected a typographical error in the fourth paragraph on page 10.1-6.

**72.48 Determination ID #NAC-15-MAG-005**

Change Description

Revised Chapter 13C of the MAGNASTOR FSAR. The changes revised technical specification bases to provide additional clarification about the requirements of LCO 3.1.2.

Chapter 13C, pages 13C-15 thru 13C-17.

---

Source of Change: 72.48 Determination ID #NAC-15-MAG-005

Originating Document: DCR(L) 71160-FSAR-6D

This DCR(L) revised the technical specification bases to provide additional clarification about the requirements of LCO 3.1.2.

1. Clarification that partial concrete cask vent blockage is the equivalent area of two inlet/outlet vents and not two completely blocked vents and that vent obstruction can be any type of accumulation within the vent that restricts airflow;
2. Additional statements reiterating that the limiting time constraint for restoring adequate concrete cask heat removal capability is 58 hours;
3. Additional statements on the implementation of LCO 3.1.2 required action A.1;
4. A typographical error is being corrected on page 13C-17 by changing "meet" to "met".
5. The current descriptions in the bases are being revised to clarify an inconsistency with the thermal evaluation of the concrete cask for partial inlet vent blockage. Specifically, all four concrete cask outlet vents must be free of blockage to ensure adequate heat removal and not two, or equivalent area.

**72.48 Determination ID #NAC-13-MAG-033**

Change Description

Revised Drawing 71160-556, added the option for standoffs at the top and bottom of the cask inner diameter for improved centering of the TSC and reduced seal stroke requirements.

Drawing 71160-556

---

Source of Change: 72.48 Determination ID #NAC-13-MAG-033

Originating Document: DCR(L) 71160-556-3A

This DCR(L) revised Drawing 71160-556, by adding the option for standoffs at the top and bottom of the cask inner diameter for improved centering of the TSC and reduced seal stroke requirements. Changes were made as follows:

Sheet 1:

1. Added Delta note 16 to read: "Standoffs at the top and bottom of the cask inner diameter may be used to improve centering of the TSC for reduced seal stroke requirements."



**72.48 Determination ID #NAC-10-MAG-057**

**Change Description**

Revised Drawing 71160-560 (Assembly, Standard Transfer Cask, MAGNASTOR): Revised the notes for weld inspection to be consistent with FSAR Chapter 10, Section 10.1.1. Added a Kevlar seal option to increase the structural capacity of the seal allowing for increased inflation pressures, which permits increased annulus circulation flow rates and corresponding annulus water pressure.

Drawing 71160-560

---

Source of Change: 72.48 Determination ID #NAC-10-MAG-057

Originating Document: DCR(L) 71160-560-1A

This DCR(L) revised Drawing 71160-560, Revision 1 by revising the notes for weld inspection to be consistent with FSAR Chapter 10, Section 10.1.1. Additionally, it added a Kevlar seal option to increase the structural capacity of the seal allowing for increased inflation pressures, which permits increased annulus circulation flow rates and corresponding annulus water pressure. Changes made were as follows:

Drawing 71160-560, Rev. 2

Sheet 1:

1. B.O.M., Item 22, Revised Material to "EPDM/KELVAR"; was "EPDM".
2. Revised Note 3 to read "VISUALLY INSPECT (VT) ALL WELDS PER ASME SECTION V, ARTICLES 1 AND 9. ACCEPTANCE PER ASME SECTION III, ARTICLE NF-5360." Was "VISUALLY INSPECT (VT) ALL WELDS. AFTER LOAD TESTING MAG. PARTICLE INSPECT (MT) ALL CRITICAL LOAD BEARING WELDS."
3. Added a note to read, "AFTER LOAD TESTING INSPECT ALL ACCESSIBLE LOAD BEARING WELDS WITH EITHER LIQUID PENETRANT (PT) OR MAGNETIC PARTICLE (MT). (PT) PER ASME SECTION V, ARTICLES 1 AND 6, ACCEPTANCE PER SECTION III, ARTICLE NF-5350. (MT) PER ASME SECTION V, ARTICLES 1 AND 7, ACCEPTANCE PER SECTION III, ARTICLE NF-5340."

**72.48 Determination ID #NAC-14-MAG-103**

Change Description

Revised Drawings 71160-581 and 71160-681, by editing the Delta Note specifying UT examination requirements for shell to bottom welds to correct reference to Article 5, which should be Article 4.

Drawings 71160-581 and 71160-681

---

Source of Change: 72.48 Determination ID #NAC-14-MAG-103

Originating Documents: DCR(L) 71160-581-4A and DCR(L) 71160-681-0A

This DCR(L) revised Drawing 71160-581, Revision 4, by revising Delta note 3, and Drawing 71160-681, Revision 0, by revising Delta note 2, specifying UT examination requirements for shell to bottom welds to correct reference to Article 5, which should be Article 4, i.e., "Ultrasonic examined Per ASME Section V, Articles 1 and 4. Acceptance per Section III, Article NB-5320.". Changes were made as follows:

Drawing 71160-581, Rev 5:

Sheet 1:

1. Revised Delta note 3 to read, "... Section V, Article 1 and 4. ...", was "... Section V, Articles 1 and 5. ...".

Drawing 71160-681, Rev 1:

Sheet 1:

1. Revised Delta note 2 to read, "... Section V, Article 1 and 4. ...", was "... Section V, Articles 1 and 5. ...".

**72.48 Determination ID #NAC-13-MAG-076**

Change Description

Revised Drawing 71160-585, added optional slot to inner port cover (initial Item 8 welded to TSC lid port) to enable the licensee to fill the port cavity with helium during port cover welding operations which facilitates helium leak testing of the inner port cover weld. An optional second slot is permitted to enable helium to flow into the port cavity without initial evacuation. The size and location of the slots are to be such that the slots can be sufficiently sealed, i.e., for all conditions of storage and transport, by the inner port cover weld.

Drawing 71160-585

---

Source of Change: 72.48 Determination ID #NAC-13-MAG-076

Originating Document: DCR(L) 71160-585-9A

This DCR(L) revised Drawing 71160-585, Revision 9, by adding the optional slot to inner port cover (initial Item 8 welded to TSC lid port) to enable the licensee to fill the port cavity with helium during port cover welding operations which facilitates helium leak testing of the inner port cover weld. An optional second slot is permitted to enable helium to flow into the port cavity without initial evacuation. The size and location of the slots are to be such that the slots can be sufficiently sealed, i.e., for all conditions of storage and transport, by the inner port cover weld. Changes were made as follows:

Drawing 71160-585, Rev. 10

Sheet 1:

1. Add delta note 11, "At the option of the licensee, one or two slots may be machined into the inner port cover to allow the introduction of helium into the port cavity. Slot size and location shall permit slot to be sealed by the inner port cover weld."

Sheet 2:

2. Zone A4, add Delta Note 11 symbol with leader pointing to the inner port cover.



**72.48 Determination ID #NAC-14-MAG-054**

Change Description

Revised Drawing 71160-585, added optional slot to inner port cover (initial Item 8 welded to TSC lid port) to enable the licensee to fill the port cavity with helium during port cover welding operations which facilitates helium leak testing of the inner port cover weld. An optional second slot is permitted to enable helium to flow into the port cavity without initial evacuation. The size and location of the slots are to be such that the slots can be sufficiently sealed, i.e., for all conditions of storage and transport, by the inner port cover weld.

Drawings 71160-585 and 71160-685

---

Source of Change: 72.48 Determination ID #NAC-14-MAG-054

Originating Document: DCR(L) 71160-585-10A and DCR(L) 71160-685-4A

This DCR(L) revised Drawing 71160-585, Revision 10, and Drawing 71160-685, Revision 4 by reducing the port cover minimum plate thickness to that specified by the ASME SA240 specification for 3/8" plate. Maximum plate thickness is specified as 0.52." Field modification of the port covers is permitted within this thickness range to aid fit up with the closure lid counterbore. Note that this does not affect the size of the attachment welds. Additionally, delta notes were revised to clarify that the outer port cover, closure ring and corresponding welds are not to extend beyond the top surface of the lid. The stresses in the port and the weld have been analyzed. The revised port cover is structurally adequate for all conditions of storage. Changes were made as follows:

Drawing 71160-585, Rev. 11

Sheet 1:

1. Revised delta note 3 as follows: "Items 16, 18 (Closure Ring), 8 (Port Cover) and corresponding welds shall not extend beyond the top surface of the closure lid assembly. As necessary to aid fit-up, the port covers (Item 8) may be field ground/machined to the minimum specified thickness." Was: "Weld surface not to extend beyond the top surface of the closure lid assembly".
2. Added delta note 3 to Item 18. Zone B6, added delta note 3 to closure ring weld callout.
3. Revised BOM for Item 8. Deleted "1/2 plate" and Add "See Note 12" in Description
4. Added Note 12 as shown below: "Port Covers (Item 8) shall have a minimum thickness governed by ASME SA240 specification for 3/8 plate. Thicker plate may be used with a maximum thickness of 0.52 inch."

Sheet 2:

5. Added delta note 3 to Items 8 and 16. Zone B8, added delta note 3 to closure ring weld callout.

Drawing 71160-685, Rev. 5

Sheet 1:

1. Revised delta note 6 as follows: "Items 9 (Closure Ring), 12 & 19 (Outer Port Cover) and corresponding welds shall not extend beyond the top surface of the closure lid assembly. As necessary to aid fit-up, the port covers (Items 8, 11, 12, 19) may be field ground/ machined to the minimum specified thickness." Was: "Weld surface not to extend beyond the top surface of the closure lid assembly".
2. Revised BOM for Items 8, 11, 12, and 19. Deleted "1/2 plate" and Added "See Note 12" in Description.
3. Added Note 12 as shown below: "Inner Port Cover (Items 8, 11) and Outer Port Cover (Items 12, 19) shall have a minimum thickness governed by ASME SA240 specification for 3/8 plate. Thicker plate may be used with a maximum thickness of 0.52 inch."

Sheet 2:

4. Added delta note 6 to Items 8, 9, 11, 12, 19.
5. Zone E8, added delta note 6 to closure ring weld callout.

**72.48 Determination ID #NAC-14-MAG-105**

Change Description

Revised Drawing 71160-602, changed the range of the wiper thickness from (.005" - .008") to (.004" - .008"). The wiper is a part of the DFC Lid assembly and its primary function is to maintain the contents within the cavity of the DFC. This change doesn't affect the functionality of the DFC.

Drawing 71160-602

---

Source of Change: 72.48 Determination ID #NAC-14-MAG-105

Originating Document: DCR(L) 71160-602-0A

This DCR(L) revised Drawing 71160-602, Revision 0 by changing the range of the wiper thickness from (.005" - .008") to (.004" - .008"). The wiper is a part of the DFC Lid assembly and its primary function is to maintain the contents within the cavity of the DFC. This change doesn't affect the functionality of the DFC. Changes were made as follows:

Drawing 71160-602, Rev. 1

Sheet 1:

1. Revised the description of Item 4, Wiper Plate in the BOM table. Is: ".004-.008 (.102-.203mm) SHEET/STRIP"; was: ".005-.008 (.127-.203mm) SHEET/STRIP".



**NAC PROPRIETARY INFORMATION REMOVED**

**72.48 Determination ID #NAC-14-MAG-087**

Change Description

Revised Proprietary Drawing 71160-674, dimensions for the cutout section in the Inner-Formed Plates (Item 1 and Item 2) were provided, which were left off of the drawing in the previous revision. A correction was made to specify the use of 6 connector pins (Item 5 or Item 10) in total. The size of chamfers implemented on the square pin (Item 9) and square connector pin (Item 10) was specified.

Proprietary Drawing 71160-674

---

Source of Change: 72.48 Determination ID #NAC-14-MAG-087

Originating Document: DCR(L) 71160-674-3PA

Drawing 71160-674, Rev. 4P  
Sheet 1:

Sheet 2:

**72.48 Determination ID #NAC-15-MAG-010**

Change Description

The list of License Drawings for the proprietary and non-proprietary versions of the FSAR are being revised for changes made via the 72.48 process.

Chapter 1, page 1.8-1

---

Source of Change: 72.48 Determination ID #NAC-15-MAG-010

Originating Document: DCR(L) 71160-FSAR-6F

This DCR(L) incorporates the list of License Drawings with the latest approved drawing revisions to the following license drawings.

- |                       |                       |
|-----------------------|-----------------------|
| 1. 71160-556, Rev. 4  | 5. 71160-602, Rev. 1  |
| 2. 71160-560, Rev. 2  | 6. 71160-674, Rev. 4P |
| 3. 71160-581, Rev. 5  | 7. 71160-681, Rev. 1  |
| 4. 71160-585, Rev. 11 | 8. 71160-685, Rev. 5  |

**Enclosure 2**

**List of Changes**

**for**

**MAGNASTOR® FSAR, Revision 7  
(Docket No 72-1031)**

**NAC International**

**July 2015**

## **List of Changes for the MAGNASTOR® FSAR, Revision 7**

### **Incorporates 72.48 changes for the period December 2014 thru June 2015**

<b>Chapter/Page/ Figure/Table</b>	<b>Source of Change</b>	<b>Description of Change</b>
<b>Note:</b> The List of Effective Pages and the Chapter Table of Contents, List of Figures, and List of Tables have been revised accordingly to reflect the list of changes detailed below.		
<b><u>Chapter 1</u></b>		
Page 1.3-7	Amendment 5, 13D	Modified text throughout Section 1.3.1.5, "Damaged Fuel Can."
Page 1.3-8	Amendment 5, 13D	Text flow changes.
Page 1.3-12	Amendment 5, 13D	Replaced Figure 1.3-4, "MAGNASTOR Damaged Fuel Can."
Page 1.4-1	Amendment 5, 13D	Modified text at the end of the second paragraph of Section 1.4, "MAGNASTOR Contents."
Page 1.8-1		
<b><u>Chapter 2</u></b>		
No changes.		
<b><u>Chapter 3</u></b>		
No changes.		
<b><u>Chapter 4</u></b>		
Pages 4.1-1 thru 4.1-3	Amendment 5, 13D	Modified Section 4.1, "Discussion," throughout.
Pages 4.1-4 thru 4.1-5	Amendment 5, 13D	Text flow changes.
Page 4.1-6	Amendment 5, 13D	Added new Figure 4.1-2, "Preferential loading Pattern for the PWR Basket with Minimum Reduced Cool Time Fuel."
Pages 4.1-7 thru 4.1-8	Amendment 5, 13D	Text flow changes.
Pages 4.4-11 thru 4.4-12	Amendment 5, 13D	Modified text throughout page 4.4-11 and at the top of page 4.4-12.
Pages 4.4-13 thru 4.4-28	Amendment 5, 13D	Text flow changes.
Pages 4.4-29 thru 4.4-30	Amendment 5, 13D	Added new text under new subheading, "Evaluation of TSC Loaded with PWR Minimum Reduced Cool Time Fuel Basket Assembly."
Page 4.4-30	Amendment 4, 13A	Added new Section 4.4.1.7, "Two-Dimensional Transfer Cask and TSC Model for Increased Loading Times of PWR 20 kW and 25kW Heat Loads."

Chapter/Page/ Figure/Table	Source of Change:	Description of Change
Page 4.4-31	Amendment 4, 13A, Amendment 5, 13D	Text flow changes.
Page 4.4-32	DCR(L) 71160-FSAR-6B NAC-15-MAG-003	Modified temperature text in the fourth paragraph on the page.
Page 4.4-33	Amendment 5, 13D	Added new text under subheading, "Normal Conditions of Storage – PWR Minimum Reduced Cool Time Fuel Basket Assembly."
Pages 4.4-34 thru 4.4-35	Amendment 4, 13A, Amendment 5, 13D	Text flow changes.
Page 4.4-36	Amendment 4, 13A	Renumbered text references to table numbers to reflect appropriate changes for Tables 4.4-16 and 4.4-17 in the second paragraph of the page; added text under subheading, "Maximum TSC Transfer Temperatures for PWR 20 kW (no additional cooling) and 25kW Heat Loads with 7 hours of cooling".
Pages 4.4-37 thru 4.4-57	Amendment 4, 13A, Amendment 5, 13D	Text flow changes.
Page 4.4-58	DCR(L) 71160-FSAR-6B NAC-15-MAG-003	Modified title of Figure 4.4-18 and replaced the figure.
Page 4.4-59	DCR(L) 71160-FSAR-6B NAC-15-MAG-003	Modified the title of Figure 4.4-19.
Pages 4.4-60 thru 4.4-62	Amendment 4, 13A, Amendment 5, 13D	Text flow changes.
Pages 4.4-63 thru 4.4-68	DCR(L) 71160-FSAR-6B NAC-15-MAG-003	Modified Tables 4.4-2, 4.4-3, 4.4-6, 4.4-8, 4.4-10 and 4.4-12.
Page 4.4-69	DCR(L) 71160-FSAR-6B NAC-15-MAG-003	Modified Tables 4.4-13 and 4.4-14.
	Amendment 4, 13A	Added new Table 4.4-15.
Pages 4.4-70 thru 4.4-71	Amendment 4, 13A	Renumbered and modified Tables to 4.4-16 and 4.4-17 and their notes.
Page 4.5-1	Amendment 5, 13D	Added three new sentences to the end of the first paragraph in Section 4.5.1, for PWR minimum reduced cool time fuel.
Page 4.5-2	DCR(L) 71160-FSAR-6B NAC-15-MAG-003	Modified the third embedded table, "Principal Component Temperatures – Off-Normal Storage of CC1/CC2 with BWR TSC," at the bottom of the page.
Page 4.6-1	DCR(L) 71160-FSAR-6B NAC-15-MAG-003 Amendment 5, 13D	Added new paragraph to the end of Section 4.6, "Accident Events.
Page 4.6-2	DCR(L) 71160-FSAR-6B NAC-15-MAG-003	Modified the embedded table, at the top of the page, in Section 4.6.1.
Pages 4.6-3 thru 4.6-4	Amendment 5, 13D	Text flow changes.
<b>Chapter 5</b>		
Page 5.1-1	Amendment 5, 13D	Modified second paragraph and added new third paragraph in Section 5.1.

Chapter/Page/ Figure/Table	Source of Change:	Description of Change
Pages 5.1-2 thru 5.1-6	Amendment 5, 13D	Text flow changes.
Page 5.8.4-2	Amendment 5, 13D	Added new first row to the embedded table near the top of the page in Section 5.8.4.2.
Page 5.8.5-2	Amendment 4, 14C Amendment 5, 14D	Modified the middle of the third paragraph in Section 5.8.5.2.1.
Page 5.8.5-3	Amendment 4, 14C Amendment 5, 14D	Modified the second and third paragraphs in Section 5.8.5.2.2.
Page 5.8.5-9	Amendment 4, 14C Amendment 5, 14D	Added Table 5.8.5-7, "Additional Assembly Cool Time (Years) Required to Load BPRA or TP (Uniform Loading)," and the associated footnote.
Page 5.8.6-1	Amendment 4, 14C Amendment 5, 14D	Modified the fourth paragraph of Section 5.8.6.
	Amendment 5, 14D	Editorial typographical correction in first line of the fifth paragraph, changing "1 800,000;" to "180,000."
Page 5.8.6-7	(Revision 7)	Moved Table 5.8.6-5 for text flow
Page 5.8.6-7	Amendment 4, 14C Amendment 5, 14D	Added new Table 5.8.6-6, "Additional Assembly Cool Time (Years) Required to Load a CEA (Uniform Loading)."
Page 5.8.7-1		Editorial change in the first sentence of Section 5.8.7, changing "kW" to "W".
Page 5.8.7-2	Amendment 4, 14C Amendment 5, 14D	Added the last sentence to the paragraph in Section 5.8.7.3, "Additional assembly cool times...shown in Table 5.8.7-2."
Page 5.8.7-5	Amendment 4, 14C Amendment 5, 14D	Added new Table 5.8.7-2 "Additional Assembly Cool Time (Years) Required When Loading Nonfuel Hardware – Three-Zone Preferential Loading."
Page 5.8.9-1	Amendment 4, 14C Amendment 5, 14D	Modified the last paragraph on the page in Section 5.8.9-1.
Page 5.8.9-56	Amendment 5, 13D	Modified Table 5.8.9-10.
Pages 5.9-1 thru 5.9.9-6	Amendment 5, 13D; 14A	Added and modified new Section 5.9, "PWR Reduced Minimum Cool Time and Alternate Preferential Heat Load Pattern Shielding Evaluation Detail."
Pages 5.10-1 thru 5.10.6-25	Amendment 5, 14A	Added new Section 5.10, "CE16 Four-Zone Preferential Heat Load Pattern Shielding Evaluation Detail."
<b>Chapter 6</b>		
Page 6.1-2	Amendment 5, 13D	Modified the third paragraph on the page.
Pages 6.1-3 thru 6.1-5	Amendment 5, 13D	Text flow changes.
Page 6.1-6	Amendment 5, 13D	Replaced Figure 6.1.1-1, "82-Assembly BWR Basket Configuration."
Page 6.1-11	Amendment 5, 13D	Modified Table 6.1.1-4, "BWR Fuel Assembly Loading Criteria (Enrichment Limits)," by adding new notes "c" and "d" to the table.
Page 6.1-13	Amendment 5, 13D	Modified Table 6.1.1-6, "Damaged Fuel Basket Bounding PWR Fuel Assembly Loading Criteria (Enrichment/Soluble Boron Limits)." by adding a new row for "CE16H1."

Chapter/Page/ Figure/Table	Source of Change:	Description of Change
Page 6.4-11	Amendment 5, 13D	Modified Table 6.4.3-4, "BWR Fuel Basket Allowable Loading (Enrichment Limits)," by adding new notes "c" and "d" to the table.
Page 6.4-12	Amendment 5, 13D	Modified Table 6.4.3-5, "Damaged Fuel Basket PWR Fuel Assembly Loading Criteria (Enrichment/Soluble Boron Limits)," by adding a new row for "CE16H1."
Page 6.7.4-1	Amendment 5, 13D	Modified the second paragraph on the page, in Section 6.7.4.
Page 6.7.4-2	Amendment 5, 13D	Text flow changes.
Page 6.7.5-1	Amendment 5, 13D	Modified the second paragraph on the page, in Section 6.7.5.
Page 6.7.6-1	Amendment 5, 13D	Modified the third paragraph on the page, in Section 6.7.6.1.
Page 6.7.6-4	Amendment 5, 13D	Modified the first paragraph on the page, under subheading "Phase I Design Modification."
Page 6.7.6-7	Amendment 5, 13D; 14A	Modified the first paragraph under Section 6.7.6.2.
Page 6.7.6-23	Amendment 5, 14A	Modified Table 6.7.6-8 by adding new fields at the bottom of the table and a new footnote.
Page 6.7.6-24	Amendment 5, 14A	Added new footnotes "b" and "c" to Table 6.7.6-9.
Page 6.7.6-28	Amendment 5, 14A	Added new footnotes "c" and "d" to Table 6.7.6-13.
Page 6.7.8-4	Amendment 5, 13D	Changed 0.56 to 0.57 at the end of the second line of the last paragraph on the page.
Page 6.7.8-81	Amendment 5, 13D	Modified Table 6.7.8-1, "Sample Results for Undamaged Fuel in DFC (Damaged Fuel Basket)," by adding a new row for "CE16H1."
Page 6.7.8-82	Amendment 5, 13D	Modified Table 6.7.8-2, "DFC Unclad Rod Array Pitch Study Results," by adding a new row for "CE16H1."
Page 6.7.8-83	Amendment 5, 13D	Modified Table 6.7.8-3, "Sample Results for Unclad Rod/Loose Pellet Fuel in DFC (Damaged Fuel Basket)," by adding a new row for "CE16H1."
Page 6.7.8-85	Amendment 5, 13D	Modified Table 6.7.8-5, "Sample DFC Fuel Mixture Height Study Results," by adding a new row for "CE16H1."
Page 6.7.8-86	Amendment 5, 13D	Modified Table 6.7.8-6, "DFC Fuel Mixture Maximum Reactivity Height for 0.036 g/cm <sup>2</sup> <sup>10</sup> B – No Inserts," by adding a new row for "CE16H1."
Page 6.7.8-87	Amendment 5, 13D	Modified Table 6.7.8-7, "DFC Fuel Mixture Maximum Reactivity Height for 0.036 g/cm <sup>2</sup> <sup>10</sup> B – Inserts," by adding a new row for "CE16H1."
Page 6.7.8-90	Amendment 5, 13D	Modified Table 6.7.8-10, "PWR Damaged Fuel Assembly Allowable Loading (Enrichment/Soluble Boron Limits)," by adding a new row for "CE16H1."

<b>Chapter/Page/ Figure/Table</b>	<b>Source of Change:</b>	<b>Description of Change</b>
<b><u>Chapter 7</u></b>		
Page 7.1-3	DCR(L) 71160-FSAR-6C NAC-15-MAG-004	Modified text in the second paragraph on the page.
Page 7.1-4	DCR(L) 71160-FSAR-6C NAC-15-MAG-004	Text flow changes.
<b><u>Chapter 8</u></b>		
Pages 8.3-15	DCR(L) 71160-FSAR-6B NAC-15-MAG-003	Modified Table 8.3-27.
<b><u>Chapter 9</u></b>		
Page 9.1-3	Amendment 5, 13D	Modified the first note of Item 15 in Section 9.1.1.
Page 9.1-4	Amendment 5, 13D	Text flow changes.
<b><u>Chapter 10</u></b>		
Page 10.1-5	Amendment 5, 13D	Modified the first sentence in Section 10.1.2.3.
Page 10.1-6	DCR(L) 71160-FSAR-6C NAC-15-MAG-004	Modified text near the end of the fourth paragraph on the page.
Page 10.1-14	DCR(L) 71160-FSAR-6B NAC-15-MAG-003	Modified the embedded table at the top of the page in Section 10.1.6.4.4.
<b><u>Chapter 11</u></b>		
No changes.		
<b><u>Chapter 12</u></b>		
No changes.		
<b><u>Chapter 13</u></b>		
Page 13C-10	Amendment 4, 13A	Modified the first paragraph for the term "BACKGROUND"; text flow at bottom of page due to deleted empty space after first paragraph where text was removed in a previous revision.
Pages 13C-11 thru 13C-12	Amendment 4, 13C	Text flow, and added text contained in parentheses at the end of the 3 <sup>rd</sup> paragraph for the term "LCO"; added a comma after "drying cycles" in the first sentence, last paragraph of the term "LCO." (Note: additional editorial changes from the Rev. 13C submittal are N/A, as the paragraph content has changed via Amendment 3 and Revision 6.)
Pages 13C-15 thru 13C-18	DCR(L) 71160-FSAR-6D NAC-15-MAG-005	Modified text throughout Section 3.1.2 and SR 3.1.2.1, where indicated.
<b><u>Chapter 14</u></b>		
No changes.		
<b><u>Chapter 15</u></b>		
No changes.		



**Enclosure 3**

**Certification of Accuracy**  
**of the**  
**MAGNASTOR® FSAR, Revision 7**  
**(Docket No 72-1031)**

**NAC International**

**July 2015**

**NAC INTERNATIONAL**  
**CERTIFICATION OF ACCURACY**  
**PURSUANT TO 10 CFR 72. 248(c)(4)(i)**

---

George Carver (Affiant), Vice President, Engineering and Licensing, of NAC International, hereinafter referred to as NAC, at 3930 East Jones Bridge Road, Norcross, Georgia 30092, being duly sworn, deposes and certifies that:

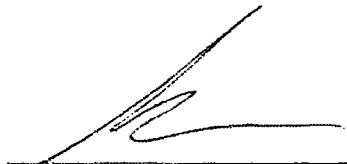
1. Affiant has reviewed the information described in Item 2, is personally familiar with the preparation, checking and verification of that information and is authorized to certify its accuracy.
2. The information being certified as accurate includes all of the changes incorporated into the MAGNASTOR Final Safety Analysis Report, Revision 7.

**STATE OF GEORGIA, COUNTY OF GWINNETT**

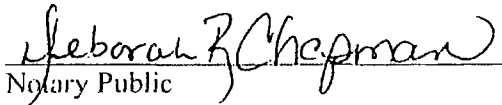
Mr. George Carver, being duly sworn, deposes and says:

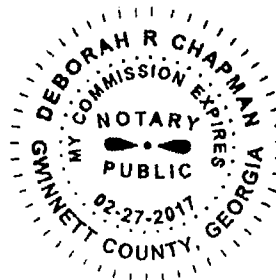
That he has read the foregoing affidavit and the matters stated therein are true and correct to the best of his knowledge, information and belief.

Executed at Norcross, Georgia, this 6<sup>th</sup> day of July, 2015.

  
\_\_\_\_\_  
George Carver  
Vice President, Engineering and Licensing  
NAC International

Subscribed and sworn before me this 6<sup>th</sup> day of July, 2015.

  
\_\_\_\_\_  
Notary Public



Enclosure 4

FSAR Changed Pages and LOEP

Docket No. 72-1031

MAGNASTOR<sup>®</sup> FSAR, Revision 7



July 2015

Revision 7

# MAGNASTOR<sup>®</sup>

(Modular Advanced Generation  
Nuclear All-purpose STORAGE)

---

## FINAL SAFETY ANALYSIS REPORT

NON-PROPRIETARY VERSION

Docket No. 72-1031



---

Atlanta Corporate Headquarters: 3930 East Jones Bridge Road, Norcross, Georgia 30092 USA  
Phone 770-447-1144, Fax 770-447-1797, [www.nacintl.com](http://www.nacintl.com)



### List of Effective Pages

#### Chapter 1

Page 1-i .....	Revision 5
Page 1-1 .....	Revision 1
Page 1.1-1 thru 1.1-5.....	Revision 5
Page 1.2-1 .....	Revision 6
Page 1.2-2 .....	Revision 5
Page 1.3-1 thru 1.3-6.....	Revision 5
Page 1.3-7 thru 1.3-8.....	Revision 7
Page 1.3-9 .....	Revision 1
Page 1.3-10 .....	Revision 4
Page 1.3-11 .....	Revision 1
Page 1.3-12 .....	Revision 7
Page 1.3-13 .....	Revision 5
Page 1.3-14 .....	Revision 6
Page 1.3-15 thru 1.3-18.....	Revision 5
Page 1.4-1 .....	Revision 7
Page 1.5-1 .....	Revision 5
Page 1.6-1 .....	Revision 2
Page 1.6-2 .....	Revision 0
Page 1.7-1 .....	Revision 0
Page 1.7-2 .....	Revision 2
Page 1.8-1 .....	Revision 7

26 drawings (see Section 1.8)

#### Chapter 2

Page 2-i thru 2-ii .....	Revision 5
Page 2-1 .....	Revision 5
Page 2.1-1 .....	Revision 5
Page 2.1-2 .....	Revision 0
Page 2.1-3 thru 2.1-5.....	Revision 5
Page 2.2-1 thru 2.2-3.....	Revision 5
Page 2.2-4 thru 2.2-5.....	Revision 0
Page 2.2-6 thru 2.2-7.....	Revision 5
Page 2.2-8 .....	Revision 6
Page 2.3-1 thru 2.3-4.....	Revision 0
Page 2.3-5 .....	Revision 5
Page 2.3-6 thru 2.3-8.....	Revision 0
Page 2.4-1 .....	Revision 0
Page 2.4-2 .....	Revision 2
Page 2.4-3 thru 2.4-4.....	Revision 5
Page 2.4-5 .....	Revision 0
Page 2.4-6 thru 2.4-7.....	Revision 5

Page 2.5-1 .....	Revision 0
Page 2.6-1 thru 2.6-2.....	Revision 0

#### Chapter 3

Page 3-i .....	Revision 6
Page 3-ii .....	Revision 5
Page 3-iii .....	Revision 6
Page 3-iv thru 3-vi .....	Revision 5
Page 3-vii .....	Revision 6
Page 3-viii .....	Revision 6
Page 3-ix .....	Revision 5
Page 3-1 .....	Revision 0
Page 3.1-1 .....	Revision 1
Page 3.1-2 .....	Revision 0
Page 3.1-3 thru 3.1-4.....	Revision 5
Page 3.1-5 thru 3.1-5.....	Revision 1
Page 3.1-6 .....	Revision 6
Page 3.2-1 thru 3.2-3.....	Revision 5
Page 3.3-1 .....	Revision 0
Page 3.4-1 .....	Revision 2
Page 3.4-2 .....	Revision 5
Page 3.4-3 .....	Revision 6
Page 3.4-4 .....	Revision 1
Page 3.4-5 .....	Revision 5
Page 3.4-6 thru 3.4-42.....	Revision 3
Page 3.4-43 thru 3.4-48.....	Revision 5
Page 3.5-1 .....	Revision 1
Page 3.5-2 thru 3.5-30.....	Revision 6
Page 3.6-1 thru 3.6-2.....	Revision 5
Page 3.6-3 thru 3.6-19.....	Revision 6
Page 3.7-1 .....	Revision 5
Page 3.7-2 thru 3.7-81.....	Revision 6
Page 3.8-1 thru 3.8-10.....	Revision 0
Page 3.9-1 .....	Revision 0
Page 3.9-2 .....	Revision 1
Page 3.10-1 .....	Revision 0
Page 3.10.1-1 .....	Revision 5
Page 3.10.1-2 thru 3.10.1-4.....	Revision 2
Page 3.10.1-5 .....	Revision 1
Page 3.10.1-6 thru 3.10.1-32.....	Revision 5
Page 3.10.2-1 thru 3.10.2-26.....	Revision 4
Page 3.10.3-1 thru 3.10.3-2.....	Revision 1
Page 3.10.3-3 .....	Revision 0

**List of Effective Pages (cont'd)**

Page 3.10.3-4 thru 3.10.3-38.....	Revision 1	Page 4.8.3-5 .....	Revision 0
Page 3.10.4-1 thru 3.10.4-2.....	Revision 1	Page 4.8.3-6 thru 4.8.3-9.....	Revision 1
Page 3.10.4-3 thru 3.10.4-9.....	Revision 0	Page 4.9-1 .....	Revision 2
Page 3.10.4-10 .....	Revision 1	Page 4.9.1-1 .....	Revision 3
Page 3.10.4-11 thru 3.10.4-14.....	Revision 0	Page 4.9.2-1 thru 4.9.2-3.....	Revision 5
Page 3.10.5-1 .....	Revision 1	Page 4.9.3-1 thru 4.9.3-3.....	Revision 3
Page 3.10.5-2 .....	Revision 2	Page 4.9.4-1 .....	Revision 2
Page 3.10.5-3 thru 3.10.5-4.....	Revision 1		
Page 3.10.6-1 thru 3.10.6-2.....	Revision 5	<u>Chapter 5</u>	
Page 3.10.6-3 .....	Revision 4	Page 5-i thru 5-ii .....	Revision 7
Page 3.10.6-4 thru 3.10.6-6.....	Revision 5	Page 5-iii .....	Revision 5
Page 3.10.6-7 thru 3.10.6-10.....	Revision 4	Page 5-iv .....	Revision 1
Page 3.10.6-11 thru 3.10.6-13.....	Revision 2	Page 5-v thru 5-vii .....	Revision 5
Page 3.10.6-14 thru 3.10.6-16.....	Revision 4	Page 5-viii .....	Revision 7
Page 3.10.6-17 thru 3.10.6-18.....	Revision 2	Page 5-ix thru 5-x.....	Revision 5
Page 3.10.6-19 .....	Revision 4	Page 5-xi thru 5-xii .....	Revision 7
Page 3.10.6-20 thru 3.10.6-21.....	Revision 2	Page 5-1 thru 5-2.....	Revision 5
Page 3.10.6-22 thru 3.10.6-34.....	Revision 4	Page 5.1-1 thru 5.1-6.....	Revision 7
Page 3.10.7-1 thru 3.10.7-2.....	Revision 0	Page 5.1-7 thru 5.1-12.....	Revision 5
Page 3.10.8-1 .....	Revision 4	Page 5.2-1 thru 5.2-12.....	Revision 5
Page 3.10.8-2 .....	Revision 2	Page 5.3-1 thru 5.3-2.....	Revision 5
Page 3.10.8-3 thru 3.10.8-8.....	Revision 0	Page 5.3-3 .....	Revision 0
Page 3.10.9-1 .....	Revision 6	Page 5.3-4 thru 5.3-5.....	Revision 1
Page 3.10.9-2 .....	Revision 4	Page 5.3-6 .....	Revision 0
Page 3.10.9-3 thru 3.10.9-11.....	Revision 0	Page 5.4-1 thru 5.4-5.....	Revision 0
Page 3.10.10-1 thru 3.10.10-8.....	Revision 5	Page 5.5-1 .....	Revision 0
		Page 5.5-2 thru 5.5-5.....	Revision 5
<u>Chapter 4</u>		Page 5.5-6 .....	Revision 0
Page 4-i thru 4-iv .....	Revision 7	Page 5.5-7 thru 5.5-10.....	Revision 1
Page 4-1 .....	Revision 0	Page 5.5-11 thru 5.5-13.....	Revision 0
Page 4.1-1 thru 4.1-8.....	Revision 7	Page 5.5-14 thru 5.5-15.....	Revision 1
Page 4.2-1 .....	Revision 0	Page 5.5-16 thru 5.5-20.....	Revision 5
Page 4.3-1 .....	Revision 0	Page 5.6-1 thru 5.6-2.....	Revision 0
Page 4.4-1 thru 4.4-10.....	Revision 5	Page 5.6-3 .....	Revision 1
Page 4.4-11 thru 4.4-71 .....	Revision 7	Page 5.6-4 thru 5.6-6.....	Revision 5
Page 4.5-1 thru 4.5-2.....	Revision 7	Page 5.6-7 .....	Revision 1
Page 4.5-3 thru 4.5-4.....	Revision 5	Page 5.6-8 .....	Revision 5
Page 4.6-1 thru 4.6-4.....	Revision 7	Page 5.6-9 .....	Revision 1
Page 4.7-1 thru 4.7-2.....	Revision 0	Page 5.6-10 thru 5.6-13.....	Revision 0
Page 4.8-1 .....	Revision 0	Page 5.7-1 thru 5.7-3.....	Revision 0
Page 4.8.1-1 thru 4.8.1-10.....	Revision 0	Page 5.8-1 .....	Revision 0
Page 4.8.2-1 thru 4.8.2-8.....	Revision 0	Page 5.8.1-1 thru 5.8.1-4.....	Revision 0
Page 4.8.3-1 thru 4.8.3-2.....	Revision 0	Page 5.8.2-1 .....	Revision 0
Page 4.8.3-3 thru 4.8.3-4.....	Revision 1	Page 5.8.2-2 thru 5.8.2-5.....	Revision 1

**List of Effective Pages (cont'd)**

Page 5.8.2-6 .....	Revision 0	Page 5.9.1-1 .....	Revision 7
Page 5.8.2-7 thru 5.8.2-13.....	Revision 1	Page 5.9.2-1 .....	Revision 7
Page 5.8.3-1 .....	Revision 5	Page 5.9.3-1 thru 5.9.3-5.....	Revision 7
Page 5.8.3-2 .....	Revision 1	Page 5.9.4-1 thru 5.9.4-2.....	Revision 7
Page 5.8.3-3 thru 5.8.3-5.....	Revision 5	Page 5.9.5-1 thru 5.9.5-2.....	Revision 7
Page 5.8.3-6 thru 5.8.3-17.....	Revision 1	Page 5.9.6-1 thru 5.9.6-4.....	Revision 7
Page 5.8.3-18 thru 5.8.3-19.....	Revision 5	Page 5.9.7-1 thru 5.9.7-23.....	Revision 7
Page 5.8.3-20 thru 5.8.3-23.....	Revision 1	Page 5.9.8-1 thru 5.9.8-28.....	Revision 7
Page 5.8.3-24 thru 5.8.3-33.....	Revision 5	Page 5.9.9-1 thru 5.9.9-6.....	Revision 7
Page 5.8.4-1 .....	Revision 5	Page 5.10-1 .....	Revision 7
Page 5.8.4-2 .....	Revision 7	Page 5.10.1-1 .....	Revision 7
Page 5.8.4-3 thru 5.8.4-30.....	Revision 0	Page 5.10.2-1 .....	Revision 7
Page 5.8.5-1 .....	Revision 5	Page 5.10.3-1 thru 5.10.3-3.....	Revision 7
Page 5.8.5-2 thru 5.8.5-3.....	Revision 7	Page 5.10.4-1 .....	Revision 7
Page 5.8.5-4 thru 5.8.5-6.....	Revision 5	Page 5.10.5-1 thru 5.10.5-4.....	Revision 7
Page 5.8.5-7 .....	Revision 0	Page 5.10.6-1 thru 5.10.6-25.....	Revision 7
Page 5.8.5-8 .....	Revision 5		
Page 5.8.5-9 .....	Revision 7	<u>Chapter 6</u>	
Page 5.8.6-1 .....	Revision 7	Page 6-i thru 6-vi .....	Revision 5
Page 5.8.6-2 thru 5.8.6-6.....	Revision 5	Page 6-1 .....	Revision 0
Page 5.8.6-7 .....	Revision 7	Page 6.1-1 .....	Revision 5
Page 5.8.7-1 thru 5.8.7-2.....	Revision 7	Page 6.1-2 thru 6.1-6.....	Revision 7
Page 5.8.7-3 .....	Revision 0	Page 6.1-7 thru 6.1-10.....	Revision 5
Page 5.8.7-4 .....	Revision 5	Page 6.1-11 .....	Revision 7
Page 5.8.7-5 .....	Revision 7	Page 6.1-12 .....	Revision 5
Page 5.8.8-1 .....	Revision 5	Page 6.1-13 .....	Revision 7
Page 5.8.8-2 thru 5.8.8-4.....	Revision 0	Page 6.2-1 .....	Revision 5
Page 5.8.8-5 thru 5.8.8-12.....	Revision 1	Page 6.2-2 thru 6.2-5.....	Revision 0
Page 5.8.8-13 thru 5.8.8-23.....	Revision 0	Page 6.3-1 .....	Revision 5
Page 5.8.8-24 thru 5.8.8-34.....	Revision 1	Page 6.3-2 .....	Revision 6
Page 5.8.8-35 thru 5.8.8-56.....	Revision 0	Page 6.3-3 .....	Revision 5
Page 5.8.8-57 thru 5.8.8-65.....	Revision 5	Page 6.3-4 thru 6.3-8.....	Revision 0
Page 5.8.8-66 thru 5.8.8-79.....	Revision 1	Page 6.3-9 .....	Revision 2
Page 5.8.8-80 thru 5.8.8-115.....	Revision 5	Page 6.4-1 .....	Revision 0
Page 5.8.9-1 .....	Revision 7	Page 6.4-2 .....	Revision 2
Page 5.8.9-2 thru 5.8.9-6.....	Revision 0	Page 6.4-3 thru 6.4-10.....	Revision 5
Page 5.8.9-7 thru 5.8.9-55.....	Revision 1	Page 6.4-11 thru 6.4-12.....	Revision 7
Page 5.8.9-56 .....	Revision 7	Page 6.5-1 thru 6.5-7.....	Revision 0
Page 5.8.9-57 thru 5.8.9-69.....	Revision 1	Page 6.6-1 .....	Revision 0
Page 5.8.10-1 thru 5.8.10-5.....	Revision 0	Page 6.7-1 .....	Revision 0
Page 5.8.11-1 thru 5.8.11-3.....	Revision 1	Page 6.7.1-1 thru 6.7.1-2.....	Revision 5
Page 5.8.12-1 thru 5.8.12-16.....	Revision 5	Page 6.7.1-3 .....	Revision 0
Page 5.8.13-1 thru 5.8.13-6.....	Revision 5	Page 6.7.1-4 .....	Revision 2
Page 5.9-1 .....	Revision 7	Page 6.7.1-5 thru 6.7.1-37.....	Revision 0

List of Effective Pages (cont'd)

Page 6.7.2-1 thru 6.7.2-2.....	Revision 0	Page 8.1-1 thru 8.1-2.....	Revision 5
Page 6.7.2-3 .....	Revision 5	Page 8.1-3 thru 8.1-4.....	Revision 6
Page 6.7.2-4 thru 6.7.2-5.....	Revision 0	Page 8.2-1 .....	Revision 1
Page 6.7.3-1 thru 6.7.3-27.....	Revision 5	Page 8.3-1 .....	Revision 5
Page 6.7.4-1 thru 6.7.4-2.....	Revision 7	Page 8.3-2 thru 8.3-8.....	Revision 1
Page 6.7.4-3 .....	Revision 0	Page 8.3-9 thru 8.3-14.....	Revision 5
Page 6.7.4-4 .....	Revision 2	Page 8.3-15 .....	Revision 7
Page 6.7.4-5 thru 6.7.4-44.....	Revision 0	Page 8.3-16 thru 8.3-17.....	Revision 5
Page 6.7.5-1 .....	Revision 7	Page 8.4-1 .....	Revision 0
Page 6.7.5-2 thru 6.7.5-7.....	Revision 0	Page 8.5-1 .....	Revision 1
Page 6.7.6-1 .....	Revision 7	Page 8.5-2 .....	Revision 6
Page 6.7.6-2 thru 6.7.6-3.....	Revision 2	Page 8.6-1 .....	Revision 1
Page 6.7.6-4 .....	Revision 7	Page 8.6-2 .....	Revision 6
Page 6.7.6-5 thru 6.7.6-6.....	Revision 2	Page 8.6-3 .....	Revision 1
Page 6.7.6-7 .....	Revision 7	Page 8.7-1 .....	Revision 2
Page 6.7.6-8 thru 6.7.6-22.....	Revision 2	Page 8.7-2 .....	Revision 0
Page 6.7.6-23 thru 6.7.6-24.....	Revision 7	Page 8.8-1 .....	Revision 2
Page 6.7.6-25 thru 6.7.6-27.....	Revision 2	Page 8.8-2 .....	Revision 3
Page 6.7.6-28 .....	Revision 7	Page 8.8-3 .....	Revision 0
Page 6.7.7-1 thru 6.7.7-27.....	Revision 0	Page 8.8-4 .....	Revision 3
Page 6.7.8-1 thru 6.7.8-3.....	Revision 5	Page 8.9-1 .....	Revision 0
Page 6.7.8-4 .....	Revision 7	Page 8.10-1 .....	Revision 0
Page 6.7.8-5 thru 6.7.8-80.....	Revision 5	Page 8.10-2 .....	Revision 1
Page 6.7.8-81 thru 6.7.8-83.....	Revision 7	Page 8.10-3 .....	Revision 6
Page 6.7.8-84 .....	Revision 5	Page 8.10-4 thru 8.10-7.....	Revision 1
Page 6.7.8-85 thru 6.7.8-87.....	Revision 7	Page 8.11-1 thru 8.11-3.....	Revision 0
Page 6.7.8-88 thru 6.7.8-89.....	Revision 5	Page 8.12-1 thru 8.12-2.....	Revision 0
Page 6.7.8-90 .....	Revision 7	Page 8.12-3 .....	Revision 6
		Page 8.13-1 thru 8.13-6.....	Revision 0
		Page 8.13-7 thru 8.13-17.....	Revision 6
<u>Chapter 7</u>			
Page 7-i .....	Revision 5	<u>Chapter 9</u>	
Page 7-1 .....	Revision 0	Page 9-i .....	Revision 5
Page 7.1-1 thru 7.1-2.....	Revision 5	Page 9-1 thru 9-2.....	Revision 2
Page 7.1-3 thru 7.1-4.....	Revision 7	Page 9.1-1 thru 9.1-2.....	Revision 5
Page 7.1-5 .....	Revision 5	Page 9.1-3 thru 9.1-4.....	Revision 7
Page 7.1-6 .....	Revision 2	Page 9.1-5 thru 9.1-20.....	Revision 5
Page 7.2-1 thru 7.2-2.....	Revision 0	Page 9.2-1 thru 9.2-2.....	Revision 5
Page 7.3-1 .....	Revision 0	Page 9.3-1 thru 9.3-3.....	Revision 5
Page 7.4-1 .....	Revision 0		
<u>Chapter 8</u>			
Page 8-i .....	Revision 6	<u>Chapter 10</u>	
Page 8-ii .....	Revision 5	Page 10-i .....	Revision 5
Page 8-1 .....	Revision 0	Page 10-1 .....	Revision 0
		Page 10.1-1 .....	Revision 5



**List of Effective Pages (cont'd)**

Page 10.1-2 .....	Revision 6	Page 13A-1 .....	Revision 0
Page 10.1-3 thru 10.1-4.....	Revision 2	Page 13B-i.....	Revision 0
Page 10.1-5 thru 10.1-6.....	Revision 7	Page 13B-1 .....	Revision 0
Page 10.1-7 thru 10.1-13.....	Revision 5	Page 13C-i.....	Revision 1
Page 10.1-14 .....	Revision 7	Page 13C-1 thru 13C-3 .....	Revision 5
Page 10.1-15 thru 10.1-23.....	Revision 5	Page 13C-4 thru 13C-9 .....	Revision 0
Page 10.2-1 thru 10.2-2.....	Revision 0	Page 13C-10 thru 13C-12 .....	Revision 7
Page 10.2-3 .....	Revision 5	Page 13C-13 thru 13C-14 .....	Revision 1
Page 10.3-1 .....	Revision 0	Page 13C-15 thru 13C-18 .....	Revision 7
Page 10.3-2 .....	Revision 1	Page 13C-19 thru 13C-21 .....	Revision 5
		Page 13C-22.....	Revision 1
<u>Chapter 11</u>		Page 13C-23 thru 13C-24 .....	Revision 5
Page 11-i .....	Revision 0	Page 13C-25 thru 13C-27 .....	Revision 2
Page 11-1 .....	Revision 0		
Page 11.1-1 thru 11.1-2.....	Revision 0	<u>Chapter 14</u>	
Page 11.2-1 .....	Revision 0	Page 14-i .....	Revision 0
Page 11.3-1 .....	Revision 0	Page 14-1 thru 14-2.....	Revision 0
Page 11.3-2 thru 11.3-3.....	Revision 5	Page 14.1-1 thru 14.1-7.....	Revision 0
Page 11.3-4 thru 11.3-6.....	Revision 0	Page 14.2-1 .....	Revision 0
Page 11.4-1 .....	Revision 0		
Page 11.5-1 .....	Revision 0	<u>Chapter 15</u>	
		Page 15-i .....	Revision 0
<u>Chapter 12</u>		Page 15-1 .....	Revision 0
Page 12-i .....	Revision 5	Page 15.1-1 .....	Revision 0
Page 12-1 .....	Revision 0	Page 15.2-1 thru 15.2-4.....	Revision 0
Page 12.1-1 thru 12.1-10.....	Revision 5	Page 15.3-1 .....	Revision 0
Page 12.2-1 .....	Revision 0		
Page 12.2-2 .....	Revision 1		
Page 12.2-3 .....	Revision 0		
Page 12.2-4 .....	Revision 1		
Page 12.2-5 .....	Revision 4		
Page 12.2-6 .....	Revision 0		
Page 12.2-7 thru 12.2-15.....	Revision 5		
Page 12.2-16 .....	Revision 0		
Page 12.2-17 .....	Revision 1		
Page 12.2-18 .....	Revision 4		
Page 12.2-19 .....	Revision 0		
Page 12.2-20 .....	Revision 5		
Page 12.3-1 thru 12.3-2.....	Revision 0		
<u>Chapter 13</u>			
Page 13-i .....	Revision 0		
Page 13-1 .....	Revision 0		
Page 13A-i .....	Revision 0		

The transfer cask penetrations can also be used for the introduction of auxiliary forced air or gas to cool the exterior of the TSC. Alternately, if auxiliary cooling is required to lower fuel cladding or TSC component temperatures, the loaded TSC may be returned to the spent fuel pool or shelf for cooling.

#### **1.3.1.5      Damaged Fuel Can**

The MAGNASTOR Damaged Fuel Can (DFC), shown in Figure 1.3-4, is provided to accommodate damaged PWR fuel assemblies or fuel debris equivalent to one PWR fuel assembly. Up to four DFCs may be loaded, one into each outer corner, in the MAGNASTOR DF Basket Assembly.

The primary function of the DFC is to confine the fuel material within the can to minimize the potential for dispersal of the fuel material into the TSC cavity. In normal operation, the DFC is in a vertical orientation.

The DFC is fabricated from Type 304 stainless steel and has an 8.7-in square inside dimension. The side plates that form the upper end of the DFC are 0.15-in thick and the tube body walls are 0.048-in thick (18-gage sheet). The DFC lid plate and bottom thicknesses total 11/16 (0.688) inch and the lid overall height is 2.32 inches. The DFC bottom plate thickness is 5/8 (0.625) inch. The DFC lid and bottom include screened drain holes.

#### **1.3.2      Operational Features**

In storage, MAGNASTOR does not require any active operational systems. The principal MAGNASTOR operational activities are loading, welding, and preparing the TSC for storage and transferring the TSC to the concrete cask. The transfer cask (MTC) is designed to meet the requirements of these operations. The transfer cask holds the TSC during fuel loading operations, provides biological shielding during TSC closure and preparation, and positions the TSC for transfer into the concrete cask. The lid design of the TSC assures structural integrity, while reducing the time and dose involved in TSC closure.

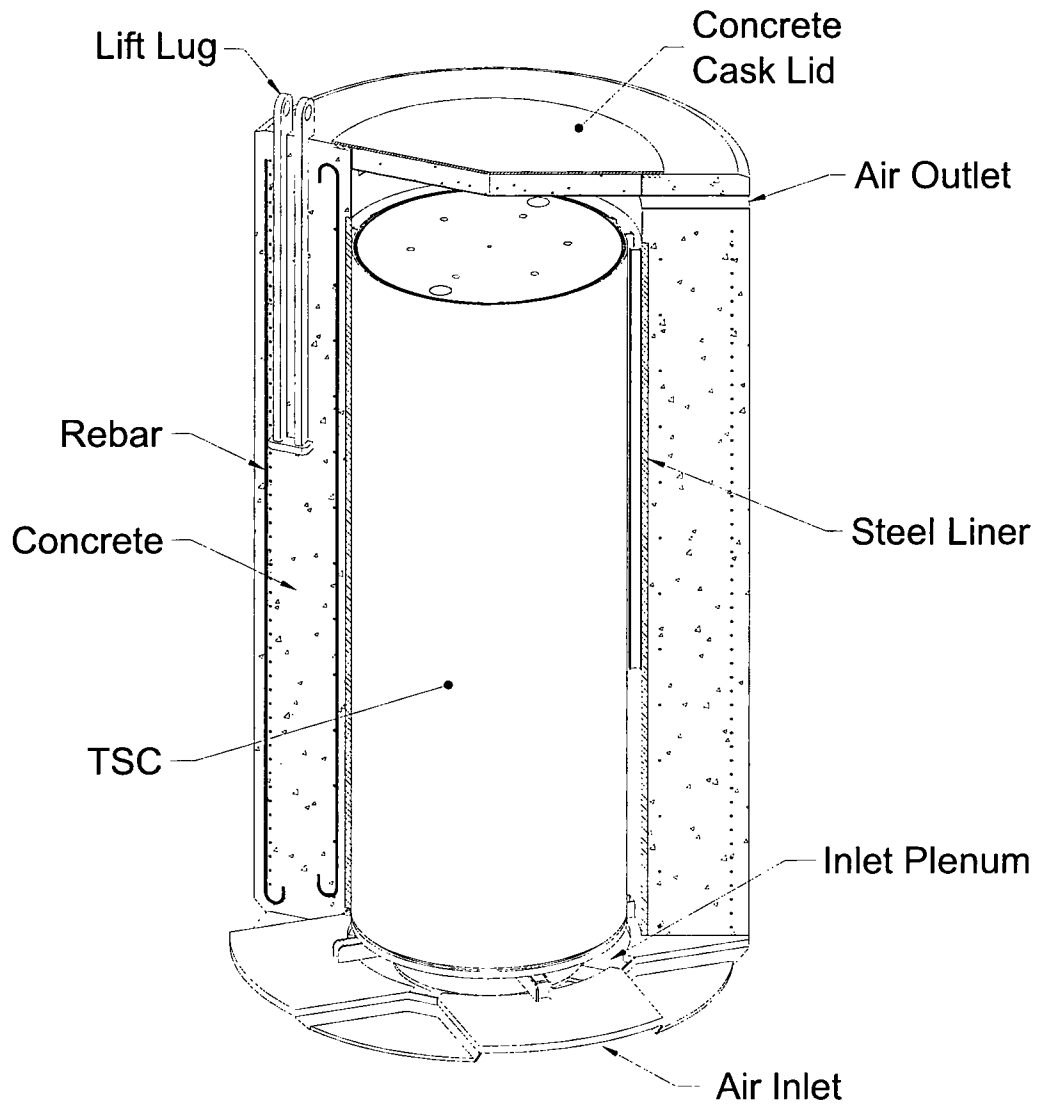
The detailed generic step-by-step operating procedures for the loading and transferring of MAGNASTOR are presented in Chapter 9. The following is a list of the major loading activities. This list assumes that the empty TSC is installed in the transfer cask.

- Fill the TSC with water or borated water if required.
- Lift the transfer cask over the pool and start the flow of water to the transfer cask annulus and lower the cask to the bottom of the pool.
- Load the selected spent fuel assemblies and damaged fuel cans (if applicable) into the TSC.
- Install the closure lid assembly.

- Remove the transfer cask from the pool and place it in the cask preparation workstation.
- Decontaminate the transfer cask.
- Lower the TSC water level and weld the closure lid to the TSC shell. Examine the weld.
- Hydrostatically test the TSC.
- Install and weld the closure ring. Examine the weld.
- Drain the remaining pool water from the TSC.
- Vacuum dry the TSC cavity. Verify cavity dryness.
- Establish a helium backfill.
- Install and weld the inner vent and drain port covers. Examine the welds.
- Helium leak test the inner vent and drain port covers.
- Install and weld the outer vent and drain port covers. Examine the welds.
- Install the TSC lifting system.
- Install the adapter plate on the concrete cask.
- Lift and place the transfer cask on the transfer adapter.
- Attach the TSC lifting system to the crane hook and raise the TSC off of the shield doors.
- Open the shield doors.
- Lower the TSC into the concrete cask (see Figure 1.3-1).
- Remove the transfer cask, transfer adapter, and TSC lifting systems.
- Install the lid on the concrete cask.
- Move the loaded concrete cask to the storage pad.
- Move the concrete cask to its designated location on the storage pad.

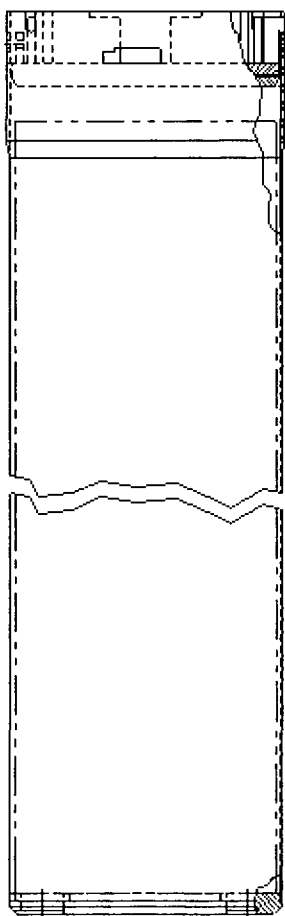
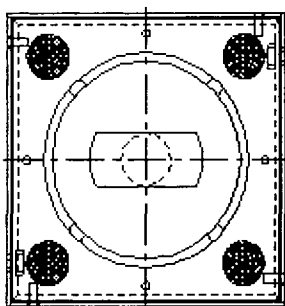
The TSC unloading and spent fuel removal from the TSC are essentially the reverse of these steps, except that weld removal and cooldown of the contents is required. This typical sequence of operations, and individual steps, may be modified by the approved site procedure to accommodate specific site requirements, as long as the requirements of the Technical Specifications and the Certificate of Compliance (CoC) are met.

Figure 1.3-3 Concrete Cask



Note: Inner rebar optional.

Figure 1.3-4 MAGNASTOR Damaged Fuel Can



#### 1.4 MAGNASTOR Contents

The MAGNASTOR system is designed to safely store up to 37 undamaged PWR fuel assemblies in the 37 PWR basket assembly or up to 87 undamaged BWR fuel assemblies in the 87 BWR basket assembly. The system is also designed to store up to four damaged fuel cans (DFCs) in the DF Basket Assembly. The DF Basket Assembly has a capacity of up to 37 undamaged PWR fuel assemblies, including four DFC locations. DFCs may be placed in up to four of the DFC locations. Each DFC may contain an undamaged PWR fuel assembly, a damaged PWR fuel assembly, or PWR fuel debris equivalent to one PWR fuel assembly. Undamaged PWR fuel assemblies may be placed directly in the DFC locations of a DF Basket Assembly.

PWR fuel assemblies may be stored with nonfuel hardware. Nonfuel hardware stored in a damaged or undamaged fuel assembly placed into a DFC is limited to steel rod inserts for guide tube dashpots and instrument tube tie components. BWR fuel assemblies may be stored with or without channels. Assemblies may contain solid filler rods or burnable absorber rods replacing fuel rods in the assembly lattice. Irradiated (i.e., activated during in-core operation) steel filler rods are limited to five rods per assembly and there may be no more than one assembly with irradiated rods per TSC. The design content conditions are specified in the CoC for MAGNASTOR. Unenriched PWR fuel assemblies are not evaluated and are not included as allowable contents. Unenriched BWR fuel assemblies are allowed with a maximum assembly average burnup of 5,000 MWd/MTU. Assemblies may contain axial end blankets. Axial end blankets may be low enriched, be unenriched, and/or contain annular fuel pellets.



## **1.8      License Drawings**

This section presents the list of License Drawings for MAGNASTOR.

<b>Drawing Number</b>	<b>Title</b>	<b>Revision No.</b>
71160-551	Fuel Tube Assembly, MAGNASTOR – 37 PWR	10NP*
71160-556	Assembly, MAGNASTOR Transfer Cask (MTC), Stainless Steel	4
71160-560	Assembly, Standard Transfer Cask, MAGNASTOR	2
71160-561	Structure, Weldment, Concrete Cask, MAGNASTOR	8
71160-562	Reinforcing Bar and Concrete Placement, Concrete Cask, MAGNASTOR	8
71160-571	Details, Neutron Absorber, Retainer, MAGNASTOR – 37 PWR	8
71160-572	Details, Neutron Absorber, Retainer, MAGNASTOR – 87 BWR	8NP*
71160-574	Basket Support Weldments, MAGNASTOR – 37 PWR	6
71160-575	Basket Assembly, MAGNASTOR – 37 PWR	11NP*
71160-581	Shell Weldment, TSC, MAGNASTOR	5
71160-584	Details, TSC, MAGNASTOR	8
71160-585	TSC Assembly, MAGNASTOR	11
71160-590	Loaded Concrete Cask, MAGNASTOR	7
71160-591	Fuel Tube Assembly, MAGNASTOR – 87 BWR	8NP*
71160-598	Basket Support Weldments, MAGNASTOR – 87 BWR	7NP*
71160-599	Basket Assembly, MAGNASTOR – 87 BWR	8NP*
71160-600	Basket Assembly, MAGNASTOR – 82 BWR	5NP*
71160-601	Damaged Fuel Can (DFC), Assembly, MAGNASTOR	0
71160-602	Damaged Fuel Can (DFC), Details, MAGNASTOR	1
71160-671	Details, Neutron Absorber, Retainer, For DF Corner Weldment, MAGNASTOR – 37 PWR	0
71160-673	Damaged Fuel Can (DFC), Spacer, MAGNASTOR	0
71160-674	DF Corner Weldment, MAGNASTOR	3NP*
71160-675	DF Basket Assembly, 37 Assembly PWR, MAGNASTOR	3NP*
71160-681	DF, Shell Weldment, TSC, MAGNASTOR	1
71160-684	Details, DF Closure Lid, MAGNASTOR	2
71160-685	DF, TSC Assembly, MAGNASTOR	5


\* Proprietary drawing replaced by nonproprietary version.




Security-Related Information Figure  
Withheld Under 10 CFR 2.390

[illegible]


# Security-Related Information Figure Withheld Under 10 CFR 2.390

 <b>NAC INTERNATIONAL</b>	
ASSEMBLY, MAGNASTOR TRANSFER CASK (MTC), STAINLESS STEEL	
PROJECT 71160	ISSUED 556
REV 4	
BY 2 OF 6	
DATE 10/10/00	


Security-Related Information Figure  
Withheld Under 10 CFR 2.390

 <b>NAC INTERNATIONAL</b>	
ASSEMBLY, MAGNASTOR TRANSFER CASK (MTC), STAINLESS STEEL	
PROJECT 71160	REV. 556
	3 6 4


Security-Related Information Figure  
Withheld Under 10 CFR 2.390

 <b>NAC INTERNATIONAL</b>	
ASSEMBLY, MAGNASTOR TRANSFER CASK (MTC), STAINLESS STEEL	
PROJECT 71160	ISSUE 556
REV 4 OF 5	

Security-Related Information Figure  
Withheld Under 10 CFR 2.390

 <b>NAC INTERNATIONAL</b>			
ASSEMBLY, MAGNASTOR TRANSFER CASK (MTC), STAINLESS STEEL			
PROJECT 71160		ISSUE 556	
		REV 5 6 4	


Security-Related Information Figure  
Withheld Under 10 CFR 2.390

 <b>NAC INTERNATIONAL</b>	
ASSEMBLY, MAGNASTOR TRANSFER CASK (MTC), STAINLESS STEEL	
PROJECT 71160	DRAWING 556
	6 6 4

A vertical scale with tick marks and labels A, B, C, D, E, and F from bottom to top.


8	7	6	5	4	3	2	1
					LICENSE 2246 Bar 9/15		

Security-Related Information Figure  
Withheld Under 10 CFR 2.390


 <b>NAC INTERNATIONAL</b>	
ASSEMBLY, STANDARD TRANSFER CASK, MAGNASTOR	
PROJECT 71160	DRAWING 560
	REV 2



# Security-Related Information Figure Withheld Under 10 CFR 2.390

 <b>NAC INTERNATIONAL</b>	
ASSEMBLY, STANDARD TRANSFER CASK, MAGNASTOR	
PROJECT 71160	ISSUANCE 560
REV 3 OF 4	

Security-Related Information Figure  
Withheld Under 10 CFR 2.390

 <b>NAC INTERNATIONAL</b>	
ASSEMBLY, STANDARD TRANSFER CASK, MAGNASTOR	
PROJECT 71160	GROUP 560
Rev 4	Rev 4


R-228764

# Security-Related Information Figure Withheld Under 10 CFR 2.390

UNLESS OTHERWISE STATED DIMENSIONS ARE IN INCHES OR FEET AND INCHES ALL DIMENSIONS ARE TO BE TOLERANCES AS A MINIMUM OF FIVE (5) THOUSANDS			NAC INTERNATIONAL	
GROUP	NAME	DATE	SHELL WELDMENT, TSC, MAGNASTOR	
GROUP 1	Bob D	6-7-11		
GROUP 2	Bob D	6-12-15		
GROUP 3	Bob D	6-10-15		
GROUP 4	Bob D	6-11-11		
GROUP 5	Bob D	6-11-11		
GROUP 6	Bob D	6-11-11		
GROUP 7	Bob D	6-11-11		
GROUP 8	Bob D	6-11-11		
GROUP 9	Bob D	6-11-11		
GROUP 10	Bob D	6-11-11		
GROUP 11	Bob D	6-11-11		
GROUP 12	Bob D	6-11-11		
GROUP 13	Bob D	6-11-11		
GROUP 14	Bob D	6-11-11		
GROUP 15	Bob D	6-11-11		
GROUP 16	Bob D	6-11-11		
GROUP 17	Bob D	6-11-11		
GROUP 18	Bob D	6-11-11		
GROUP 19	Bob D	6-11-11		
GROUP 20	Bob D	6-11-11		
GROUP 21	Bob D	6-11-11		
GROUP 22	Bob D	6-11-11		
GROUP 23	Bob D	6-11-11		
GROUP 24	Bob D	6-11-11		
GROUP 25	Bob D	6-11-11		
GROUP 26	Bob D	6-11-11		
GROUP 27	Bob D	6-11-11		
GROUP 28	Bob D	6-11-11		
GROUP 29	Bob D	6-11-11		
GROUP 30	Bob D	6-11-11		
GROUP 31	Bob D	6-11-11		
GROUP 32	Bob D	6-11-11		
GROUP 33	Bob D	6-11-11		
GROUP 34	Bob D	6-11-11		
GROUP 35	Bob D	6-11-11		
GROUP 36	Bob D	6-11-11		
GROUP 37	Bob D	6-11-11		
GROUP 38	Bob D	6-11-11		
GROUP 39	Bob D	6-11-11		
GROUP 40	Bob D	6-11-11		
GROUP 41	Bob D	6-11-11		
GROUP 42	Bob D	6-11-11		
GROUP 43	Bob D	6-11-11		
GROUP 44	Bob D	6-11-11		
GROUP 45	Bob D	6-11-11		
GROUP 46	Bob D	6-11-11		
GROUP 47	Bob D	6-11-11		
GROUP 48	Bob D	6-11-11		
GROUP 49	Bob D	6-11-11		
GROUP 50	Bob D	6-11-11		
GROUP 51	Bob D	6-11-11		
GROUP 52	Bob D	6-11-11		
GROUP 53	Bob D	6-11-11		
GROUP 54	Bob D	6-11-11		
GROUP 55	Bob D	6-11-11		
GROUP 56	Bob D	6-11-11		
GROUP 57	Bob D	6-11-11		
GROUP 58	Bob D	6-11-11		
GROUP 59	Bob D	6-11-11		
GROUP 60	Bob D	6-11-11		
GROUP 61	Bob D	6-11-11		
GROUP 62	Bob D	6-11-11		
GROUP 63	Bob D	6-11-11		
GROUP 64	Bob D	6-11-11		
GROUP 65	Bob D	6-11-11		
GROUP 66	Bob D	6-11-11		
GROUP 67	Bob D	6-11-11		
GROUP 68	Bob D	6-11-11		
GROUP 69	Bob D	6-11-11		
GROUP 70	Bob D	6-11-11		
GROUP 71	Bob D	6-11-11		
GROUP 72	Bob D	6-11-11		
GROUP 73	Bob D	6-11-11		
GROUP 74	Bob D	6-11-11		
GROUP 75	Bob D	6-11-11		
GROUP 76	Bob D	6-11-11		
GROUP 77	Bob D	6-11-11		
GROUP 78	Bob D	6-11-11		
GROUP 79	Bob D	6-11-11		
GROUP 80	Bob D	6-11-11		
GROUP 81	Bob D	6-11-11		
GROUP 82	Bob D	6-11-11		
GROUP 83	Bob D	6-11-11		
GROUP 84	Bob D	6-11-11		
GROUP 85	Bob D	6-11-11		
GROUP 86	Bob D	6-11-11		
GROUP 87	Bob D	6-11-11		
GROUP 88	Bob D	6-11-11		
GROUP 89	Bob D	6-11-11		
GROUP 90	Bob D	6-11-11		
GROUP 91	Bob D	6-11-11		
GROUP 92	Bob D	6-11-11		
GROUP 93	Bob D	6-11-11		
GROUP 94	Bob D	6-11-11		
GROUP 95	Bob D	6-11-11		
GROUP 96	Bob D	6-11-11		
GROUP 97	Bob D	6-11-11		
GROUP 98	Bob D	6-11-11		
GROUP 99	Bob D	6-11-11		
GROUP 100	Bob D	6-11-11		

PROJECT	71160	DRAWING	581	SHEET	3
DRAWING TITLE		LICENSE		1 of 2	


Security-Related Information Figure  
Withheld Under 10 CFR 2.390

 <b>NAC INTERNATIONAL</b>	
SHELL WELDMENT, TSC, MAGNASTOR	
PROJECT 71160	REVISION 581
REV 3	REV 3

# Security-Related Information Figure Withheld Under 10 CFR 2.390

<small>UNLESS OTHERWISE STATED          BACKGROUND AND BACKGROUND CHECKS          OF ALL PERSONS SHALL BE          CONDUCTED BY THE BUREAU          ALL BUREAU REPORTS SHALL BE          REPRODUCED AS A COPY          OF THE BUREAU REPORT</small>			GROUP	NAME	DATE	<b>NAC INTERNATIONAL</b> TSC ASSEMBLY, MAGNASTOR	
				<i>[Signature]</i>	10/28/19		
				<i>[Signature]</i>	10/29/19		
				<i>[Signature]</i>	10/29/19		
				<i>[Signature]</i>	10/29/19		
<small>ALL DISPOSITIONS ARE IN ACCORD          EMPLOYER'S PURPOSES TO BE USED FOR          IDENTIFICATION PURPOSES ONLY          NOT AGENCY 71160-590/500</small>				<i>[Signature]</i>	10/29/19	PROJECT	71160
<small>ISSUING OFFICE</small>			LICENSE	<i>[Signature]</i>	10/30/19	CHARGE	585
						1	3


Security-Related Information Figure  
Withheld Under 10 CFR 2.390

 <b>NAC INTERNATIONAL</b>	
TSC ASSEMBLY, MAGNASTOR	
PROJECT 71160	REV 585
2 2	3 11

# Security-Related Information Figure Withheld Under 10 CFR 2.390


<b>NAC</b> <b>INTERNATIONAL</b>	
TSC ASSEMBLY, MAGNASTOR	
PROJECT 71160	REVISION 585
Rev 3 of 3	

# Security-Related Information Figure Withheld Under 10 CFR 2.390

UNLESS OTHERWISE STATED 1. ENDORSEMENT AND ENDORSEMENT 2. ENDORSEMENT AND ENDORSEMENT		GROUP		NAME	DATE	 <b>NAC INTERNATIONAL</b>	<b>DAMAGED FUEL CAN (DFC). DETAILS. MAGNASTOR</b>
ALL TRUCKS (TRUCKS) ARE IN THE OF POWER (POWER)		GROUP		NAME	DATE		
		GROUP		NAME	DATE		
		GROUP		NAME	DATE		
		GROUP		NAME	DATE		
ALL ENDORSEMENT ARE IN POWER		GROUP		NAME	DATE	<b>PROJECT 71160</b>	<b>6021</b>
MAGNASTOR (MAGNASTOR) ARE IN THE OF POWER (POWER)		GROUP		NAME	DATE		
		GROUP		NAME	DATE		
		GROUP		NAME	DATE		
		GROUP		NAME	DATE		
MAGNASTOR (MAGNASTOR) ARE IN THE OF POWER (POWER)		GROUP		NAME	DATE	<b>PROJECT 71160</b>	<b>6021</b>
		GROUP		NAME	DATE		
		GROUP		NAME	DATE		
		GROUP		NAME	DATE		
		GROUP		NAME	DATE		



Security-Related Information Figure  
Withheld Under 10 CFR 2.390


 NAC INTERNATIONAL	
DAMAGED FUEL CAN (DFC), DETAILS, MAGNASTOR	
PROJECT 71160	602
Rev 2 of 2	

R-228766

# Security-Related Information Figure Withheld Under 10 CFR 2.390

UNLESS OTHERWISE STATED EXCLUDED FROM CLASSIFICATION GUIDE BY THE NAME 71160-685			NAC INTERNATIONAL	
GROUP	NAME	DATE		
1	DF, SHELL WELDMENT, TSC, MAGNASTOR	5-17-13		
2	6-22-15	6-22-15		
3	6-10-15	6-10-15		
4	6-10-15	6-10-15		
5	6-10-15	6-10-15		
6	6-10-15	6-10-15		
7	6-10-15	6-10-15		
8	6-10-15	6-10-15		
ALL INFORMATION ARE IN NOTES EXCLUDED SUBJECTS TO REVIEW OF RETOR				
NOT REVENUE 71160-685				
ISSUING FPM LICENSE				
Royce Ben				
5/12/15				
PROJECT 71160				
681				
No. 1 of 2				


Security-Related Information Figure  
Withheld Under 10 CFR 2.390

 <b>NAC INTERNATIONAL</b>		
DF, SHELL WELDMENT, TSC, MAGNASTOR		
PROJECT	71160	REV 1
DATE		681
BY		2
APP'D		2


# Security-Related Information Figure Withheld Under 10 CFR 2.390

UNLESS OTHERWISE STATED SIGNATURES AND TELEPHONE NUMBERS OF ALL PERSONS PARTICIPATING			NAC INTERNATIONAL	
ALL PERSONS PARTICIPATING ARE TO BE CONSIDERED AS A UNIT, WITHIN OF PROPER TOLERANCE			DF, TSC ASSEMBLY, MAGNASTOR	
GROUP	NAME	DATE		
GROUP	NAME	DATE		
GROUP	NAME	DATE		
GROUP	NAME	DATE		
GROUP	NAME	DATE		
ALL SIGNATURES ARE TO BE CONSIDERED AS A UNIT, WITHIN OF PROPER TOLERANCE				
PROJECT ASSEMBLY 71160-590/301				
SIGNATURE TYPE: LICENSE				
NAME: Roy W. Carr			PROJECT: 71160	
			DRAWING: 685	
			SHEET: 1 OF 3	

# Security-Related Information Figure Withheld Under 10 CFR 2.390

 <b>NAC INTERNATIONAL</b>		
DF, TSC ASSEMBLY, MAGNASTOR		
PROJECT	71160	REV
		685 3
		2 3

Security-Related Information Figure  
Withheld Under 10 CFR 2.390

 <b>NAC INTERNATIONAL</b>	
DF, TSC ASSEMBLY, MAGNASTOR	
PROJECT 71160	WORKSHEET 685
OF 3 OF 3	

## Chapter 4 Thermal Evaluation

### Table of Contents

4	THERMAL EVALUATION .....	4-1
4.1	Discussion .....	4.1-1
4.2	Thermal Properties of Materials .....	4.2-1
4.3	Technical Specifications for Components .....	4.3-1
4.4	Normal Storage Conditions.....	4.4-1
4.4.1	Thermal Analysis Models .....	4.4-1
4.4.2	Test Model .....	4.4-31
4.4.3	Maximum Temperatures for PWR and BWR Fuel Configurations.....	4.4-31
4.4.4	Maximum Internal Pressures for PWR and BWR TSCs .....	4.4-37
4.5	Off-Normal Events.....	4.5-1
4.5.1	Off-Normal Storage Events .....	4.5-1
4.5.2	Off-Normal Transfer Phase Events for PWR Fuel .....	4.5-4
4.6	Accident Events .....	4.6-1
4.6.1	Analysis of Maximum Anticipated Ambient Heat Load .....	4.6-1
4.6.2	Fire Accident.....	4.6-2
4.6.3	Full Blockage of Concrete Cask Air Inlets .....	4.6-3
4.6.4	Maximum TSC Internal Pressure for Accident Events.....	4.6-4
4.7	References.....	4.7-1
4.8	Thermal Evaluation Detail.....	4.8-1
4.8.1	Benchmark of the Two-Dimensional Axisymmetric Methodology for TSC Thermal Analyses for MAGNASTOR .....	4.8.1-1
4.8.2	Methodology to Compute the Porous Media Constants .....	4.8.2-1
4.8.3	Benchmark Evaluation of the Two-Dimensional Axisymmetric Methodology for Annular Cooling in the Concrete Cask for MAGNASTOR .....	4.8.3-1
4.9	Thermal Contingency Events During PWR TSC Preparation and Transfer Operations.....	4.9-1
4.9.1	Water Phase Contingency Events for PWR Fuel.....	4.9.1-1
4.9.2	Draining and Vacuum Drying Phase Contingency Events for PWR Fuel....	4.9.2-1
4.9.3	TSC Transfer Phase Contingencies for PWR Fuel.....	4.9.3-1
4.9.4	Post TSC Transfer Phase Contingency Events for PWR Fuel.....	4.9.4-1

## List of Figures

Figure 4.1-1	Definition of the Preferential Loading Pattern for the PWR Basket Assembly .....	4.1-5
Figure 4.1-2	Preferential Loading Pattern for the PWR Basket with Minimum Reduced Cool Time Fuel .....	4.1-6
Figure 4.4-1	Two-Dimensional Model of Concrete Cask Loaded with PWR TSC .....	4.4-41
Figure 4.4-2	Computational Mesh for the Two-Dimensional Axisymmetric CFD Model of the Concrete Cask .....	4.4-42
Figure 4.4-3	Axial Power Distribution for the PWR Fuel Assembly .....	4.4-43
Figure 4.4-4	Axial Power Distribution for the BWR Fuel Assembly .....	4.4-44
Figure 4.4-5	PWR Peak Fuel Cladding Temperature versus TSC Internal Pressure .....	4.4-45
Figure 4.4-6	Two-Dimensional Finite Element Model of the PWR Fuel Basket .....	4.4-46
Figure 4.4-7	Two-Dimensional Finite Element Model of the BWR Fuel Basket .....	4.4-47
Figure 4.4-8	14×14 PWR Fuel Assembly Two-Dimensional Model .....	4.4-48
Figure 4.4-9	10×10 BWR Fuel Assembly Two-Dimensional Model .....	4.4-49
Figure 4.4-10	Neutron Absorber Model for PWR Fuel Tube .....	4.4-50
Figure 4.4-11	BWR Fuel Tube Configuration with Channel and Neutron Absorber .....	4.4-51
Figure 4.4-12	BWR Fuel Tube Configuration with Channel, but without the Neutron Absorber.....	4.4-52
Figure 4.4-13	Two-Dimensional Model of Transfer Cask Loaded with a PWR TSC .....	4.4-53
Figure 4.4-14	Temperature (°F) Distribution for the CC1/CC2 Concrete Cask and TSC Containing a Design Basis PWR Heat Load.....	4.4-54
Figure 4.4-15	Air Velocity (m/s) in the CC1/CC2 Concrete Cask Annulus for the Design Basis PWR Heat Load .....	4.4-55
Figure 4.4-16	Three-Dimensional ANSYS Model of the PWR Canister for Vacuum Drying Condition .....	4.4-56
Figure 4.4-17	Detailed View of the Three-Dimensional ANSYS Model of the PWR Canister for Vacuum Drying Condition.....	4.4-57
Figure 4.4-18	Three-Dimensional ANSYS Model of the BWR Canister for MTC Vacuum Drying Analyses .....	4.4-58
Figure 4.4-19	Detailed View of the Three-Dimensional ANSYS Model of the BWR Canister for MTC Vacuum Drying Analyses .....	4.4-59
Figure 4.4-20	CC3 Concrete Cask Inlet Model Geometry .....	4.4-60
Figure 4.4-21	CC3 Concrete Cask Inlet Model Mesh (Bottom Surface) .....	4.4-61
Figure 4.4-22	Two-Dimensional Finite Element Model of the DF Basket Assembly .....	4.4-62
Figure 4.8-1	Two-Dimensional Model of the 24 PWR Assembly Thermal Test Configuration .....	4.8.1-7
Figure 4.8-2	ANSYS Model for Determination of the Benchmark Basket Thermal Properties .....	4.8.1-8
Figure 4.8-3	Temperature Profile from the Benchmark Cask Cavity Inner Surface.....	4.8.1-9
Figure 4.8-4	Axial Power Distribution Curve for the 15×15 PWR Fuel Assembly.....	4.8.1-9
Figure 4.8-5	Temperature Contours for the Benchmark Cask Thermal Test .....	4.8.1-10



**List of Figures (cont'd)**

Figure 4.8-6	Cross-Sectional View of the Three-Dimensional FLUENT Model of a 17×17 PWR Fuel Assembly .....	4.8.2-5
Figure 4.8-7	Three-Dimensional FLUENT Model of a Fuel Assembly Grid .....	4.8.2-6
Figure 4.8-8	Three-Dimensional FLUENT Quarter-Symmetry Model for the Flow Around the Grid .....	4.8.2-7
Figure 4.8-9	Cross-Sectional View of the Three-Dimensional FLUENT Model of a 10×10 BWR Fuel Assembly .....	4.8.2-8
Figure 4.8-10	Two-Dimensional Axisymmetric FLUENT Model of the VSC-17 .....	4.8.3-6
Figure 4.8-11	ANSYS Model for Effective Properties Calculation .....	4.8.3-7
Figure 4.8-12	Temperature Profiles for the Canister Surface .....	4.8.3-8
Figure 4.8-13	Temperature Profiles for the Concrete Liner Surface.....	4.8.3-9

### List of Tables

Table 4.1-1	Summary of Thermal Design Conditions for Storage for MAGNASTOR .....	4.1-7
Table 4.1-2	Maximum Allowable Material Temperatures.....	4.1-8
Table 4.4-1	Effective Thermal Conductivities for 14×14 PWR Fuel Assemblies for Helium Backfill.....	4.4-63
Table 4.4-2	Effective Thermal Conductivities for 10×10 BWR Fuel Assemblies for Helium Backfill.....	4.4-63
Table 4.4-3	Maximum Component Temperatures for Normal Condition Storage of Design Basis PWR and BWR Heat Loads.....	4.4-64
Table 4.4-4	Helium Mass Per Unit Volume for MAGNASTOR TSCs.....	4.4-64
Table 4.4-5	Maximum Fuel Temperature for Water Phase – PWR.....	4.4-65
Table 4.4-6	Maximum Fuel Temperature for Water Phase – BWR .....	4.4-65
Table 4.4-7	Maximum Fuel Temperature for Helium Phase – PWR.....	4.4-66
Table 4.4-8	Maximum Fuel Temperature for Helium Phase – BWR .....	4.4-66
Table 4.4-9	Durations and the Temperature at the End of the Duration for the First Vacuum Stage (PWR).....	4.4-67
Table 4.4-10	Durations and the Temperature at the End of the Duration for the First Vacuum Stage (BWR) .....	4.4-67
Table 4.4-11	Durations and the Temperature at the End of the Duration for the Second Vacuum Stage (PWR).....	4.4-68
Table 4.4-12	Durations and the Temperature at the End of the Duration for the Second Vacuum Stage (BWR) .....	4.4-68
Table 4.4-13	MTC to Concrete Cask (PWR) Transfer Times and Temperatures.....	4.4-69
Table 4.4-14	MTC to Concrete Cask (BWR) Transfer Times and Temperatures .....	4.4-69
Table 4.4-15	TFR to Concrete Cask (PWR) Transfer Times and Temperatures for 20 kW (no cooling) and 25 kW (7 hours of cooling).....	4.4-69
Table 4.4-16	Durations Allowed and the Maximum PWR Fuel Clad Temperatures for the Operation Using Reduced Vacuum Times, Reduced Cooling Time and Eight Hours of Handling.....	4.4-70
Table 4.4-17	Durations Allowed and the Maximum BWR Fuel Clad Temperatures for the Operation Using Reduced Vacuum Times, Reduced Cooling Time and Eight Hours of Handling.....	4.4-71

#### 4.1 Discussion

MAGNASTOR consists of a TSC, concrete cask, and a transfer cask. In long-term storage, the fuel, including fuel contained in damaged fuel cans and PWR minimum reduced cool time fuel, is loaded in a basket structure positioned within the TSC. The TSC is placed in the concrete cask, which provides passive radiation shielding, structural protection and natural convection cooling. The transfer cask is used to handle the TSC. The thermal performance of the concrete cask containing a loaded TSC with design basis fuel, and the performance of the transfer cask containing a loaded TSC with design basis fuel are evaluated in this chapter.

The thermal evaluation considers normal conditions and off-normal and accident events of storage. Each of these conditions can be described in terms of the environmental temperature, use of solar insolation, and the condition of the air inlets as shown in Table 4.1-1. The evaluation of the different phases of the transfer operation is accomplished by altering the properties of the medium in the canister to correspond to water or helium.

In order for the heat from the stored spent fuel assemblies, including fuel contained in damaged fuel cans and PWR minimum reduced cool time fuel, to be rejected to the ambient environment via the concrete cask or the transfer cask, the decay heat from the contents is transferred to the TSC surface. The MAGNASTOR baskets for the PWR and the BWR fuel assemblies use all three heat transfer modes—radiation, conduction and convection—to transfer the heat to the TSC surface. The basket design enhances convection heat transfer. Helium is used as the backfill gas in the TSC because its thermal conductivity is better than other allowable backfill gases. The basket is comprised of full-length carbon steel tubes that provide a significant path for conduction heat transfer. Radiation is a significant mode of heat transfer in the fuel region and between the outer surface of the basket and the TSC shell.

The significant thermal design feature of the concrete cask is the passive convective airflow around the outside of the TSC. Cool (ambient) air enters at the bottom of the concrete cask through four air inlets. Heated air exits through the four air outlets in the upper concrete cask body. Radiant heat transfer occurs from the TSC shell to the concrete cask liner, which then transmits heat to the annular airflow. Conduction through the concrete cask, although not significant, is included in the analytical model. Natural circulation of air through the concrete cask annulus, in conjunction with radiation from the TSC surface, maintains the fuel cladding temperature and all component temperatures below their design limits.

The MAGNASTOR design basis heat load is 35.5 kW for PWR fuel. The fuel loading may be in the 37 PWR Basket Assembly, i.e., up to 37 undamaged PWR fuel assemblies, or up to 37 PWR

minimum reduced cool time fuel, or in the DF Basket Assembly, which has a capacity of up to 37 undamaged fuel assemblies including four DFC locations. Damaged fuel cans may be located in the DFC locations at the four outer corners of the DF basket assembly (Figure 2.2-3 and License Drawing 71160-675). Both the PWR fuel basket and the DF basket assembly can accommodate a uniform heat load of 959 W per assembly, or a preferential loading pattern as shown in Figure 4.1-1. The preferential loading pattern identified in Figure 4.1-1 defines three values of heat generation that place the fuel assemblies with the maximum heat generation rate in an intermediate region of fuel storage locations. The PWR fuel basket can also accommodate a various heat load per assembly for the PWR minimum reduced cool time fuel with a preferential loading pattern, as shown in Figure 4.1-2. Analyses are performed using the two-dimensional axisymmetric model with the same fluid resistances and material properties for both the preferential and uniform loading patterns of the standard PWR fuels, as well as for the preferential load pattern for the PWR minimum reduced cool time fuel. The calculated maximum fuel temperature is essentially the same for both loading configurations for standard PWR fuels. The maximum temperatures at the radial location of the center of a preferential loaded fuel assembly with the 1.2 kW heat load is determined to be 689°F. At this same radial location, the calculated temperature for the uniform heat load is 684°F. This small increase is a localized bounding temperature response due to the localized increased heat generation for the preferential loading configuration. As shown in Sections 4.4.1.6 and 4.4.3 and as concluded in Sections 4.5 and 4.6, the maximum fuel temperature for the DF basket assembly configuration is bounded by that for the standard PWR basket configuration. The analysis for the PWR minimum reduced cool time fuel with the preferential loading pattern (Figure 4.1-2) is also performed using the modified two-dimensional axisymmetric model. As shown in Sections 4.4.1 and 4.4.3 and as concluded in Sections 4.5 and 4.6, the maximum fuel temperature for the PWR minimum reduced cool time fuel configuration is bounded by that for the standard PWR basket configuration.

The identical maximum fuel cladding temperature calculated for both the PWR fuel basket and the DF basket assembly loading configurations, resulting from identical total heat and small differences in inner region heat (4%), demonstrates efficiencies in the alternate PWR preferential loading configuration. Placement of the highest heat load for the preferential loading configuration in an intermediate radial location balances system performance. The thermal loading basis for the PWR analyses in this chapter uses the preferential loading since it represents the system loading with maximum heat concentration. The maximum fuel temperature reduction for the PWR minimum reduced cool time fuel also states that placement of the highest heat load in an intermediate radial location, plus the low heat in the basket center nine

(9) slots, enhances system performance. The BWR fuel basket can accommodate 87 fuel assemblies with a uniform design basis total heat load of 33 kW, or 379 watts, per assembly.

The thermal evaluation applied different component temperature limits and allowable stress limits for long-term conditions versus short-term conditions. Normal storage operation is considered to be a long-term condition. Off-normal and accident events are considered to be short-term conditions. Thermal evaluations are performed for the design basis PWR and BWR fuels for all design conditions. The maximum allowable material temperatures for long-term and short-term conditions are provided in Table 4.1-2.

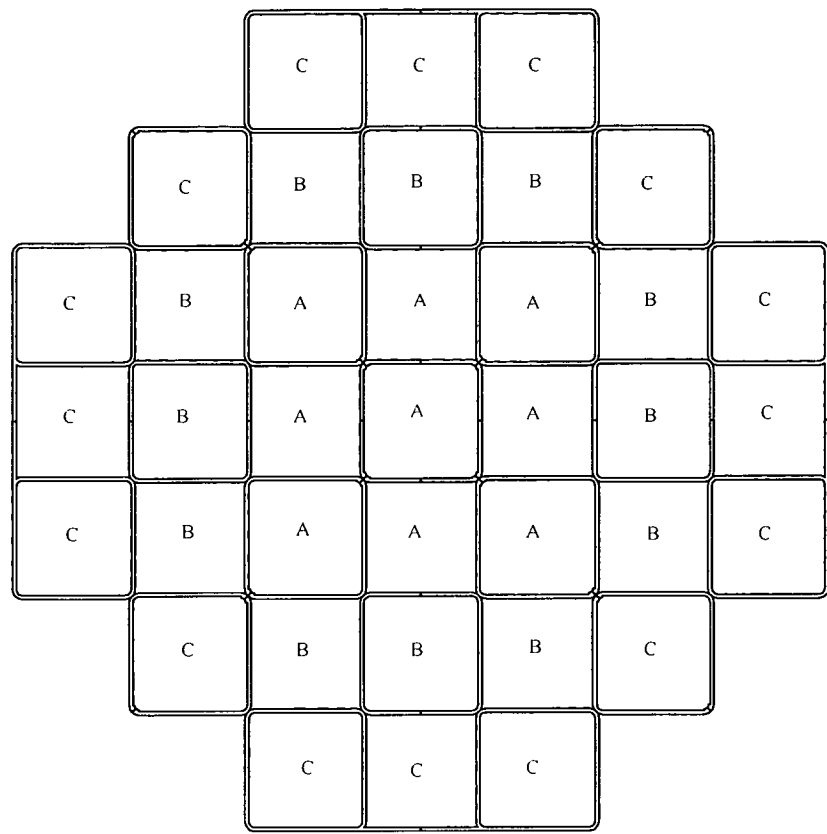
During normal conditions of storage and off-normal and accident events, the concrete cask must reject the decay heat from the TSC to the environment without exceeding the system components temperature limits. In addition, to ensure fuel rod integrity for normal conditions of storage, the spent fuel must be maintained at a sufficiently low temperature in an inert atmosphere to preclude thermally induced fuel rod cladding deterioration. To preclude fuel degradation, the maximum cladding temperature under normal conditions of storage and canister transfer operations is limited to 752°F (400°C) per ISG-11 [2]. The maximum cladding temperature for off-normal and accident events is limited to 1,058°F (570°C). For the structural components of the storage system, the thermally induced stresses, in combination with pressure and mechanical load stresses, are limited to the material allowable stress levels.

Thermal evaluations for normal conditions of storage and canister transfer operations are presented in Section 4.4. The finite element method is used to compute the effective properties for the basket, neutron absorber and fuel region. The thermal solutions for the concrete cask and transfer cask are obtained using finite element and finite volume methodologies. Thermal models used in the evaluation of normal and transfer conditions are described in Section 4.4.1.

A summary of the thermal evaluation results for normal conditions of storage is provided in Table 4.4-3 for the PWR and the BWR cases. Table 4.4-5 through Table 4.4-15 contain the maximum fuel cladding temperatures for the different phases of the transfer operations for the PWR and BWR cases. Thermal evaluation results for off-normal and accident events are presented in Sections 4.5 and 4.6, respectively. Comparison of the evaluation results shows that the standard PWR basket evaluation bounds that of the DF basket assembly and also bounds that of the PWR minimum reduced cool time fuel basket assembly. The results demonstrate that the calculated temperatures are less than the allowable fuel cladding and component temperatures for all normal (long-term) storage conditions and for short-term events. As shown in Chapter 3, the thermally induced stresses, combined with pressure and mechanical load stresses, are also within allowable limits.

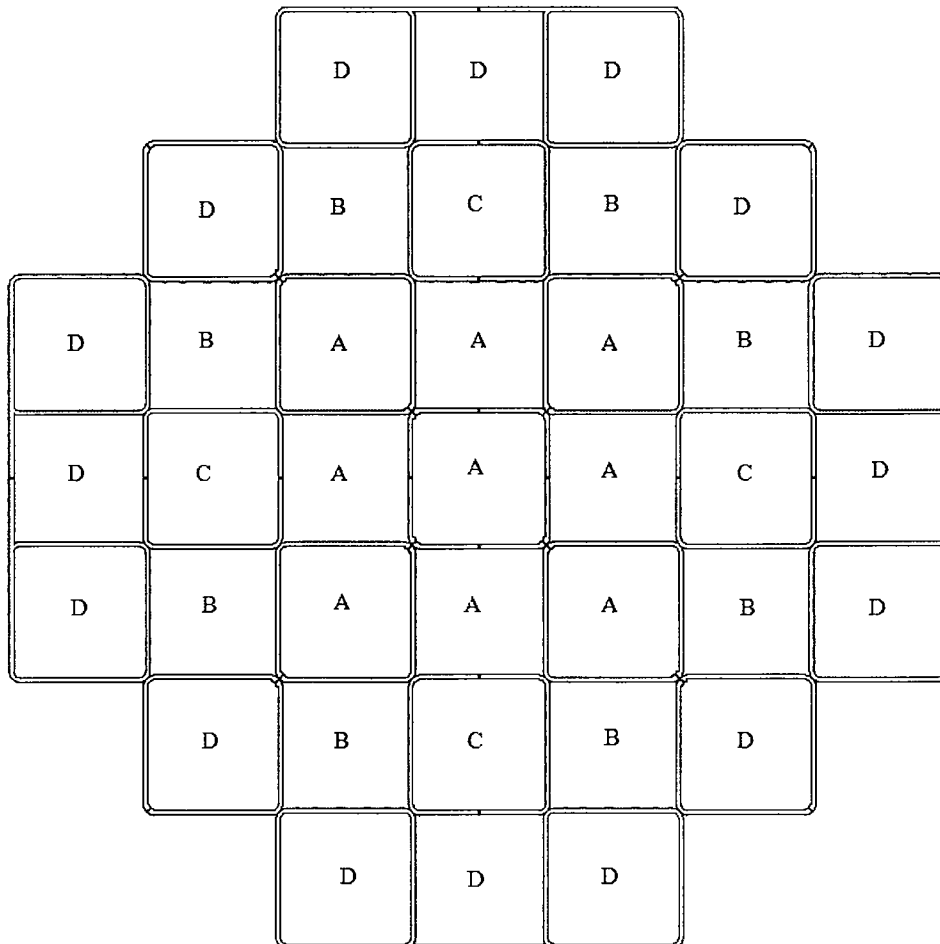
As discussed in Section 4.4.1, for TSC that is less than fully loaded, empty fuel storage locations shall begin at the center of the basket and continue outward, as required in an approximately symmetric pattern.

Figure 4.1-1      Definition of the Preferential Loading Pattern for the PWR Basket Assembly



Zone Identification	A	B	C
Maximum Heat Load per Assembly (kW)	0.922	1.20	0.80
Total Number of Fuel Assemblies	9	12	16

Figure 4.1-2 Preferential Loading Pattern for the PWR Basket with Minimum Reduced Cool Time Fuel



Zone Description	Designator	Heat Load [Watts]	No. of Assemblies
Inner Ring	A	513	9
Middle Ring	B	1300	8
Middle Ring	C	1800	4
Outer Ring	D	830	16



**Table 4.1-1 Summary of Thermal Design Conditions for Storage for MAGNASTOR**

Condition		Environmental Temperature (°F)	Solar Insolation <sup>a</sup>	Condition of Concrete Cask Inlets
Normal		76 <sup>b</sup>	Yes	All inlets open
Off-Normal - Half Air Inlets Blocked		76	Yes	Half inlets blocked
Off-Normal - Severe Heat		106	Yes	All inlets open
Off-Normal - Severe Cold		-40	No	All inlets open
Accident - Extreme Heat		133	Yes	All inlets open
Accident - All Air Inlets Blocked		76	Yes	All inlets blocked
Accident - Fire	During Fire	1475	Yes	All inlets open
	Before and After Fire	76	Yes	All inlets open

<sup>a</sup> Solar Insolation per 10 CFR 71 [3]:

Curved Surface: 400 g cal/cm<sup>2</sup> (1475 Btu/ft<sup>2</sup>) for a 12-hour period.

Flat Horizontal Surface: 800 g cal/cm<sup>2</sup> (2950 Btu/ft<sup>2</sup>) for a 12-hour period.

<sup>b</sup> Maximum average annual temperature in the 48 contiguous United States is 75.6°F. [25]

Table 4.1-2 Maximum Allowable Material Temperatures

Material	Temperature Limits (°F)		Reference
	Long Term	Short Term	
Concrete	200(B)/300(L) <sup>a</sup>	350	ACI-349 [4] NUREG-1567 [20]
Fuel Clad			
PWR Fuel	752	752/1,058 <sup>b</sup>	ISG-11 [2] and PNL-4835 [5]
BWR Fuel	752	752/1,058 <sup>b</sup>	
NS-4-FR	300	300	JAPC [6]
Chemical Copper Lead	600	600	Baumeister [7]
ASME SA693 17-4PH Type 630 Stainless Steel	650	800	ASME Code [8] ARMCO [9]
ASME SA240 Type 304 Stainless Steel	800	800	ASME Code [8]
ASME SA537 Class 1 Carbon Steel	800	850/1,000 <sup>c</sup>	ASME Code [8] ASME Code Case N-707 [26]
ASTM A588 Carbon Steel	700	700	ASME Code Case N-71-17 [10] ASTM Standard [19]
ASTM A350 LF2 Carbon Steel	700	700	ASTM Standard [19]
ASTM A36 Carbon Steel	700	700	ASME Code Case N-71-17 [10] ASTM Standard [19]
ASME SA695 Type B Grade 40 and SA696 Type C Carbon Steel	800	800	ASME Code [8]

<sup>a</sup> B and L refer to bulk temperature and local temperature, respectively.

<sup>b</sup> 752°F TSC transfer operations; 1,058°F off-normal and accident events.

<sup>c</sup> 850°F TSC transfer operations; 1,000°F off-normal and accident events.

$k_s$  ----- thermal conductivity associated with the  
solid portion of the porous media model

The model of loaded TSC for the PWR minimum reduced cool time fuel is identical to the first model for standard PWR fuel, except for the mesh of the basket region. The basket zone is remeshed to match the variation of the heat generation of the preferential fuel heating pattern of the minimum reduced cool time fuel configuration.

### **Heat Generation**

The heat generation for the fuel is applied to the active fuel region of the TSC model (see Figure 4.4-1) for the PWR and the BWR fuel assemblies. The maximum design basis heat loads to be considered for the PWR and the BWR fuel basket configurations are 35.5 kW and 33 kW, respectively. The maximum design basis heat load to be considered for the DF basket assembly is 35.5 kW.

For the PWR fuel basket, two patterns of heat generation are considered. First, a uniform loading of 35.5 kW or 959 W in each fuel location is considered. The axial power distribution for PWR fuel, as shown in Figure 4.4-3, is included in applying the heat generation. Second, an optional heat generation pattern, as shown in Figure 4.1-1 is also considered and has the same total heat load of 35.5 kW. The application of the heat generation for this condition incorporates an axial distribution and a radial distribution. The area over which each fuel assembly heat load is distributed in Figure 4.1-1 is determined on the basis of the cross-section of the fuel tubes containing the specific heat loads identified as A, B and C in Figure 4.1-1. The heat generation values specified in Figure 4.1-1 are considered to be the maximum permissible heat generation in each fuel location for this configuration. It is noted that maximum fuel assembly heat load in Figure 4.1-1 is 25% greater than the heat load for the uniform condition. The fuel heat load in the center of the basket in Figure 4.1-1, Zone A, at 0.922 kW is only 4% less than the uniform heat loading at 0.96 kW per assembly. The use of hotter assemblies in the Zone B ring results in slightly more flow in the Zone B region with the higher heat load, but simultaneously presents a bounding condition over the uniform loading of the entire basket since the edge of Zone A temperatures is increased by the influence from the higher heat in Zone B. An analysis using a 40 kW preferential loading with a more aggressive annular turbulence model (K-ε) and a reduced flow resistance showed that the preferential heat distribution increased the maximum fuel temperatures by 6°F. With the reduction of the maximum heat load to 35.5 kW, the 6°F difference in maximum fuel cladding temperature will decrease, but will still produce temperatures equal to or greater than the uniform heat load configuration. Third, an optional heat generation pattern, as shown in Figure 4.1-2 is also considered and has the same total heat load of 35.5 kW. The application of the heat generation for this condition incorporates an axial distribution and a radial distribution. The area over which each fuel assembly heat load is

distributed in Figure 4.1-2 is determined on the basis of the cross-section of the fuel tubes containing the specific heat loads identified as A, B, C and D in Figure 4.1-2. The heat generation values specified in Figure 4.1-2 are considered to be the maximum permissible heat generation in each fuel location for this configuration.

In one of the three analyses performed for the DF basket assembly, the uniform loading heat generation rate of undamaged fuel is applied to the standard fuel slots and a compacted heat generation rate (over the lower 103 inches of the active fuel region considering a 50% compaction of the fuel debris) is considered for the four damaged fuel can slots. In the other two analyses, the uniform loading heat generation rate of standard fuel assemblies is applied to the active fuel region of the basket.

For the BWR fuel basket, only a uniform thermal loading pattern is considered. The design basis heat load for BWR fuel is 33 kW, which corresponds to a maximum heat load of 379 watts for each of the 87 fuel assemblies. The axial power distribution for the BWR fuel is shown in Figure 4.4-4. For some BWR fuel assembly enrichments, the five fuel locations in the center of the BWR basket will not be loaded. In this configuration, the fuel assembly decay heat is limited to 379 watts. The configuration with a partially loaded fuel basket containing BWR fuel assemblies with a maximum heat load of 379 watts per assembly is considered to be bounded by the fully loaded BWR fuel basket configuration. Temperatures obtained from analyses performed using the maximum heat load in conjunction with a fully loaded BWR basket are considered to bound the results for a partially loaded basket.

#### **Pressure of the Helium Backfill**

To drive the convection internal to the TSC, it is necessary to increase the density of the helium. Since the free volume in the TSC remains constant, the density of the backfill gas can be increased by backfilling the TSC to a range of pressures and temperatures that would result in an increase in the density. In the MAGNASTOR design, the TSC is backfilled with helium to meet the density listed in Table 4.4-4. Since the gas in the model is characterized as an ideal gas, the increased density in the analysis can be indirectly obtained by specifying a pressure in the TSC region. For the PWR normal condition, the density of helium in the TSC associated with a pressure of 7 atm (g) is (0.76g/liter). It is important to assess the effect of the helium density on the performance of the system. The evaluation of the sensitivity of the peak fuel temperature to the pressure is performed using the PWR model described in this section. The condition requiring a change is the pressure that is applied to the TSC region of the model. The results of the model solutions for pressures of 1 atm (g), 3 atm (g), 5 atm (g) and 7 atm (g) are shown as a graph in Figure 4.4-5. As shown in Figure 4.4-5, the variation of the peak cladding temperature with the pressure specified inside the TSC is a nonlinear function. The peak cladding temperature decreases sharply when the pressure increases from 1 atm to 3 atm. Subsequent

increases in the pressure to 5 atm and 7 atm do not result in the same rate of decrease of the clad temperature as for the 1 atm and 3 atm cases. The model of the TSC in the concrete cask has two regions of convection separated by a TSC shell. Heat can only be transferred through the shell from the TSC internal region to the annulus region outside the TSC. The flow characteristics in the annulus region are primarily affected by the total heat generation being transferred through the TSC shell, as well as the geometry of the annulus. As the pressure (and the associated mass) of the gas in the TSC is increased, the buoyancy force inside the TSC is increased. This increases the mass flow rate of the TSC gas so that the ability to reject heat from the fuel is also increased. This would tend to reduce the maximum clad temperature. However, the flow in the annulus is not expected to be significantly affected by the velocity of the gas internal to the TSC. Therefore, regardless of the buoyancy force inside the TSC, the maximum clad temperature is limited by the shell temperature, which is controlled by the annulus flow. At some pressure level, an increase in the TSC pressure (and mass) of the gas would not significantly decrease the fuel clad temperature, which would imply a reduced derivative of the clad temperature with respect to the pressure. This is the characteristic of the curve in Figure 4.4-5, which implies that further increase in the pressure does not result in a significant reduction of the clad temperature. There is an advantage in operating in this regime of the curve in that the sensitivity of the clad temperature due to a reduction in the helium density is reduced. This evaluation demonstrates that even with a 10% loss of density, the peak clad fuel temperatures for the design basis heat load remain under 752°F (400°C). The calculated maximum temperatures from this evaluation show that there is an acceptable 10 psig tolerance for the minimum helium backfill pressure.

#### **Modeling of the Air Inlet with Shield Bars**

The inlet region of the CC3 concrete cask is designed with shield bars for enhanced shielding. The flow resistances of the inlet vent airway of the concrete cask, which includes shield bars, are calculated using a three-dimensional FLUENT CFD model (see Figures 4.4-20 and 4.4-21). Half of the inlet is modeled because of symmetry. The symmetry plane passes between the top and bottom walls of the air inlet. The computed viscous and inertial resistance coefficients are applied to the inlet region of the two-dimensional axisymmetric concrete cask and to the TSC model corresponding to the CC3 concrete cask. The inlet region is defined as a porous region without the geometric details of the inlet. For each applied pressure gradient between inlet and outlet boundaries, the average axial velocity in the model is determined. Five sets of the average static pressure drop between the flow inlet and outlet boundaries as a function of the average axial velocity in the domain are obtained and curve fitted as:

$$\Delta P = 0.1451 \times V + 1.222 \times V^2$$

where,  $\Delta P$  is the average static pressure drop and  $V$  is the average axial velocity.

The pressure drop is related to the source term in the momentum equation for a homogenous porous medium according to:

$$\Delta P = \left( \frac{\mu}{\alpha} V + \frac{1}{2} C_p V^2 \right) \Delta n$$

where  $\Delta n$  is the porous medium thickness,  $\rho$  is air density,  $\mu$  is air viscosity,  $1/\alpha$  is the viscous resistance coefficient, and  $C$  is the inertial resistance coefficient.

Comparing the previous equations and substituting the geometry of the inlet and the material properties of air at ambient temperature, the viscous resistance and inertial resistance coefficients are:

$$1/\alpha = 9051 \text{ 1/m}^2 \quad C = 2.633 \text{ 1/m.}$$

The viscous and inertial resistance coefficients are divided by the porosity and porosity squared, respectively, to get the resistance coefficient for the 100% open area used in modeling the inlet region as a porous zone in the concrete cask thermal analysis. The porosity of the model is determined to be 0.9282 for the air inlet with additional shield bars.

### **Mesh Sensitivity Evaluation**

With respect to the sensitivity of the calculated fuel cladding, concrete cask and TSC temperatures to the number of divisions of the finite volume cells, this need only be addressed for the regions containing fluid flow. For the solid regions, such as the concrete or the steel components, the sensitivity evaluation of cell refinement is not required.

There are two fluid regions in the model: the airflow annulus region outside the TSC, and the helium region inside the TSC. Each of these fluid regions uses a different fluid flow model. The TSC internal flow is modeled utilizing a laminar flow model; the airflow in the annulus region is modeled using a turbulent flow model.

In the concrete cask annulus region, the modeling accuracy of the turbulent flow depends not on the usual refined mesh near the wall, as for a laminar flow condition, but on the value of  $y^+$ , as previously discussed. The cell divisions in the annulus region have been set to permit the  $y^+$  to be less than unity, which is acceptable according to FLUENT documentation. Therefore, further refinement of the annulus region would not provide a more accurate temperature result.

For the helium flow in the TSC (laminar flow), the largest velocities are in the downcomer regions and, essentially, the entire heat load must be transferred to the TSC shell. The focus of the sensitivity evaluation is the number of cell divisions in the downcomer region. The largest velocity gradients in the downcomer regions occur in the radial direction, not in the axial direction. To determine the sensitivity of the radial divisions in the downcomer region, the

number of radial divisions modeled was increased by a factor of two. The axial divisions in the downcomer region remain the same. The mesh refinement in the air annulus and in the concrete cask remains unchanged. The condition used in the evaluation corresponded to the normal condition using a uniform heat loading of 40 kW, which bounds the design basis condition for the 35.5 kW. The results of this evaluation showed that the maximum fuel temperature changed by less than 1°F for the increased refinement mesh. The temperature of the TSC shell showed a decrease of 2°F for the mesh with the increased refinement. This indicates that the maximum fuel temperature is relatively insensitive to the mesh refinement in the downcomer region.

### **Heat Transfer by Radiation**

Thermal radiation in all fluid (air and helium) regions has been considered in the model, specifically the following.

- Thermal radiation across the air annulus between the TSC shell and the concrete cask liner.
- Thermal radiation across the air gap above the TSC lid and in the isolated air region below the pedestal of the concrete cask.
- Thermal radiation across the helium downcomer region between the fuel basket and the TSC shell.

The discrete ordinates (DO) radiation model in FLUENT is used to solve the radiative heat transfer equation with emissivity values applied on the solid material surfaces.

Radiation in the porous media fuel region is modeled by using equivalent thermal conductivities that include the effects of heat transfer by radiation. The model of the porous media region in FLUENT is enclosed by a vertical wall that separates the porous region from the downcomer. The wall is comprised of two sides; one side facing the inner surface of the canister and the other facing the interior region of the porous media. An emissivity corresponding to electroless nickel is applied to the side facing the canister surface. On the side of the wall facing the interior region of the porous media, an emissivity of zero is applied to avoid incorporating the radiation already taken into account using the effective properties for the basket.

#### **4.4.1.2 Two-Dimensional Fuel Basket Models**

The purpose of the two-dimensional fuel basket model is to determine the effective thermal conductivity of the basket region in the axial and radial directions. The effective conductivities are used in the two-dimensional axisymmetric concrete cask and TSC models, and the two-dimensional axisymmetric transfer cask and TSC models. Two types of media are considered in the TSC: helium and water. The fuel assemblies and neutron absorbers in the fuel basket model are shown as homogeneous regions with effective thermal properties, which are determined by

the two-dimensional fuel assembly models and the two-dimensional fuel tube models described in Sections 4.4.1.3 and 4.4.1.4, respectively. The analyses performed in Section 4.4.1.3 identify that the PWR fuel assembly with the minimum conductivity is the 14×14. The properties of the PWR 14×14 fuel assembly are used in the evaluation of the effective properties for the PWR basket in this section. For the BWR assembly, the bounding fuel assembly type is the 10×10, which is used to determine the effective properties for the BWR basket.

Since the effective properties for the fuel basket correspond to the basket region, which is comprised of full-length fuel tubes, it is only necessary to consider a cross-section of the basket with a two-dimensional planar model. Due to symmetry of the basket designs, only a 1/8-section model is required for the PWR and the BWR fuel baskets. ANSYS is used to perform the conduction analysis using the models shown in Figure 4.4-6 for the PWR fuel basket and Figure 4.4-7 for the BWR fuel basket. The models include only radiation and conduction heat transfer. Radiation heat transfer is incorporated into the effective properties for the fuel assemblies and the neutron absorbers. Each fuel basket model takes into account the size of the cells in the basket – i.e., those cells formed directly by the fuel tube, and those cells formed by adjacent fuel tubes. The neutron poison is contained only on the inner surface of the basket tubes. The exterior tubes, which form the boundary of the downcomer region, may not have neutron absorbers on the adjacent surface of the interfacing fuel tubes. In the condition where the neutron absorber sheet is not required for criticality control, aluminum plates may be installed as an alternative to maintain thermal properties. The PWR and BWR fuel basket models evaluated in this section use the conductivity of the neutron poison defined in Chapter 8.

Additionally, it is conservatively assumed for both the PWR and BWR fuel baskets that a gap between the fuel tubes exists for the full length of the tube without any contact, as shown in Figure 4.4-6 and Figure 4.4-7. The gap between the fuel tubes is modeled as being 0.01 inch, and the conduction through the gap is based on the presence of either helium or water, depending on the condition.

The effective thermal conductivity ( $K_{eff}$ ) of the fuel basket region in the radial direction is determined by considering the basket region as a solid cylinder with heat generation.

Considering the temperature at the center of the TSC to be  $T_{max}$ , the effective thermal conductivity ( $K_{eff}$ ) is shown:

$$K_{eff} = \frac{Q}{4\pi H(T_{max} - T_o)} = \frac{Q}{4\pi H\Delta T} \quad [15]$$

where:

$Q$  ----- total heat generated by the fuel (Btu/hr)



H	-----	length of the active fuel region (in)
$T_o$	-----	boundary temperature of the basket
$\Delta T$	-----	$T_{\max} - T_o$ (°F)

The value of  $\Delta T$  is obtained from thermal analysis using the two-dimensional models shown in Figure 4.4-6 and Figure 4.4-7, with the boundary temperature constrained to be  $T_o$ . The effective conductivity ( $K_{\text{eff}}$ ) is then determined by using the stated expression. The analysis is repeated by applying different boundary temperatures so that temperature-dependent conductivities can be determined.

The effective properties for the DF basket assembly are determined using the same methodology as used for the standard PWR basket, except for the modification to the model, as listed.

1. A  $\frac{1}{4}$ -section model is used as shown in Figure 4.4-22.
2. The contents of the DFC locations in the DF basket assembly are conservatively modeled as helium, which has a lower conductivity.
3. Thermal conductivities of the steel plates forming the basket corner slot in the model are factored to reflect the actual plate thickness.

#### 4.4.1.3 Two-Dimensional Fuel Assembly Models

The two-dimensional fuel assembly models include the fuel pellets, cladding, and the media occupying the space between fuel rods. The media is considered to be helium for storage conditions, and water or helium for transfer conditions. The two-dimensional finite element models of the fuel assemblies are used to determine the effective conductivities for the PWR and BWR fuel assemblies. The effective conductivities are used in the two-dimensional fuel basket models described in Section 4.4.1.2. For the PWR fuel assemblies, four separate types are considered: 14×14, 15×15, 16×16 and 17×17. For the BWR fuel assemblies, four separate types are considered: 7×7, 8×8, 9×9 and 10×10. For the BWR fuel assembly, a fuel channel is considered since it may be present and it will result in bounding fuel cladding temperatures. Therefore, it is only necessary to address a single fuel configuration for each of the fuel assembly types.

The two-dimensional fuel assembly models include the fuel pellets, cladding, media between fuel rods, media between the fuel rods and the inner surface of the fuel tube (PWR), or between the fuel rods and the inner surface of the fuel channel (BWR), and a gap between the fuel pellets and cladding. The media are considered to be helium for storage, and water or helium for transfer conditions. Modes of heat transfer modeled include conduction and radiation between individual fuel rods for the steady-state condition. ANSYS PLANE55 conduction elements and MATRIX50 radiation elements are used to model conduction and radiation. (Radiation is not considered for the water condition.) Radiation elements are defined between fuel rods and

between the fuel rods and the fuel tube (PWR) or the fuel channel (BWR). A typical PWR fuel assembly finite element model is shown in Figure 4.4-8, which corresponds to the 14×14 fuel assembly. The BWR fuel assembly model only considers the region up to the inner surface of the channel, and a typical BWR fuel assembly is shown in Figure 4.4-9, which corresponds to the 10×10 fuel assembly.

The effective conductivity for the fuel is determined by using an equation defined in a Sandia National Laboratory Report [15]. The equation is used to determine the maximum temperature of a square cross-section of an isotropic homogeneous fuel with a uniform volumetric heat generation. At the boundary of the square cross-section, the temperature is constrained to be uniform. The expression for the temperature at the center of the fuel is given by:

$$T_c = T_e + 0.29468 (Qa^2 / K_{eff})$$

where:

$T_c$	-----	the temperature at the center of the fuel (°F)
$T_e$	-----	the temperature applied to the exterior of the fuel (°F)
$Q$	-----	volumetric heat generation rate (Btu/hr-in <sup>3</sup> )
$a$	-----	half length of the square cross-section of the fuel (inch)
$K_{eff}$	-----	effective thermal conductivity for the isotropic homogeneous fuel (Btu/hr-in-°F)

Volumetric heat generation (Btu/hr-in<sup>3</sup>) based on the design heat load is applied to the pellets. The effective conductivity is determined based on the heat generated and the temperature difference from the center of the model to the edge of the model. Temperature-dependent effective properties are established by performing multiple analyses using different boundary temperatures. The effective conductivity in the axial direction and the effective density of the fuel assembly are calculated on the basis of the material area ratio. The effective specific heat is computed on the basis of a weighted mass average.

For the PWR fuel assemblies, the 14×14 fuel assembly is shown to have the effective properties that correspond to the minimum values, as shown in Table 4.4-1 for both fuel tube configurations, i.e., with and without neutron absorber.

For the BWR fuel assemblies, the 10×10 fuel assembly is shown to have the effective properties that correspond to the minimum values, as shown in Table 4.4-2.

**4.4.1.4      Two-Dimensional Neutron Absorber Models**

The two-dimensional neutron absorber model is used to calculate the effective conductivities of the neutron absorber, the neutron absorber retainer, and the fuel channel (for BWR only). These

effective conductivities are used in the two-dimensional fuel basket models (Section 4.4.1.2). A total of three neutron absorber models is required: one PWR model (for the PWR 14×14) and two BWR models—one with the neutron absorber plate and channel, and one with the channel but without the neutron absorber plate, corresponding to the enveloping configurations of the 10×10 BWR fuel assembly.

The configurations shown in the neutron absorber models in Figure 4.4-10 and Figure 4.4-11 for PWR and BWR fuel, respectively, incorporate the neutron absorber (and the channel for the BWR). The configuration shown in Figure 4.4-12 is for the BWR fuel tube with the channel, but without the neutron absorber.

As shown in Figure 4.4-10, the PWR fuel tube model includes the neutron absorber, the stainless steel retainer, and the gaps between the neutron absorber and the stainless steel retainer and the surface of the fuel tube. Two conditions of media are considered in the gaps: helium and water.

ANSYS PLANE55 conduction elements and LINK31 radiation elements are used to construct the model. The model consists of four layers of conduction elements and two sets of radiation elements (radiation elements are not used for the water condition) that are defined at the gaps (two for each gap). The thickness of the model (x-direction) is the distance measured from the outside surface of the stainless steel retainer to the inside surface of the fuel tube (assuming the neutron absorber is centered between the retainer and the fuel tube, and there is no contact for the length of the basket). The gap size between the neutron absorber and the adjacent surfaces is 0.002 inch.

The BWR fuel assemblies may include a fuel channel, as compared to the PWR assemblies, which have no fuel channel. Therefore, two effective conductivity models are necessary for the BWR: one model with the neutron absorber plate (a total of six layers of materials) and a fuel channel; and the other model with a fuel channel, but with a gap replacing the neutron absorber plate (a total of two layers of materials).

As shown in Figure 4.4-11, the first BWR neutron absorber model includes the fuel channel, the retainer, the neutron absorber and associated gaps. As shown in Figure 4.4-12, the second BWR neutron absorber model includes the fuel channel and the gap between the fuel channel and the fuel tube surface.

Heat flux is applied at the left side of the model (retainer for PWR model and fuel channel for BWR model), and the temperature at the right boundary of the model is specified. The heat flux is determined based on the design heat load. The maximum temperature of the model (at the left boundary) and the temperature difference ( $\Delta T$ ) across the model are calculated by the ANSYS model. The effective conductivity ( $K_{xx}$ ) is determined using the following formula.

$$q = K_{xx} (A/L) \Delta T$$

or

$$K_{xx} = q L / (A \Delta T)$$

where:

$K_{xx}$	-----	effective conductivity (Btu/hr-in-°F) in X direction in Figure 4.4-10 through Figure 4.4-12
$q$	-----	heat rate (Btu/hr)
$A$	-----	area (in <sup>2</sup> )
$L$	-----	length (thickness) of model (in)
$\Delta T$	-----	temperature difference across the model (°F)

The temperature-dependent conductivity is determined by varying the temperature constraints at one boundary of the model and solving for the temperature difference. The effective conductivity for the parallel path (the Y direction in Figure 4.4-10) is calculated by the following.

$$K_{yy} = \frac{\sum K_i t_i}{L}$$

where:

$K_i$	-----	thermal conductivity of each layer (Btu/hr-in-°F)
$t_i$	-----	thickness of each layer (in)
$L$	-----	total length (thickness) of the model (in)

#### 4.4.1.5 Two-Dimensional Transfer Cask and TSC Model for Operations Involving 24-Hour Cooling

During the transfer condition, the TSC in the transfer cask is subjected to four separate conditions.

- The water phase when the lid is being welded to the TSC.
- The drying phase during which helium is present while vacuum drying to remove moisture from the TSC and the annulus circulating water cooling system is operating.
- The helium backfilled phase when the TSC closure is completed and the transfer cask cooling water system is operating (24 hours of cooling).
- The operation of transferring the helium-backfilled TSC into the concrete cask with the transfer cask annulus circulating water cooling system drained.

In this section, analyses are performed to support the use of 24-hour cooling after the drying phase and prior to loading of the canister into the concrete cask. The use of the 24-hour cooling

permits the maximum time for the drying phase and the maximum time to transfer the canister into the concrete cask. Section 4.4.1.6 describes the evaluation of an alternate system drying operational cycle permitting the cool time to be minimized and the loading of the canister into the concrete cask to be limited to eight hours.

The first step is considered to be steady-state conditions for all heat loads. For vacuum drying operations, there is no time limit for the PWR basket with heat loads less than or equal to 25 kW, and no time limit for the BWR basket with heat loads less than or equal to 29 kW. The time in vacuum drying is administratively controlled for the PWR basket with heat loads greater than 25 kW, and for the BWR basket with heat loads greater than 29 kW, to ensure the maximum fuel cladding temperature is less than the allowable temperature. For high heat loads greater than 25 kW for the PWR basket and greater than 29 kW for the BWR basket, the 24-hour helium-backfilled phase is needed for both systems. The maximum time allowed for loading the helium-backfilled TSC into the concrete cask without operating the transfer cask annulus circulating water cooling system is determined by transient analyses. During the operational sequence of TSC loading, an Annulus Circulating Water cooling System (ACWS) may be used to flow water through the annulus to cool and maintain a specified temperature for the TSC external shell. Alternative cooling methods, such as reverse ACWS, or any other equivalent site-approved annulus cooling system or by fully submerging the TSC with the lid removed or the transfer cask annulus seals deflated, may also be used. The annulus cooling methods, when used, are designed to accommodate design basis heat loads without additional heat rejection from the transfer cask to the environment. The annulus cooling methods, i.e., ACWS and reverse ACWS, may be generically referred to as "ACWS" for discussion purposes.

Note that the MAGNASTOR transfer cask is provided in two configurations, MTC1 and MTC2. The main difference between these two configurations is the material used for the cask shells and shield door (carbon steel for MTC1 and stainless steel for MTC2). The thermal models described in the following sections consider carbon steel properties for the cask shells and shield door. Since the radial conductance of the cask body is governed by the NS-4-FR material, and the water or air in the annulus between the canister and the cask shells carries out the majority of the heat, the cask shell material has an insignificant effect on the TSC and its contents. Therefore, the thermal models are applicable to both the MTC1 and MTC2 configurations.

#### **Evaluation of the Water Phase With Annulus Circulating Water Cooling System**

The model that includes water in the TSC treats the entire cavity as though it is filled with water. Since it is necessary to remove some water from the TSC during the closure lid welding operation, the water level in the TSC may be below the top of the fuel basket. The fuel tubes are designed with holes in the sides to permit the water to flow from the center of the TSC to the downcomer region of the TSC. The two-dimensional axisymmetric transfer cask and TSC

models are used to evaluate the transfer operation for PWR fuels and BWR fuels. The components comprising the transfer cask and TSC model are shown in Figure 4.4-13 for the PWR configuration. The BWR model is identical to the PWR model except for a slight difference in the dimensions. The TSC portion of the model is identical to the model employed in Section 4.4.1.1, with the exception that one of the conditions in the transfer operations uses water in the TSC instead of helium. The model for the TSC, described in Section 4.4.1.1, uses effective properties for the fuel basket region. For the water condition, the methodology described in Sections 4.4.1.2, 4.4.1.3, and 4.4.1.4 is used to determine the effective properties for the fuel basket region. For the condition of water in the TSC, no contribution due to radiation was considered; only conduction was taken into account for the effective properties. The porous media constants for the fuel basket region need not be recomputed since they are dependent on the fuel assembly and fuel basket geometry only. However, during the analytical evaluation of the water phase, the pressure drop in the fuel basket region due to the water requires the use of the viscosity, which is input as a material property. Since the maximum water temperature in the TSC is significantly below 212°F, the water is expected to remain in the liquid state, and the use of properties for the liquid state is acceptable. The transfer cask and the water annulus between the transfer cask and the TSC are also included in the model. The transfer cask is represented by effective properties. The transfer cask wall is comprised of four different materials: 1) a carbon steel inner shell; 2) a lead gamma shield layer; 3) an NS-4-FR neutron absorber layer; and 4) a carbon steel outer shell. Effective thermal conductivity for the transfer cask in the radial direction treats the four different cask wall materials as being in series. The effective thermal conductivity for the transfer cask wall in the axial direction treats the four different cask wall materials as being in parallel. The model also contains the shield doors of the transfer cask. While the inlets to the transfer cask are tubes in the side walls of the transfer cask, they are included in the model as straight sections parallel to the annulus. The following conditions are applied to the model for the steady-state evaluation of the water phase with the annulus circulating water cooling system.

- The outer surfaces of the transfer cask are considered to be adiabatic and without the application of solar insolation.
- The inlet water temperature for the annulus between the TSC and the transfer cask is specified to be 100°F.
- The driving force for the water flow in the annulus between the TSC and the transfer cask is natural convection. Water is supplied to the annulus inlets by an annulus circulating water cooling system.
- The heat generation internal to the TSC is modeled as 15, 20, 25, 30 and 35.5 kW for PWR fuels. The heat loads in Zones A, B and C, as defined in Figure 4.1-1, are factored based on the heat load for heat loads other than 35.5 kW. For the heat load of 35.5kW, the heat loads in Zones A, B and C are 0.922 kW, 1.20 kW and 0.80 kW, respectively.

The heat generation internal to the TSC is modeled as 15, 20, 25, 30 and 33 kW for BWR fuels with a uniform heat distribution.

- The flow in the TSC and in the annulus region is treated as being laminar for both the water and helium conditions of the TSC.
- Radiation heat transfer is removed from the solution.

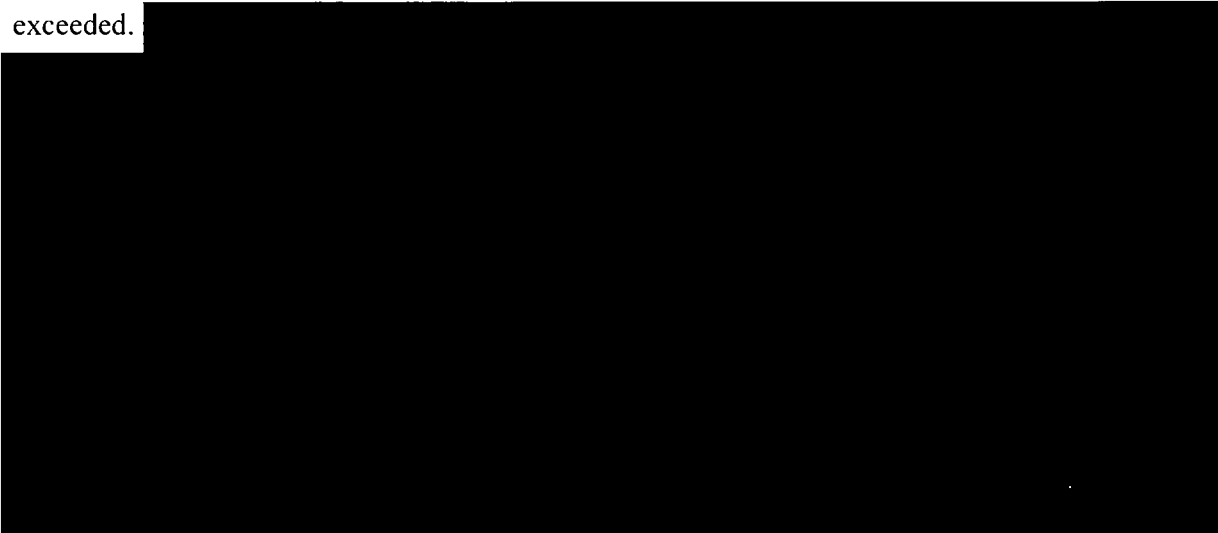


#### Evaluation of the Drying Phase-Vacuum Drying System

A Vacuum Drying System (VDS) is used to evacuate and dry the TSC cavity by vaporization and removal of the water vapor and other gases from the cavity through the vent and drain port openings. During the vacuum drying phase, convection is not considered in the TSC cavity region. Conduction helium properties are utilized during the low-pressure drying process [27].

The transfer cask model used for the thermal transient analysis is comprised of a three-dimensional ANSYS model, as shown in Figure 4.4-16 and Figure 4.4-17 for PWR fuel and Figure 4.4-18 and Figure 4.4-19 for BWR fuel. During the vacuum drying phase, the annulus circulating water cooling system is a normal operating system that allows the heat from the TSC to be rejected in the same manner as for the water phase. The transfer cask annulus circulating water cooling system is an operational convenience and not a safety-related system, since the transfer cask can be submerged in the spent fuel pool (with the annulus seals deflated) at any point in time during the vacuum drying operation without resulting in thermal shock to the transfer cask system. The temperature profile on the TSC outer diameter from the water phase analysis is applied to the TSC surface for each heat load.

Effective properties for the PWR and BWR fuel regions, the neutron absorber, and the helium inside the TSC are employed, and they are described in Sections 4.4.1.3 and 4.4.1.4, respectively. These two models are used to determine the allowable time in vacuum, depending on the heat load, to ensure that the fuel cladding temperature limit of 752°F (400°C) is not exceeded.



Transient analyses are performed to determine the maximum system temperature following the backfill helium condition for heat loads greater than 25 kW for PWR fuel and greater than 29 kW for BWR fuel. Analyses are performed for the 35.5 kW PWR and the 33 kW BWR design basis heat loads using the same two-dimensional FLUENT model used for analysis of the water phase condition with modified material properties and boundary conditions. The initial temperature field of the transient evaluation to simulate the helium backfill condition is obtained from the analysis results at the end of the vacuum drying process (ANSYS results) for the respective heat load.



The FLUENT model used to analyze the cooldown transient defines the locations at which initial temperatures are required from the ANSYS results. For each node in the FLUENT model, there are eight node points in the circumferential direction in the ANSYS 45-degree symmetry model to compute the average temperature for the respective locations. The ANSYS model employs linear temperature shape functions across each element, so that interpolation between nodes and within an element provides temperatures that are consistent with the nodal temperature in the ANSYS results. The peak temperatures, which occur at the center line of the model, are transferred to the respective FLUENT node locations as initial temperatures in order to provide an upper bounding initial condition, conserving system heat provided to the FLUENT model.

The design basis heat load provides bounding temperatures and minimum times for vacuum and the longest time for helium cooling when needed. With the identification of the temperature after the backfill condition, the time in vacuum for the potential cooling cycles can be determined, since the temperature time history will follow the same time dependency as for the initial vacuum condition.

The system thermal transient history may be represented by an initial vacuum drying cycle followed by a postulated system cooling cycle of 24 hours, followed by a second system vacuum drying cycle that is followed by a second 24-hour cooling period preceding the TSC transfer to the concrete cask. It is noted that the 24-hour cooling period returns the system to a steady-state condition for the design basis heat load, providing a bounding operating cycle for all heat loads less than the design basis. Similarly, cooling the system for a period of 24 hours provides maximum TSC transfer time from the transfer cask to the concrete cask when the water is drained from the annulus cooling system. Additional analyses defining system response to these conditions are addressed in the following discussions.

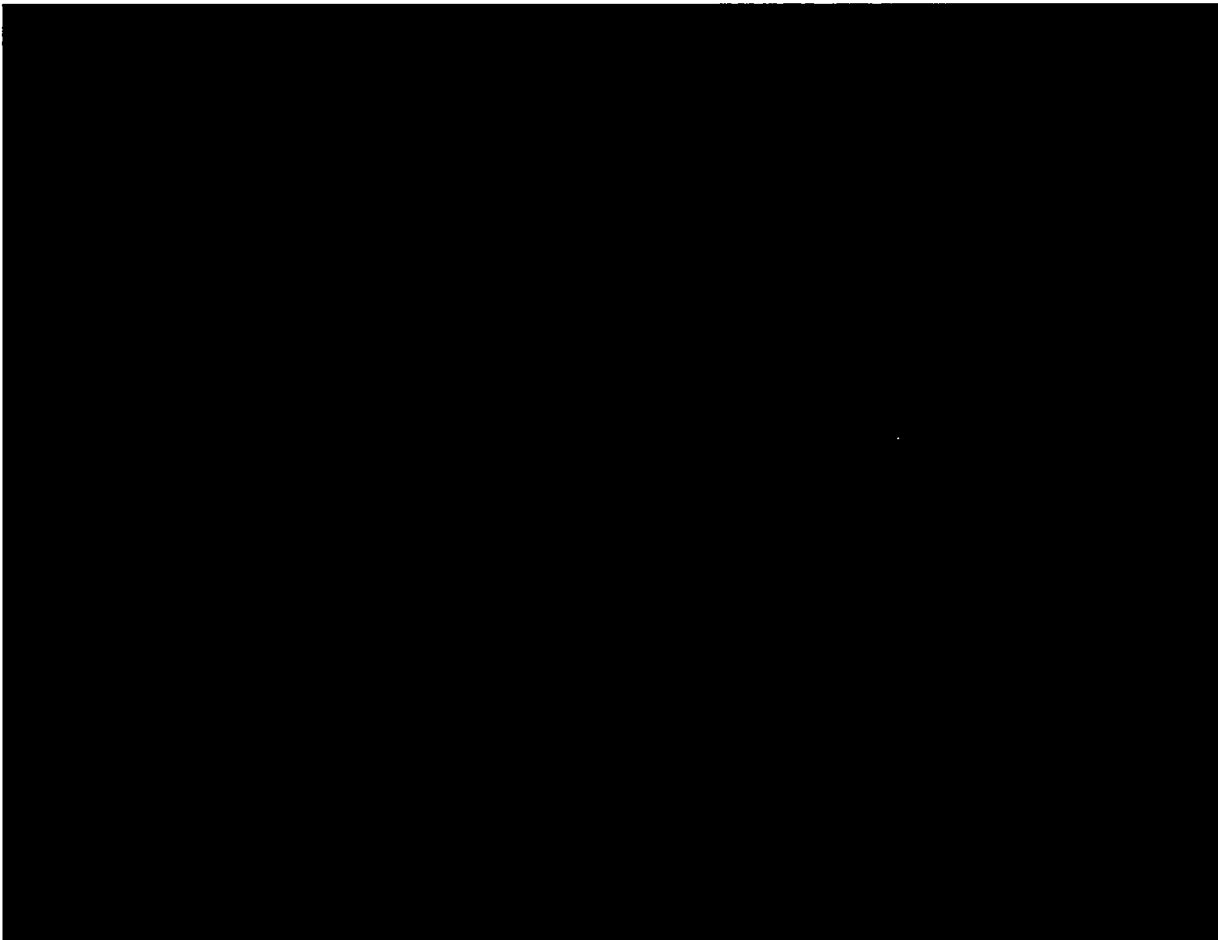
### **Mesh Sensitivity Evaluation**

The vacuum drying operation uses a three-dimensional ANSYS model to determine the thermal response of the fuel, shown in Figure 4.4-16 and Figure 4.4-18 for PWR and BWR fuel, respectively. Sensitivity of the mesh density is performed for the PWR design basis heat load of 35.5 kW. The finite element model uses an ANSYS element with a linear shape function for calculating the temperature within each element and uses a minimum of six elements in the fuel assembly cross-section plane. Temperature variation in the fuel region is expected to be parabolic since the heat generation is constant within any specified axial cross-section. Using a minimum of six elements permits development of an analytical parabolic distribution. To confirm the adequacy of the mesh density for the axial divisions, the number of elements in the basket region shown in Figure 4.4-16 was doubled, and the transient condition using design basis heat was rerun. The maximum fuel clad temperature was determined to be 1°F less than the

temperature for the solution with one-half the element density. The results from this mesh sensitivity evaluation validate that the maximum fuel temperature is relatively insensitive to mesh refinement in the fuel region.

**Evaluation of the Helium Phase With Annulus Circulating Water Cooling System**

Following the completion of vacuum drying and final cavity evacuation, the TSC is backfilled and pressurized with a measured mass of helium per the Technical Specifications to establish the cavity atmosphere for the normal condition of storage. The transfer cask and TSC remain in this helium phase condition until the TSC is placed into the concrete cask. During the helium phase, the transfer cask annulus cooling system will be used until the TSC preparations for transfer to the concrete cask are completed. Steady-state analyses for heat loads of 15, 20, 25, 30 and 35.5 kW for PWR fuel, and with heat loads of 15, 20, 25, 30 and 33 kW for BWR fuel, are performed using the model for the helium phase. The evaluation of this condition is performed to determine the initial condition for the operation in which the TSC is placed into the concrete cask with the transfer cask annulus cooling system drained.



**Evaluation of Moving the TSC into the Concrete Cask**

The transfer cask is used to load the TSC into the concrete cask. During this phase, there is no active auxiliary annulus cooling of the transfer cask, i.e. annulus cooling water system disconnected from the transfer cask, seals deflated, and annulus water drained. The transfer cask annulus is filled with ambient air, which is allowed to flow in through the reduced annulus inlet. This operation is time-limited to control the fuel cladding temperature to less than 752°F (400°C). The thermal performance of the transfer cask in this operation is evaluated for four transient conditions. Two transient conditions are for the PWR fuels with heat loads of 25 kW and 35.5kW, and two cases are for the BWR fuels with heat loads of 25 kW and 33 kW. The initial conditions for the four transient analyses are obtained from the steady-state analyses with water in the transfer cask annulus described previously in the section titled “Evaluation of the Helium Phase with Annulus Circulating Water Cooling System” for the corresponding heat load.

**4.4.1.6      Two-Dimensional Transfer Cask and TSC Model for Operations Involving Minimum Cooling Time and a Loading Time of Eight Hours**

Operational experience can lead to enhancement in the draining, vacuum drying and welding operations to minimize the need for maximum times for drying and loading operations or the potential need for cycles in the vacuum drying phase. Operational experience will reduce loading times and reduce staff radiation exposure. The following discussion presents the operational controls to be implemented.

Even with the absence of additional cycles for vacuum drying or the use of the 24-hour cool time, the TSC in the transfer cask is still subjected to four separate operational boundary conditions.

- The water phase when the lid is being welded to the TSC.
- The drying phase during which helium is present while vacuum drying to remove moisture from the TSC.
- The helium-backfilled phase is minimized to seven hours or less. It is during this time that the TSC port covers are welded and the transfer cask annulus circulating water cooling system (or equivalent) is operating, or the TSC is submerged in the spent fuel pool (with the annulus seals deflated).
- The eight hours for the operation of transferring the helium-backfilled TSC into the concrete cask with the transfer cask annulus circulating water cooling system drained.

Regardless of the time in the vacuum drying or loading operation, the response of the TSC and transfer cask in the water phase (inside the TSC) is not affected. With cooling water in the annulus, the time to remain in this condition is not altered from the system analyses or results reported in Section 4.4.1.5 for the water phase.

Without the additional cool time (of 24 hours), the initial temperatures of the TSC and fuel are significantly increased upon entering the loading phase (where the water in the annulus is drained and replaced by air). Reducing the time in the vacuum phase, as compared to the times shown in Table 4.4-9 (PWR) and Table 4.4-10 (BWR), the temperatures at the start of the condition leading to the transfer of the TSC to the concrete cask can be reduced to a level that allows eight hours for the transfer loading time.

To determine the vacuum and cool time limits, the models and their results described in Section 4.4.1.5 are used. The temperature time histories computed for the heat loads identified in Table 4.4-9 (PWR) and Table 4.4-10 (BWR) are used to identify the maximum fuel clad temperatures at the end of the reduced vacuum times for the individual heat loads. The transient analyses for the condition of the helium backfill, in conjunction with water in the annulus as described in Section 4.4.1.5, identify the temperature increase expected for the fuel clad for the range of heat loads upon backfilling the TSC with helium. Analyses in Section 4.4.1.5 identify that the maximum increase in the temperature of the fuel for the bounding PWR and BWR heat loads is 44°F and 34°F, respectively. The 44°F PWR increase and the 34°F BWR increase correspond to the design basis heat load bound the temperature for all other heat loads of the PWR or BWR fuel assemblies. The maximum temperature increase is conservatively added to the maximum fuel clad temperature occurring at the end of the reduced time in vacuum. This temperature is used to confirm that an additional eight hours for the TSC in the transfer cask with air in the annulus is equal to, or less than, the maximum fuel clad temperatures determined in Section 4.4.1.5.

### **Evaluation of TSC Loaded with DF Basket Assembly**

The flow resistance for a single zone DF basket assembly is slightly lower than the flow resistance for the standard PWR basket. The thicker side plates forming the basket corner slots for the damaged fuel can enhance the basket assembly conductance in the basket axial direction. Therefore, the thermal analysis results for the standard PWR basket bound the results for the DF basket assembly, as demonstrated by three representative analyses performed for the DF basket assembly for the transfer condition. Maximum fuel temperatures for all three analyses for the DF basket assembly are lower than those for the standard PWR basket. The three analyses are: 1) For the water phase, the 35.5 kW steady-state case (FLUENT CFD analysis) with helium inside the canister and water in the annulus between the canister and the transfer cask inner shell; 2) For the drying phase, the 25 kW steady-state case (ANSYS analysis) with helium inside the canister and water in the annulus between the canister and the transfer cask inner shell; 3) For the drying phase, the 35.5 kW transient case (ANSYS analysis) with helium inside the canister and water in the annulus between the canister and the transfer cask inner shell. Cases with helium inside the canister are selected because they yield higher fuel temperatures than cases with water inside the canister.

### **Evaluation of TSC Loaded with PWR Minimum Reduced Cool Time Fuel Basket Assembly**

The PWR minimum reduced cool time fuel basket assembly loads the four (4) hottest fuel of 1.8kW at the outer zone of the basket (Zone C, Figure 4.1-2), in addition to all center nine (9) fuels with low heat loads of 513Watts. This loading pattern significantly removes the heat from the basket center, consequently, reduces the maximum fuel temperature, compared with the maximum fuel temperature for the standard PWR basket assembly with the same total heat load. Therefore, the thermal analysis results for the standard PWR basket bound the results for the PWR minimum reduced cool time fuel basket assembly, as demonstrated by the analysis performed for the PWR minimum reduced cool time fuel basket assembly for the vacuum drying condition. The transient analysis (ANSYS analysis) with helium inside the canister and water in the annulus between the canister and the transfer cask inner shell is performed for the same duration (24 hours) of vacuum drying and same heat load (35.5kW) for the PWR minimum reduced cool time fuel basket assembly as for the standard PWR basket assembly. The maximum fuel temperature for the vacuum transient analysis is 630°F or 10°F lower than the standard PWR basket assembly at the end of 24 hour vacuum drying of 640°F (Table 4.4-9). The vacuum transient analysis for the canister is selected because it yields higher fuel temperatures than the steady state analyses with helium (with convection) or water inside the

canister for the same heat load. The reduction in the maximum temperature is expected since the maximum heat load is removed from the center of the basket.

#### **4.4.1.7      Two-Dimensional Transfer Cask and TSC Model for Increased Loading Times of PWR 20 kW and 25kW Heat Loads**

Reduced heat loads can minimize the requirement for TSC cooling prior to the operation of transferring the helium-backfilled TSC into the concrete cask with the transfer cask ACWS drained.

Regardless of the heat load, the TSC in the transfer cask is still subjected to four separate operational boundary conditions.

- The water phase when the lid is being welded to the TSC. The ACWS or the site equivalent is active during this phase.
- The drying phase during which helium is present while vacuum drying to remove moisture from the TSC. For the 20kW heat load, the vacuum time is unlimited (Table 4.4-9). For 25 kW, the vacuum time is limited to 50 hours to reduce the fuel clad temperature at the vacuum condition (Table 4.4-16). The ACWS or the site equivalent is active during this phase.
- The helium-backfilled phase is minimized so that for 20 kW, there is no additional cooling time, and for the 25 kW heat load, the cooling time is limited to a minimum of seven hours. It is during this time that the TSC port covers are welded and the transfer cask ACWS or site equivalent is operating.
- Transferring the helium-backfilled TSC into the concrete cask with the transfer cask ACWS drained.

To determine the cool time limits, the PWR TSC/transfer cask model described in Section 4.4.1.5 is used. Due to the minimum 20 kW heat load, the transfer cask model with air in the annulus was solved as a steady state problem. For this solution, there was no additional time with the TSC backfilled with helium and the operating ACWS.

Using the PWR TSC/transfer cask model described in Section 4.4.1.5, a transient evaluation is performed using an initial cooling period of 7 hours. During this 7 hour period the ACWS or its site equivalent is operated to reduce the fuel clad temperature prior to the transfer condition. After the 7 hours of cooling, the water in the annulus between the TSC and the transfer cask is replaced with air. During the transfer phase of the TSC into the concrete cask, air is allowed to flow up through the annulus. The transient is continued until the fuel clad temperature reaches 730°F.

#### **4.4.2      Test Model**

MAGNASTOR is conservatively designed by analysis. Therefore, no physical model is employed for thermal analysis. The benchmark provided in Section 4.8.1 provides confirmation that the analysis methodology employed for the MAGNASTOR design is conservative.

#### **4.4.3      Maximum Temperatures for PWR and BWR Fuel Configurations**

##### **Normal Conditions of Storage**

The temperature distributions and maximum component temperatures for MAGNASTOR for normal conditions of storage are provided in this section. System components of the CC1/CC2 concrete cask containing a PWR and BWR TSC and the CC3 concrete cask containing a PWR TSC are addressed separately. The temperature distributions in the CC1/CC2 concrete cask containing the BWR TSC are similar to those of the same system with the PWR TSC and are, therefore, not presented.

The temperature distribution in the CC1/CC2 concrete cask and the TSC containing the PWR design basis fuel (uniform heat load) for normal conditions of storage is shown in Figure 4.4-14. The air velocity distribution in the annulus between the TSC and the concrete cask liner for the normal conditions of storage for PWR fuel for the CC1/CC2 configuration is shown in Figure 4.4-15. The maximum component temperatures for the normal conditions of storage are summarized in Table 4.4-3. Note that the bounding temperatures from CC1/CC2 and CC3 analyses are conservatively used as the maximum component temperatures for the CC4 configuration. It is noted that these system thermal performance results are based on an average annual ambient temperature of 76°F at sea level pressure and standard air density properties. Site-specific conditions are to be evaluated to assure thermal margins are maintained for steady-state storage conditions at the intended MAGNASTOR ISFSI site.

As shown in Figure 4.4-14, the peak fuel temperature for the normal storage condition occurs near the top of the fuel basket and, based on the uniform spacing of the isotherms at the centerline of the TSC, the temperature varies monotonically from the TSC bottom to the peak near the top of the fuel basket. This is indicative that the dominant mode of heat rejection from the fuel is by convection due to the helium flow circulating within the TSC.

The calculated temperatures at the TSC surface for the normal storage condition are higher than the concrete liner or surface, indicating that radiation heat transfer occurs across the concrete cask to TSC annulus.

To confirm that the concrete cask heat removal system is operable, one of the following two surveillance options with a frequency of 24 hours is required: (1) Visually verify all concrete

cask air inlet and outlet screens are free of blockage; (2) Verify the difference between the concrete cask air outlet average temperature and the ambient temperature is less than 119°F, 127°F, 134°F and 119°F for the concrete cask configuration CC1/CC2-PWR, CC1/CC2-BWR, CC3-PWR and CC4-PWR, respectively. The allowable temperature differences are determined based on the maximum calculated temperature difference between air outlet and ambient and the calculated minimum temperature margin for concrete and fuel temperatures for all normal and off-normal conditions.

#### **Normal Conditions of Storage – PWR Configuration with DF Basket Assembly**

The thermal evaluation for the concrete cask loaded with a TSC containing a DF basket assembly in storage conditions is performed based on configuration CC3 using the two-dimensional axisymmetric FLUENT CFD models described in Section 4.4.1.1. Three cases are considered:

Case 1: The active fuel region is modeled as a single porous zone with a single lumped resistance coefficient. The uniform loading heat generation rate (based on a total heat load of 35.5 kW) is applied to the active fuel region. The calculated maximum fuel temperature is 704°F.

Case 2: The active fuel region is modeled as two parallel porous zones radially, with a resistance coefficient for the outer zone of 16 basket slots (which include the four damaged fuel can slots) and a separate resistance coefficient for the inner zone of 21 basket slots. The uniform loading heat generation rate is applied to the active fuel region. The calculated maximum fuel temperature is 707°F.

Case 3: The active fuel region is modeled the same way as in Case 2. The uniform loading heat generation rate is considered for the standard fuel assemblies. The decay heat is considered to be concentrated at the lower 103 inches of the active fuel region based on a 50% compaction ratio of debris for the four damaged fuel can slots. The calculated maximum fuel temperature is 709°F.

The maximum fuel temperatures from the Case 1 through Case 3 analyses are lower than the maximum fuel temperature (718°F) for the corresponding standard PWR basket, as shown in Table 4.4-3. Therefore the standard PWR basket analyses bound those for the DF basket assembly.



**Normal Conditions of Storage – PWR Minimum Reduced Cool Time Fuel Basket Assembly**

The thermal evaluation for the concrete cask loaded with a TSC containing the PWR minimum reduced cool time fuel basket assembly for normal storage condition is performed based on configuration CC3 using the modified two-dimensional axisymmetric FLUENT CFD model described in Section 4.4.1.1. The model used for the analysis of the TSC containing PWR minimum reduced cool time fuel basket assembly for normal storage conditions is identical to the model described in Section 4.4.1.1, except for the re-meshed basket zones in the basket radial direction to match locations of the heat generation due to the preferential loading.

The maximum fuel temperature of the analysis is 698°F, 20°F lower than the maximum fuel temperature (718°F) for the corresponding standard PWR basket, as shown in Table 4.4-3. The maximum temperature for the fuel heat load in Figure 4.1-2 is lower since the maximum fuel heat load is no longer at the center of the basket. Therefore the standard PWR basket analyses bound those for the PWR minimum reduced cool time fuel basket assembly.

**Transfer Condition for 24-Hour Cooling and Multiple Vacuum Drying Cycles**

The maximum component temperatures for MAGNASTOR during the transfer operation are reported in this section for operational procedures using 24 hours of cooling. The transfer operation is comprised of four separate phases: the water phase, the drying phase, the helium phase, and the TSC transfer phase. The water phase and the helium phase are not time limited due to the normal use of the transfer cask annulus cooling water system (ACWS), reverse ACWS, or site-approved ACWS equivalent. The transfer cask annulus cooling system is an operational convenience and not a safety-related system, since the transfer cask can be fully submerged (with the annulus seals deflated) in the spent fuel pool at any point in time during the transfer operation without resulting in thermal shock to the transfer cask system. The annulus cooling system maintains the TSC shell at a temperature significantly lower than the temperature corresponding to the normal conditions of storage. The maximum temperatures for the water phase are listed in Table 4.4-5 and Table 4.4-6 for PWR fuel and BWR fuel, respectively. The maximum temperatures for the helium phase are listed in Table 4.4-7 and Table 4.4-8 for PWR fuel and BWR fuel, respectively. Using the reverse ACWS model described in Section 4.4.1.5,

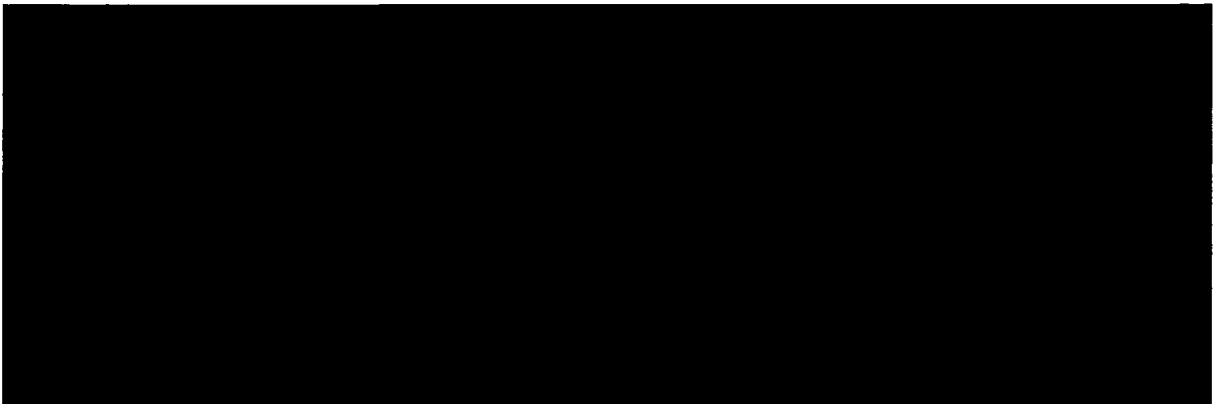
method. Table 4.4-9 and Table 4.4-10 present times for the vacuum drying for heat loads greater than 25 kW for PWR fuel and

greater than 29 kW for BWR fuel that are administratively controlled to maintain the fuel cladding temperature below the 752°F limit.

If additional vacuum drying is required for heat loads requiring administrative controls to meet the specified cavity dryness criteria, additional drying cycles can be performed following 24 hours of cooling the TSC, either with the annulus cooling water system or by returning the transfer cask and TSC to the spent fuel pool. Table 4.4-11 and Table 4.4-12 show the second vacuum time and maximum fuel temperatures at the end of the duration for PWR fuel and BWR fuel, respectively. Note that the PWR fuel cladding temperatures shown in Table 4.4-5, 4.4-7, and 4.4-9 are bounded by the PWR fuel cladding temperatures for the normal storage steady-state conditions in Table 4.4-3. Therefore, the normal condition design bases PWR heat load fuel cladding and component temperatures, such as for the fuel basket (including damaged fuel cans, as applicable) and the TSC, bound the maximum temperatures for any phase of the transfer condition for the fuel basket and TSC components.

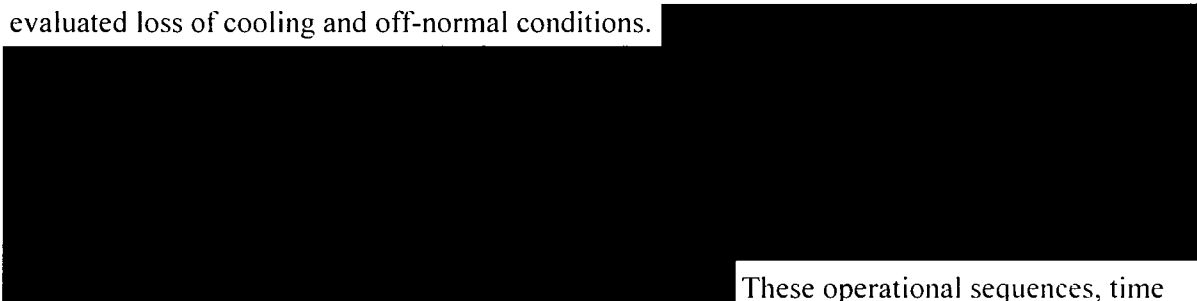
The time for TSC transfer to the concrete cask is administratively limited to ensure that the maximum fuel cladding temperature is bounded by the design bases heat load normal condition storage temperature. Table 4.4-13 and Table 4.4-14 show the duration and the maximum fuel temperature at the end of the TSC placement in the concrete cask for both PWR fuel and BWR fuel, respectively. The time duration for the transfer operation is determined by modeling the water material properties in the annulus as air, as described in Section 4.4.1.5.

The off-normal condition for use of the annulus cooling system corresponds to loss of cooling by the ACWS, or equivalent site-approved annulus cooling system. This can occur during the water phase or the drying phase of transfer operations.



In the event of loss of cooling occurring during the vacuum drying phase, the TSC is first backfilled with 75 psig (+10, -0 psi) helium, and is then returned to the pool, where it is cooled for a minimum of 24 hours prior to continuing vacuum drying operations.

The loading procedures in Chapter 9 provide normal operational loading sequences. The MAGNASTOR System Operating Manual prepared in accordance with the FSAR analyses provides cask loading and unloading sequence alternatives, including time limitations for all evaluated loss of cooling and off-normal conditions.



These operational sequences, time limits and corrective actions will ensure that the fuel cladding and system component temperatures do not exceed design allowable values.

#### **Transfer Condition for Minimum Cooling Time and Eight Hours of Canister Transfer**

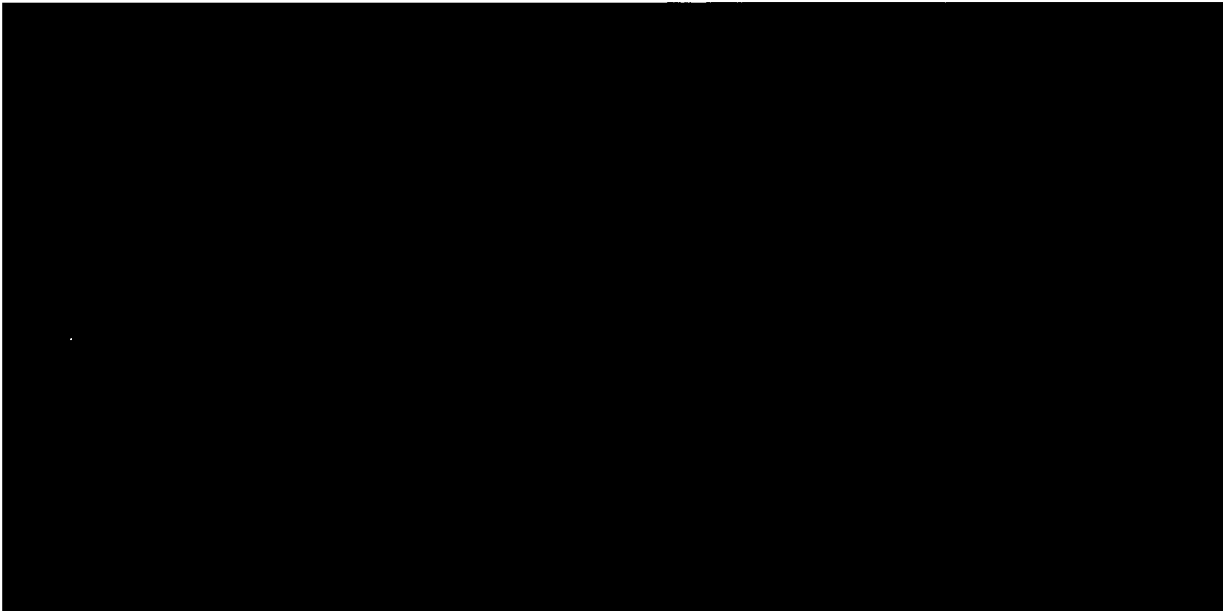
The maximum component temperatures for MAGNASTOR during the transfer operation are reported in this section for operational procedures using the minimum cooling time and eight hours of TSC transfer time (as determined by the evaluation in Section 4.4.1.6). The transfer operation is comprised of four separate phases: the water phase, the drying phase (reduced time as compared to the evaluations in Section 4.4.1.5), the helium phase (minimized cooling time), and the TSC transfer phase (limited to eight hours). The water phase and the helium phase permit indefinite time due to the normal use of the transfer cask annulus cooling system, or an equivalent cooling system. The annulus cooling system maintains the TSC shell at a temperature

significantly lower than the temperature corresponding to the normal conditions of storage. The maximum temperatures for the water phase are listed in Table 4.4-5 and Table 4.4-6 for PWR fuel and BWR fuel, respectively.

Heat load-dependent vacuum drying times reported in Table 4.4-9 and Table 4.4-10 confirm that for the same heat loads, the PWR fuel clad temperatures bound the BWR fuel clad temperatures. The temperatures reported in Table 4.4-16 and Table 4.4-17 are for the maximum PWR and BWR clad temperatures, respectively, at the end of the reduced vacuum time, the reduced cool time, and the eight hours of transfer time. These results confirm that the maximum clad temperatures have significant margin relative to the 752°F fuel clad temperature limit.

For system operations that are outside the sequence presented in Table 4.4-16 or Table 4.4-17, as a result of equipment failure or some other event that extends drying and transfer operations, additional vacuum drying, helium cooling, and/or transfer times will be implemented in accordance with the actions described in the preceding section, “Transfer Condition for 24-Hour Cooling and Multiple Vacuum Drying Cycles.”

**Maximum TSC Transfer Temperatures for PWR 20 kW (no additional cooling) and 25kW Heat Loads with 7 hours of cooling**



#### **4.4.4        Maximum Internal Pressures for PWR and BWR TSCs**

The maximum TSC internal operating pressures for normal conditions of storage are calculated in the following sections for the TSCs containing PWR and BWR design basis fuel assemblies.

##### **Maximum Internal Pressure for the TSC Containing PWR Fuel**

The internal pressure of a TSC containing PWR fuel assemblies is a function of fuel type, burnup, initial enrichment, cool time, fuel condition (failure fraction), presence or absence of nonfuel hardware, TSC length, and the backfill gases in the TSC. Gases included in the pressure evaluation of a TSC containing PWR fuel include fuel rod fission, decay, backfill gases and integral fuel burnable absorber (IFBA) generated gas, gas generated by the nonfuel hardware components (assembly control components contain boron as the absorber material), and TSC backfill gases. Each of the PWR fuel types is separately evaluated to determine a bounding pressure for a TSC containing PWR fuel assemblies. Evaluations are performed for all contents in the standard basket (undamaged fuel) and in the damaged fuel basket configuration. The damaged fuel basket represents a bounding configuration due to the additional volume displacement by the thicker corner weldment plates and the presence of the DFC canisters themselves.

Fission gases include all fuel material generated gases, including helium generated by long-term actinide decay. Based on detailed SAS2H calculations, the quantity of fission and decay gases rises as burnup and cool time are increased and enrichment is decreased. The maximum gas available for release is calculated based on 70,000 MWd/MTU burnup cases at an enrichment of 1.9 wt %  $^{235}\text{U}$  and a cool time of 40 years for maximum fissile material assemblies in each major PWR fuel class. For other PWR fuel assembly types, fission and decay gases are determined by ratioing the fissile material mass to the maximum fissile material mass assemblies.

Fuel rod backfill pressure varies significantly among the PWR fuel types. Based on a literature review, a 500 psig backfill is assigned to Westinghouse and CE core fuel types. A maximum backfill pressure of 435 psig is assigned to B&W core assemblies. Backfill gas quantities are based on the fresh fuel free volume between the fuel pellet stack and the fuel rod cladding, including the plenum volume, and a backfill temperature of 68°F.

Burnable poison rod assemblies (BPRAs) placed within the TSC may contribute additional gas quantities due to n-alpha reaction of  $^{10}\text{B}$  during in-core operation. A portion of the neutron poison population is formed by  $^{10}\text{B}$ . Other neutron poisons, such as gadolinium and erbium, do not produce a significant amount of helium nuclides (alpha particles). BPRAs in this section is a general term used to describe a range of absorbers including, but not necessarily limited to,

Westinghouse Pyrex (borosilicate glass) BPRA and WABA (wet annular burnable absorber) configurations, as well as B&W BPRA and shim rods used in CE cores. The CE shim rods replace standard fuel rods to form a complete assembly array. The quantity of helium available for release from the BPRA is directly related to the initial boron content of the fuel rods and the release fraction of gas from the matrix material. The gas released from either of the low-temperature, solid matrix BPRA materials is likely to be limited, but no release fractions were available in open literature. Consequently, a 100% release fraction is applied. Initial boron content in the Westinghouse and B&W BPRA is based on a uniform absorber concentration of  $0.0063 \text{ g/cm}^{10}\text{B}$ . The maximum number of poison rods is 16 for Westinghouse  $14 \times 14$  fuel assemblies, 20 for Westinghouse and B&W  $15 \times 15$  fuel assemblies, and 24 for Westinghouse and B&W  $17 \times 17$  fuel assemblies. The length of the absorber rods is conservatively taken as the active fuel length. CE core shim rods are modeled at  $0.0126 \text{ g/cm}^{10}\text{B}$  for 16, 12, and 12 rods applied to CE-manufactured  $14 \times 14$ ,  $15 \times 15$ , and  $16 \times 16$  fuel assemblies, respectively.

Fuel rods may contain integral fuel burnable absorbers (IFBAs). The absorber is typically zirconium diboride and, as such, will generate helium gas as part of the neutron capture process. IFBA assemblies are generally used as an alternative or augmentation to BPRA use. The IFBA loading employed in the pressure analysis is based on NUREG-6760 as  $2.355 \text{ mg}^{10}\text{B}/\text{inch}$  in 156 rods. To bound the presence of both BPRA and IFBA materials in a fuel assembly, when loaded, the cask pressure calculations assume a design basis IFBA loading in the fuel assembly with a design basis BPRA inserted into the assembly guide tubes prior to loading into the storage system. Rather than accounting for the IFBA rods as an individual component, the pressure calculations double the BPRA gases for non-CE fuel assembly types (bound the combined inventory of IFBA and BPRA based on linear loading and number of rods affected).

Under normal operating conditions, the helium backfill for a TSC containing PWR fuel assemblies is at a maximum average gas temperature of  $465^\circ\text{F}$  and a pressure of 103 psig. Nominal helium densities for both PWR and BWR fuel types are shown in Table 4.4-4. Maximum system backfill pressure at operating conditions is set by the use of the operating procedures documented in Chapter 9. This approach ensures that an acceptable helium density is established in the canister prior to sealing. Free volumes inside the two classes of TSCs containing PWR fuel are 9,900 and 10,300 liters for TSCs containing the undamaged fuel basket and 9,600 liters for the TSCs containing the damaged fuel basket. The free volumes do not include PWR fuel assembly and nonfuel hardware components, since these vary for each assembly type, but do account for axial spacers and DFC displaced volume in the case of the damaged fuel basket. The free volume of the TSC is obtained by subtracting the assembly volume. The assembly volume includes the fuel skeleton, fuel rods and nonfuel hardware. For

the Westinghouse BPRAs, the Pyrex volume is employed since it displaces more volume than the WABA rods.

The TSC internal pressure is determined by summing the partial pressures of the TSC helium backfill gas and the released gases from the fuel and the poison rods. The partial pressure due to the fuel and neutron poison rod gases is determined by the ideal gas correlation ( $PV=nRT$ ) and the applicable rod release fractions and failure rates. For normal conditions, a 1% rod failure fraction is applied. For failed fuel rods, the releasable molar quantity of the fission and actinide decay gas is 30%, with 100% of the rod backfill gas being released. The normal condition average temperature of the gases released from the fuel rods and neutron poison inserts is conservatively set to 485°F (525 K) in the partial pressure calculation.

The TSC is evaluated for normal condition pressure for each of the PWR fuel types, with insert. The maximum normal condition pressure for a TSC containing PWR fuel assemblies is 104 psig. At a 1% rod failure fraction, the quantity of gas released from the fuel and neutron poison rods is minimal, resulting in no significant effect on system pressure.

The calculated maximum pressure of 104 psig allows for a 6 psig tolerance on the TSC helium backfill prior to reaching the 110 psig system pressure used in the Chapter 3 normal condition structural evaluations. Significantly higher pressure margins exist in the off-normal and accident pressures. Off-normal and accident pressures were calculated at 119 psig (10% fuel failure and off-normal thermal conditions) and 226 psig (100% fuel failure, see Section 4.6.4), and these calculated values are significantly lower than the established pressure limits of 130 psig for off-normal and 250 psig for accident condition pressures that are used in the structural calculations.

#### **Maximum Internal Pressure for the TSC Containing BWR Fuel**

Maximum internal pressures are determined for the BWR fuel in the same manner as those documented for the TSC containing PWR fuel. Primary differences for the BWR evaluations, versus those for the PWR, include a rod backfill gas pressure of 132 psig, a maximum burnup of 60,000 MWd/MTU used to generate fission gases, and the absence of neutron poison gases (no nonfuel hardware in the BWR system). The 132 psig rod backfill pressure used in this analysis is significantly higher than the 6 atmosphere (g) maximum pressure reported in open literature. Free volumes, without fuel assemblies, in the TSC containing BWR fuel types are 9,900 and 10,300 liters.

A bounding normal condition average temperature of 525 K is used for the partial pressure analysis of the fuel rod gases. The maximum normal condition pressure for a TSC containing BWR fuel is 104 psig.

The calculated maximum pressure of 104 psig allows for a 6 psig tolerance on the TSC helium backfill prior to reaching the 110 psig system pressure employed in the Chapter 3 normal

condition structural evaluations. Significantly higher pressure margins exist in the off-normal and accident pressures. Off-normal and accident pressures were calculated at 112 psig (10% fuel failure and off-normal thermal conditions) and 159 psig (100% fuel failure, see Section 4.6.4) and are conservatively bounded by the 130 psig off-normal and 250 psig accident condition pressures that were employed in the structural calculations.

#### **TSC Backfill Helium Tolerances**

Due to measurement and instrument uncertainties in the canister backfill operation, a range of allowed helium backfill density (g/liter) is determined in this section.

Any increase in backfill density is limited by the associated rise in pressure, which in turn is limited to the structural analysis inputs (110 psig for the limiting normal condition). As documented in the pressure evaluations, a 6 psi tolerance is acceptable prior to reaching system pressures employed in the structural analysis. Assuming a constant temperature, which is conservative as increased backfill density would enhance heat transfer and increase system pressure, and applying the ideal gas law make backfill density directly proportional to pressure. Relying on a 6 psi tolerance on a nominal pressure of 104 psig (119 psia) allows for a 5% increase in backfill density.

A decrease in backfill density is limited by thermal constraints. Lower helium density reduces convective heat capability of the system and, thereby, raises fuel clad temperature. Thermal analysis in Section 4.4.1.1 states that a 10% decrease in backfill density is acceptable while remaining below the maximum allowed clad temperature limit of 752°F.

Table 4.4-4 lists the pressure and temperature limited upper and lower bound helium backfill densities.



Figure 4.4-1 Two-Dimensional Model of Concrete Cask Loaded with PWR TSC

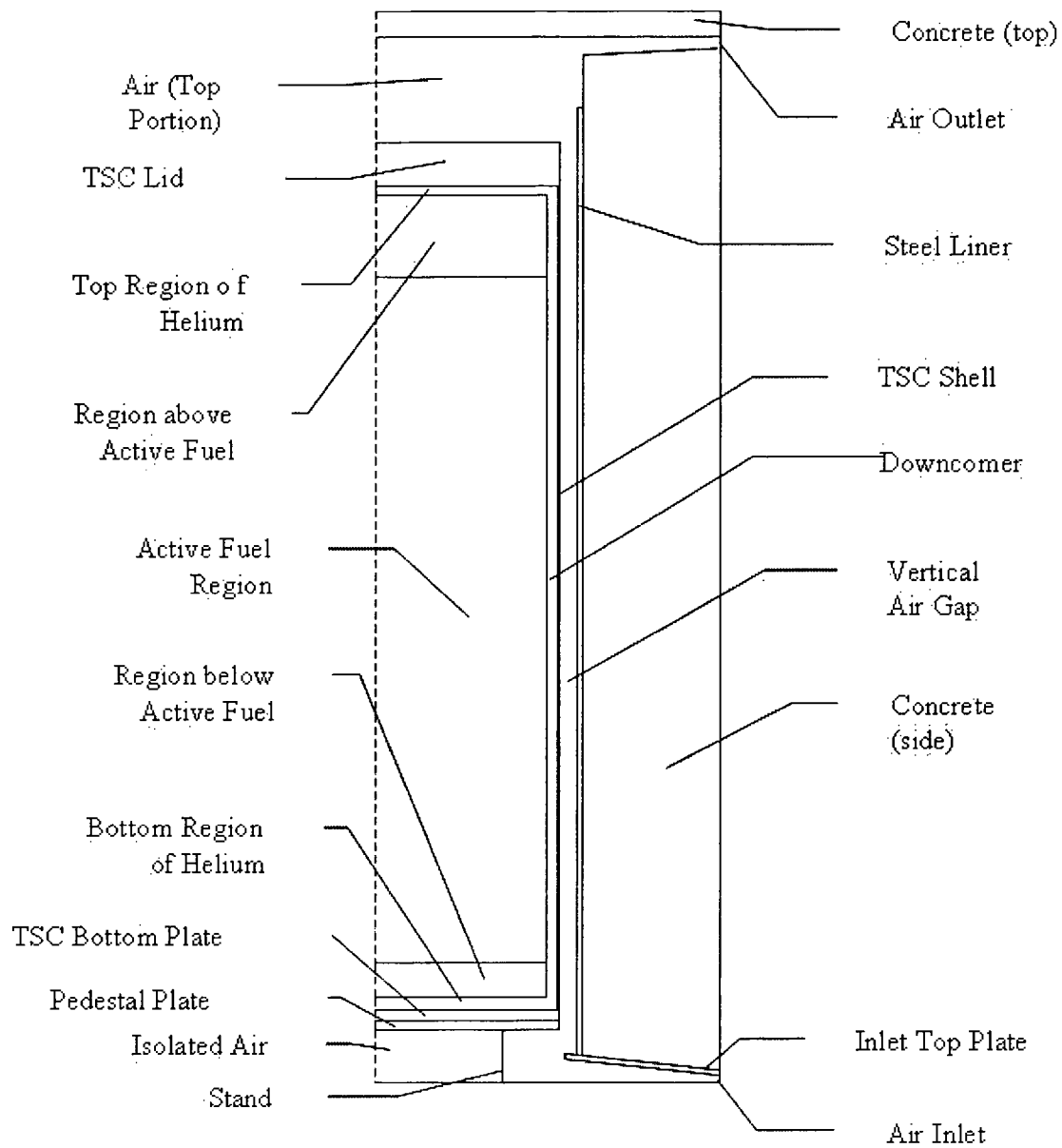


Figure 4.4-2      Computational Mesh for the Two-Dimensional Axisymmetric CFD Model  
of the Concrete Cask

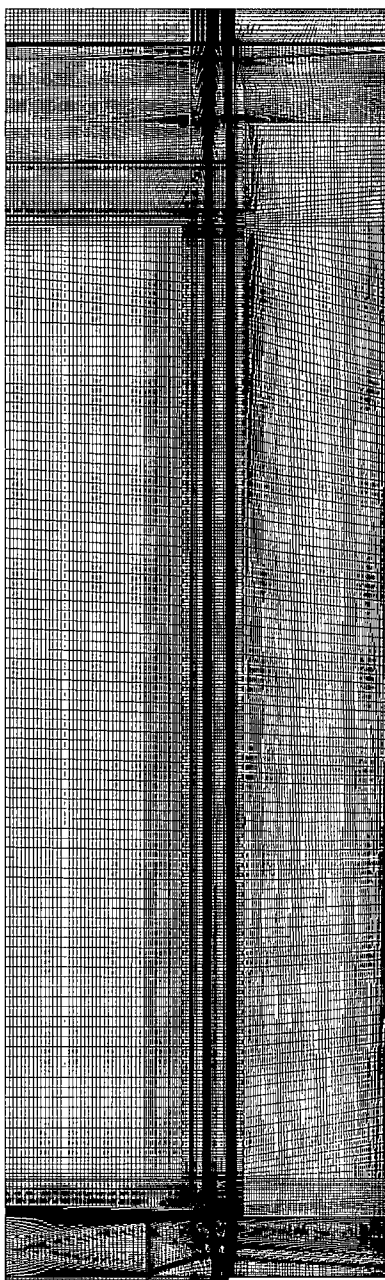


Figure 4.4-3 Axial Power Distribution for the PWR Fuel Assembly

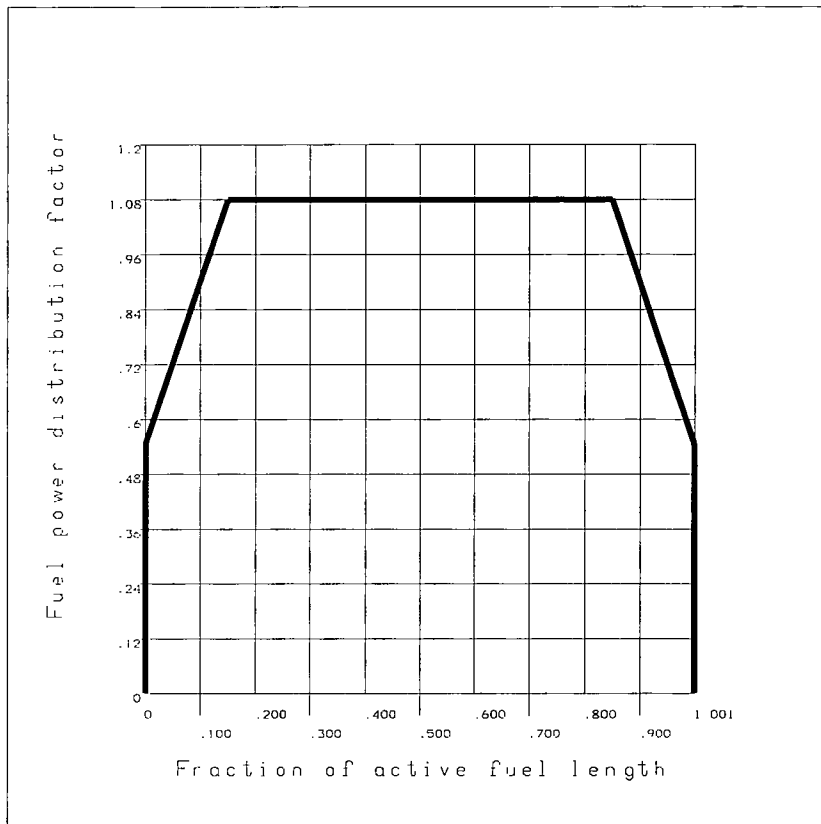


Figure 4.4-4 Axial Power Distribution for the BWR Fuel Assembly

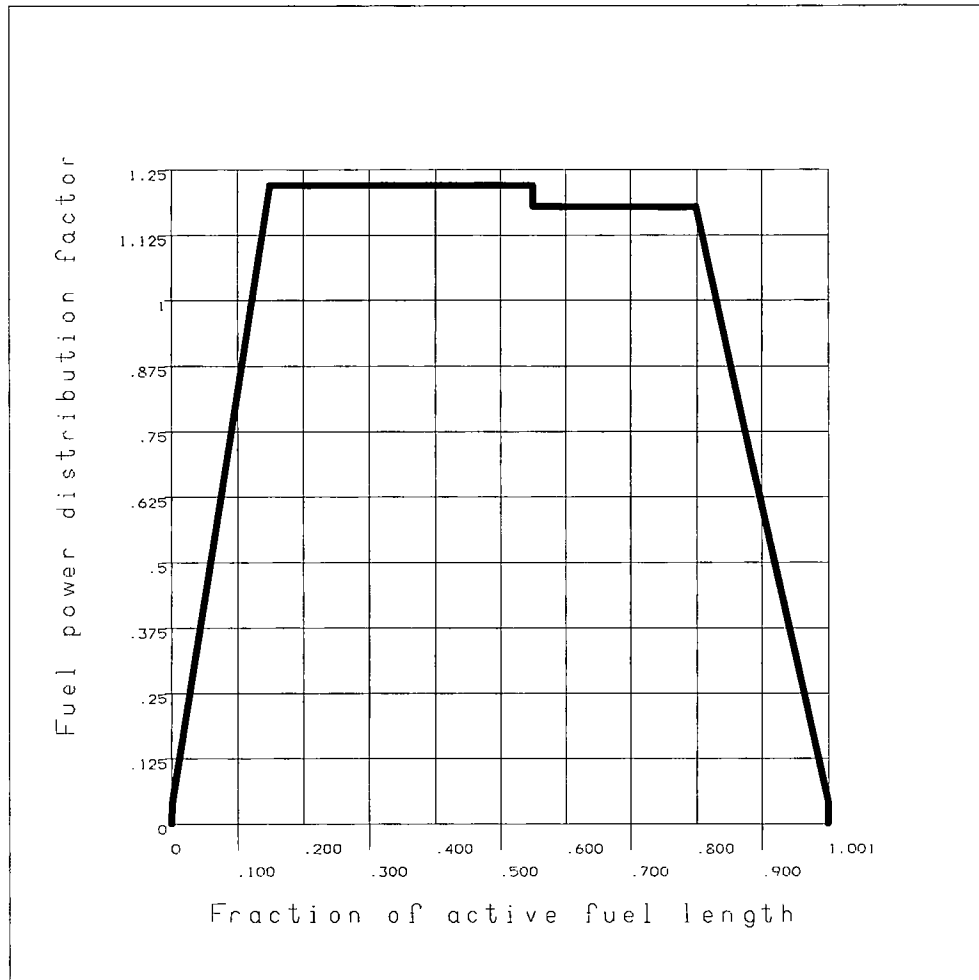


Figure 4.4-5 PWR Peak Fuel Cladding Temperature versus TSC Internal Pressure

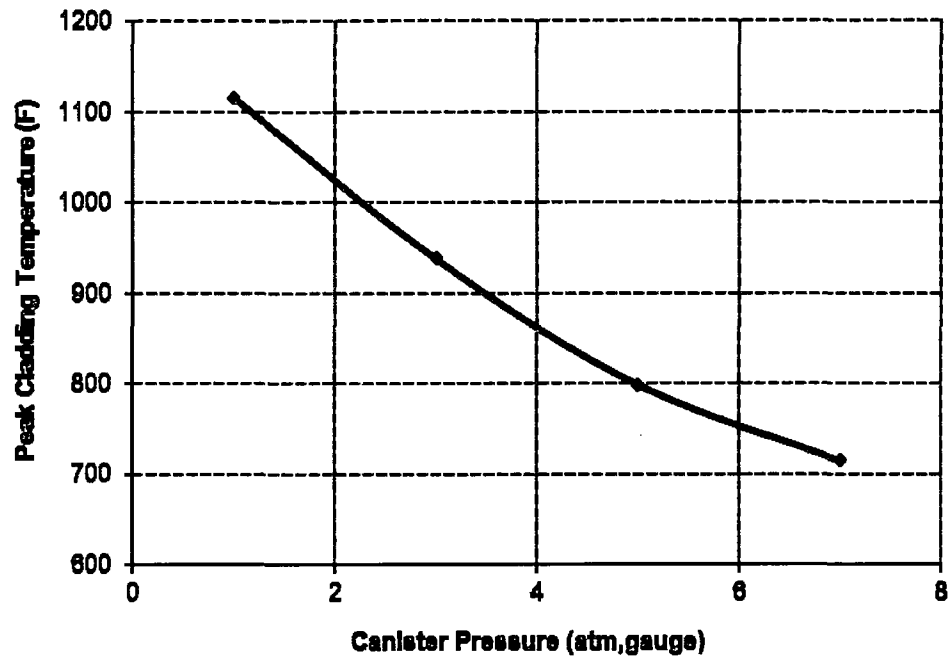


Figure 4.4-6 Two-Dimensional Finite Element Model of the PWR Fuel Basket

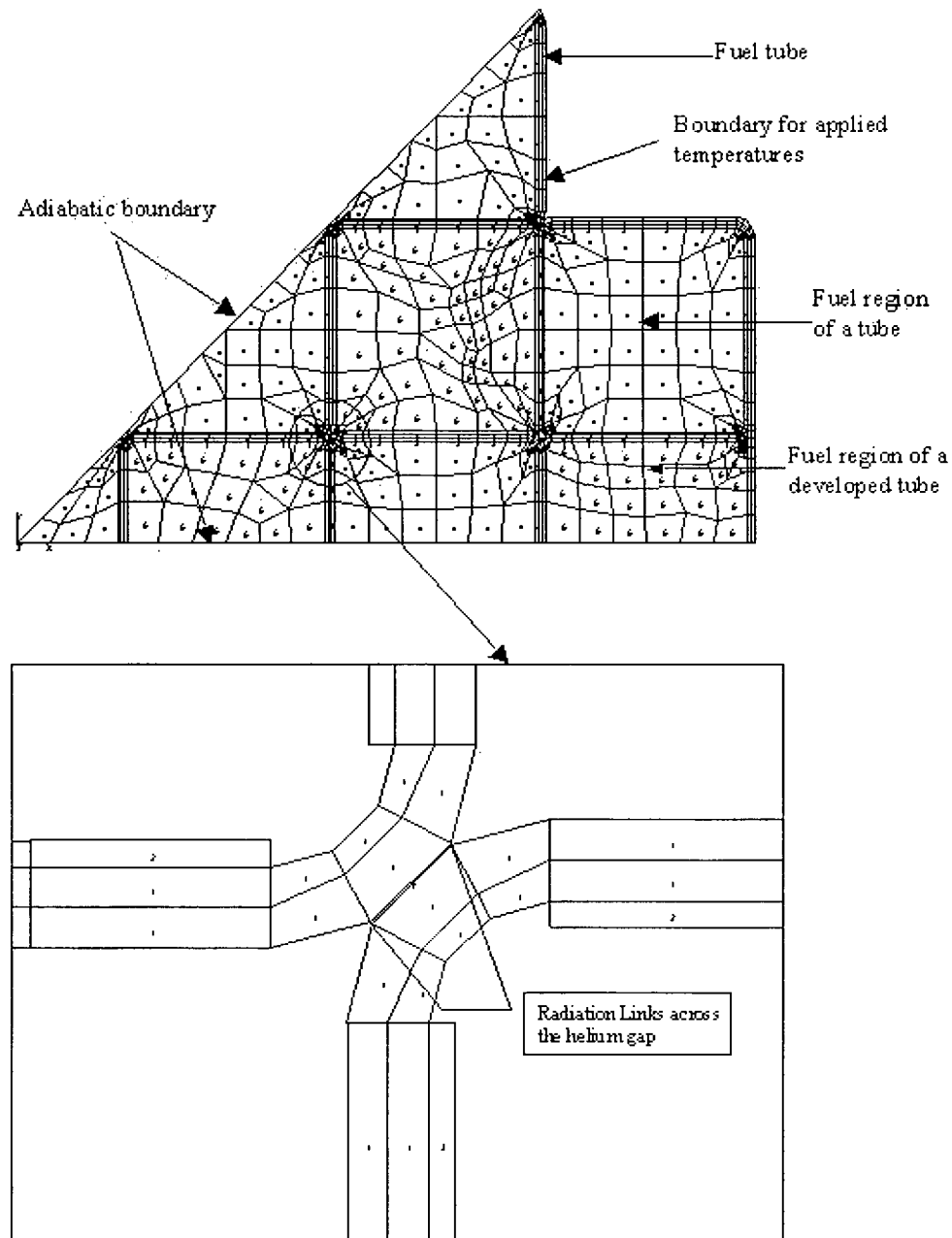


Figure 4.4-7 Two-Dimensional Finite Element Model of the BWR Fuel Basket

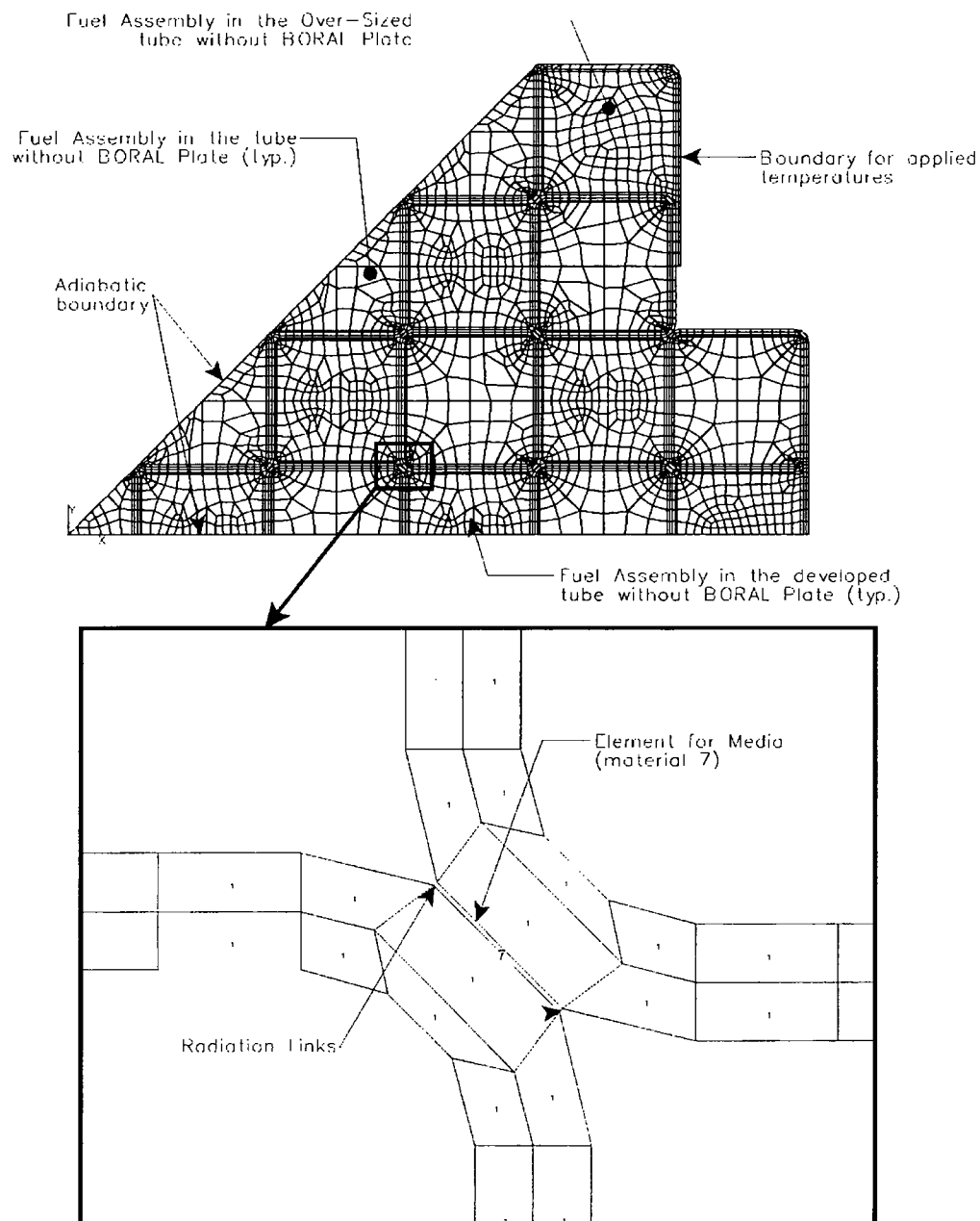
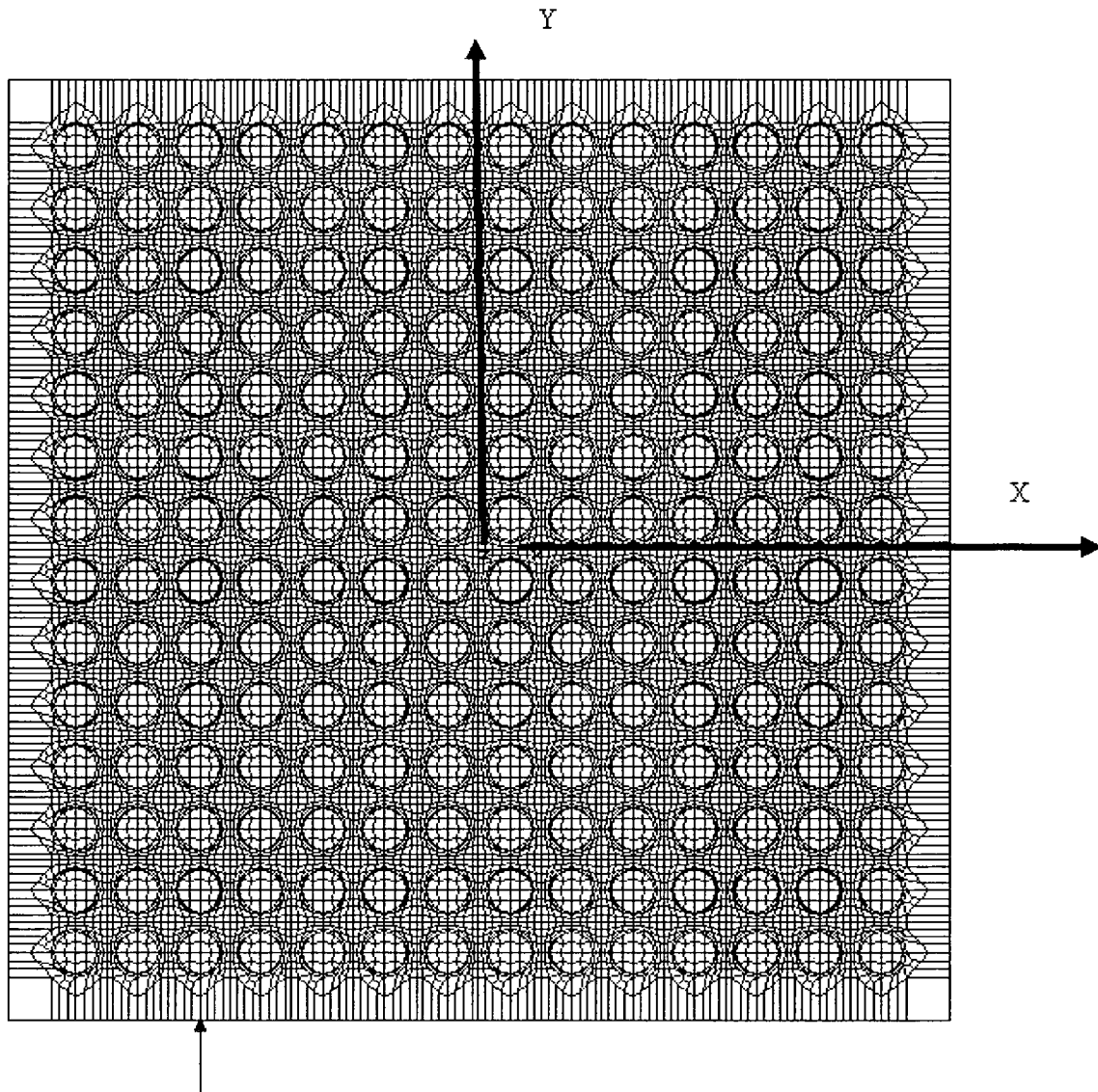


Figure 4.4-8 14×14 PWR Fuel Assembly Two-Dimensional Model



Temperature boundary condition applied along the edge of the model.

Note: X and Y correspond to the in-plane directions of the fuel assembly, while Z is out of the plane and corresponds to the axial direction of the fuel assembly.



Figure 4.4-9 10×10 BWR Fuel Assembly Two-Dimensional Model

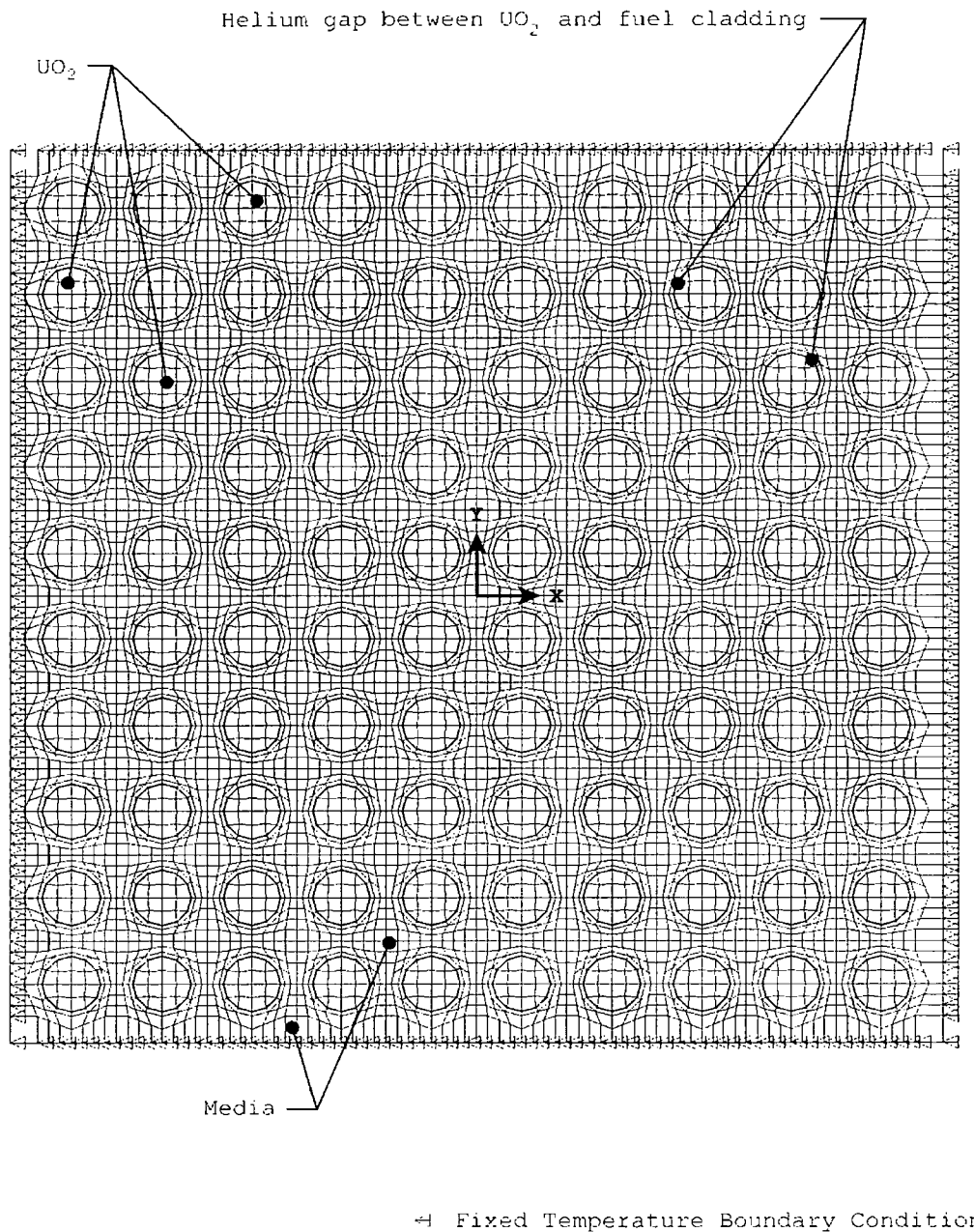
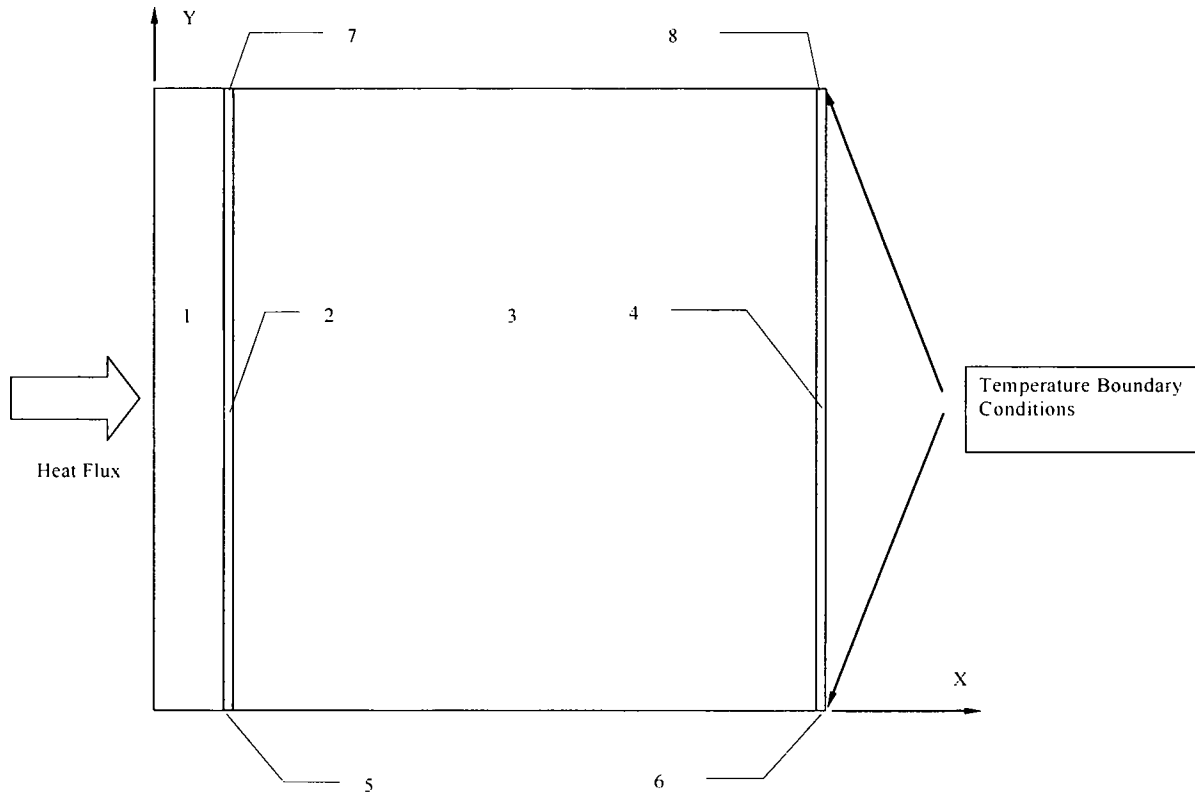
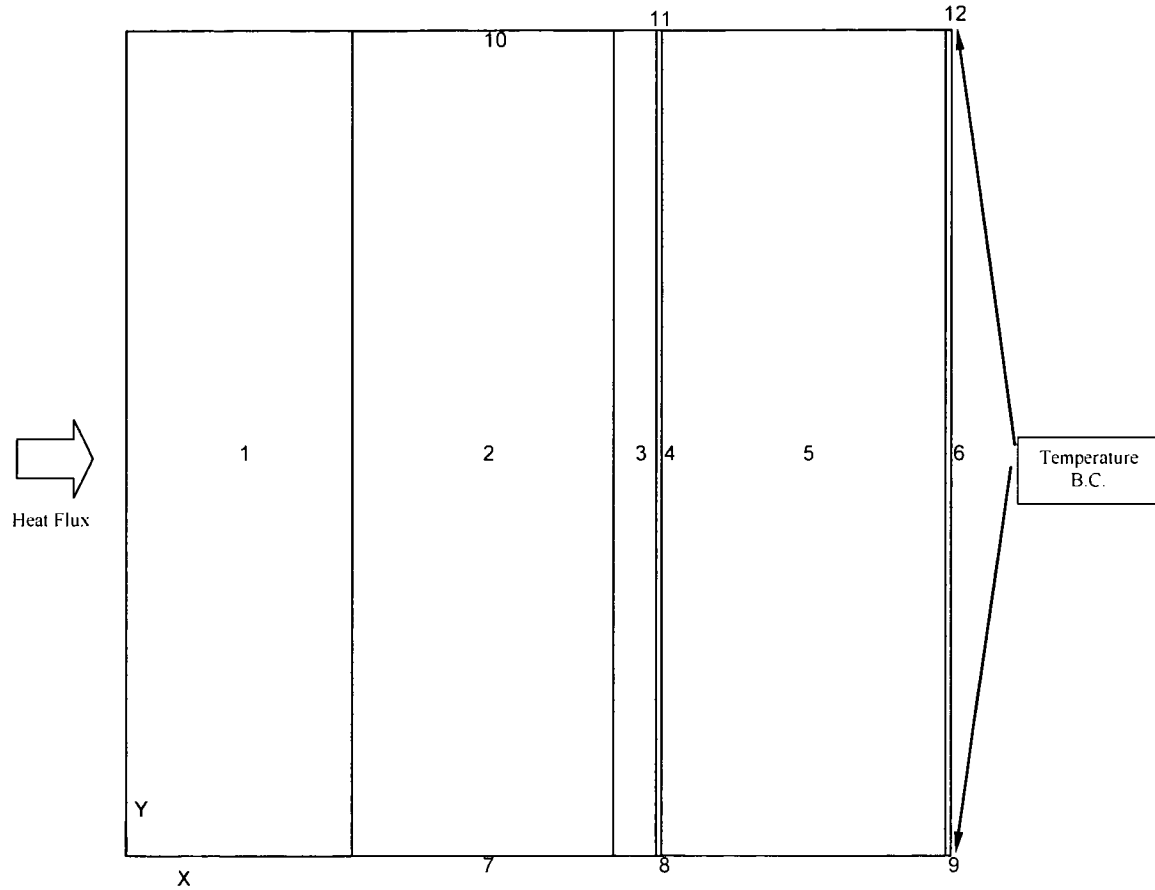


Figure 4.4-10 Neutron Absorber Model for PWR Fuel Tube



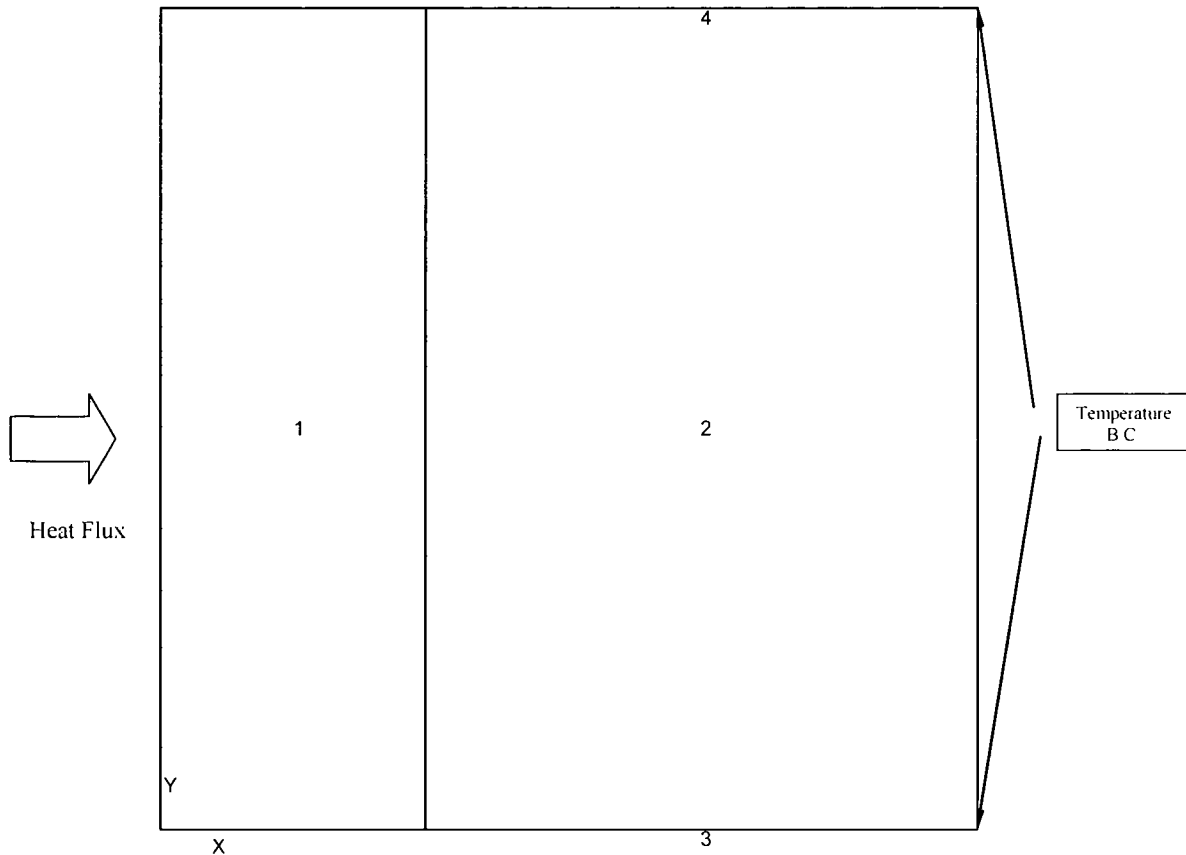
Element Number	Description
1	Stainless Steel Retainer Strip
2	Media – Helium or water
3	Neutron Absorber
4	Media – Helium
5,7	Radiation Links (between stainless steel and neutron absorber)
6,8	Radiation Links (between aluminum and nickel plated carbon steel)

Figure 4.4-11 BWR Fuel Tube Configuration with Channel and Neutron Absorber



Element Number	Description
1	Zirconium-based alloy (BWR fuel channel)
2, 4, 6	Media – Helium or water
3	Stainless Steel Retainer Strip
5	Neutron Absorber
7, 10	Radiation Links (between zirconium-based alloy and stainless steel)
8, 11	Radiation Links (between stainless steel and aluminum)
9, 12	Radiation Links (between aluminum and nickel-plated carbon steel)

Figure 4.4-12 BWR Fuel Tube Configuration with Channel, but without the Neutron Absorber



Element Number	Description
1	Zirconium-based alloy (BWR fuel channel)
2	Media ---- Helium or water
3, 4	Radiation Links (between zirconium-based alloy and nickel-plated carbon steel)

Figure 4.4-13 Two-Dimensional Model of Transfer Cask Loaded with a PWR TSC

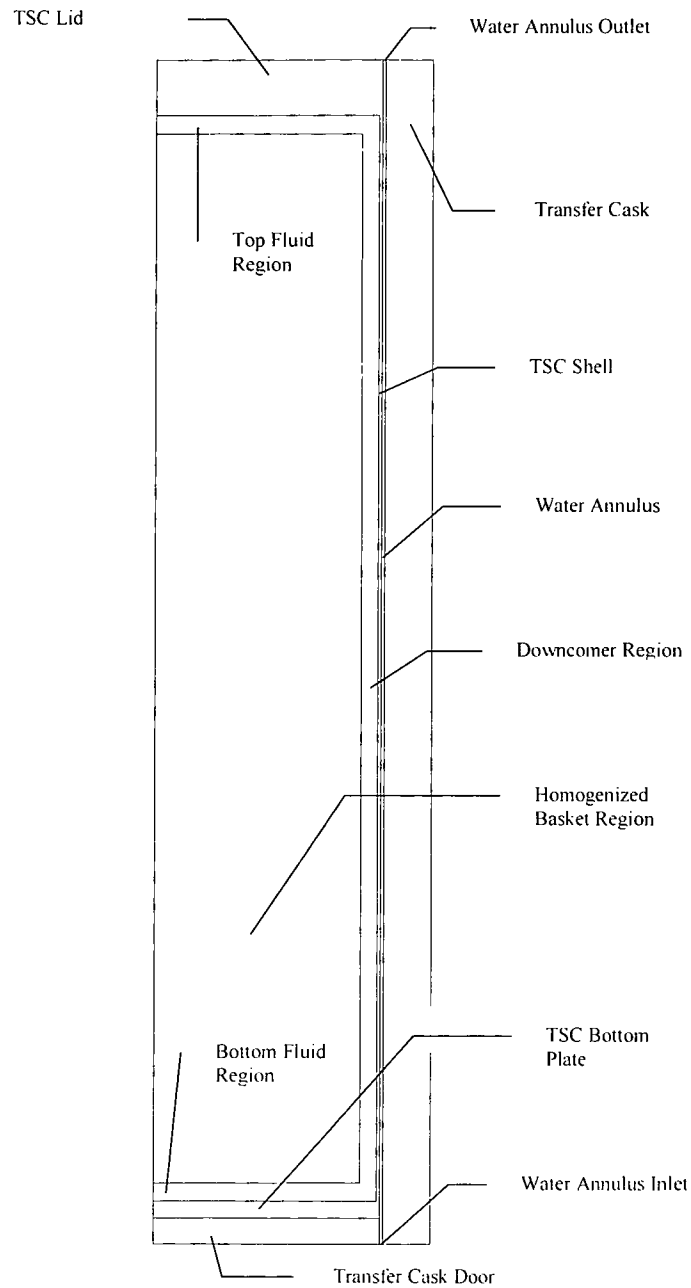


Figure 4.4-14 Temperature (°F) Distribution for the CC1/CC2 Concrete Cask and TSC  
Containing a Design Basis PWR Heat Load

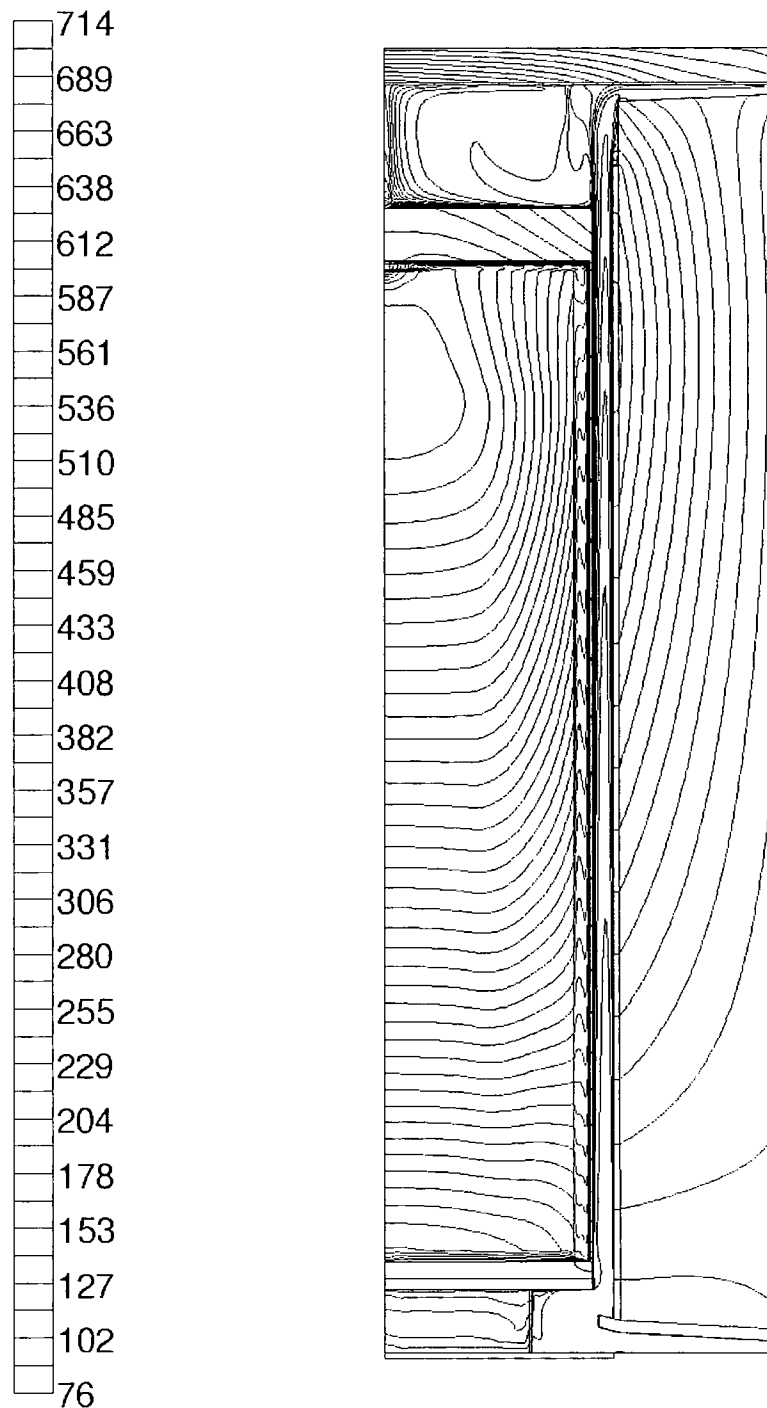


Figure 4.4-15 Air Velocity (m/s) in the CC1/CC2 Concrete Cask Annulus for the Design Basis PWR Heat Load

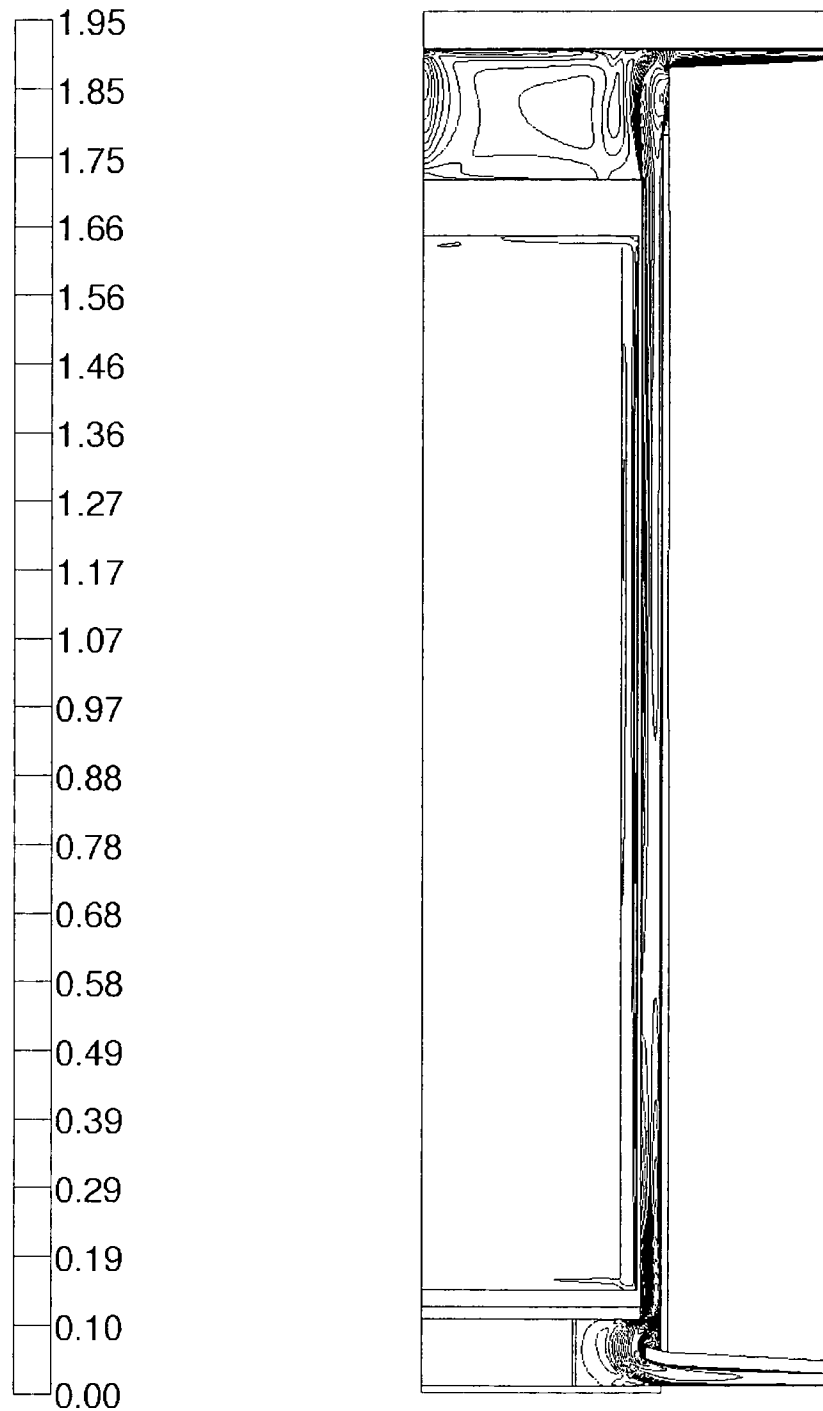


Figure 4.4-16 Three-Dimensional ANSYS Model of the PWR Canister for Vacuum Drying Condition

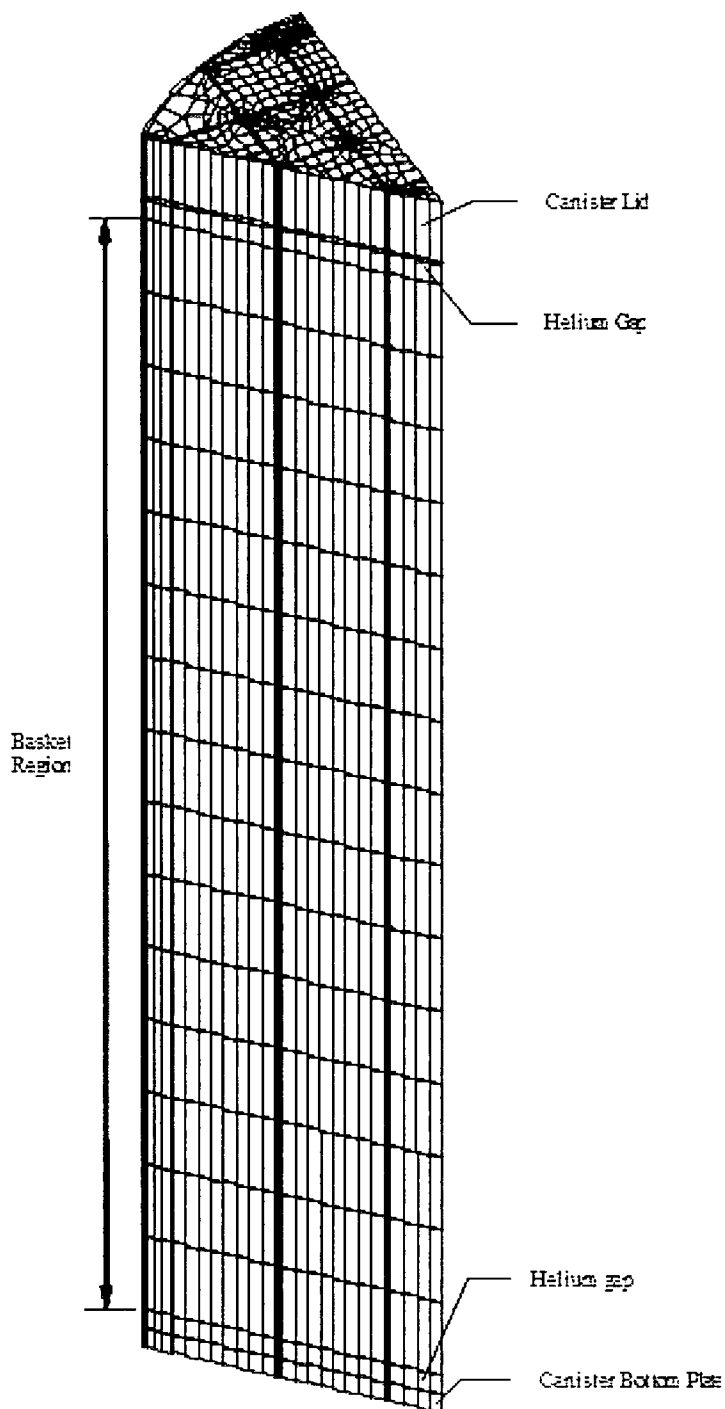




Figure 4.4-17 Detailed View of the Three-Dimensional ANSYS Model of the PWR Canister  
for Vacuum Drying Condition

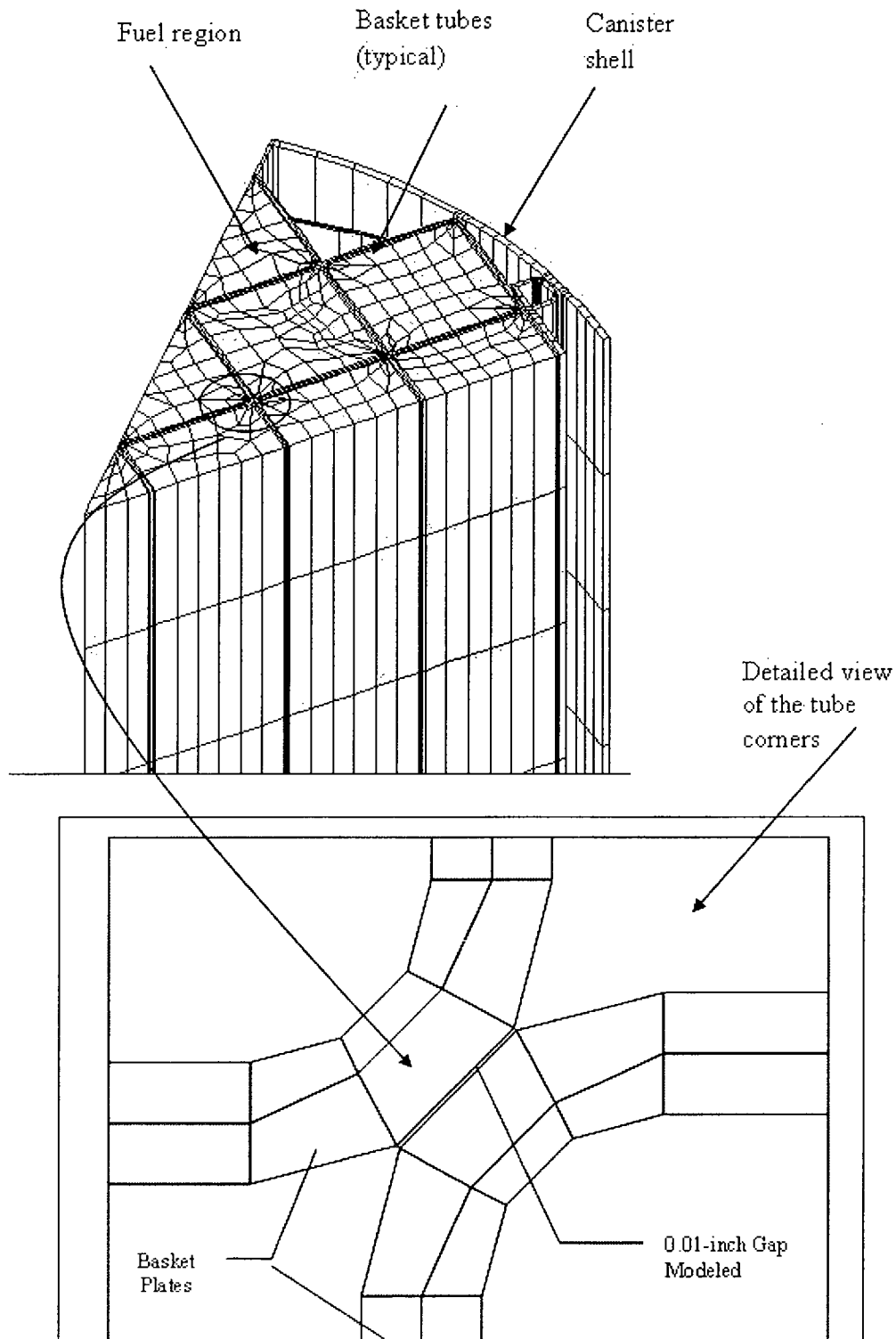


Figure 4.4-18 Three-Dimensional ANSYS Model of the BWR Canister for MTC Vacuum Drying Analyses

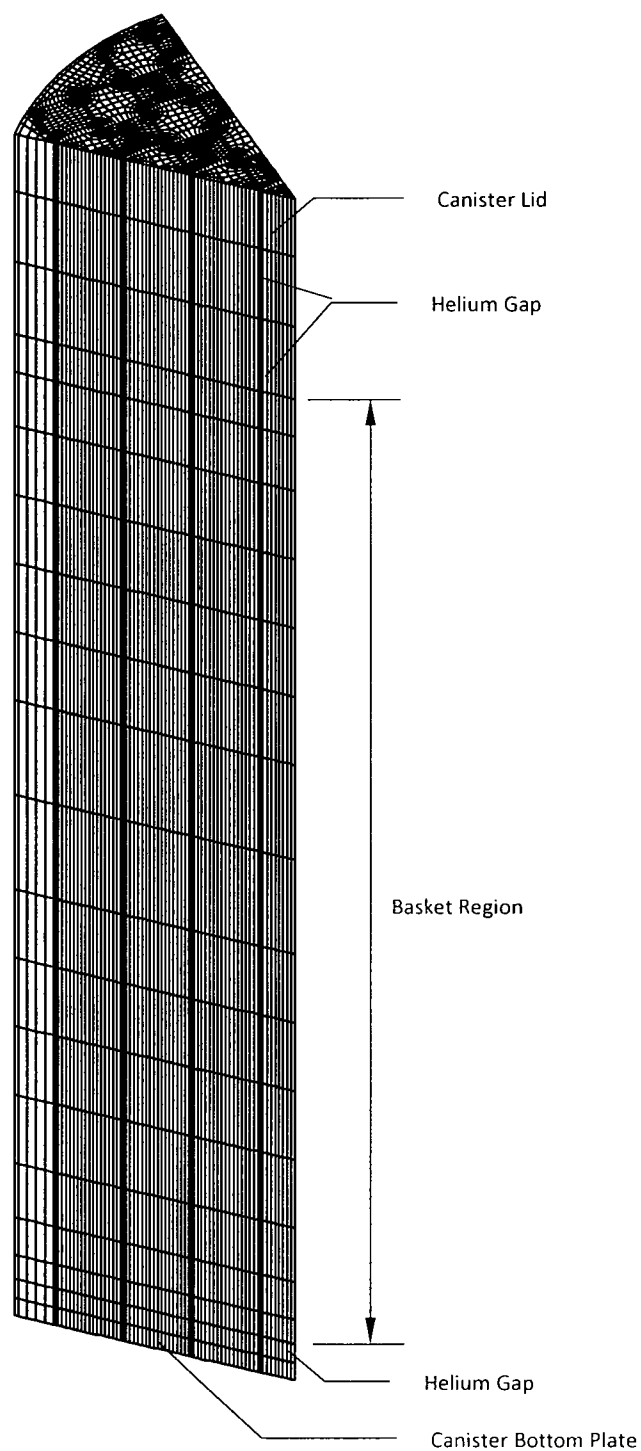


Figure 4.4-19 Detailed View of the Three-Dimensional ANSYS Model of the BWR Canister for MTC Vacuum Drying Analyses

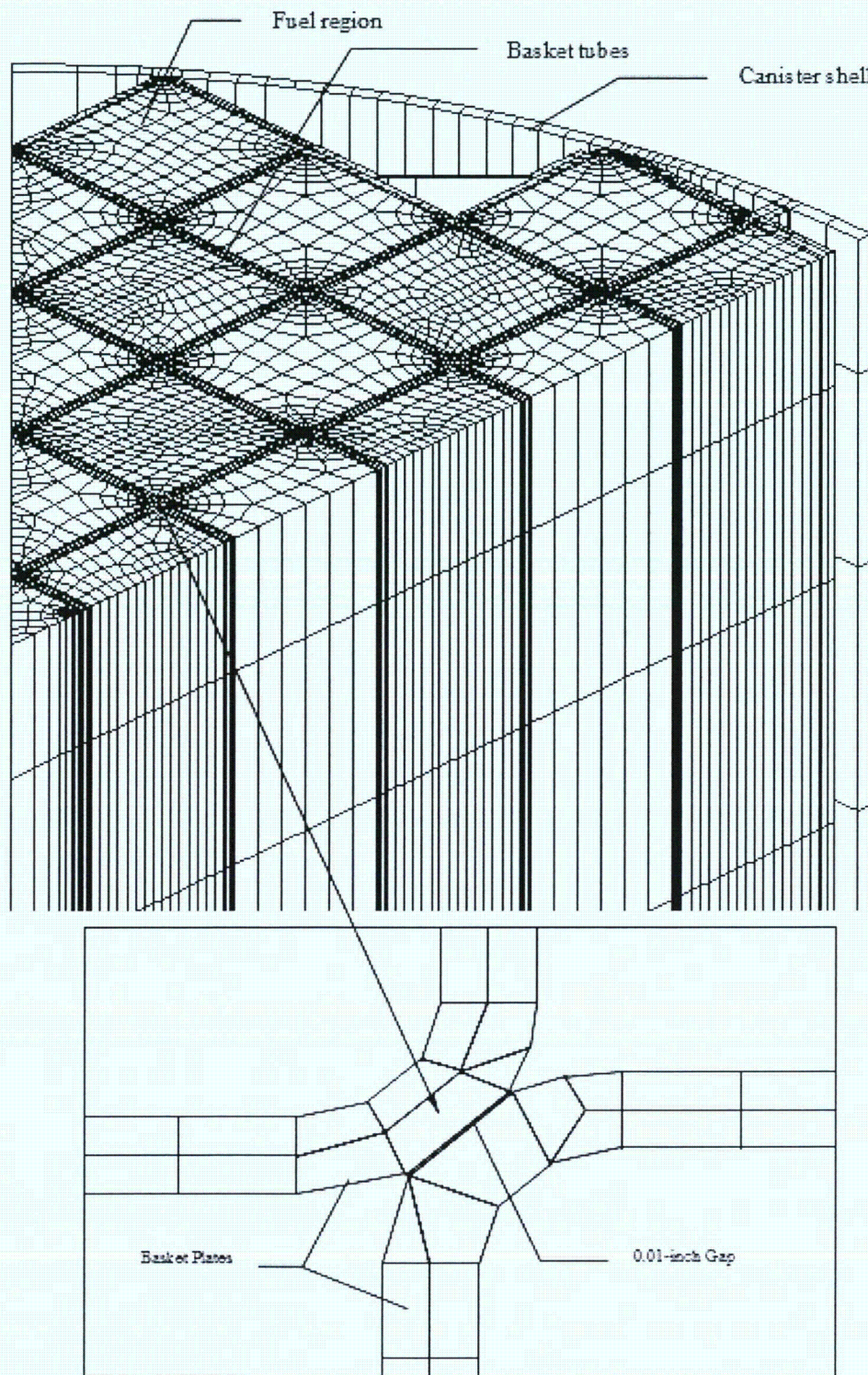
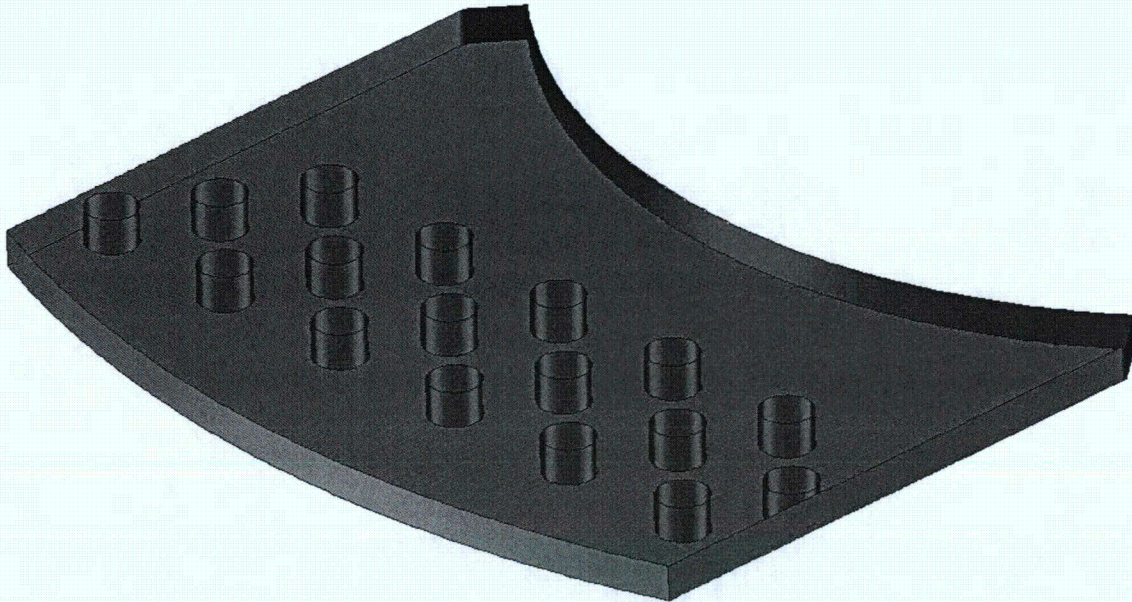




Figure 4.4-20 CC3 Concrete Cask Inlet Model Geometry



Note: The symmetry plane is the top surface (not shown).

Figure 4.4-21 CC3 Concrete Cask Inlet Model Mesh (Bottom Surface)

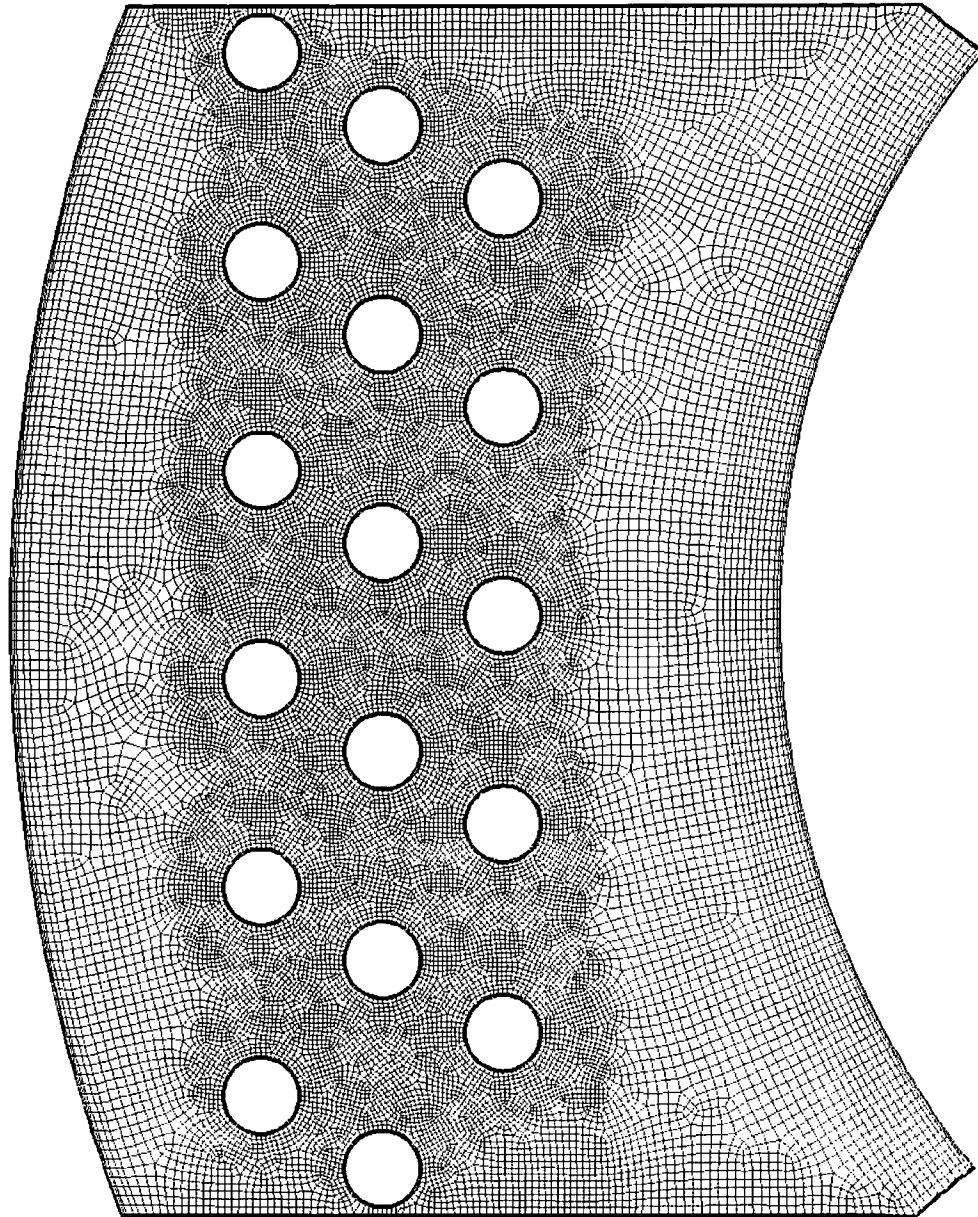
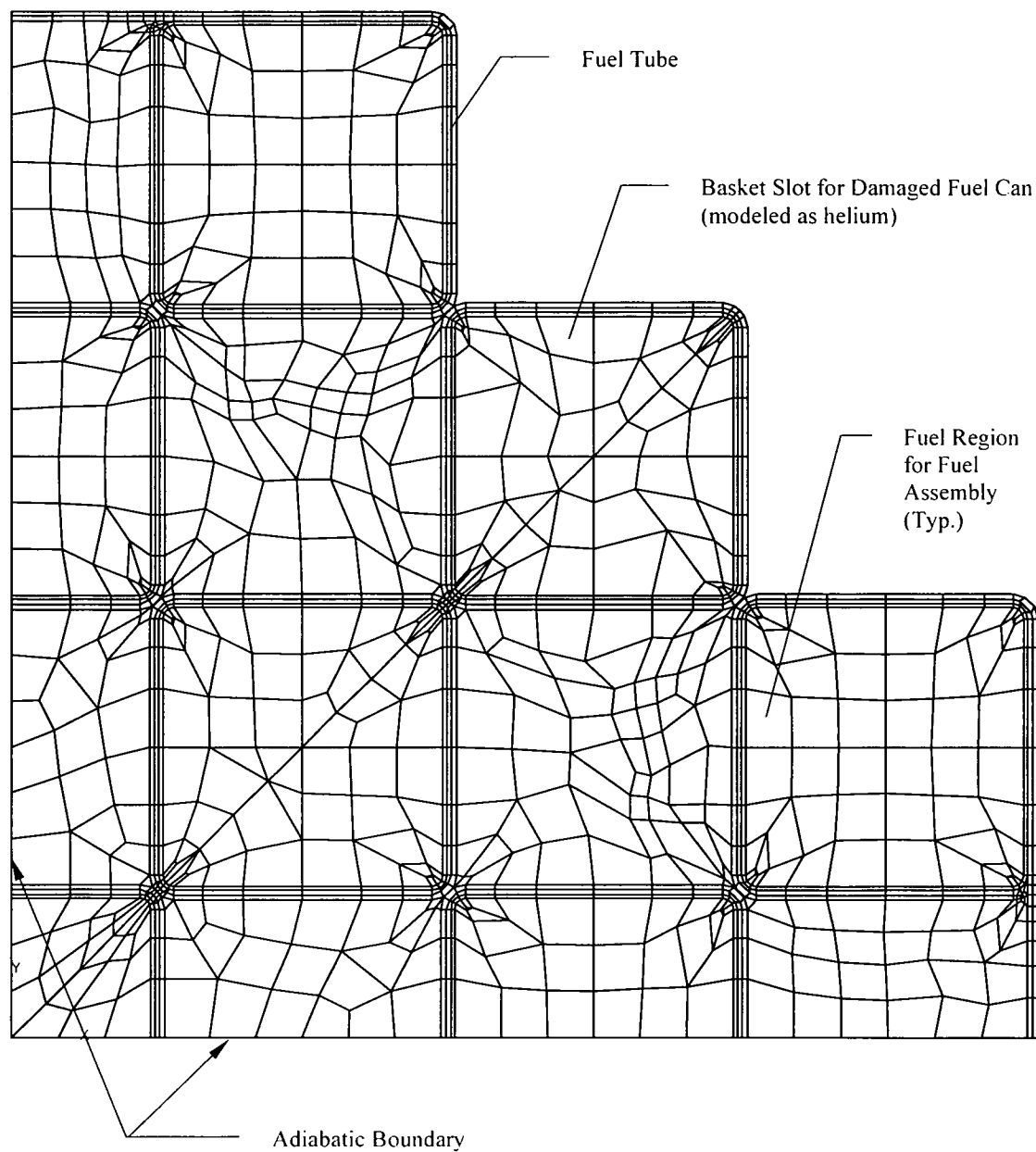


Figure 4.4-22 Two-Dimensional Finite Element Model of the DF Basket Assembly



**Table 4.4-1 Effective Thermal Conductivities for 14×14 PWR Fuel Assemblies for Helium Backfill**

For fuel assemblies in fuel tubes with the neutron absorber:

Conductivity <sup>a</sup> (Btu/hr-in-°F)	Temperature (°F)			
	221	415	612	813
K <sub>xx</sub>	0.019	0.026	0.036	0.048
K <sub>yy</sub>	0.019	0.026	0.036	0.048
K <sub>zz</sub>	0.124	0.115	0.111	0.112

For fuel assemblies in positions without the neutron absorber:

Conductivity <sup>a</sup> (Btu/hr-in-°F)	Temperature (°F)			
	222	417	615	816
K <sub>xx</sub>	0.019	0.025	0.034	0.044
K <sub>yy</sub>	0.019	0.025	0.034	0.044
K <sub>zz</sub>	0.127	0.117	0.114	0.115

**Table 4.4-2 Effective Thermal Conductivities for 10×10 BWR Fuel Assemblies for Helium Backfill**

Conductivity <sup>a</sup> (Btu/hr-in-°F)	Temperature (°F)			
	192	394	597	801
K <sub>xx</sub>	0.020	0.028	0.039	0.052
K <sub>yy</sub>	0.020	0.028	0.039	0.052
K <sub>zz</sub>	0.134	0.125	0.122	0.125

<sup>a</sup> K<sub>xx</sub> and K<sub>yy</sub> correspond to the in-plane directions and K<sub>zz</sub> corresponds to the axial direction in the basket.

**Table 4.4-3 Maximum Component Temperatures for Normal Condition  
Storage of Design Basis PWR and BWR Heat Loads**

Component		Maximum Temperatures (°F)				Allowable Temperature (°F)
		CC1/CC2		CC3	CC4	
		PWR	BWR	PWR	PWR	
Fuel Cladding		714	695	718	718	752
Fuel Basket <sup>a</sup>		714	695	718	718	800
TSC Shell		457	436	462	462	800
Concrete	local	271	241	256	271	300
	bulk	160	153	155	160	200

**Table 4.4-4 Helium Mass Per Unit Volume for MAGNASTOR TSCs**

Fuel Type	Helium Density (g/liter)		
	Nominal	Lower Bound	Upper Bound
PWR	0.763	0.694	0.802
BWR	0.774	0.704	0.814

<sup>a</sup> The maximum fuel cladding temperature is conservatively used.



Table 4.4-5 Maximum Fuel Temperature for Water Phase – PWR

HEAT LOAD (KW)	T <sub>MAX</sub> OF FUEL (°F)	T <sub>MAX</sub> OF CANISTER OD (°F)
35.5	131	118
30	127	116
25	124	114
20	120	112
15	116	109

Table 4.4-6 Maximum Fuel Temperature for Water Phase – BWR

HEAT LOAD (KW)	T <sub>MAX</sub> OF FUEL (°F)	T <sub>MAX</sub> OF CANISTER OD (°F)
33	129	117
30	127	116
25	124	114
20	120	112
15	116	109

**Table 4.4-7 Maximum Fuel Temperature for Helium Phase – PWR**

HEAT LOAD (KW)	T <sub>MAX</sub> OF FUEL (°F)	T <sub>MAX</sub> OF CANISTER OD (°F)
35.5	424	124
30	388	122
25	350	119
20	311	116
15	273	113

**Table 4.4-8 Maximum Fuel Temperature for Helium Phase – BWR**

HEAT LOAD (KW)	T <sub>MAX</sub> OF FUEL (°F)	T <sub>MAX</sub> OF CANISTER OD (°F)
33	419	123
30	396	122
25	358	119
20	319	116
15	279	116

**Table 4.4-9 Durations and the Temperature at the End of the Duration for the First Vacuum Stage (PWR)**

Heat Load (kW)	Vacuum Duration (hours)	T <sub>MAX</sub> at Steady State or at the End of the Duration (°F)	
		Fuel	Basket
15	No limit	509	483
20	No limit	627	599
25	No limit	739	709
30	32	643	614
35.5	24	640	612

**Table 4.4-10 Durations and the Temperature at the End of the Duration for the First Vacuum Stage (BWR)**

Heat Load (kW)	Vacuum Duration (hours)	T <sub>MAX</sub> at Steady State or at the End of the Duration (°F)	
		Fuel	Basket
15	No limit	444	431
20	No limit	547	532
25	No limit	647	630
29	No limit	723	706
30	44	656	639
33	33	645	628

**Table 4.4-11 Durations and the Temperature at the End of the Duration for the Second Vacuum Stage\* (PWR)**

Heat Load (kW)	Helium Backfill Duration (hours)	T <sub>MAX</sub> of Fuel/Basket at the End of the Helium Backfill (°F)	Second Vacuum Duration (hours)	T <sub>MAX</sub> of Fuel/Basket at the End of the Second Vacuum (°F)
35.5	24	460	11	640

\* For the cases with heat load higher than 25 kW, the duration and temperatures at the end of the duration shown in this table can be conservatively used.

**Table 4.4-12 Durations and the Temperature at the End of the Duration for the Second Vacuum Stage\* (BWR)**

Heat Load (kW)	Helium Backfill Duration (hours)	T <sub>MAX</sub> of Fuel/Basket at the End of the Helium Backfill (°F)	Second Vacuum Duration (hours)	T <sub>MAX</sub> of Fuel/Basket at the End of the Second Vacuum (°F)
33	24	447	16	645

\* For the cases with heat load larger than 29 kW, the duration and temperatures at the end of the duration shown in this table can be conservatively used.

Table 4.4-13      MTC to Concrete Cask (PWR) Transfer Times and Temperatures



Table 4.4-14      MTC to Concrete Cask (BWR) Transfer Times and Temperatures

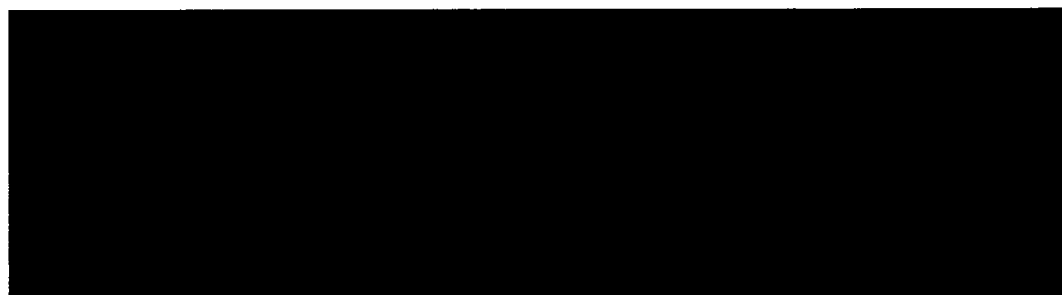


Table 4.4-15      TFR to Concrete Cask (PWR) Transfer Times and Temperatures for 20 kW (no cooling) and 25 kW (7 hours of cooling)

Heat Load (kW)	Allowed Duration (hours)	T <sub>MAX</sub> of Fuel/Basket at the End of the Transfer from TFR to Concrete Cask (°F)
≤ 20	No Limit	
≤ 25	70.5	

Table 4.4-16 Durations Allowed and the Maximum PWR Fuel Clad Temperatures for  
the Operation Using Reduced Vacuum Times, Reduced Cooling Time  
and Eight Hours of Handling

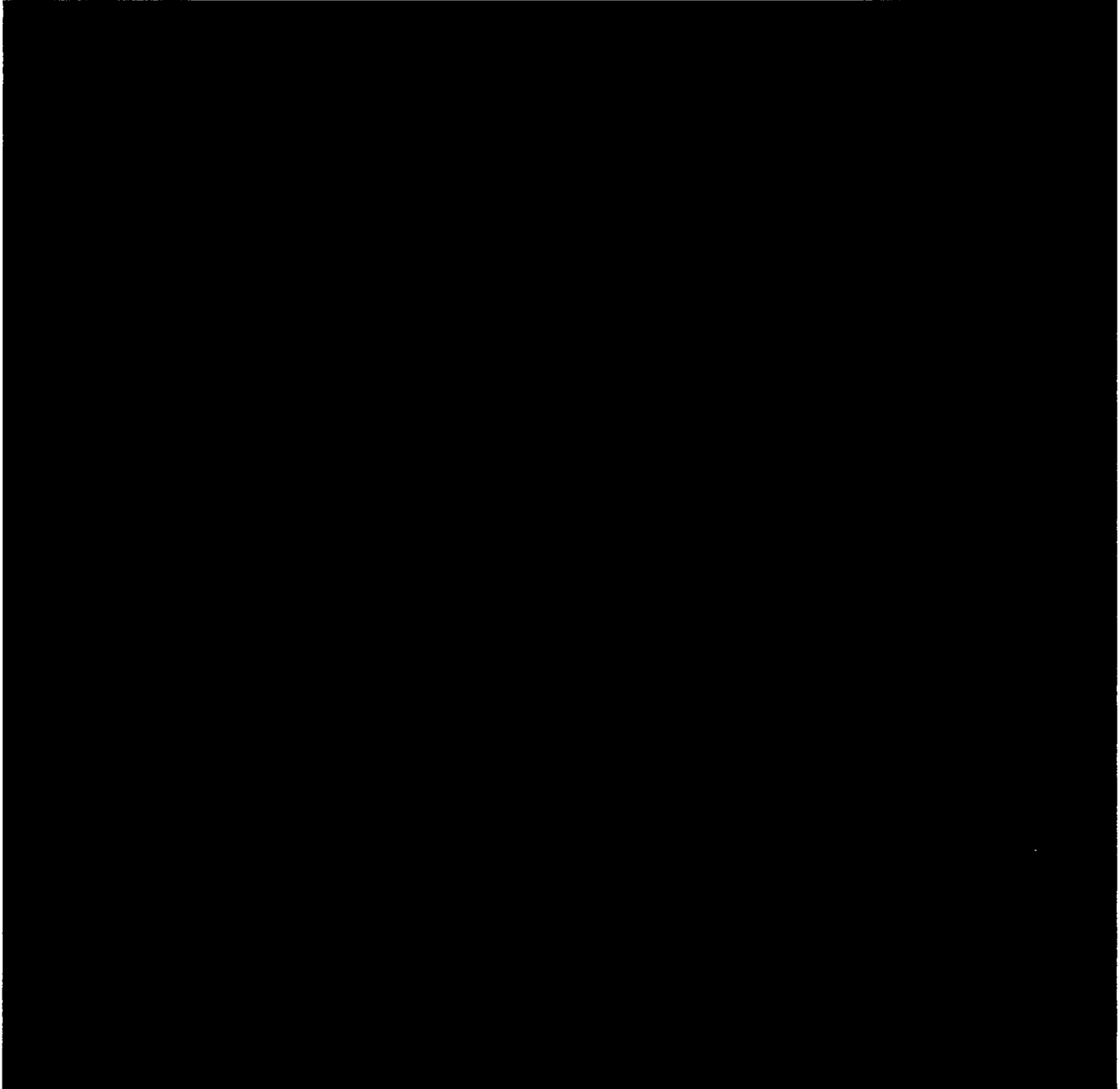
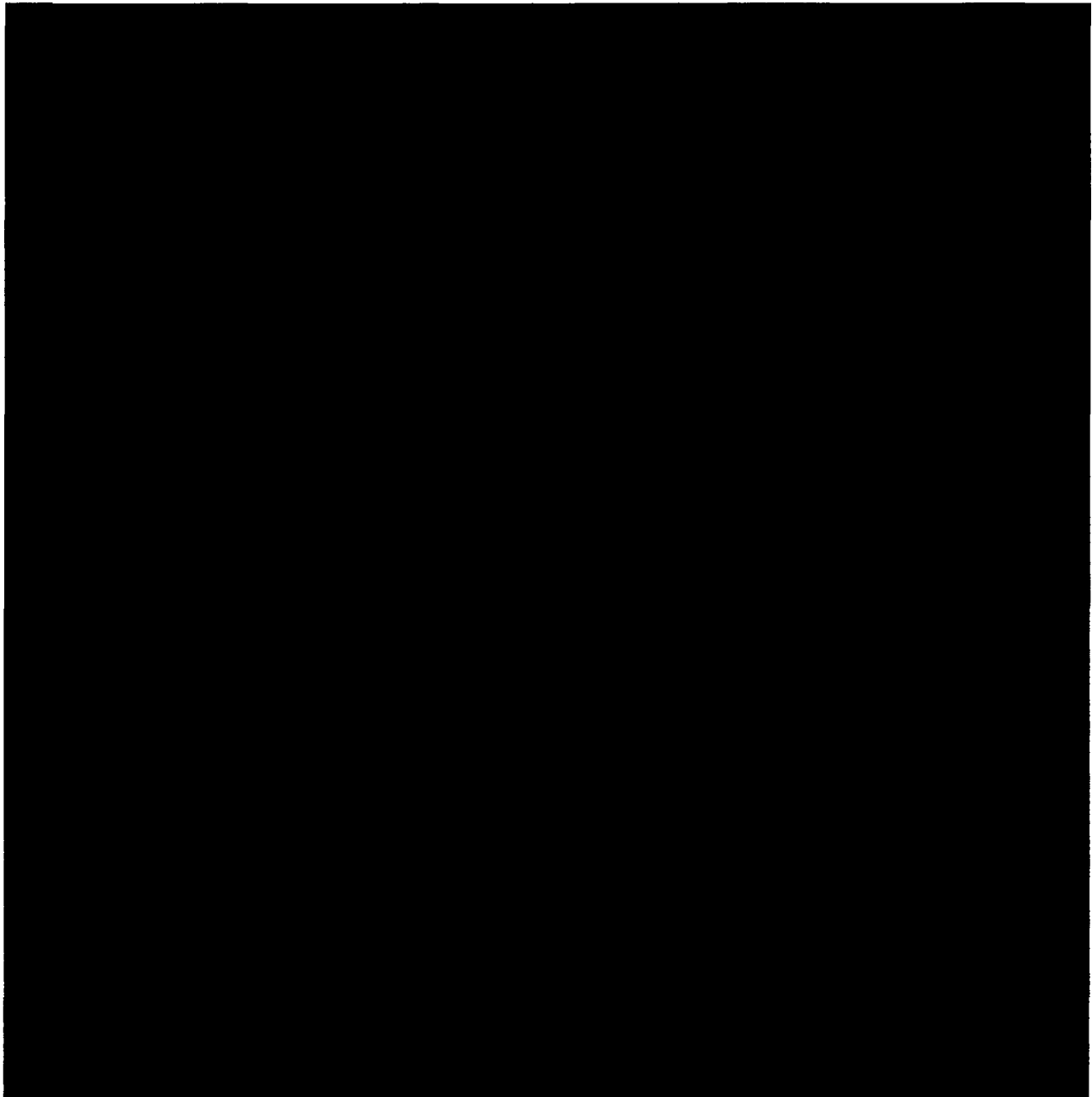


Table 4.4-17      Durations Allowed and the Maximum BWR Fuel Clad Temperatures for  
the Operation Using Reduced Vacuum Times, Reduced Cooling Time  
and Eight Hours of Handling



#### 4.5 Off-Normal Events

This section evaluates postulated off-normal storage and off-normal transfer phase events that might occur once during any calendar year of operation. The actual occurrence of any of these events is, therefore, infrequent.

##### 4.5.1 Off-Normal Storage Events

The concrete cask and TSC model described in Section 4.4.1.1 is used for the evaluation of the concrete cask and TSC for the off-normal events: severe ambient temperature conditions (106°F and -40°F) and the half-blocked air inlets condition. The evaluation of the off-normal events for variations in the ambient temperature only requires a change to the boundary condition temperature. For the half-blocked air inlets condition, the air inlet condition is modified to permit only half of the air flow into the inlet. The design basis heat loads of 35.5 kW and 33 kW are used in the evaluations of the concrete cask and TSC containing PWR and BWR fuels, respectively. As shown in Section 4.4.1 and Section 4.4.3, the analysis results for the standard PWR basket bound the analysis results for the DF basket assembly for normal conditions due to the higher thermal conductivity of the DF basket assembly. This conclusion is valid for the off-normal conditions for the same reasons. As shown in Section 4.4.3, the analysis results for the standard PWR basket bound the analysis results for the PWR minimum reduced cool time fuel basket assembly for normal conditions due to the heat distribution of the preferential loading of the PWR minimum reduced cool time fuel basket assembly. The heat distribution for the preferential loading removes the maximum heat load from the basket center. This conclusion is valid for the off-normal conditions for the same reasons.

The principal component temperatures for each of the off-normal events, discussed previously, are summarized in the following tables, along with the allowable temperatures. Note that the maximum fuel cladding temperatures are conservatively used as the maximum fuel basket temperatures. As the tables show, the component temperatures for the concrete cask and TSC containing PWR and BWR fuels are within the allowable values for the off-normal storage events.

Principal Component Temperatures – Off-Normal Storage of CC1/CC2 with PWR TSC

Component	106°F Ambient, Maximum Temperatures (°F)	-40°F Ambient, Maximum Temperatures (°F)	76°F Ambient/Half Blocked Air Inlets Temperatures (°F)	Allowable Temperature (°F)
Fuel Cladding	752	603	717	1,058
Fuel Basket	752	603	717	1,000
TSC Shell	485	336	459	800
Concrete	311	118	274	350



Principal Component Temperatures – Off-Normal Storage of CC3 with PWR TSC

Component	106°F Ambient, Maximum Temperatures (°F)	-40°F Ambient, Maximum Temperatures (°F)	76°F Ambient/Half Blocked Air Inlets Temperatures (°F)	Allowable Temperature (°F)
Fuel Cladding	756	617	720	1,058
Fuel Basket	756	617	720	1,000
TSC Shell	490	353	465	800
Concrete	296	96	259	350

Principal Component Temperatures – Off-Normal Storage of CC4 with PWR TSC

Component	106°F Ambient, Maximum Temperatures (°F)	-40°F Ambient, Maximum Temperatures (°F)	76°F Ambient/Half Blocked Air Inlets Temperatures (°F)	Allowable Temperature (°F)
Fuel Cladding	756	617	720	1,058
Fuel Basket	756	617	720	1,000
TSC Shell	490	353	465	800
Concrete	311	118	274	350

Principal Component Temperatures – Off-Normal Storage of CC1/CC2 with BWR TSC

Component	106°F Ambient, Maximum Temperatures (°F)	-40°F Ambient, Maximum Temperatures (°F)	76°F Ambient/Half Blocked Air Inlets Temperatures (°F)	Allowable Temperature (°F)
Fuel Cladding	733	585	698	1,058
Fuel Basket	733	586	698	1,000
TSC Shell	464	318	438	800
Concrete	282	99	247	350

There are no adverse consequences due to these off-normal events. The maximum component temperatures are less than the allowable temperature limits.

#### **4.6            Accident Events**

This section presents the evaluations of the thermal accident design events, which address very low probability events that might occur once during the lifetime of the ISFSI or hypothetical events that are postulated because their consequences may result in the maximum potential impact on the surrounding environment. Three thermal accident events are evaluated in this section: maximum anticipated heat load, fire accident and full blockage of the air inlets. The maximum TSC internal pressure for the bounding accident conditions is evaluated in Section 4.6.4.

The concrete cask and TSC model described in Section 4.4.1.1 is used for the evaluation of the concrete cask and TSC for these thermal accident events. Since the CC3 concrete cask containing the PWR TSC has the same heat load and almost the same thermal mass as the CC1/CC2 concrete cask containing the PWR TSC, the thermal response is essentially the same for CC1/CC2 and CC3 for the fire accident and the full blockage event.

As shown in Section 4.4.1 and Section 4.4.3, the analysis results for the standard PWR basket bound the analysis results for the DF basket assembly for normal conditions due to the higher thermal conductivity of the DF basket assembly. This conclusion is valid for the accident conditions for the same reasons.

As shown in Section 4.4.3, the analysis results for the standard PWR basket bound the analysis results for the PWR minimum reduced cool time fuel basket assembly for normal conditions due to the heat distribution of the preferential loading of PWR minimum reduced cool time fuel basket assembly. This conclusion is valid for the accident conditions for the same reasons.

##### **4.6.1            Analysis of Maximum Anticipated Ambient Heat Load**

This section evaluates the concrete cask and the TSC for the postulated accident event of an ambient temperature of 133°F. A steady state condition is considered in the thermal evaluation of the system for this accident event.

Using the same methods and thermal models described in Section 4.4.1.1 for the normal conditions of storage, thermal evaluations are performed for the concrete cask and the TSC with its contents for this accident condition. All boundary conditions in the model are the same as those used for the normal condition evaluation, except that an ambient temperature of 133°F is used. The maximum calculated temperatures of the principal PWR and BWR cask component, with the corresponding allowable temperatures, are as follows.

Component	Maximum Temperature (°F)				Allowable Temperature (°F)
	CC1/CC2		CC3	CC4	
	PWR	BWR	PWR	PWR	
Fuel Cladding	786	767	790	790	1,058
Fuel Basket	786	767	790	790	1,000
TSC Shell	510	489	514	514	850
Concrete	347	318	332	347	350

Note that the maximum fuel cladding temperatures are conservatively considered to be the maximum basket temperatures. This evaluation shows that the component temperatures are within the allowable temperatures for the extreme ambient temperature conditions.

#### 4.6.2 Fire Accident

A fire may be caused by flammable material or by a transport vehicle. While it is possible that a transport vehicle could cause a fire while transferring a loaded storage cask at the ISFSI, this fire will be confined to the vehicle and will be rapidly extinguished by the persons performing the transfer operations or by the site fire crew. Fuel in the fuel tanks of the concrete cask transport vehicle and/or prime mover (maximum 50 gallons) is the only flammable liquid that could be near a concrete cask, and potentially at, or above, the elevation of the surface on which the cask is supported. The fuel carried by other onsite vehicles or by other equipment used for ISFSI operations and maintenance, such as air compressors or electrical generators, is considered not to be within the proximity of a loaded cask on the ISFSI pad. Site-specific analysis of fire hazards will evaluate the specific equipment used at the ISFSI and determine any additional controls required.

The analyzed area is a 15×15-foot square, less the 136 in-diameter footprint of the concrete cask, corresponding to the center-to-center distance of the concrete casks on the ISFSI pad. The potential depth (D) of the 50-gallon pool of flammable liquid is calculated as follows.

$$D = \frac{50 \times 231}{15 \times 15 \times 144 - 3.14 \times 128^2 / 4} = 0.6 \text{ in.}$$

With a burning rate of 5 in/hr, the fire would continue for 7.2 minutes. The fire accident evaluation in this section conservatively considers an 8-minute fire. The temperature of the fire is taken to be 1,475°F, which is specified for the fire accident event in 10 CFR 71.73c [3].

The fire condition is an accident event and is initiated with the concrete cask in a normal operating steady-state condition. To determine the maximum temperatures of the concrete cask components, the two-dimensional axisymmetric model of the concrete cask and TSC for the PWR configuration described in Section 4.4.1.1 is used to perform a transient analysis. The PWR

configuration is considered to bound the BWR configuration due to the higher initial temperatures of the normal condition.

The initial condition of the fire accident transient analysis is based on the steady-state analysis results for the normal condition of storage, which corresponds to an ambient temperature of 100°F in conjunction with solar insolation (as specified in Section 4.4.1.1). The fire condition is implemented by applying a boundary temperature condition of 1,475°F at the air inlet and the lower surface of the steel plate forming the top of the air inlet for eight minutes. This boundary condition temperature is applied as a stepped boundary condition. During the eight-minute fire, solar insolation is also applied to the outer surface of the concrete cask. At the end of the eight minutes, the temperature at the inlet is reset to the ambient temperature of 100°F. The cooldown phase is continued for an additional 10.7 hours to observe the maximum TSC shell temperature and the average temperature of the TSC contents.

The maximum fuel temperature increased by less than 3°F, thus remaining well below the accident event temperature limit of 1,058°F. The maximum temperature of the TSC shell increases to 512°F due to the fire condition. The limited duration of the fire, the large thermal capacitance of the concrete cask, and the minimal thermal conductivity limit the local region where the concrete temperatures exceed 300°F to less than 10 inches above the top surface of the air inlets. These results confirm that the operation of the concrete cask is not adversely affected during and after the fire accident condition.

#### **4.6.3      Full Blockage of Concrete Cask Air Inlets**

This section evaluates the concrete cask for the transient condition of full blockage of the air inlets at the normal storage condition temperature (100°F).

The accident temperature conditions are evaluated using the concrete cask and TSC thermal models described in Section 4.4.1.1. The transient analysis assumes initial normal storage conditions, with the sudden loss of convective cooling of the TSC. This is simulated by removing the inlet and outlet conditions from the model. Heat is then rejected from the TSC to the concrete cask liner only by radiation and convection. The loss of convective cooling to the ambient environment results in a sustained heat-up of the TSC and its contents and the concrete cask. The maximum fuel cladding temperature, maximum basket temperature, and the maximum concrete bulk temperature remain less than the allowable accident temperatures for approximately 72 hours after the initiation of the event. However, the internal pressure in the TSC cavity will reach the analyzed maximum pressure condition of 250 psig in approximately 58 hours after the initiation of a complete blockage event.

The evaluation demonstrates that there are no adverse consequences due to this accident, provided that debris is cleared from at least two air inlets within 58 hours based on the steady-state evaluation of the half-blocked air inlet condition in Section 4.5.

#### **4.6.4      Maximum TSC Internal Pressure for Accident Events**

Accident event pressures are evaluated with the method and inputs documented in the normal condition pressure evaluation (Section 4.4.4). System conditions incorporated in the accident analysis are an increased rod failure fraction and an increase in the average gas temperature of the TSC. A 100% rod failure fraction is applied in the system pressure calculation in conjunction with normal system temperatures. The second accident pressure evaluation applies the bounding thermal accident TSC average gas temperature to a TSC with a 1% (normal condition) fuel failure fraction. The bounding thermal accident, and associated pressure increase, is the result of the air inlets full blocked thermal evaluation. The average TSC gas temperature applied in the thermal accident pressure evaluation is a conservative 684°F compared to 677°F calculated for this condition. Maximum calculated TSC internal pressures for the PWR and BWR systems are documented as follows.

<b>System</b>	<b>100% Fuel Failure</b>	<b>Inlets Blocked</b>
PWR (undamaged fuel basket)	221 psig	130 psig
PWR (damaged fuel basket)	226 psig	130 psig
BWR	159 psig	129 psig

## Chapter 5 Shielding Evaluation

### Table of Contents

5	SHIELDING EVALUATION .....	5-1
5.1	Cask Shielding Discussion and Dose Results .....	5.1-1
5.1.1	Transfer Cask Shielding Discussion and Dose Results .....	5.1-1
5.1.2	Concrete Cask Shielding Discussion and Dose Results .....	5.1-4
5.1.3	Offsite Dose Discussion and Results .....	5.1-5
5.2	Source Specification .....	5.2-1
5.2.1	Gamma Source .....	5.2-3
5.2.2	Neutron Source .....	5.2-4
5.2.3	Bounding Gamma and Neutron Spectrum .....	5.2-5
5.3	Axial Burnup Profile .....	5.3-1
5.4	Axial Source Profile .....	5.4-1
5.4.1	Neutron and Gamma Source Rates Related to Burnup .....	5.4-1
5.5	Model Specification .....	5.5-1
5.5.1	Description of Radial and Axial Shielding Configurations .....	5.5-2
5.5.2	MCNP Detector Mesh Definition .....	5.5-3
5.5.3	NAC-CASC Model .....	5.5-3
5.5.4	Offsite Particulate and Gas Release .....	5.5-4
5.5.5	Shield Regional Densities .....	5.5-5
5.6	Shielding Evaluation .....	5.6-1
5.6.1	Calculation Methods .....	5.6-1
5.6.2	Flux-to-Dose Rate Conversion Factors .....	5.6-3
5.6.3	Cask Dose Rate and Exposure Results .....	5.6-3
5.6.4	NAC-CASC Dose Evaluation .....	5.6-4
5.6.5	Surface Contamination Release .....	5.6-4
5.7	References .....	5.7-1
5.8	Shielding Evaluation Detail .....	5.8-1
5.8.1	Contents Description .....	5.8.1-1
5.8.2	Response Function Method .....	5.8.2-1
5.8.3	37-Assembly PWR System .....	5.8.3-1
5.8.4	87-Assembly BWR System .....	5.8.4-1
5.8.5	PWR Nonfuel Hardware Components - BPRA and Thimble Plug .....	5.8.5-1
5.8.6	Nonfuel Hardware Component – Reactor Control Elements .....	5.8.6-1
5.8.7	Preferential Loading of PWR Fuel .....	5.8.7-1

Table of Contents (cont'd)

5.8.8	Sample Input Files .....	5.8.8-1
5.8.9	Cool-Time Tables .....	5.8.9-1
5.8.10	Axial Zoned Fuel/End Blanket Discussion.....	5.8.10-1
5.8.11	Transfer Cask Moderator Condition Study.....	5.8.11-1
5.8.12	PWR Damaged Fuel .....	5.8.12-1
5.8.13	Nonfuel Hardware Components – Neutron Sources, Reconstituted Assemblies, and Hafnium Flux Reduction Assemblies.....	5.8.13-1
5.9	PWR Reduced Minimum Cool Time and Alternate Preferential Heat Load Pattern Shielding Evaluation Detail .....	5.9-1
5.9.1	Contents Description.....	5.9.1-1
5.9.2	Response Function Method.....	5.9.2-1
5.9.3	Undamaged Fuel - Uniform Heat Load Pattern Evaluation.....	5.9.3-1
5.9.4	PWR Nonfuel Hardware Components - BPRA and Thimble Plug .....	5.9.4-1
5.9.5	Nonfuel Hardware Component – Reactor Control Elements .....	5.9.5-1
5.9.6	Preferential Loading of PWR Fuel .....	5.9.6-1
5.9.7	Sample Input Files .....	5.9.7-1
5.9.8	Cool-Time Tables .....	5.9.8-1
5.9.9	Damaged Fuel .....	5.9.9-1
5.10	CE16 Four-Zone Preferential Heat Load Pattern Shielding Evaluation Detail .....	5.10-1
5.10.1	Contents Description.....	5.10.1-1
5.10.2	Response Function Method.....	5.10.2-1
5.10.3	Preferential Loading of CE 16x16 Fuel at a Minimum Cool time of 4 Years .....	5.10.3-1
5.10.4	Nonfuel Hardware Component – Reactor Control Elements .....	5.10.4-1
5.10.5	Damaged Fuel .....	5.10.5-1
5.10.6	Cool-Time Tables .....	5.10.6-1

**List of Figures (cont'd)**

Figure 5.8.8-12	Concrete Cask Sample Input File – Damaged PWR Fuel TSC – Lower End Fitting Damaged Fuel.....	5.8.8-89
Figure 5.8.8-13	CC4 Sample Input File.....	5.8.8-102
Figure 5.8.10-1	Millstone Sample Axial Burnup Profiles.....	5.8.10-3
Figure 5.8.11-1	PWR TSC Flood Study – Radial Surface Dose Rate Profile .....	5.8.11-2
Figure 5.8.11-2	PWR TSC Flood Study – Top Axial Surface Dose Rate Profile .....	5.8.11-2
Figure 5.8.11-3	BWR TSC Flood Study – Radial Surface Dose Rate Profile .....	5.8.11-3
Figure 5.8.11-4	BWR TSC Flood Study – Top Axial Surface Dose Rate Profile .....	5.8.11-3
Figure 5.8.12-1	Dose Rate Profile Comparison at Radial Surface of Transfer Cask – Active Fuel Damaged PWR Fuel – CE 14×14 .....	5.8.12-5
Figure 5.8.12-2	Dose Rate Profile Comparison at Top Surface of Transfer Cask – Active Fuel Damaged PWR Fuel – WE 14×14 .....	5.8.12-5
Figure 5.8.12-3	Dose Rate Profile Comparison at Bottom Surface of Transfer Cask – Active Fuel Damaged PWR Fuel – WE 14×14 .....	5.8.12-6
Figure 5.8.12-4	Dose Rate Profile at Radial Surface of Transfer Cask – Lower End Fitting Damaged PWR Fuel – WE 14×14 .....	5.8.12-6
Figure 5.8.12-5	Dose Rate Profile at Bottom Surface of Transfer Cask – Lower End Fitting Damaged PWR Fuel – WE 14×14 .....	5.8.12-7
Figure 5.8.12-6	Dose Rate Profile Comparison at Radial Surface of Standard Concrete Cask – Active Fuel Damaged PWR Fuel – CE 14×14.....	5.8.12-7
Figure 5.8.12-7	Dose Rate Profile Comparison at Top Surface of Standard Concrete Cask – Active Fuel Damaged PWR Fuel – CE 16×16 .....	5.8.12-8
Figure 5.8.12-8	Dose Rate Profile at Radial Surface of Concrete Cask – Lower End Fitting Damaged PWR Fuel – WE 14×14 .....	5.8.12-8
Figure 5.8.12-9	Concrete Cask Inlet Dose Rate Profile – Lower End Fitting Damaged PWR Fuel – WE 14×14.....	5.8.12-9
Figure 5.8.12-10	Schematic of DF Basket Assembly Configuration for PWR SNF with DFCs.....	5.8.12-10
Figure 5.8.12-11	Dose Rate Profile Comparison at Radial Surface of Transfer Cask – Active Fuel Damaged PWR Fuel – CE 14×14 – All Source Regions.	5.8.12-11
Figure 5.8.12-12	Dose Rate Profile Comparison at Radial Surface of Transfer Cask – Active Fuel Damaged PWR Fuel – WE 14×14 – All Source Regions and BPRAs.....	5.8.12-11
Figure 5.8.12-13	Dose Rate Profile Comparison at Radial Surface of Standard Storage Cask – Active Fuel Damaged PWR Fuel – CE 14×14 – All Source Regions .....	5.8.12-12
Figure 5.8.12-14	Dose Rate Profile Comparison at Radial Surface of Standard Storage Cask – Active Fuel Damaged PWR Fuel – WE 14×14 – All Source Regions and BPRAs.....	5.8.12-12
Figure 5.8.12-15	Dose Rate Profile Comparison at Radial Surface of CC4 Concrete Cask – Active Fuel Damaged PWR Fuel – CE 14x14.....	5.8.12-13
Figure 5.8.12-16	Dose Rate Profile Comparison at Top Surface of CC4 Concrete Cask – Active Fuel Damaged PWR Fuel – WE 14x14 .....	5.8.12-13



### List of Figures (cont'd)

Figure 5.8.12-17	Dose Rate Profile at Radial Surface of CC4 – Lower End Fitting Damaged PWR Fuel .....	5.8.12-14
Figure 5.8.12-18	CC4 Inlet Dose Rate Profile – Lower End Fitting Damaged PWR Fuel .....	5.8.12-14
Figure 5.8.13-1	Reconstituted Assembly Radial Dose Rate Comparison – Storage Cask.....	5.8.13-4
Figure 5.8.13-2	Reconstituted Assembly Radial Dose Rate Comparison – Transfer Cask.....	5.8.13-4
Figure 5.8.13-3	SAS2H Input for HFRA Source .....	5.8.13-5
Figure 5.9.3-1	Concrete Cask Side Dose Rate Profile at Various Distances – PWR (CC4).....	5.9.3-3
Figure 5.9.3-2	Concrete Cask Side Surface Dose Rate Profile by Source – PWR (CC4).....	5.9.3-4
Figure 5.9.6-1	Schematic of PWR Fuel 1.8 kW Preferential Loading Pattern.....	5.9.6-3
Figure 5.9.7-1	Transfer Cask Sample Input File – Preferential Zone B1 .....	5.9.7-2
Figure 5.9.7-2	Storage Cask Sample Input File – Preferential Zone B2 .....	5.9.7-10
Figure 5.9.9-1	Schematic of DF Basket Assembly Configuration for PWR SNF with DFCs .....	5.9.9-4
Figure 5.10.3-1	Schematic of PWR Fuel 1.8 kW Preferential Loading Pattern.....	5.10.3-2
Figure 5.10.5-1	Schematic of DF Basket Assembly Configuration for PWR SNF with DFCs .....	5.10.5-2

**List of Tables (cont'd)**

Table 5.8.4-9	BWR Bounding Surface Current Input Data <sup>a</sup> .....	5.8.4-30
Table 5.8.4-10	Rectangular Controlled Area Boundary for the 2×10 BWR Cask Array.....	5.8.4-30
Table 5.8.5-1	Sample Core Type BPRA Hardware Summary – Westinghouse 15×15 Core .....	5.8.5-7
Table 5.8.5-2	Bounding Regional Nonfuel Hardware Masses .....	5.8.5-7
Table 5.8.5-3	Allowed BPRA Burnup and Cool-time Combinations .....	5.8.5-8
Table 5.8.5-4	BPRA Dose Rate Contributions – Westinghouse 14×14 .....	5.8.5-8
Table 5.8.5-5	Allowed Thimble Plug Burnup and Cool-time Combinations.....	5.8.5-9
Table 5.8.5-6	Thimble Plug Dose Rate Contributions – Westinghouse 14×14.....	5.8.5-9
Table 5.8.5-7	Additional Assembly Cool Time (Years) Required to Load BPRA or TP (Uniform Loading).....	5.8.5-9
Table 5.8.6-1	Bounding CEA Descriptions.....	5.8.6-5
Table 5.8.6-2	CEA Dose Rate Contributions – Westinghouse 17×17.....	5.8.6-5
Table 5.8.6-3	Gamma Source Comparison for CEA Primary Absorber Materials .....	5.8.6-6
Table 5.8.6-4	Dose Rates from Ag-In-Cd Based CEAs as a Function of Exposure and Cool Time .....	5.8.6-7
Table 5.8.6-5	CEA Maximum Exposure and Minimum Cool Time Summary.....	5.8.6-7
Table 5.8.6-6	Additional Assembly Cool Time (Years) Required to Load a CEA (Uniform Loading) .....	5.8.6-7
Table 5.8.7-1	Preferential Pattern Dose Rate Results.....	5.8.7-4
Table 5.8.7-2	Additional Assembly Cool Time (Years) Required When Loading Nonfuel Hardware – Three-Zone Preferential Loading .....	5.8.7-5
Table 5.8.9-1	Low Burnup PWR Fuel Loading Table .....	5.8.9-2
Table 5.8.9-2	Loading Table for PWR Fuel – 959 W/Assembly .....	5.8.9-3
Table 5.8.9-3	Loading Table for PWR Fuel – 1,200 W/Assembly .....	5.8.9-8
Table 5.8.9-4	Loading Table for PWR Fuel – 922 W/Assembly .....	5.8.9-13
Table 5.8.9-5	Loading Table for PWR Fuel – 800 W/Assembly .....	5.8.9-18
Table 5.8.9-6	Loading Table for PWR Fuel – 911 W/Assembly .....	5.8.9-23
Table 5.8.9-7	Loading Table for PWR Fuel – 1,140 W/Assembly .....	5.8.9-31
Table 5.8.9-8	Loading Table for PWR Fuel – 876 W/Assembly .....	5.8.9-39
Table 5.8.9-9	Loading Table for PWR Fuel – 760 W/Assembly .....	5.8.9-47
Table 5.8.9-10	Low Burnup BWR Fuel Loading Table .....	5.8.9-56
Table 5.8.9-11	Loading Table for BWR Fuel – 379 W/Assembly .....	5.8.9-57
Table 5.8.9-12	Loading Table for BWR Fuel – 360 W/Assembly.....	5.8.9-62
Table 5.8.10-1	Zoned Fuel and Profile Effects on Source Magnitudes.....	5.8.10-4
Table 5.8.10-2	Millstone Zoned Fuel Effects on Source Magnitudes .....	5.8.10-5
Table 5.8.12-1	Damaged Fuel Material Summary – 14b PWR Fuel.....	5.8.12-15
Table 5.8.12-2	Transfer Cask Maximum Damaged PWR Fuel Dose Rates.....	5.8.12-15
Table 5.8.12-3	Standard Concrete Cask Maximum Damaged PWR Fuel Dose Rates .	5.8.12-16
Table 5.8.12-4	CC4 Maximum Damaged PWR Fuel Dose Rates.....	5.8.12-16
Table 5.8.13-1	HFRA vs. BPRA Source Comparison.....	5.8.13-6

**List of Tables (cont'd)**

Table 5.9.3-1	Maximum CC4 Surface Dose Rates – Reduced Cool Time .....	5.9.3-5
Table 5.9.4-1	Additional Assembly Cool Time (Years) Required to Load BPRA or TP .....	5.9.4-1
Table 5.9.4-2	Reduced Cool Time Combined Dose Rate Results .....	5.9.4-2
Table 5.9.5-1	Westinghouse CEA Dimensions .....	5.9.5-2
Table 5.9.5-2	Calculated WE 14x14 CEA Activated Mass.....	5.9.5-2
Table 5.9.5-3	CEA Dose Rate Contributions – Westinghouse 14x14.....	5.9.5-2
Table 5.9.5-4	Additional Assembly Cool Time (Years) Required to Load CEA.....	5.9.5-2
Table 5.9.6-1	Preferential Pattern Dose Rate Results.....	5.9.6-4
Table 5.9.8-1	Loading Table for PWR Fuel – 959 W/Assembly .....	5.9.8-2
Table 5.9.8-2	Loading Table for PWR Fuel – 513 W/Assembly .....	5.9.8-5
Table 5.9.8-3	Loading Table for PWR Fuel – 1,300 W/Assembly .....	5.9.8-8
Table 5.9.8-4	Loading Table for PWR Fuel – 1,800 W/Assembly .....	5.9.8-11
Table 5.9.8-5	Loading Table for PWR Fuel – 830 W/Assembly .....	5.9.8-14
Table 5.9.8-6	Loading Table for PWR Fuel – 487 W/Assembly .....	5.9.8-17
Table 5.9.8-7	Loading Table for PWR Fuel – 1235 W/Assembly .....	5.9.8-20
Table 5.9.8-8	Loading Table for PWR Fuel – 1710 W/Assembly .....	5.9.8-23
Table 5.9.8-9	Loading Table for PWR Fuel – 788 W/Assembly .....	5.9.8-26
Table 5.9.9-1	Damaged Fuel Material Summary – 14b PWR Fuel.....	5.9.9-5
Table 5.9.9-2	Preferentially Loaded Stainless Steel MTC Maximum Damaged Fuel Dose Rates .....	5.9.9-5
Table 5.9.9-3	Uniformly Loaded CC4 Maximum Damaged PWR Fuel Dose Rates.....	5.9.9-6
Table 5.9.9-4	Preferentially Loaded CC4 Maximum Damaged PWR Fuel Dose Rates .....	5.9.9-6
Table 5.10.3-1	Preferential Pattern Dose Rate Results.....	5.10.3-3
Table 5.10.4-1	CEA Dose Rate Contributions – CE 16x16 .....	5.10.4-1
Table 5.10.4-2	Additional Assembly Cool Time (Years) Required to Load CEA.....	5.10.4-1
Table 5.10.5-1	Preferentially Loaded Carbon Steel MTC Maximum Damaged CE16 Fuel Dose Rates.....	5.10.5-3
Table 5.10.5-2	Preferentially Loaded CC Maximum Damaged CE16 Fuel Dose Rates .....	5.10.5-4
Table 5.10.6-1	Loading Table for CE 16x16 Fuel – 513 W/Assembly.....	5.10.6-2
Table 5.10.6-2	Loading Table for CE 16x16 Fuel – 1,300 W/Assembly .....	5.10.6-5
Table 5.10.6-3	Loading Table for CE 16x16 Fuel – 1,800 W/Assembly .....	5.10.6-8
Table 5.10.6-4	Loading Table for CE 16x16 Fuel – 830 W/Assembly .....	5.10.6-11
Table 5.10.6-5	Loading Table for CE 16x16 Fuel – 487 W/Assembly .....	5.10.6-14
Table 5.10.6-6	Loading Table for CE 16x16 Fuel – 1235 W/Assembly .....	5.10.6-17
Table 5.10.6-7	Loading Table for CE 16x16 Fuel – 1710 W/Assembly .....	5.10.6-20
Table 5.10.6-8	Loading Table for CE 16x16 Fuel – 788 W/Assembly .....	5.10.6-23

## 5.1 Cask Shielding Discussion and Dose Results

The TSC is loaded and sealed inside a transfer cask and then moved into a concrete cask for placement on the ISFSI pad. Dose evaluations are performed for the various TSC contents when the TSC is inside the transfer cask or the concrete cask.

With the exception of the offsite dose discussion, the dose results are presented based on bounding heat loads and corresponding source terms based on a 35.5 kW PWR cask heat load and a 35 kW BWR cask heat load. Offsite dose results are produced by similar bounding values of a 40 kW PWR cask heat load and a 38 kW BWR cask heat load. Thermal evaluations restrict BWR payloads to 33 kW. Cool time tables for the thermally restricting payloads are listed in Section 5.8.9. Based on the code validation discussion in Section 5.2, a 5% uncertainty is applied to the heat loads for fuel burnups above 45 GWd/MTU. This results in an extension in minimum allowed cool time for high burnup fuel assemblies. All dose rates calculated at higher cask heat loads are bounding for the reduced heat load. For any fuel type, burnup, initial enrichment, and cool time combination allowed, additional cool time and, therefore, reduced sources are associated with the lower cask heat load. This conclusion applies also to the PWR preferential loading patterns.

A reduced minimum cool time of 2.5 years and four-zone preferential loading pattern (max 1.8 kW/assy heat load) are evaluated in Section 5.9 for undamaged or damaged PWR assemblies in the CC4 or MTC2.

Dose rates (detector tallies) in this chapter are calculated using Monte Carlo methods and, therefore, contain a result and statistical uncertainty of the result. The statistical uncertainty is expressed as a percentage and referred to as fractional standard deviation (FSD) or relative uncertainty.

### 5.1.1 Transfer Cask Shielding Discussion and Dose Results

The transfer cask radial shield is comprised of steel inner and outer shells connected by solid steel top and bottom forgings. The shell encloses a lead gamma shield and a solid borated polymer (NS-4-FR) neutron shield. The TSC shell and the basket internal structure provide additional radial shielding. The transfer operation bottom shielding is provided by the TSC bottom plate and solid steel transfer cask doors. The TSC closure lid provides radiation shielding at the top of the TSC.

The three-dimensional transfer cask shielding analysis provides a complete, nonhomogenized representation of the transfer cask and TSC structure. The model assumes the following TSC/transfer cask configuration for all dose rate evaluations.

- **Dry canister cavity**  
The majority of the TSC operations, in particular closure lid welding, are performed with the TSC cavity filled with water. Evaluating a dry canister cavity is conservative. Note that the water filling the TSC/transfer cask annulus between the inflatable seals is modeled. Transfer cask dose rates from a wet canister, while containing an increased neutron source due to a higher subcritical multiplication resulting from a higher  $k_{\text{eff}}$ , are lower than those of the dry system due to the additional radiation shielding provided by the water within and surrounding the source region. PWR and BWR confirmatory calculations comparing dry, wet and partially flooded canister configurations are included in Section 5.8.11.
- **6-in auxiliary weld shield**  
Closure lid weld operations are typically performed with an automated weld system that is mounted on a weld platform. The presence of this platform provides significant auxiliary shielding during the TSC closure operation.
- **Homogenization of the fuel assembly into five source regions**  
While TSC and concrete cask features are discretely modeled, the fuel assembly is homogenized into upper and lower end-fitting (nozzle) regions, upper and lower plenum regions (lower plenum regions are modeled only for B&W fuel assemblies), and an active fuel region. For shielded applications, such as in the heavily shielded spent fuel transfer and concrete casks, homogenizing the fuel region does not introduce a significant bias in the dose results presented.

#### **5.1.1.1      Undamaged Fuel Dose Rates**

The carbon steel and stainless steel transfer cask maximum calculated dose rates are shown in Table 5.1.3-1 and Table 5.1.3-4. Payload types producing maximum surface dose rates are listed in Table 5.1.3-3 and Table 5.1.3-6. TSC surface contamination release dose rates are shown in Section 5.6.5. Dose rates are based on a three-dimensional Monte Carlo analysis using surface detectors. Uncertainty in Monte Carlo results is indicated in parentheses. Further detail on the detector geometry is included in Section 5.5. There is no design basis off-normal or accident event that will affect the shielding performance of the transfer cask.

Transfer cask top-, side-, and bottom-surface average dose rates are 254 (1.1 %) mrem/hr, 895 (<1%) mrem/hr, and 3,000 (<1%) mrem/hr, respectively. Access to the bottom of the cask is limited to pool-to-workstation transfer operations and the workstation-to-vertical concrete cask transfer operations. Site ALARA plans should specify limited access to areas below and around the loaded transfer cask during lifting and transfer operations.

#### **5.1.1.2      Damaged PWR Fuel Dose Rates**

Damaged PWR fuel assemblies may be loaded in damaged fuel cans in the four corner assembly locations of the PWR damaged fuel basket. DFC slots are locations 4, 8, 30 and 34 in Figure 5.8.12-10. To ensure that the worst case configuration is considered, two damaged fuel scenarios are evaluated.

The first scenario assumes the damaged fuel collects over the active fuel length of the fuel assembly. This scenario is modeled by filling the fuel assembly interstitial volume with  $\text{UO}_2$  and increasing the fuel neutron, gamma and n-gamma source consistent with this increase in mass. Dose rate profiles for the 37-assembly undamaged assemblies are compared with profiles for 33 undamaged and 4 damaged assemblies in Section 5.8.12. Based on the self-shielding of the added mass compensating for the increase in source, damaged fuel dose rates for the first scenario are bounded by either the corresponding undamaged fuel dose rates or the second damaged fuel scenario.

In the second scenario, damaged fuel is assumed to migrate from the active fuel into the lower end fitting region of the fuel assembly, filling all the modeled void space. However, no credit is taken for the reduction in the lower end fitting hardware dose rate due to the added  $\text{UO}_2$  mass and self-shielding nor for the reduction in fuel mass migrated from the active fuel region. In this case, transfer cask bottom surface dose rates increase due to the addition of damaged fuel. The transfer cask bottom axial dose rate increases 53 mrem/hr, increasing the bottom axial dose rate by approximately 0.9 percent. Radial dose rates for PWR fuel increase, but remain less than the bounding BWR fuel.

Damaged fuel dose rates are computed using the carbon steel transfer cask, as it produces higher dose rates than the stainless steel transfer cask due to the higher density of stainless steel versus carbon steel.

Damaged fuel maximum dose rates in the carbon steel transfer cask are summarized in Table 5.1.3-9.

### **5.1.2      Concrete Cask Shielding Discussion and Dose Results**

The concrete cask is composed of body and lid components. The body contains the air inlets, air outlets, and the cavity for TSC placement. The lid provides environmental closure for the TSC. The radial shield design is comprised of a carbon steel inner liner surrounded by concrete. The concrete contains radial and axial rebar for structural support. As in the transfer cask, the TSC shell provides additional radial shielding. The concrete cask top shielding design is comprised of the TSC lid and concrete cask lid. The concrete cask lid incorporates both concrete and steel plate to provide additional gamma shielding. The bottom shielding is comprised of the stainless steel TSC bottom plate, the pedestal/air inlet structure, and a carbon steel base plate. Radiation streaming paths consist of air inlets located at the bottom and air outlets located above the top of the TSC, and above the annulus between the concrete cask body and the TSC. Air inlets and outlets are radial openings to the concrete cask. The inlets and outlets are axially offset from the source regions to minimize dose and meet ALARA principles.

No auxiliary shielding is considered in the concrete cask shielding evaluation. All components relevant to safety performance are explicitly included in the concrete cask model. Homogenization of materials used in the models is limited to the fuel assembly as described in Section 5.1.1.

#### **5.1.2.1      Undamaged Fuel Dose Rates**

Refer to Table 5.1.3-2, Table 5.1.3-5, and Table 5.1.3-7 for a summary of the concrete cask normal condition and accident event maximum calculated dose rates for the standard (CC1/CC2), augmented shield (CC3), and short, standard (CC4) cask configurations. Listed maximum dose rates include fuel and nonfuel hardware contributions. Payload types producing maximum surface dose rates are listed in Table 5.1.3-3, Table 5.1.3-6, and Table 5.1.3-8. Refer to Section 5.6.5 for TSC surface contamination release dose rates. Dose rates are based on three-dimensional Monte Carlo analysis using surface detectors. Further detail on the detector geometry is included in Section 5.5.

The maximum concrete cask side (cylindrical) average surface dose rate is 58 (<1%) mrem/hour. On the concrete cask top (disk), the average surface dose rate is 104 (2%) mrem/hour. Average dose rates for the standard shielding concrete cask are more than twice as high on the radial surface and approximately 20% higher on the axial surface than the augmented shielding cask configuration for the PWR system (augmented cask shield analysis limited to PWR payloads). The maximum inlet and outlet dose rates are 434 and 59 mrem/hr, respectively. No design basis normal condition or accident event exposes the bottom of the concrete cask.

#### **5.1.2.2      Damaged PWR Fuel Dose Rates**

The two damaged fuel scenarios described in Section 5.1.1.2 are also evaluated for the concrete cask.

The first scenario assumes the damaged fuel collects over the active fuel length of the fuel assembly. Dose rate profiles for the 37- undamaged assemblies are compared with profiles for 33 undamaged and 4 damaged assemblies in Section 5.8.12. Based on the self-shielding of the added mass compensating for the increase in source, damaged fuel dose rates for the first scenario are bounded by either the corresponding undamaged fuel dose rates or the second damaged fuel scenario.

In the second scenario, damaged fuel is assumed to migrate from the active fuel into the lower end fitting region of the fuel assembly, filling all the modeled void space. In this case, concrete cask inlet and radial dose rates increase due to the addition of damaged fuel. The concrete cask inlet dose rate increase is 38 mrem/hr, increasing the inlet dose rate by approximately 9 percent. The maximum concrete cask radial dose rate increases to 82.3 mrem/hr, an increase of approximately 4 percent.

Damaged fuel dose rates are computed using the standard concrete cask (CC1/CC2) or the short, standard concrete cask (CC4), as they produce higher dose rates than the augmented shield concrete cask.

Damaged fuel maximum dose rates in the standard concrete cask are summarized in Table 5.1.3-10.

#### **5.1.3      Offsite Dose Discussion and Results**

Contributions from concrete casks to site radiation dose exposure are limited to either radiation emitted from the concrete cask surface or a hypothetical release of surface contamination from the TSC. As documented in Section 5.6.5, there is no significant site dose effect from the expected surface contamination of the system. The TSCs are comprised of a welded shell, bottom plate and lid structure. The vent and drain ports in the lid are covered by redundant welded plates. There is, therefore, no credible leakage from the system, and no significant effluent source can be released from the TSC contents. Details on the TSC confinement boundary are provided in Chapter 7, with leakage test information provided in Section 10.1.3.

Controlled area boundary exposure from the concrete cask surface radiation is evaluated using the NAC-CASC code. (As previously stated, NAC-CASC is a modified version of SKYSHINE-



III.) NAC-CASC calculates the direct dose rate as well as the air scattered contribution of the total dose rate. As the detectors are below the top surface of the cask, only the cylindrical shell (radial) cask surface current contributes a direct component to the total dose rate. NAC-CASC primary enhancements to SKYSHINE-III allow the input of an angular surface current, the input of cylindrical shell (side) and disk (top) geometries, and the accounting of concrete cask self-shielding (i.e., radiation emitted from one cask intersecting another cask in the array—in particular, front/back row interaction in the array). The cylindrical shell and top surfaces are Monte Carlo sampled to generate the surface current input into the code. Each of the sampled locations represents a point source to which the SKYSHINE-III line beam response functions are applicable.

The NAC-CASC (SKYSHINE-III) method assumes that radiation emitted from the source does not interact with the cask/source structure after emission (beyond the additional routines added by NAC to account for self-shielding). This assumption does not represent a significant effect on site dose rates as the calculated surface current is near normal to the surface and any backscatter to the cask from the air surrounding the array would then require a second backscatter from the cask surface to reach a detector location. As detector locations for site exposure are at significant distances from the array (typically 100+ meters), there would not be a significant contribution from radiation having undergone such repeated large angle scatter.

Both a single cask and a 2×10 array of casks are evaluated for site exposure evaluations. Each cask in the array is assigned the maximum dose (surface current) source allowed by the cask loading tables. A combination of the maximum cask side and top dose cases provides for a conservative estimate on the controlled area boundary exposure, since the different fuel types produce the highest cask surface dose components.

The full-year exposure for site boundary (controlled area boundary) results is based on 8,760 hours of exposure.

#### **5.8.4        87-Assembly BWR System**

This section presents the detailed evaluation of the concrete and transfer casks loaded with BWR fuel assemblies.

##### **5.8.4.1        BWR Fuel and Basket Models**

The three-dimensional shielding evaluation includes a homogenized fuel assembly model and a detailed three-dimensional basket model.

###### **5.8.4.1.1      Fuel Assembly Model**

Based on the fuel assembly physical parameters provided in Table 5.8.1-4 and the hardware masses in Table 5.8.1-5, homogenized treatments of fuel assembly source regions are developed. The homogenized fuel assembly is represented in the model as a stack of boxes with width equal to the fuel assembly width. The height of each box corresponds to the modeled height of the corresponding assembly region.

Sample fuel and nonfuel hardware homogenizations for the source regions for the 08b assembly are shown in Table 5.8.4-1 and Table 5.8.4-2, respectively. The resulting fuel compositions on an atom/barn-cm basis are shown in Table 5.8.4-3. Similar compositions sets are generated for the remaining fuel assembly hybrids. Note that the Zirc-2 fuel assembly channel is not included in the model.

###### **5.8.4.1.2      Basket Model**

The basket is composed of coated carbon steel tubes, pinned together at the corners, and held together by side and corner weldments. Forty-five fuel tubes, in combination with the weldments, form 89 fuel openings. Two openings are located below the vent port covers. To minimize exposure and meet ALARA constraints, basket capacity is reduced to 87 assemblies. Pin spacers maintain the tube axial spacing within the TSC cavity. Each tube contains four metallic composite neutron absorber sheets. In dry storage and transfer, the presence of the neutron absorber sheets provides minimal shielding and could, therefore, be removed without a significant increase in exposure. Key basket characteristics are shown in Table 5.8.4-4. Radial and axial sketches of basket within the TSC are shown in Figure 5.8.4-1 and Figure 5.8.4-2.

##### **5.8.4.2        Minimum Cool-time Specification**

SAS2H generates heat loads for all BWR fuel types listed in Section 5.8.1.2. Based on a 35 kW per cask (0.402 kW per assembly) heat load, minimum allowed cool times for each fuel type are calculated. Calculated heat loads account for fuel material (actinide and fission product) and

hardware (light element) generated sources. Minimum cool times are conservatively rounded up to the nearest one-tenth of a year. A sample minimum cool time calculation for the 09b hybrid BWR assembly is shown in Table 5.8.4-5. The resulting minimum cool times are listed in an assembly specific loading table (see Table 5.8.4-6). Note that cool times for maximum assembly average burnups less than or equal to 30,000 MWd/MTU are not tabulated since they are equal to four years for all seven BWR fuel types. However, the following minimum enrichments for these assembly average burnups must be invoked.

Max. Assembly Avg. Burnup (MWd/MTU)	Min. Assembly Avg. Initial Enrichment (wt % <sup>235</sup> U)
5,000	0.7
10,000	1.3
15,000	1.5
20,000	1.7
25,000	1.9
30,000	2.1

Note that the loading table removes combinations of high burnup and low enrichment (e.g., 60 GWd/MTU and 1.9 wt% <sup>235</sup>U) from the payload definition. Source term data covering these combinations is generated, but produces unrealistic source terms due to the complete consumption of fissile uranium early in the burnup cycle and the SAS2H input of a fixed power density. To maintain power density, ORIGEN-S (SAS2H) will substantially increase flux levels, which would not occur during core operation of the assembly, to produce fissile material and to produce power by nonthermal fission. The increased flux level “breeds” higher actinides, which in turn increase source significantly. Since a high burnup and low enrichment combination would require repeated reinsertion of a burned assembly, the combination is excluded.

Minimum cool time tables for the thermal analysis limited heat load are included in Section 5.8.9.

#### 5.8.4.3 Transfer Cask Dose Rates

Using the dose response method, cask dose rates are tabulated for all allowed cool time, assembly average burnup, and initial enrichment combinations for each of the assembly types. Maximum dose rates as a function of distance from the cask surface are shown in Figure 5.8.4-3 for the cask radial surface, Figure 5.8.4-5 for the cask top, and Figure 5.8.4-7 for the cask bottom. Breakdowns of the cask surface radial and top dose rates into the source components are shown

### 5.8.5 PWR Nonfuel Hardware Components - BPRA and Thimble Plug

The PWR fuel assembly basket is designed to store nonfuel components inside the fuel assembly. Nonfuel components that may be stored include the following:

- BPRAs (Burnable Poison Rod Assemblies)

Burnable poison rods are employed in the majority of PWR cores as either replacement rods for fuel rods, typical of CE cores, or as BPRAs in Westinghouse and B&W cores. Common types of BPRAs are Westinghouse Pyrex BPRAs, Westinghouse WABA, and B&W/Framatome  $\text{Al}_2\text{O}_3\text{-B}_4\text{C}$  zirconium alloy rods. BPRAs are composed of a set of rods made from an absorber material suspended from a spider structure located on the top-end fitting of the assembly. BPRAs are designed to reduce reactivity in fresh fuel, but may remain in a fuel assembly for more than one cycle. Potential BPRA source regions are the top-end fitting, top plenum, and active fuel regions. The amount of activated material depends on the number of absorber (poison) rods attached to the BPRA and the material of the BPRA. Guide tube locations not occupied by absorber rods are typically occupied by short plug rods extending into the upper plenum region of the assembly. BPRA rods may be composed of activated material such as steel or a relatively inert material such as zirconium alloy. Table 5.8.5-1 provides a summary of Westinghouse 15×15 core BPRA types and the maximum regional masses chosen for the analysis. BPRAs for the remaining Westinghouse and B&W cores are treated similarly. A summary of BPRA characteristics for fuel placed into the transfer and storage systems is listed in Table 5.8.5-2. Poison rods replacing fuel rods are enveloped in the shielding analysis since they are typically constructed with a zirconium alloy clad and do not contain a significant amount of activated material, in particular compared to the fuel rod that they replace.

- Thimble Plugs

Thimble plugs are similar to BPRAs in that they are attached to a spider resting on the end-fitting tie plate. Thimble plugs extend into the upper plenum region of the fuel assembly and block flow through the guide tubes during in-core operations. Thimble plug components do not extend into the active fuel region. They may be reused in multiple cycles and can experience significantly higher burnup than BPRAs. Thimble plug masses evaluated for each core are shown in Table 5.8.5-2.

#### 5.8.5.1 Modeling Detail

Dose rates for BPRA and thimble plug components are estimated using fuel assembly response functions for the hardware source regions of interest. Credit is taken for the increased region masses and the associated increase in self-shielding. The BPRA and thimble plug activated hardware is primarily composed of stainless steel. A 0.8 g/kg  $^{59}\text{Co}$  impurity is applied against this material. Full cask loads containing up to 37 nonfuel hardware components (i.e., one in each assembly) are evaluated and allowed for storage. There are no restrictions on the number of components per TSC, location of component within the TSC, or mixture of BPRA and thimble plug components with other nonfuel hardware within a TSC.

#### 5.8.5.2 Dose Rate and Heat Load Impact

To minimize impact of off-site boundary and occupational dose evaluations, the maximum dose rate contribution of the nonfuel assembly hardware on the radial surface of the concrete cask is limited to 7.5 mrem/hr. This limit is reduced for the B&W BPRAs that do not contain activated hardware in the active fuel region. BPRAs are evaluated to a maximum burnup of 70 GWd/MTU, with thimble plug burnup being limited to an equivalent 180 GWd/MTU. The BPRAs and thimble plugs for each core configuration are independently evaluated.

##### 5.8.5.2.1 BPRA

Table 5.8.5-3 lists the allowed BPRA loading configurations expressed in burnup and cool-time limits or curie limits. The radiation source for the BPRAs is dominated by  $^{60}\text{Co}$  gammas. Therefore, the spectrum of the activated BPRAs is not decay time sensitive. As a result of the dominant  $^{60}\text{Co}$  contribution, the burnup/cool-time loading table reflects the cool-time increase required to decay to a limiting  $^{60}\text{Co}$  curie content for each assembly type at each burnup level. System users may choose to directly implement the burnup/cool-time tables on a generic fuel type basis or to determine site-specific minimum BPRA cool times based on the  $^{60}\text{Co}$  curie limit in Table 5.8.5-3.

Maximum and average dose rate contributions from BPRAs on the concrete and transfer cask surfaces are listed in Table 5.8.5-4. The BPRA radial profile from the cask configuration and fuel assembly which produces maximum radial dose rates (CC4 with Westinghouse 14 × 14 assembly) is shown in Figure 5.8.5-1. The addition of the BPRA increases the maximum reported dose rates, as demonstrated in Figure 5.8.5-2 for a Westinghouse 14×14 assembly.

The maximum decay heat produced by a full cask load of BPRAs (37) is 0.44 kW. For any of the fuel assemblies evaluated, an increase in cool time, shown in Table 5.8.5-7, is necessary to accommodate loading the BPRAs. An increase in cool time will also decrease the fuel source

term. Therefore, the strict application of increased fuel assembly minimum cool time without considering the corresponding reduction in fuel dose rates is conservative.

#### **5.8.5.2.2 Thimble Plugs**

Table 5.8.5-5 lists the allowed thimble plug loading configurations expressed in burnup and cool-time limits or curie limits. The radiation source for the thimble plugs is dominated by  $^{60}\text{Co}$  gammas. Therefore, the spectrum of the activated thimble plugs is not decay time sensitive. As a result of the dominant  $^{60}\text{Co}$  contribution, the burnup/cool-time loading table reflects the cool time increase required to decay to a limiting  $^{60}\text{Co}$  curie content for each assembly type at each burnup level. System users may choose to directly implement the burnup/cool-time tables on a generic fuel type basis or to determine site-specific minimum thimble plug cool times based on the  $^{60}\text{Co}$  curie limit in Table 5.8.5-5.

Maximum and average dose rate contributions from thimble plugs on the concrete and transfer cask surfaces are listed in Table 5.8.5-6. The concrete cask axial profile for the thimble plugs is shown in Figure 5.8.5-3. The addition of the thimble plugs does not increase the maximum reported dose rates, as demonstrated in Figure 5.8.5-4 for a Westinghouse 14×14 assembly.

The maximum decay heat produced by a full cask load of thimble plugs (37) is 0.04 kW. For any of the fuel assemblies evaluated, an increase in cool time, shown in Table 5.8.5-7, is necessary to accommodate loading the thimble plugs. An increase in cool time will also decrease the fuel source term. Therefore, the strict application of increased fuel assembly minimum cool time without considering the corresponding reduction in fuel dose rates is conservative.

#### 5.8.5.2.3 Combination of Fuel, BPRA, and Thimble Plug Dose Rates

Maximum PWR system dose rates are reported for the conservative combination of fuel, BPRA, and thimble plug dose rates. At each cask/detector surface combination, with the exception of the concrete and transfer cask sides, this combination is straightforward based on the hardware sources being the dominant contributor to the total. On the sides of the casks, the fuel sources comprise most of the total, and the elevation of the maximum dose rate due to fuel, BPRA, and thimble plug may not coincide. As shown in the previous sections, BPRA loading affects the maximum dose rate while thimble plugs do not.

The combined maxima are listed as follows.

Cask / Dose Location	Fuel		Combined	
	Assembly	Max. Dose Rate (mrem/hr)	Assembly	Max. Dose Rate (mrem/hr)
Standard Shield Concrete Cask Top	CE 16×16	378	CE 16×16	378
Standard Shield Concrete Cask Radial	CE 14×14	76.7	WE 14×14	79.3
Standard Shield Concrete Cask Inlet	WE 14×14	425	WE 14×14	434
Standard Shield Concrete Cask Outlet	CE 16×16	38.3	CE 16×16	38.3
Carbon Steel Transfer Cask Top	WE 14×14	451	WE 14×14	546
Carbon Steel Transfer Cask Radial	CE 14×14	939	WE 14×14	942
Carbon Steel Transfer Cask Bottom	WE 14×14	5,824	WE 14×14	5,908
Augmented Shield Concrete Cask Top	WE 14×14	350	WE 14×14	408
Augmented Shield Concrete Cask Radial	CE 14×14	36.5	WE 14×14	37.1
Augmented Shield Concrete Cask Inlet	WE 14×14	117	WE 14×14	119
Augmented Shield Concrete Cask Outlet	B&W 17×17	21.8	WE 14×14	26.2
Stainless Steel Transfer Cask Top	B&W 17×17	505	WE 14×14	568
Stainless Steel Transfer Cask Radial	CE 14×14	922	WE 14×14	945
Stainless Steel Transfer Cask Bottom	WE 14×14	5,239	WE 14×14	5,326
CC4 Top	WE 14×14	316	WE 14×14	365
CC4 Radial	CE 14×14	76.8	WE 14×14	79.5
CC4 Inlet	WE 14×14	112.4	WE 14×14	115
CC4 Outlet	B&W 17×17	36.8	B&W 17×17	42.8

**Table 5.8.5-5 Allowed Thimble Plug Burnup and Cool-time Combinations**

Burnup (GWd/MTU)	Cool Time (yrs)				
	WE 14×14	WE 15×15	B&W 15×15	WE 17×17	B&W 17×17
45	2.0	3.5	7.0	5.0	6.0
90	6.0	7.0	10.0	9.0	10.0
135	7.0	9.0	12.0	10.0	12.0
180	8.0	9.0	14.0	12.0	12.0
<sup>60</sup> Co Activity (Ci)	63.5	64.1	56.9	64.0	63.6

**Table 5.8.5-6 Thimble Plug Dose Rate Contributions – Westinghouse 14×14**

Cask / Dose Location	Maximum Dose (mrem/hr)	Average Dose (mrem/hr)
Standard Shield Concrete Cask Top	42	11
Standard Shield Concrete Cask Radial	7.3	1.4
Standard Shield Concrete Cask Outlet	3.4	--
Carbon Steel Transfer Cask Top	95	28
Carbon Steel Transfer Cask Radial	152	16
Augmented Shield Concrete Cask Top	57	9.9
Augmented Shield Concrete Cask Radial	4.0	0.7
Augmented Shield Concrete Cask Outlet	4.1	--
Stainless Steel Transfer Cask Top	102	38
Stainless Steel Transfer Cask Radial	154	16
CC4 Top	48.9	10.8
CC4 Radial	8.6	10.8
CC4 Outlet	7.3	--

**Table 5.8.5-7 Additional Assembly Cool Time (Years) Required to Load BPRA or TP (Uniform Loading)**

	BPRA	TP
CE 14x14 <sup>a</sup>	--	--
WE 14x14	0.5	0.1
WE 15x15	0.5	0.1
B&W 15x15	0.1	0.1
CE 16x16 <sup>a</sup>	--	--
WE 17x17	0.5	0.1
B&W 17x17	0.1	0.1

<sup>a</sup> BPRA's and TP's are not evaluated for CE fuel.



### 5.8.6 Nonfuel Hardware Component – Reactor Control Elements

Reactor control element (e.g., CEAs and RCCAs) material quantities and the core region in which the material was exposed to the neutron activation flux were obtained from the DOE characteristics database [30]. Bounding mass quantities activated in the assembly top and gas plenum regions are listed in Table 5.8.6-1 for the seven analyzed assembly configurations. Similar to the fuel assembly hardware evaluation, the plenum material is activated at a 0.2 flux factor, with top material activation at a 0.1 flux factor (0.05 for the CE 16×16 fuel). Material above the top is not considered to be activated to a significant extent and is, therefore, not modeled. In the shielding evaluation, the source material activated in the plenum region of the fuel assembly is located at the bottom of the active fuel region. This is the result of the full insertion of the CEA into the assembly under storage conditions. The CEA material classified as that in the top assembly region is modeled directly above the active fuel region. To minimize the increased dose due to loading of CEAs, only the center nine basket locations are allowed to contain the added source.

CEA response functions are evaluated in groups 11 through 15 based on the significant energy lines of the Ag-In-Cd, inconel, and stainless steel light element spectra. CEAs may also contain hafnium as the primary absorber nuclide. As seen in table 5.8.6-3, the source for hafnium components of the absorber is not significant when compared to the source of steel/inconel or Ag-In-Cd based absorbers. The minimum cool time for CEAs is set uniformly at 10 years, with a maximum exposure of 180 GWd/MTU to assess dose effects on the system.

Maximum CEA dose rates are calculated for the Westinghouse 17×17 bounding CEA description due to the significant amount of Ag-In-Cd and steel/inconel activated in the assembly upper plenum region. Results are shown in Table 5.8.6-2. On the sides of the concrete and transfer casks, the additive dose rate does not affect the maximum dose rates. At the concrete cask inlets and transfer cask bottom, loading of CEAs significantly increases the maximum dose rates.

The maximum decay heat produced by a loading of nine CEAs is 0.62 kW. For any of the fuel assemblies evaluated, an increase in cool time, shown in Table 5.8.6-6, is necessary to accommodate loading a CEA. As an increase in cool time will also decrease the fuel source term, the strict application of increased cool time without a recalculation of fuel dose rates is conservative.

The cask system is evaluated for higher CEA burnup/exposure than the 180,000 MWd/MTU, 10-year-cooled case used to establish baseline dose rate effects. The effects of higher burnup/exposure on steel/inconel absorber and the steel hardware of other absorbers is evaluated by reviewing the source spectrum in Table 5.8.6-3 that demonstrates that the overwhelming majority of the source is in energy groups 12 and 13, which correspond to the <sup>60</sup>Co energy lines.

Figure 5.8.6-1 is then used to compare the source strength in groups 12 and 13 with higher exposures at a cool time of 12 years. The figure demonstrates that the increase in cool time is enough to reduce the source to less than the 180 GWd/MTU and 10-year-cooled source. A similar comparison is made in Figure 5.8.6-2 for group 15 of the Ag-In-Cd absorber. Group 15 was chosen for the comparison as it represents the group producing maximum energy and source magnitude. As shown in Figure 5.8.6-2, due to the longer half life of the isotopes producing these gamma rays, additional cool time is required. The complete source spectrum is, therefore, used to determine dose rate effects on the system with minimum cool times of 14 and 20 years for maximum exposures of 270 and 360 GWd/MTU, respectively. As shown in Table 5.8.6-4, these exposure/cool time combinations are bounded by the baseline 180,000 MWd/MTU, 10-year cool time state point.

Table 5.8.6-5 lists the exposure cool time combinations applicable to all CEA types.

**Table 5.8.6-4 Dose Rates from Ag-In-Cd Based CEAs as a Function of Exposure and Cool Time**

Cask / Dose Location	180 GWd/MTU, 10 Years		270 GWd/MTU, 14 Years		360 GWd/MTU, 20 Years	
	Maximum	Average	Maximum	Average	Maximum	Average
Concrete Cask Radial	3.6	0.3	3.6	0.3	3.6	0.3
Concrete Cask Inlet	32	--	32	--	32	--
Transfer Cask Radial	0.9	<0.1	0.7	<0.1	0.4	<0.1
Transfer Cask Bottom	2527	848	2193	739	1849	625

**Table 5.8.6-5 CEA Maximum Exposure and Minimum Cool Time Summary**

Maximum Exposure (GWd/MTU)	Minimum Cool Time (yrs)
180	10
270	14
360	20

**Table 5.8.6-6 Additional Assembly Cool Time (Years) Required to Load a CEA (Uniform Loading)**

Assembly	Cool Time
CE 14x14	0.2
WE 14x14	2.0
WE 15x15	3.1
B&W 15x15	0.2
CE 16x16	0.2
WE 17x17	2.9
B&W 17x17	0.2

### 5.8.7 Preferential Loading of PWR Fuel

In order to envelop fuel assemblies with heat loads higher than 959 W, a three-zone preferential loading pattern is proposed as follows.

Zone Description	Designator	Heat Load [W/assy]	# Assemblies
Inner Ring	A	922	9
Middle Ring	B	1,200	12
Outer Ring	C	800	16

Preferential and uniform loading patterns limit total cask heat load to 37 kW. As will be seen in the results section, the maximum dose rate for the preferential loading pattern is less than that calculated for a uniform pattern.

A sketch of the PWR basket and loading pattern is shown in Figure 5.8.7-1.

Minimum cool time tables for the preferential heat load pattern are included in Section 5.8.9. The method and models for the preferential loading pattern shielding evaluations are identical to those of the uniform loading pattern with the exception of requiring three sets of response functions, one for each zone. Source spectrum varies as a result of changes in burnup, initial enrichment and minimum cool time and, therefore, requires cask dose responses (dose per unit source in each spectrum energy group) for each of the zones. The dose responses from each ring, accounting for the differences in the number of assemblies per zone, are added to arrive at the dose rate for a fully loaded cask.

#### 5.8.7.1 Input File Setup

Based on a three-zone pattern, the source and tally descriptions are modified in the MCNP models to consider the sources in the appropriate basket locations with the proper scaling on the tally cards. For each cask/detector combination, three sets of runs (A, B and C) are needed to characterize the dose rate response.

#### 5.8.7.2 Results

Maximum and average surface dose rates for the preferential pattern are shown in Table 5.8.7-1, with the corresponding limiting results for the uniform pattern. The maximum dose rates for the analyzed preferential loading pattern are less than or statistically unchanged from those calculated for a uniform pattern at each detector surface for both casks.

The concrete cask radial and top axial average dose rates are less than or statistically unchanged in the preferential pattern. Therefore, using the uniform pattern to characterize the restricted area

and controlled area boundaries is acceptable. Although the transfer cask top and bottom average dose rates are slightly higher for the preferential pattern, the maximum dose rates on the top of the cask, which are higher for the uniform pattern, are the dominant contributor to occupational exposures. Bottom dose rates do not contribute to occupational exposures. As such, the occupational exposure evaluations for TSC transfer are also conservative.

#### **5.8.7.3      Cool-time Tables**

Cool times for the three preferential loading pattern heat loads are shown in Table 5.8.9-3 through Table 5.8.9-5. Results are not shown for burnups of  $\leq 30$  GWd/MTU. The minimum enrichments and cool times (as a function of burnup) for  $\leq 30$  GWd/MTU fuel are listed in Table 5.8.9-1. Additional assembly cool times for loading nonfuel hardware, including BPRAs, TPs, and CEAs, are shown in Table 5.8.7-2.

**Table 5.8.7-2 Additional Assembly Cool Time (Years) Required When Loading Nonfuel Hardware – Three-Zone Preferential Loading**

Assy		Three-Zone		
		A	B	C
CE 14x14	BP	--	--	--
	TP	--	--	--
	CEA	0.2	0.1	0.2
WE 14x14	BP	0.5	0.2	0.7
	TP	0.1	0.1	0.1
	CEA	2.3	0.7	4.1
WE 15x15	BP	0.6	0.2	0.8
	TP	0.1	0.1	0.1
	CEA	3.4	1.5	4.5
B&W 15x15	BP	0.1	0.1	0.1
	TP	0.1	0.1	0.1
	CEA	0.2	0.1	0.2
CE 16x16	BP	--	--	--
	TP	--	--	--
	CEA	0.2	0.1	0.3
WE 17x17	BP	0.6	0.2	0.7
	TP	0.1	0.1	0.1
	CEA	3.3	1.4	4.3
B&W 17x17	BP	0.1	0.1	0.1
	TP	0.1	0.1	0.1
	CEA	0.2	0.1	0.2

## 5.8.9 Cool-Time Tables

### 5.8.9.1 PWR

PWR system performance is evaluated for a cask heat load of 35.5 kW with preferential (1.2 kW max) and uniform (959 W/assy) heat load patterns. Minimum cool times are summarized for the uniform and preferential heat load patterns.

Allowed low burnup (up to 30,000 MWd/MTU) fuel loadings are shown in Table 5.8.9-1. Note that the listed minimum cool times at each burnup step are bounding for all fuel types and initial enrichments above the minimum enrichment specified. Collapsing the fuel type and initial enrichment-dependent minimum cool time matrix to a single value may result in a minimum cool time longer than individual values presented for higher burnups in the detailed tables that follow.

The minimum cool time tables account for potential uncertainties in the source generation abilities of SAS2H at burnups greater than 45 GWd/MTU by reducing allowed heat loads by 5 percent. Fuel assembly loading tables at greater than 45 GWd/MTU are, therefore, generated for a cask heat load of 33.725 kW with preferential (1.14 kW max) and uniform (911 W/assy) heat load patterns.

The 5% penalty adjusted three-zone preferential loading pattern is as follows.

Zone Description	Designator	Heat Load [W/assy]	# Assemblies
Inner Ring	A	876	9
Middle Ring	B	1,140	12
Outer Ring	C	760	16

Table 5.8.9-2 contains the minimum cool times for a uniform heat load of 959 W/assy ( $\leq 45$  GWd/MTU) PWR fuel. Greater than 45 GWd/MTU uniform heat load minimum cool times are listed in Table 5.8.9-6. Table 5.8.9-3 through Table 5.8.9-5 contain the minimum cool times for the preferential loading of  $\leq 45$  GWd/MTU with higher burnup fuel cool times listed in Table 5.8.9-7 through Table 5.8.9-9.

Decay heat associated with loading nonfuel components requires an increase in the minimum fuel assembly cool time. The incremental cool time increase required to load nonfuel components are documented in Sections 5.8.5, 5.8.6, and 5.8.7.

Table 5.8.9-1 Low Burnup PWR Fuel Loading Table

Max. Assembly Avg. Burnup (MWd/MTU)	Min. Assembly Avg. Initial Enrichment (wt% <sup>235</sup> U)	Minimum Cool Time (yrs)			
Heat Load per Assy	--	959 W	800 W	922 W	1,200 W
10,000	1.3	4.0	4.0	4.0	4.0
15,000	1.5	4.0	4.0	4.0	4.0
20,000	1.7	4.0	4.0	4.0	4.0
25,000	1.9	4.0	4.3	4.0	4.0
30,000	2.1	4.4	5.2	4.5	4.0



#### 5.8.9.2 BWR

Thermal analysis limits the BWR cask heat load to below that used in the cask shielding analysis. Minimum fuel assembly cool times are, therefore, required for a 33 kW cask heat load (379 W/assembly). Due to potential uncertainties in the source generation abilities of SAS2H, allowed heat load is reduced by an additional 5%, to 360 W/assembly, for fuel with burnups greater than 45 GWd/MTU. Minimum cool times for fuel with burnup greater than 30 GWd/MTU, but  $\leq 45$  GWd/MTU, are listed in Table 5.8.9-11 with high burnup fuel cool times shown in Table 5.8.9-12.

Allowed low burnup (up to 30,000 MWd/MTU) fuel loadings are shown in Table 5.8.9-10. Note that the listed minimum cool times at each burnup step are bounding for all fuel types and initial enrichments above the minimum enrichment specified. Collapsing the fuel type and initial enrichment dependent minimum cool time matrix to a single value may result in a minimum cool time longer than individual values presented for higher burnups.

Table 5.8.9-10 Low Burnup BWR Fuel Loading Table

Max. Assembly Avg. Burnup (MWd/MTU)	Min. Assembly Avg. Initial Enrichment (wt% <sup>235</sup> U)	Minimum Cool Time (yrs)
5,000	0.7	4.0
10,000	1.3	4.0
15,000	1.5	4.0
20,000	1.7	4.0
25,000	1.9	4.0
30,000	2.1	4.3

**5.9      PWR Reduced Minimum Cool Time and Alternate Preferential Heat Load Pattern Shielding Evaluation Detail**

This section contains evaluation detail for Westinghouse 14x14 fuel assemblies with a minimum cool time of 2.5 years loaded in the CC4 and stainless steel MTC. This section includes uniform loading and four zone preferential loading with a maximum assembly heat load of 1.8 kW. Evaluations are documented for undamaged and damaged fuel. The minimum cool time for the Westinghouse 14x14 CEAs was reduced to 2.5 years from the previous minimum cool time of 10 years.

Evaluation methods and models are based on those described in Section 5.8, with changes limited to those associated with reducing minimum permitted cool time to 2.5 years, modeling a four region preferential heat loading pattern, and allowing WE 14x14 CEAs to be cooled 2.5 years. Activated mass of the WE 14x14 CEA was calculated based on the known dimensions of the WE 15x15 CEA (see Section 5.9.5).

Uniform heat load evaluations at a minimum cool time of 2.5 years are included in Section 5.9.3. Preferential loading for heat load is discussed in Section 5.9.6. The effects of nonfuel hardware components to dose rates and heat load are discussed in Sections 5.9.4 and 5.9.5. Model differences, dose rates and minimum loading time impacts resulting from the damaged fuel basket configuration are discussed in Section 5.9.9.

**5.9.1      Contents Description**

Three-dimensional models of the loaded TSC within the stainless steel transfer or CC4 concrete cask require the relative elevations of the various source regions, hardware masses, and in-core condition to describe source and shielding models. The elevation of each of the assembly regions also defines the volume into which the fuel assembly is homogenized.

As described in Section 5.2, PWR fuel assemblies were surveyed to construct hybrids containing maximum fuel and hardware masses. Section 5.8.1 contains geometry data of the Westinghouse 14x14 hybrid used in this evaluation. Sample in-core characteristics are also contained in Section 5.8.1.

### 5.9.2 Response Function Method

The evaluation of reduced minimum cool time in the CC4 and MTC use the response function method described in Section 5.8.2.

Response functions for the transfer and storage cask (generated using MCNP) solve the particle transport equations at each relevant spectrum line using Monte Carlo techniques. The results of the individual spectrum lines are then statistically summed. As the basket is loaded uniformly (or in a four-region pattern for the 1.8 kW preferential loading pattern), the dose rate response can be calculated for a source located in multiple fuel assembly locations using Monte Carlo sampling within MCNP. For the uniform loading, the basket position variable is, therefore, not required within the summation. Note that the term is still accounted for directly within the MCNP run. For the four-region preferential loading scenario, the summation is limited to the dose rate response contribution of the four zones.

The response function method allows the MCNP weight window (acceleration) map to be optimized for a particular source energy, producing an increased number of particles scoring per source particle. The response function also allows for a significant reduction in the number of MCNP shielding runs, thereby increasing the number of particles per MCNP run (based on fixed computer resources). For example, a single PWR fuel type has approximately 20,000 source runs associated with it, requiring the same number of MCNP runs to determine a complete dose rate set. The same dose rate set for fuel gamma and neutron cases may be generated using approximately 20 MCNP runs (one per relevant neutron and gamma energy line) using the response function.

Section 5.8.2 demonstrates the applicability of the response method to determine the dose rates of the MAGNASTOR concrete cask and transfer cask systems.

### **5.9.3      Undamaged Fuel - Uniform Heat Load Pattern Evaluation**

This section presents the detailed evaluations of the concrete and transfer casks loaded with PWR fuel assemblies at a minimum cool time of 2.5 years are based on models developed in Section 5.8 for a PWR undamaged fuel basket configuration with a payload of 37 fuel assemblies and no inserts. This section applies a uniform heat load pattern to determine system dose rates at a minimum cool time of 2.5 years. Preferential loading is discussed in Section 5.9.6. The effects of nonfuel hardware components to dose rates and heat load are discussed in Sections 5.9.4 and 5.9.5. Model differences, dose rates and minimum loading time impacts resulting from the damaged fuel basket configuration are discussed in Section 5.9.9.

#### **5.9.3.1      PWR Fuel and Basket Models**

The three-dimensional shielding evaluation includes a homogenized fuel assembly model and a detailed three-dimensional basket model. These models are discussed in length in Section 5.8.3.

#### **5.9.3.2      Minimum Cool-time Specification**

The 2.5-year evaluation method is identical to that employed in Section 5.8.3.2 other than the change allowing load tables to contain data down to 2.5 years rather than limiting content to 4 years minimum. The method is repeated in the following two paragraphs.

SAS2H generates heat loads based on the fuel data listed in Section 5.8.1.1. Based on the desired 35.5 kW system heat load, minimum allowed cool times for the matrix of initial enrichment and burnup are calculated. Calculated heat loads account for fuel material (actinide and fission product) and hardware (light element) generated sources. Minimum cool times are conservatively rounded up to the nearest one-tenth of a year. The resulting minimum cool times are listed in assembly specific loading tables.

The loading table removes combinations of high assembly average burnup and low enrichment (e.g., 60 GWd/MTU and 1.9 wt%  $^{235}\text{U}$ ) from the contents definition. Source term data covering these combinations produces unrealistic source terms due to the complete consumption of fissile uranium early in the burnup cycle and the SAS2H input of a fixed power density. To maintain power density, ORIGEN-S (SAS2H) will substantially increase flux levels, which would not occur during core operation of the assembly, to produce fissile material and to produce power by non-thermal fission. The increased flux level “breeds” higher actinides, which in turn increase source significantly. Since a high burnup and low enrichment combination would require repeated reinsertion of a burned assembly, the combination is excluded.

Minimum cool time tables, based on 2.5 years minimum cool time, are included in Section 5.9.8.

### **5.9.3.3      Stainless Steel Transfer Cask Dose Rates**

Using the dose response method, transfer cask dose rates are tabulated for all allowed cool times, assembly average burnup, and initial enrichment combinations for the hybrid Westinghouse 14x14 fuel type (ng14b). Reducing the minimum cool time to 2.5 years has no impact on the bounding source terms for the stainless steel MTC. Bounding source term cool times remain above the previous minimum cool time of 4 years. No new dose rates are evaluated for the uniformly loaded stainless steel MTC.

### **5.9.3.4      CC4 Dose Rates**

Using the dose response method, concrete cask dose rates are tabulated for all allowed cool times, assembly average burnup, and initial enrichment combinations for the hybrid Westinghouse 14x14 fuel type (ng14b). The reduction in minimum cool time results in a new bounding source term for the radial dose rates. The three other detector locations (Top, Inlet, and Outlet) remain bounded by previous evaluations.

Maximum dose rates as a function of distance from the CC4 radial surface are shown in Figure 5.9.3-1. A breakdown of the CC4 radial surface dose rates into the source components is shown in Figure 5.9.3-2. Refer to Table 5.9.3-1 for the maximum concrete cask surface dose rates and the contents that develop the dose rates. Reducing the minimum cool time to 2.5 years significantly increases radial dose rates on the CC4.

### **5.9.3.5      NAC-CASC Site Boundary Evaluation**

The previous section demonstrated that the WE14x14 CC4 average radial dose rate is 68 mrem/hr. This evaluation was based on a bounding assessment at 2.5 year minimum cool time and 35.5 kW maximum system heat load. Design basis input to the site boundary analysis is an average radial dose rate of 57 mrem/hr, which was based on an assessment of 4.0 year minimum cool time and 40.0 kW maximum system heat load. For site boundary dose rates the increased radial dose component can be accounted for by conservatively increasing reported single cask and array yearly dose and exposure values by 20%. This will conservatively neglect the smaller height CC evaluated at the reduced cool time (with the associated lower surface area for emission) and reduced axial dose components versus the 40 kW design basis source.

Figure 5.9.3-1 Concrete Cask Side Dose Rate Profile at Various Distances – PWR (CC4)

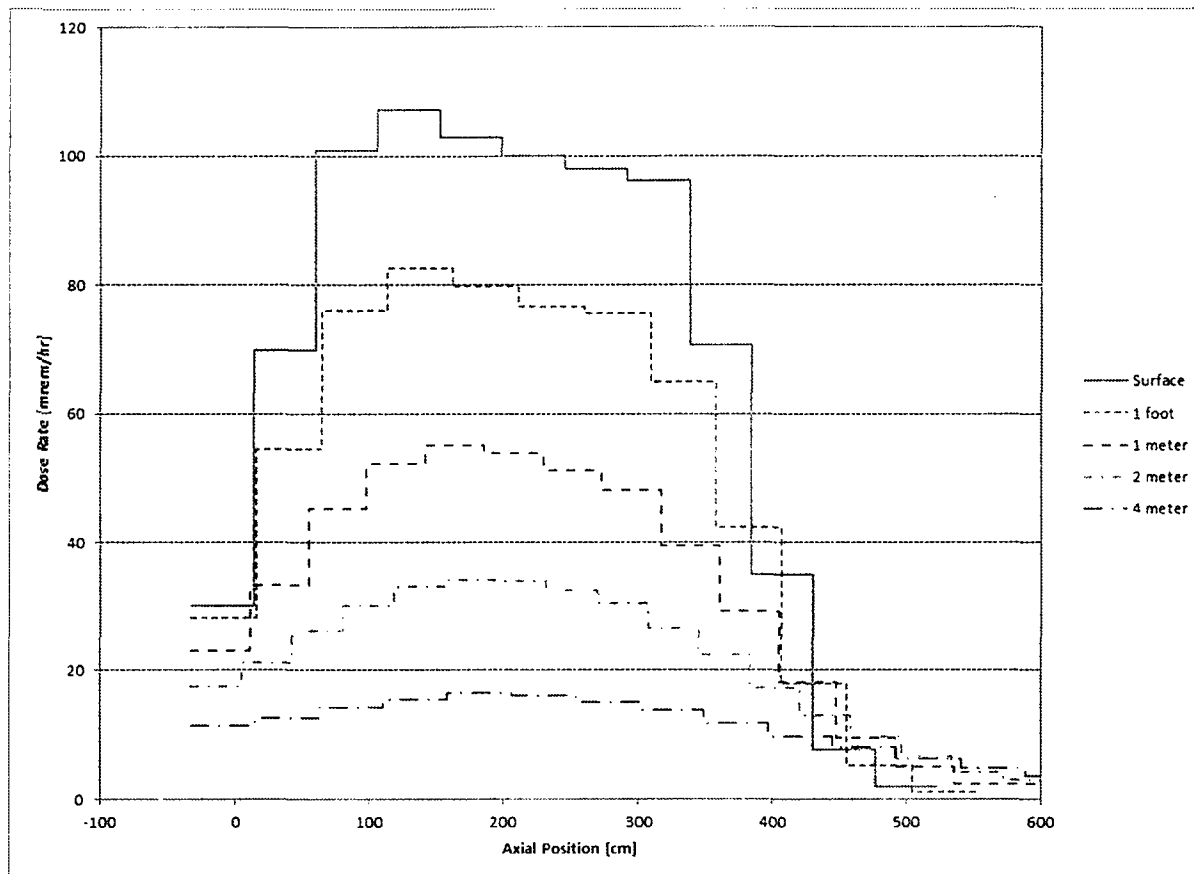




Figure 5.9.3-2 Concrete Cask Side Surface Dose Rate Profile by Source – PWR  
(CC4)

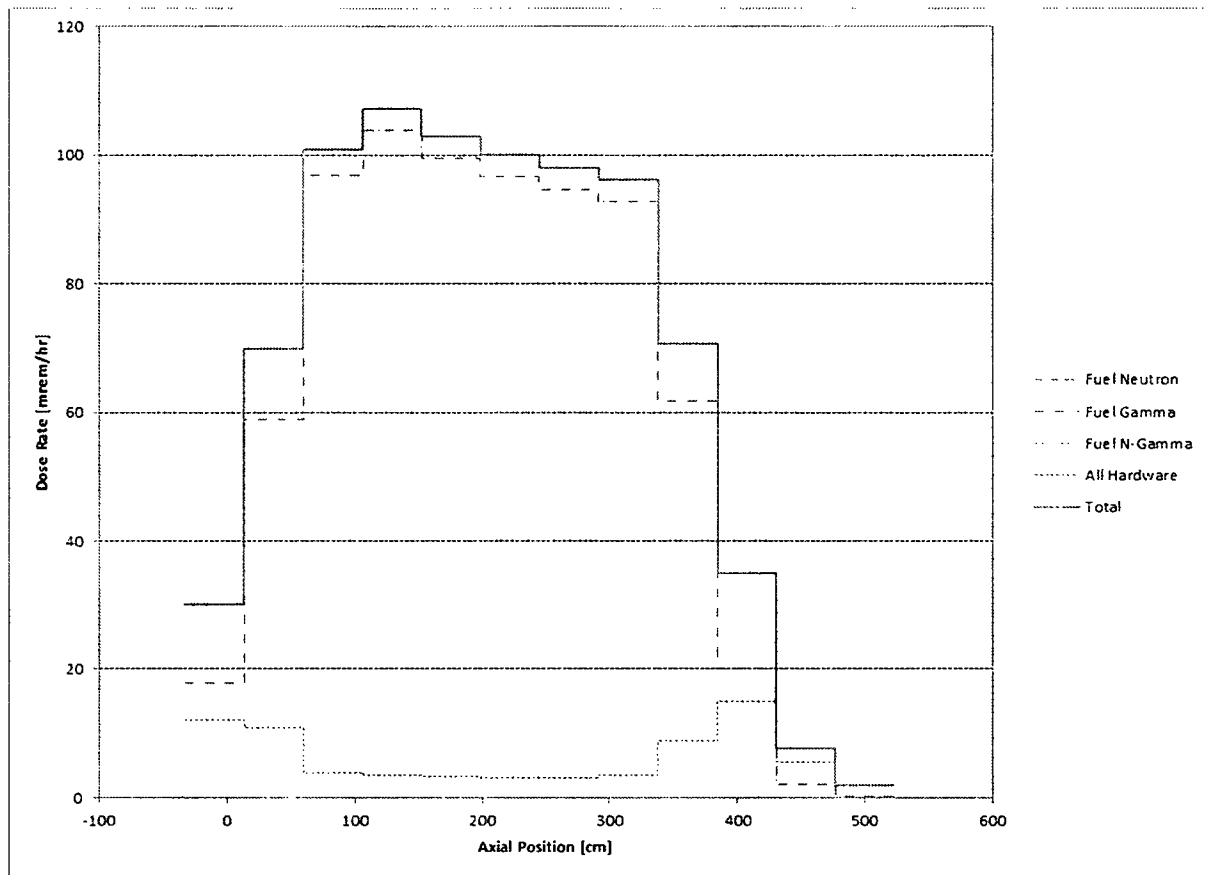


Table 5.9.3-1 Maximum CC4 Surface Dose Rates – Reduced Cool Time

Surface	Fuel Type	Cool Time (yrs)	Assembly Average Burnup (GWd/MTU)	Initial Enrichment (wt% <sup>235</sup> U)	Maximum Dose Rate (mrem/hr)	Average Dose Rate (mrem/hr)
Radial	14b	2.6	20	3.9	107.4	68.4

#### 5.9.4 PWR Nonfuel Hardware Components - BPRA and Thimble Plug

The PWR fuel assembly basket is designed to store nonfuel components inside the fuel assembly. The BPRA and TP evaluations were not changed from Section 5.8.5; refer to that section for expanded explanation of the BPRA and TP nonfuel hardware components. Additional assembly cool time required to load the nonfuel hardware components is shown in Table 5.9.4-1. The table includes results for the preferential loading described in Section 5.9.6.

**Table 5.9.4-1 Additional Assembly Cool Time (Years) Required to Load BPRA or TP**

Zone:	A	B1	B2	C	Uniform
Additional Cool Time BPRA:	1.4	0.1	0.1	0.7	0.5
Additional Cool Time TP:	0.2	0.1	0.1	0.1	0.1

##### 5.9.4.1 Combination of Fuel, BPRA, and Thimble Plug Dose Rates

Maximum combined dose rates at the cask radial surface are calculated for the reduced minimum cool time. The combined dose rate is listed in Table 5.9.4-2 for the uniform loading.

Table 5.9.4-2 Reduced Cool Time Combined Dose Rate Results

Cask / Dose Location	Fuel		Combined	
	Assembly	Max. Dose Rate (mrem/hr)	Assembly	Max. Dose Rate (mrem/hr)
CC4 Radial	WE 14×14	107.4	WE 14×14	113.9

#### 5.9.5 Nonfuel Hardware Component – Reactor Control Elements

Reactor control element (e.g., CEAs and RCCAs) material quantities and the core region in which the material was exposed to the neutron activation flux were obtained from the DOE characteristics database [30] for previous sections. This database assumes the Westinghouse 14x14 CEA is fully inserted when calculating activated CEA masses which severely overestimates the activated CEA mass. During typical core operation only the tips of the CEA rods are located within a significant neutron flux field. Rod tips are above the active fuel region at full withdrawal limiting activated regions to the plenum and assembly top regions. Activation volumes and masses for the WE 14x14 assembly type CEA are calculated in this section to more accurately evaluate the heat and dose contribution from the CEAs.

As the WE 14x14 CEA rod dimensions are not known the rod dimensions of the WE 15x15 CEA are used to approximate volumes and masses for the 14x14 CEA. The WE 15x15 CEA rod to guide tube gap is applied to the WE 14x14 assembly to approximate the 14x14 CEA rod outer diameter. The cone on the bottom of the CEA rod is assumed the same length. The CEA is assumed inserted to the top of the active fuel region. Using the calculated CEA rod cross section and the length of the upper nozzle and upper plenum the activated mass of the WE 14x14 CEA is calculated.

Mass quantities activated in the assembly top and gas plenum regions are listed in Table 5.9.5-2. Similar to the fuel assembly hardware evaluation, the plenum material is activated at a 0.2 flux factor, with top material activation at a 0.1 flux factor. Material above the top is not considered to be activated to a significant extent and is, therefore, not modeled. In the shielding evaluation, the source material activated in the plenum region of the fuel assembly is located at the bottom of the active fuel region. This is the result of the full insertion of the CEA into the assembly under storage conditions. To minimize the increased dose due to loading of CEAs, only the center nine basket locations are allowed to contain the added source. The minimum cool time of the CEA is reduced to 2.5 years.

Results are shown in Table 5.9.5-3. On the sides of the concrete and transfer casks, the additive dose rate does not affect the maximum dose rates. At the concrete cask inlets and transfer cask bottom, loading of CEAs significantly increases the maximum dose rates.

The maximum decay heat produced by loading a single CEA is 18.5 W. An increase in assembly cool time required to allow loading of a CEA is shown in Table 5.9.5-4. As an increase in cool time will also decrease the fuel source term, the strict application of increased cool time without a recalculation of fuel dose rates is conservative.

**Table 5.9.5-1 Westinghouse CEA Dimensions**

	Dimension	14x14 [Calculated]	15x15 [Known]
RCCA Rod OD	inch	0.398	0.4395
RCCA Rod ID	inch	0.359	0.4005
Lower Plug OD	inch	0.398	0.4395
Lower Plug Length	inch	1.125	1.125
Conical Section Length	inch	0.625	0.625

**Table 5.9.5-2 Calculated WE 14x14 CEA Activated Mass**

Material	Neutron Zone	WE 14x14
Steel/Inconel	Top	0.169
Ag-In-Cd	Top	0.860
Steel/Inconel	Gas Plenum	0.593
Ag-In-Cd	Gas Plenum	1.820

**Table 5.9.5-3 CEA Dose Rate Contributions – Westinghouse 14x14**

Cask / Dose Location	Maximum Dose (mrem/hr)	Average Dose (mrem/hr)
Stainless Steel Transfer Cask Radial	1.41	0.2
Stainless Steel Transfer Cask Bottom	1654.1	546.2
CC4 Radial	0.53	< 0.1
CC4 Inlet	3.41	--

**Table 5.9.5-4 Additional Assembly Cool Time (Years) Required to Load CEA**

Zone:	A	B1	B2	C	Uniform
Additional Cool Time CEA:	2.2	0.2	0.1	1.0	0.7

#### 5.9.6 Preferential Loading of PWR Fuel at a Minimum Cool time of 2.5 Years

In order to envelop fuel assemblies with heat loads higher than 959 W, a four-zone preferential loading pattern is proposed as follows.

Zone Description	Designator	Heat Load [W/assy]	# Assemblies
Inner Ring	A	513	9
Middle Ring	B1	1,300	8
	B2	1,800	4
Outer Ring	C	830	16

Preferential and uniform loading patterns limit total cask heat load to 35.5 kW. As will be seen in the results section, the maximum dose rate for the preferential loading pattern is less than that calculated for a uniform pattern.

A sketch of the PWR basket and loading pattern is shown in Figure 5.9.6-1.

Minimum cool time tables for the preferential heat load pattern are included in Section 5.9.8. The method and models for the preferential loading pattern shielding evaluations are identical to those of the uniform loading pattern with the exception of requiring three sets of response functions, one for each zone. Source spectrum varies as a result of changes in burnup, initial enrichment and minimum cool time and, therefore, requires cask dose responses (dose per unit source in each spectrum energy group) for each of the zones. The dose responses from each ring, accounting for the differences in the number of assemblies per zone, are added to arrive at the dose rate for a fully loaded cask.

##### 5.9.6.1 MCNP Input File Setup

Based on a four-zone pattern, the source and tally descriptions are modified in the MCNP models to consider the sources in the appropriate basket locations with the proper scaling on the tally cards. For each cask/detector combination, four sets of runs (A, B1, B2 and C) are needed to characterize the dose rate response.

##### 5.9.6.2 MTC and CC4 Dose Rates

Maximum and average surface dose rates for the preferential pattern are shown in Table 5.9.6-1, with the corresponding limiting results for the uniform pattern. The maximum dose rates for the analyzed preferential loading pattern are less than or statistically unchanged from those

calculated for a uniform pattern at each detector surface for both casks with the exception of MTC bottom dose rates. Maximum MTC bottom dose rates are increased minimally ( $< 7\%$ ).

The concrete cask radial and top axial average dose rates are less than or statistically unchanged in the preferential pattern. Therefore, using the uniform pattern to characterize the restricted area and controlled area boundaries is acceptable.



Figure 5.9.6-1 Schematic of PWR Fuel 1.8 kW Preferential Loading Pattern

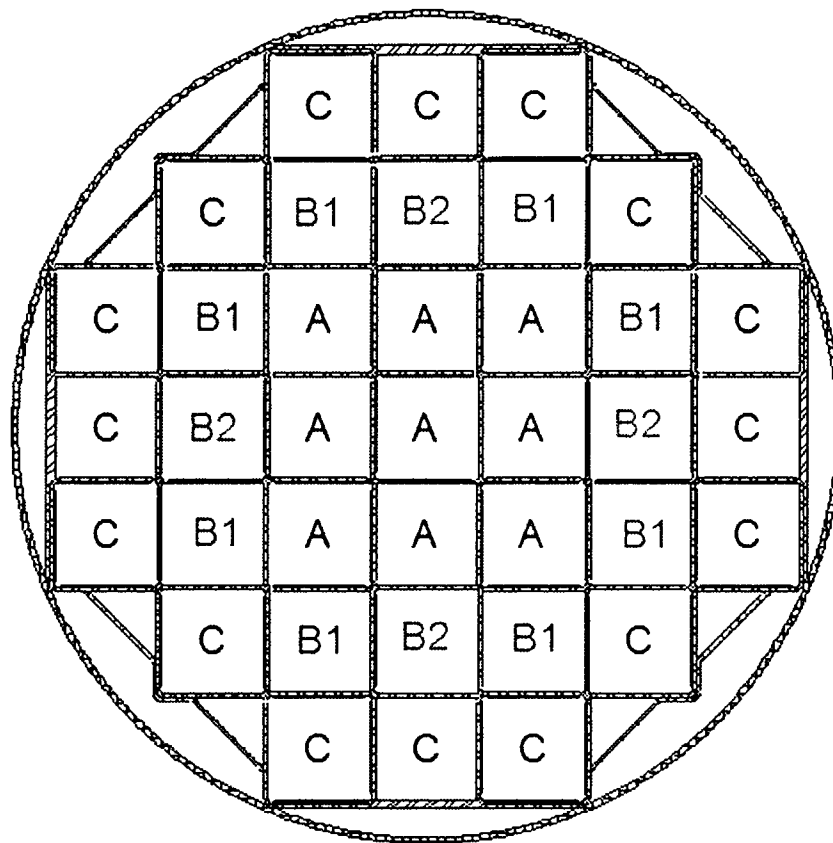


Table 5.9.6-1 Preferential Pattern Dose Rate Results

Cask / Dose Location	Uniform		Preferential	
	Avg. Dose Rate (mrem/hr)	Max. Dose Rate (mrem/hr)	Avg. Dose Rate (mrem/hr)	Max. Dose Rate (mrem/hr)
Stainless Steel MTC Radial	628	883	689	888
Stainless Steel MTC Top	216	466	221	464
Stainless Steel MTC Bottom	2,713	5,239	2,687	5,630
CC4 Radial	68.4	107.4	67.1	103.2
CC4 Top	61.5	315	58.3	288.4
CC4 Inlet	--	112.4	--	103.3
CC4 Outlet	--	35.4	--	35.7

### 5.9.7 Sample Input Files

This section contains sample input files for the four zone preferential loading pattern. Figure 5.9.7-1 provides the preferential zone B1 loading pattern for the stainless steel transfer cask. Figure 5.9.7-2 provides the preferential zone B2 loading pattern for concrete cask. All other modeling configurations (i.e. damaged fuel) are unchanged from those presented in Section 5.8.8.

**Figure 5.9.7-1 Transfer Cask Sample Input File – Preferential Zone B1**

```
MAGNASTOR Duke Transfer Cask - trfShwDryRadFg_ngl4b_B107g
C Radial Biasing - Fuel Gamma Source
C Fuel Assembly Cells - ngl4b - v1.0
1 1 -2.5071 -1 u=6 $ Lower Nozzle
2 2 -2.7253 -2 +1 u=6 $ Lower Plenum
3 3 -3.9171 -3 +2 u=6 $ Fuel
4 4 -1.0067 -4 +3 u=6 $ Upper Plenum
5 5 -2.8608 -5 +4 u=6 $ Upper Nozzle
6 0 +5 u=6 $ Outside
C Cells - Fuel Tube v1.0
7 8 -7.8212 -8 +7 u=5 $ Tube
8 13 -2.6507 -9 -7 u=5 $ Poison
9 13 -2.6507 -10 -7 u=5 $ Poison
10 13 -2.6507 -11 -7 u=5 $ Poison
11 13 -2.6507 -12 -7 u=5 $ Poison
12 0 -7 #8 #9 #10 #11 u=5 $ Space Inside Tube
13 0 +7 +8 u=5 $ Space Below and Outside Tube
C Cells - PWR Basket v1.0
14 0 -13 -14 fill=5 trcl = ( -23.5331 70.5993 0.0000 ) u=4 $ Assy loc 1
15 like 14 but fill=5 trcl = ( 23.5331 70.5993 0.0000 ) u=4 $ Assy loc 3
16 like 14 but fill=5 trcl = ( -47.0662 47.0662 0.0000 ) u=4 $ Assy loc 4
17 like 14 but fill=5 trcl = ( 0.0000 47.0662 0.0000 ) u=4 $ Assy loc 6
18 like 14 but fill=5 trcl = ( 47.0662 47.0662 0.0000 ) u=4 $ Assy loc 8
19 like 14 but fill=5 trcl = ( -70.5993 23.5331 0.0000 ) u=4 $ Assy loc 9
20 like 14 but fill=5 trcl = ( -23.5331 23.5331 0.0000 ) u=4 $ Assy loc 11
21 like 14 but fill=5 trcl = ( 23.5331 23.5331 0.0000 ) u=4 $ Assy loc 13
22 like 14 but fill=5 trcl = ( 70.5993 23.5331 0.0000 ) u=4 $ Assy loc 15
23 like 14 but fill=5 trcl = ( -47.0662 0.0000 0.0000 ) u=4 $ Assy loc 17
24 like 14 but fill=5 trcl = ( 0.0000 0.0000 0.0000 ) u=4 $ Assy loc 19
25 like 14 but fill=5 trcl = ( 47.0662 0.0000 0.0000 ) u=4 $ Assy loc 21
26 like 14 but fill=5 trcl = ( -70.5993 -23.5331 0.0000 ) u=4 $ Assy loc 23
27 like 14 but fill=5 trcl = ( -23.5331 -23.5331 0.0000 ) u=4 $ Assy loc 25
28 like 14 but fill=5 trcl = ( 23.5331 -23.5331 0.0000 ) u=4 $ Assy loc 27
29 like 14 but fill=5 trcl = ( 70.5993 -23.5331 0.0000 ) u=4 $ Assy loc 29
30 like 14 but fill=5 trcl = ( -47.0662 -47.0662 0.0000 ) u=4 $ Assy loc 30
31 like 14 but fill=5 trcl = ( 0.0000 -47.0662 0.0000 ) u=4 $ Assy loc 32
32 like 14 but fill=5 trcl = ( 47.0662 -47.0662 0.0000 ) u=4 $ Assy loc 34
33 like 14 but fill=5 trcl = ( -23.5331 -70.5993 0.0000 ) u=4 $ Assy loc 35
34 like 14 but fill=5 trcl = ( 23.5331 -70.5993 0.0000 ) u=4 $ Assy loc 37
35 8 -7.8212 -15 #22 #29 u=4 $ Side support +x
36 8 -7.8212 -16 #19 #26 u=4 $ Side support -x
37 8 -7.8212 -17 #14 #15 u=4 $ Side support +y
38 8 -7.8212 -18 #33 #34 u=4 $ Side support -y
39 8 -7.8212 -19 +20 +21 u=4 $ Corner
40 8 -7.8212 -21 +22 +20 +15.2 +16.1 +17.4 +18.3
#14 #15 #19 #22 #26 #29 #33 #34 u=4 $ Corner diagonal
41 0 #14 #15 #16 #17 #18 #19 #20 #21 #22 #23 #24
#25 #26 #27 #28 #29 #30 #31 #32 #33 #34
#35 #36 #37 #38 #39 #40 u=4 $ Outside Basket Structure
C Cells - PWR Canister Cavity v1.0
42 0 -23 fill=6 trcl = ( -23.5331 70.5993 0.0000 ) u=3 $ Assy loc 1
43 like 42 but fill=6 trcl = ( 0.0000 70.5993 0.0000 ) u=3 $ Assy loc 2
44 like 42 but fill=6 trcl = ( 23.5331 70.5993 0.0000 ) u=3 $ Assy loc 3
45 like 42 but fill=6 trcl = ( -47.0662 47.0662 0.0000 ) u=3 $ Assy loc 4
46 like 42 but fill=6 trcl = ( -23.5331 47.0662 0.0000 ) u=3 $ Assy loc 5
47 like 42 but fill=6 trcl = ( 0.0000 47.0662 0.0000 ) u=3 $ Assy loc 6
48 like 42 but fill=6 trcl = ( 23.5331 47.0662 0.0000 ) u=3 $ Assy loc 7
49 like 42 but fill=6 trcl = ( 47.0662 47.0662 0.0000 ) u=3 $ Assy loc 8
50 like 42 but fill=6 trcl = ( -70.5993 23.5331 0.0000 ) u=3 $ Assy loc 9
51 like 42 but fill=6 trcl = ( -47.0662 23.5331 0.0000 ) u=3 $ Assy loc 10
52 like 42 but fill=6 trcl = ( -23.5331 23.5331 0.0000 ) u=3 $ Assy loc 11
53 like 42 but fill=6 trcl = ( 0.0000 23.5331 0.0000 ) u=3 $ Assy loc 12
54 like 42 but fill=6 trcl = ( 23.5331 23.5331 0.0000 ) u=3 $ Assy loc 13
55 like 42 but fill=6 trcl = ( 47.0662 23.5331 0.0000 ) u=3 $ Assy loc 14
56 like 42 but fill=6 trcl = ( 70.5993 23.5331 0.0000 ) u=3 $ Assy loc 15
57 like 42 but fill=6 trcl = ( -70.5993 0.0000 0.0000 ) u=3 $ Assy loc 16
58 like 42 but fill=6 trcl = ( -47.0662 0.0000 0.0000 ) u=3 $ Assy loc 17
```

```
59 like 42 but fill=6 trcl = ( -23.5331 0.0000 0.0000 ) u=3 $ Assy loc 18
60 like 42 but fill=6 trcl = ( 0.0000 0.0000 0.0000 ) u=3 $ Assy loc 19
61 like 42 but fill=6 trcl = ( 23.5331 0.0000 0.0000 ) u=3 $ Assy loc 20
62 like 42 but fill=6 trcl = ( 47.0662 0.0000 0.0000 ) u=3 $ Assy loc 21
63 like 42 but fill=6 trcl = ( 70.5993 0.0000 0.0000 ) u=3 $ Assy loc 22
64 like 42 but fill=6 trcl = ( -70.5993 -23.5331 0.0000 ) u=3 $ Assy loc 23
65 like 42 but fill=6 trcl = ( -47.0662 -23.5331 0.0000 ) u=3 $ Assy loc 24
66 like 42 but fill=6 trcl = ( -23.5331 -23.5331 0.0000 ) u=3 $ Assy loc 25
67 like 42 but fill=6 trcl = ( 0.0000 -23.5331 0.0000 ) u=3 $ Assy loc 26
68 like 42 but fill=6 trcl = ( 23.5331 -23.5331 0.0000 ) u=3 $ Assy loc 27
69 like 42 but fill=6 trcl = ( 47.0662 -23.5331 0.0000 ) u=3 $ Assy loc 28
70 like 42 but fill=6 trcl = ( 70.5993 -23.5331 0.0000 ) u=3 $ Assy loc 29
71 like 42 but fill=6 trcl = ( -47.0662 -47.0662 0.0000 ) u=3 $ Assy loc 30
72 like 42 but fill=6 trcl = ( -23.5331 -47.0662 0.0000 ) u=3 $ Assy loc 31
73 like 42 but fill=6 trcl = ( 0.0000 -47.0662 0.0000 ) u=3 $ Assy loc 32
74 like 42 but fill=6 trcl = ( 23.5331 -47.0662 0.0000 ) u=3 $ Assy loc 33
75 like 42 but fill=6 trcl = ( 47.0662 -47.0662 0.0000 ) u=3 $ Assy loc 34
76 like 42 but fill=6 trcl = ( -23.5331 -70.5993 0.0000 ) u=3 $ Assy loc 35
77 like 42 but fill=6 trcl = ( 0.0000 -70.5993 0.0000 ) u=3 $ Assy loc 36
78 like 42 but fill=6 trcl = ( 23.5331 -70.5993 0.0000 ) u=3 $ Assy loc 37
79 0 #42 #43 #44 #45 #46 #47 #48 #49 #50 #51 #52 #53 #54
#55 #56 #57 #58 #59 #60 #61 #62 #63 #64 #65 #66 #67
#68 #69 #70 #71 #72 #73 #74 #75 #76 #77 #78 fill=4 u=3 $ Cavity
C Cells - Canister w/Weld Shield v1.0
80 0 -24 #92 #93 fill=3 u=2 $ Cavity
81 7 -7.9400 -31 +24.3 u=2 $ Canister Bottom
82 0 -25 +24.2 -28 trcl = ( 62.7565 43.1314 0.0000 ) u=2 $ Bottom Drain Port
83 14 -3.9700 -26 +28 -30 trcl = ( 62.7565 43.1314 0.0000 ) u=2 $ Middle Drain Port
84 0 -27 +30 -31.2 trcl = ( 62.7565 43.1314 0.0000 ) u=2 $ Top Drain Port
85 like 82 but trcl = ( -62.7565 -43.1314 0.0000 ) u=2 $ Bottom Vent Port
86 like 83 but trcl = ( -62.7565 -43.1314 0.0000 ) u=2 $ Middle Vent Port
87 like 84 but trcl = ( -62.7565 -43.1314 0.0000 ) u=2 $ Top Vent Port
88 7 -7.9400 -31 -24.3 +24.1 u=2 $ Canister Shell
89 8 -7.8212 -31 -24.1 +24.2 -29 #82 #83 #85 #86 u=2 $ Lower lid
90 7 -7.9400 -31 -24.1 +29 #83 #84 #86 #87 u=2 $ Upper lid
91 7 -7.9400 (-32 +35 +36) : (-33 +35 +36) : (-34 +35 +36) u=2 $ Weld Shield
92 8 -7.8212 -39 +38 +37 -24.2 trcl = ( 62.7565 43.1314 0.0000 ) u=2 $ Drain port
shield
93 8 -7.8212 -39 +38 +37 -24.2 trcl = ( -62.7565 -43.1314 0.0000 ) u=2 $ Vent port
shield
94 0 +31 #91 u=2 $ Outside void
C Transfer Cask Cells - v1.2_ngl4b
95 0 -57 #108 fill=2 ( 0.0000 0.0000 7.0350 ) u=1 $ Canister and Weld Shield
96 0 -40 -41 +57 -48 u=1 $ Gap MTC to Canister below seal
97 6 -0.9982 -40 -41 +57 -49 +48 u=1 $ Gap between seals
98 0 -40 -41 +57 +49 #108 u=1 $ Gap MTC to Canister above seal
99 7 -7.9400 -40 +41 -46 u=1 $ Bottom forging
100 7 -7.9400 -42 +41 +46 -47 u=1 $ Inner shell
101 0 -43 +42 +46 -47 u=1 $ Gap
102 10 -11.344 -44 +43 +46 -47 u=1 $ Lead shell
103 11 -1.6316 -45 +44 +46 -47 u=1 $ NS4FR shell
104 7 -7.9400 -40 +45 +46 -47 u=1 $ Outer shell
105 7 -7.9400 -40 +41 +47 u=1 $ Top forging
106 7 -7.9400 (-50 +51 -56) : (-50 -52 -56) u=1 $ Door rail
107 7 -7.9400 -55 -53 +54 -56 +57 u=1 $ Door steel
108 7 -7.9400 -59 +58 -40 u=1 $ Weld bar
109 0 +40 #106 #107 +57 u=1 $ Void
C Detector Cells - Radial Biasing
400 0 -400 fill=1 $ Surface
500 0 -500 +400 $ 1ft
600 0 -600 +400 +500 $ 1m
700 0 -700 +400 +500 +600 $ 2m
800 0 -800 +400 +500 +600 +700 $ 4m
900 0 +400 +500 +600 +700 +800 $ Exterior
C Fuel Assembly Surfaces - ngl4b - v1.0
1 RPP -9.8590 9.8590 -9.8590 9.8590 0.0000 8.0975 $ Lower Nozzle
2 RPP -9.8590 9.8590 -9.8590 9.8590 0.0000 9.8374 $ Lower Plenum
3 RPP -9.8590 9.8590 -9.8590 9.8590 0.0000 378.6454 $ Fuel
```

4 RPP -9.8590 9.8590 -9.8590 9.8590 0.0000 400.3040 \$ Upper Plenum  
5 RPP -9.8590 9.8590 -9.8590 9.8590 0.0000 409.1940 \$ Upper Nozzle  
6 PZ 255.7094 \$ Flood elevation  
C Surfaces - Fuel Tube v1.0  
7 RPP -11.6015 11.6015 -11.6015 11.6015 7.6200 439.4200 \$ Tube void  
8 RPP -12.3952 12.3952 -12.3952 12.3952 7.6200 430.5300 \$ Tube  
9 RPP -11.6015 -11.2840 -10.2362 10.2362 9.2075 428.9425 \$ Poison left  
10 RPP 11.2840 11.6015 -10.2362 10.2362 9.2075 428.9425 \$ Poison right  
11 RPP -10.2362 10.2362 11.2840 11.6015 9.2075 428.9425 \$ Poison top  
12 RPP -10.2362 10.2362 -11.6015 -11.2840 9.2075 428.9425 \$ Poison bottom  
C Surfaces - PWR Basket v1.0  
13 RPP -12.3952 12.3952 -12.3952 12.3952 0.0000 439.4200 \$ Tube opening  
14 8 RPP -16.6370 16.6370 -16.6370 16.6370 0.0000 439.4200 \$ Tube radius  
15 RPP 81.8833 83.7883 -33.1851 33.1851 7.6200 430.5300 \$ Side support +x  
16 RPP -83.7883 -81.8833 -33.1851 33.1851 7.6200 430.5300 \$ Side support -x  
17 RPP -33.1851 33.1851 81.8833 83.7883 7.6200 430.5300 \$ Side support +y  
18 RPP -33.1851 33.1851 -83.7883 -81.8833 7.6200 430.5300 \$ Side support -y  
19 RPP -60.2552 60.2552 -60.2552 60.2552 7.6200 430.5300 \$ Corner outer  
20 RPP -59.4614 59.4614 -59.4614 59.4614 7.6200 430.5300 \$ Corner inner  
21 8 RPP -78.6267 78.6267 -78.6267 78.6267 7.6200 430.5300 \$ Corner dia. outer  
22 8 RPP -77.8329 77.8329 -77.8329 77.8329 7.6200 430.5300 \$ Corner dia. inner  
C Surfaces - PWR Canister Cavity v1.0  
23 RPP -9.8595 9.8595 -9.8595 9.8595 0.0000 409.1941 \$ Assy opening  
C Surfaces - Canister w/Weld Shield v1.0  
24 RCC 0.0000 0.0000 0.0000 0.0000 0.0000 439.4200 90.1700 \$ Cavity  
25 CZ 2.6924 \$ Bot Cylinder Radius  
26 CZ 6.7691 \$ Mid Cyclinder Radius  
27 CZ 7.4041 \$ Top Cylinder Radius  
28 PZ 450.8500 \$ Port plane bot/mid  
29 PZ 452.1200 \$ Lower/upper lid  
30 PZ 459.4860 \$ Port plane mid/top  
31 RCC 0.0000 0.0000 -6.9950 0.0000 0.0000 469.2750 91.4500 \$ Canister  
32 RCC 0.0000 0.0000 462.2800 0.0000 0.0000 5.0800 78.1050 \$ Weld shield bot  
33 RCC 0.0000 0.0000 467.3600 0.0000 0.0000 5.0800 71.7550 \$ Weld shield mid  
34 RCC 0.0000 0.0000 472.4400 0.0000 0.0000 5.0900 66.6750 \$ Weld shield top  
35 RCC 62.7565 43.1314 462.2800 0.0000 0.0000 15.2500 8.8900 \$ Weld shield cutout +x+y  
36 RCC -62.7565 -43.1314 462.2800 0.0000 0.0000 15.2500 8.8900 \$ Weld shield cutout -x-y  
37 PZ 433.0700 \$ Port shield elevation  
38 CZ 2.8575 \$ Port shield ID  
39 CZ 5.0800 \$ Port shield OD  
C Transfer Cask Surfaces - v1.2 ngl4b  
40 RCC 0.0000 0.0000 0.0000 0.0000 0.0000 471.1700 111.7600 \$ Cask (Without Rail / Doors)  
41 CZ 92.7100 \$ Cavity  
42 CZ 94.6150 \$ Inner shell  
43 CZ 94.7420 \$ Gap  
44 CZ 102.8700 \$ Lead shell  
45 CZ 108.5850 \$ NS4FR shell  
46 PZ 30.4800 \$ Bottom forging  
47 PZ 435.6100 \$ Top forging  
48 PZ 3.9116 \$ Lower Elevation Water Jacket  
49 PZ 463.3214 \$ Upper Elevation Water Jacket  
50 RPP -104.0765 104.0765 -111.7600 111.7600 -12.7000 0.0000 \$ Door container  
51 PY 97.0026 \$ Inside rail +y  
52 PY -97.0026 \$ Inside rail -y  
53 PY 96.5200 \$ Door +y  
54 PY -96.5200 \$ Door -y  
55 RHP 0.0000 0.0000 -12.7000 0.0000 0.0000 12.7000 \$ Door prism  
108.4699 0.0000 0.0000 89.7374 -73.7172 0.0000  
-89.7374 -73.7172 0.0000  
56 RCC 0.0000 0.0000 -12.7000 0.0000 0.0000 12.7000 111.7600 \$ Door container  
57 RCC 0.0000 0.0000 0.0500 0.0000 0.0000 484.5550 91.4400 \$ Canister and Weld Shield  
58 CZ 90.8049 \$ Weld bar inner  
59 RCC 0.0000 0.0000 469.3150 0.0000 0.0000 1.9050 92.7100 \$ Weld bar outer  
C Radial Detector DRA (Surface)  
400 RCC 0.0000 0.0000 -12.8000 0.0000 0.0000 497.4550 111.8600  
401 PZ 20.3637  
402 PZ 53.5273

403 PZ 86.6910  
404 PZ 119.8547  
405 PZ 153.0183  
406 PZ 186.1820  
407 PZ 219.3457  
408 PZ 252.5093  
409 PZ 285.6730  
410 PZ 318.8367  
411 PZ 352.0003  
412 PZ 385.1640  
413 PZ 418.3277  
414 PZ 451.4913  
C Radial Detector DRB (1ft)  
500 RCC 0.0000 0.0000 -43.2800 0.0000 0.0000 558.4150 142.3400  
501 PZ -6.0523  
502 PZ 31.1753  
503 PZ 68.4030  
504 PZ 105.6307  
505 PZ 142.8583  
506 PZ 180.0860  
507 PZ 217.3137  
508 PZ 254.5413  
509 PZ 291.7690  
510 PZ 328.9967  
511 PZ 366.2243  
512 PZ 403.4520  
513 PZ 440.6797  
514 PZ 477.9073  
C Radial Detector DRC (1m)  
600 RCC 0.0000 0.0000 -112.8000 0.0000 0.0000 697.4550 211.8600  
601 PZ -77.9273  
602 PZ -43.0545  
603 PZ -8.1817  
604 PZ 26.6910  
605 PZ 61.5638  
606 PZ 96.4365  
607 PZ 131.3093  
608 PZ 166.1820  
609 PZ 201.0548  
610 PZ 235.9275  
611 PZ 270.8003  
612 PZ 305.6730  
613 PZ 340.5458  
614 PZ 375.4185  
615 PZ 410.2913  
616 PZ 445.1640  
617 PZ 480.0368  
618 PZ 514.9095  
619 PZ 549.7823  
C Radial Detector DRD (2m)  
700 RCC 0.0000 0.0000 -212.8000 0.0000 0.0000 897.4550 311.8600  
701 PZ -167.9273  
702 PZ -123.0545  
703 PZ -78.1818  
704 PZ -33.3090  
705 PZ 11.5638  
706 PZ 56.4365  
707 PZ 101.3093  
708 PZ 146.1820  
709 PZ 191.0548  
710 PZ 235.9275  
711 PZ 280.8003  
712 PZ 325.6730  
713 PZ 370.5458  
714 PZ 415.4185  
715 PZ 460.2913  
716 PZ 505.1640  
717 PZ 550.0368  
718 PZ 594.9095

719 PZ 639.7823  
C Radial Detector DRE (4m)  
800 RCC 0.0000 0.0000 -412.8000 0.0000 0.0000 1297.4550 511.8600  
801 PZ -347.9273  
802 PZ -283.0545  
803 PZ -218.1818  
804 PZ -153.3090  
805 PZ -88.4363  
806 PZ -23.5635  
807 PZ 41.3093  
808 PZ 106.1820  
809 PZ 171.0548  
810 PZ 235.9275  
811 PZ 300.8003  
812 PZ 365.6730  
813 PZ 430.5458  
814 PZ 495.4185  
815 PZ 560.2913  
816 PZ 625.1640  
817 PZ 690.0368  
818 PZ 754.9095  
819 PZ 819.7823

C  
C Materials List - Common Materials - v1.0  
C  
C Homogenized Lower Nozzle  
m1 24000 -1.9000E-01 25055 -2.0000E-02 26000 -6.9500E-01  
28000 -9.5000E-02  
C Homogenized Lower Plenum  
m2 24000 -1.0000E-03 50000 -1.5000E-02  
26000 -1.2500E-03 7014 -5.0000E-04  
40000 -9.8225E-01  
C Homogenized UO2 Fuel - Dry  
m3 92235 -3.6891E-02 40000 -1.6011E-01 24000 -1.6300E-04  
92238 -7.0092E-01 50000 -2.4450E-03 7014 -8.1499E-05  
8016 -9.9186E-02 26000 -2.0375E-04  
C Homogenized Upper Plenum  
m4 24000 -1.4890E-01 50000 -3.2622E-03 25055 -1.5650E-02  
26000 -5.4413E-01 7014 -1.0874E-04 28000 -7.4340E-02  
40000 -2.1362E-01  
C Homogenized Upper Nozzle  
m5 24000 -1.9000E-01 25055 -2.0000E-02 26000 -6.9500E-01  
28000 -9.5000E-02  
C Water  
m6 1001 2 8016 1  
C Stainless Steel  
m7 24000 -0.190 25055 -0.020 26000 -0.695  
28000 -0.095  
C Carbon Steel  
m8 26000 -0.99 6012 -0.01  
C Aluminum  
m9 13027 -1.0  
C Lead  
m10 82000 -1.0  
C NS-4-FR  
m11 5010 -9.3127E-04 13027 -2.1420E-01 6000 -2.7627E-01  
5011 -3.7721E-03 1001 -6.0012E-02 7014 -1.9815E-02  
8016 -4.2500E-01  
C Concrete  
m12 26000 -0.014 20000 -0.044 14000 -0.337  
1001 -0.010 8016 -0.532 11023 -0.029  
13027 -0.034  
C Vent Port Middle Cylinder  
m14 24000 -0.190 25055 -0.020 26000 -0.695  
28000 -0.095  
C Neutron Absorber  
m13 13027 -0.7470 5010 -0.0356 5011 -0.1624  
6012 -0.0549



```
phys:p 100 0 0 0 1    $ Disable Doppler energy broadening
C
C Cell Importances
C
imp:p 1 113r 0
C
C PWR Source Definition - Fuel Gamma Response to Group 7
C
sdef x=d1 y=d2 z=d3 erg=d4 cell=400:95:80:d5:3
si1  -9.85901 9.85901
sp1   0 1
si2  -9.85901 9.85901
sp2   0 1
si3 a 9.8374 19.0576 28.2778 37.4980 46.7182 55.9384 65.1586
      323.3242 332.5444 341.7646 350.9848 360.2050 369.4252 378.6454
sp3 d 0.5470 0.6358 0.7247 0.8135 0.9023 0.9912 1.0800
      1.0800 0.9912 0.9023 0.8135 0.7247 0.6358 0.5470
si4   3.000E+00 4.000E+00
sp4   0 1
C Source Information
si5 l      42 43 44
      45 46 47 48 49
      50 51 52 53 54 55 56
      57 58 59 60 61 62 63
      64 65 66 67 68 69 70
      71 72 73 74 75
      76 77 78
C Source Probability
sp5      0.0 0.0 0.0
      0.0 1.0 0.0 1.0 0.0
      0.0 1.0 0.0 0.0 0.0 1.0 0.0
      0.0 0.0 0.0 0.0 0.0 0.0 0.0
      0.0 1.0 0.0 0.0 0.0 1.0 0.0
      0.0 1.0 0.0 1.0 0.0
      0.0 0.0 0.0
mode p
nps 400000000
C
C ANSI/ANS-6.1.1-1977 - Gamma Flux-to-Dose Rate Conversion Factors
C (mrem/hr)/(photons/cm2-sec)
C
de0  0.01 0.03 0.05 0.07 0.1 0.15 0.2
      0.25 0.3 0.35 0.4 0.45 0.5 0.55
      0.6 0.65 0.7 0.8 1 1.4 1.8
      2.2 2.6 2.8 3.25 3.75 4.25 4.75
      5 5.25 5.75 6.25 6.75 7.5 9
      11 13 15
df0  3.96E-03 5.82E-04 2.90E-04 2.58E-04 2.83E-04 3.79E-04 5.01E-04
      6.31E-04 7.59E-04 8.78E-04 9.85E-04 1.08E-03 1.17E-03 1.27E-03
      1.36E-03 1.44E-03 1.52E-03 1.68E-03 1.98E-03 2.51E-03 2.99E-03
      3.42E-03 3.82E-03 4.01E-03 4.41E-03 4.83E-03 5.23E-03 5.60E-03
      5.80E-03 6.01E-03 6.37E-03 6.74E-03 7.11E-03 7.66E-03 8.77E-03
      1.03E-02 1.18E-02 1.33E-02
C
C Weight Window Generation - Radial
C
wwg 2 0 0 0 0
wvp:p 5 3 5 0 -1 0
mesh geom=cyl ref=65 0 201 origin=0.1 0.1 -513
      imesh 90.2 91.4 92.7 94.6 102.9 108.6 111.8 611.8
      iints 5 1 1 1 3 1 1 1
      jmesh 500 513 520 528 530 898 920 929 959 997 1497
      jints 1 1 1 1 1 1 1 1 1 1 1
      kmesh 1
      kints 1
C wwge:p 1e-3 1 20
fc2 Radial Surface Tally
f2:p +400.1
fm2 8.0000E+00
```

```
fs2  -401 -402 -403 -404 -405 -406
      -407 -408 -409 -410 -411 -412
      -413 -414 T
tf2
fc12 Radial 1ft Tally
f12:p +500.1
fm12 8.0000E+00
fs12  -501 -502 -503 -504 -505 -506
      -507 -508 -509 -510 -511 -512
      -513 -514 T
tf12
fc22 Radial 1m Tally
f22:p +600.1
fm22 8.0000E+00
fs22  -601 -602 -603 -604 -605 -606
      -607 -608 -609 -610 -611 -612
      -613 -614 -615 -616 -617 -618
      -619 T
tf22
fc32 Radial 2m Tally
f32:p +700.1
fm32 8.0000E+00
fs32  -701 -702 -703 -704 -705 -706
      -707 -708 -709 -710 -711 -712
      -713 -714 -715 -716 -717 -718
      -719 T
tf32
fc42 Radial 4m Tally
f42:p +800.1
fm42 8.0000E+00
fs42  -801 -802 -803 -804 -805 -806
      -807 -808 -809 -810 -811 -812
      -813 -814 -815 -816 -817 -818
      -819 T
tf42
C
C
C Print Control
C
prdump -30 -60 1 2
print
C
C Random Number Generator
C
rand gen=2 seed=19073486328125 stride=152917 hist=1
C
C Rotation Matrix
C
C 5.625 degree rotation around z-axis
*TR1 0.0 0.0 0.0 5.625 95.625 90 -84.375 5.625 90 90 90 0
C 11.25 degree rotation around z-axis
*TR2 0.0 0.0 0.0 11.250 101.250 90 -78.750 11.250 90 90 90 0
C 16.875 degree rotation around z-axis
*TR3 0.0 0.0 0.0 16.875 106.875 90 -73.125 16.875 90 90 90 0
C 22.5 degree rotation around z-axis
*TR4 0.0 0.0 0.0 22.500 112.500 90 -67.500 22.500 90 90 90 0
C 28.125 degree rotation around z-axis
*TR5 0.0 0.0 0.0 28.125 118.125 90 -61.875 28.125 90 90 90 0
C 33.75 degree rotation around z-axis
*TR6 0.0 0.0 0.0 33.750 123.750 90 -56.250 33.750 90 90 90 0
C 39.375 degree rotation around z-axis
*TR7 0.0 0.0 0.0 39.375 129.375 90 -50.625 39.375 90 90 90 0
C 45 degree rotation around z-axis
*TR8 0.0 0.0 0.0 45.000 135.000 90 -45.000 45.000 90 90 90 0
C 50.625 degree rotation around z-axis
*TR9 0.0 0.0 0.0 50.625 140.625 90 -39.375 50.625 90 90 90 0
C 56.25 degree rotation around z-axis
*TR10 0.0 0.0 0.0 56.250 146.250 90 -33.750 56.250 90 90 90 0
C 61.875 degree rotation around z-axis
```

\*TR11 0.0 0.0 0.0 61.875 151.875 90 -28.125 61.875 90 90 90 0  
C 67.5 degree rotation around z-axis  
\*TR12 0.0 0.0 0.0 67.500 157.500 90 -22.500 67.500 90 90 90 0  
C 73.125 degree rotation around z-axis  
\*TR13 0.0 0.0 0.0 73.125 163.125 90 -16.875 73.125 90 90 90 0  
C 78.75 degree rotation around z-axis  
\*TR14 0.0 0.0 0.0 78.750 168.750 90 -11.250 78.750 90 90 90 0  
C 84.375 degree rotation around z-axis  
\*TR15 0.0 0.0 0.0 84.375 174.375 90 -5.625 84.375 90 90 90 0  
C 95.625 degree rotation around z-axis  
\*TR16 0.0 0.0 0.0 95.625 185.625 90 5.625 95.625 90 90 90 0  
C 101.25 degree rotation around z-axis  
\*TR17 0.0 0.0 0.0 101.250 191.250 90 11.250 101.250 90 90 90 0  
C 106.875 degree rotation around z-axis  
\*TR18 0.0 0.0 0.0 106.875 196.875 90 16.875 106.875 90 90 90 0  
C 112.5 degree rotation around z-axis  
\*TR19 0.0 0.0 0.0 112.500 202.500 90 22.500 112.500 90 90 90 0  
C 118.125 degree rotation around z-axis  
\*TR20 0.0 0.0 0.0 118.125 208.125 90 28.125 118.125 90 90 90 0  
C 123.75 degree rotation around z-axis  
\*TR21 0.0 0.0 0.0 123.750 213.750 90 33.750 123.750 90 90 90 0  
C 129.375 degree rotation around z-axis  
\*TR22 0.0 0.0 0.0 129.375 219.375 90 39.375 129.375 90 90 90 0  
C 135 degree rotation around z-axis  
\*TR23 0.0 0.0 0.0 135.000 225.000 90 45.000 135.000 90 90 90 0  
C 140.625 degree rotation around z-axis  
\*TR24 0.0 0.0 0.0 140.625 230.625 90 50.625 140.625 90 90 90 0  
C 146.25 degree rotation around z-axis  
\*TR25 0.0 0.0 0.0 146.250 236.250 90 56.250 146.250 90 90 90 0  
C 151.875 degree rotation around z-axis  
\*TR26 0.0 0.0 0.0 151.875 241.875 90 61.875 151.875 90 90 90 0  
C 157.5 degree rotation around z-axis  
\*TR27 0.0 0.0 0.0 157.500 247.500 90 67.500 157.500 90 90 90 0  
C 163.125 degree rotation around z-axis  
\*TR28 0.0 0.0 0.0 163.125 253.125 90 73.125 163.125 90 90 90 0  
C 168.75 degree rotation around z-axis  
\*TR29 0.0 0.0 0.0 168.750 258.750 90 78.750 168.750 90 90 90 0  
C 174.375 degree rotation around z-axis  
\*TR30 0.0 0.0 0.0 174.375 264.375 90 84.375 174.375 90 90 90 0

**Figure 5.9.7-2 Storage Cask Sample Input File – Preferential Zone B2**

```

MAGNASTOR VCC - strShldryRadFg_ngl4b_B207g
C Radial Biasing - Fuel Gamma Source
C Fuel Assembly Cells - ngl4b - vl.1
1 1 -2.5071 -1 u=6 $ Lower Nozzle
2 2 -2.7253 -2 +1 u=6 $ Lower Plenum
3 3 -3.9171 -3 +2 u=6 $ Fuel
4 4 -1.0067 -4 +3 u=6 $ Upper Plenum
5 5 -2.8608 -5 +4 u=6 $ Upper Nozzle
6 0 +5 u=6 $ Outside
C Cells - Fuel Tube vl.3
7 8 -7.8212 -8 +7 u=5 $ Tube
8 9 -2.6336 -9 : -10 : -11 : -12 u=5 $ Poison
9 0 #7 #8 -6 u=5 $ Outside below PFE
10 0 #7 #8 +6 u=5 $ Outside above PFE
C Cells - PWR Basket vl.5
11 0 -13 -14 fill=5 trcl = ( -23.5331 70.5993 0.0000 ) u=4 $ Assy loc 1
12 like 11 but fill=5 trcl = ( 23.5331 70.5993 0.0000 ) u=4 $ Assy loc 3
13 like 11 but fill=5 trcl = ( -47.0662 47.0662 0.0000 ) u=4 $ Assy loc 4
14 like 11 but fill=5 trcl = ( 0.0000 47.0662 0.0000 ) u=4 $ Assy loc 6
15 like 11 but fill=5 trcl = ( 47.0662 47.0662 0.0000 ) u=4 $ Assy loc 8
16 like 11 but fill=5 trcl = ( -70.5993 23.5331 0.0000 ) u=4 $ Assy loc 9
17 like 11 but fill=5 trcl = ( -23.5331 23.5331 0.0000 ) u=4 $ Assy loc 11
18 like 11 but fill=5 trcl = ( 23.5331 23.5331 0.0000 ) u=4 $ Assy loc 13
19 like 11 but fill=5 trcl = ( 70.5993 23.5331 0.0000 ) u=4 $ Assy loc 15
20 like 11 but fill=5 trcl = ( -47.0662 0.0000 0.0000 ) u=4 $ Assy loc 17
21 like 11 but fill=5 trcl = ( 0.0000 0.0000 0.0000 ) u=4 $ Assy loc 19
22 like 11 but fill=5 trcl = ( 47.0662 0.0000 0.0000 ) u=4 $ Assy loc 21
23 like 11 but fill=5 trcl = ( -70.5993 -23.5331 0.0000 ) u=4 $ Assy loc 23
24 like 11 but fill=5 trcl = ( -23.5331 -23.5331 0.0000 ) u=4 $ Assy loc 25
25 like 11 but fill=5 trcl = ( 23.5331 -23.5331 0.0000 ) u=4 $ Assy loc 27
26 like 11 but fill=5 trcl = ( 70.5993 -23.5331 0.0000 ) u=4 $ Assy loc 29
27 like 11 but fill=5 trcl = ( -47.0662 -47.0662 0.0000 ) u=4 $ Assy loc 30
28 like 11 but fill=5 trcl = ( 0.0000 -47.0662 0.0000 ) u=4 $ Assy loc 32
29 like 11 but fill=5 trcl = ( 47.0662 -47.0662 0.0000 ) u=4 $ Assy loc 34
30 like 11 but fill=5 trcl = ( -23.5331 -70.5993 0.0000 ) u=4 $ Assy loc 35
31 like 11 but fill=5 trcl = ( 23.5331 -70.5993 0.0000 ) u=4 $ Assy loc 37
32 8 -7.8212 -15 #19 #26 u=4 $ Side support +x
33 8 -7.8212 -16 #16 #23 u=4 $ Side support -x
34 8 -7.8212 -17 #11 #12 u=4 $ Side support +y
35 8 -7.8212 -18 #30 #31 u=4 $ Side support -y
36 8 -7.8212 -19 +20 +21 u=4 $ Corner
37 8 -7.8212 -21 +22 +20 +15.2 +16.1 +17.4 +18.3
#11 #12 #16 #19 #23 #26 #30 #31 u=4 $ Corner diagonal
38 0 -6 #11 #12 #13 #14 #15 #16 #17 #18 #19 #20 #21
#22 #23 #24 #25 #26 #27 #28 #29 #30 #31
#32 #33 #34 #35 #36 #37 u=4 $ Basket below PFE
39 0 +6 #11 #12 #13 #14 #15 #16 #17 #18 #19 #20 #21
#22 #23 #24 #25 #26 #27 #28 #29 #30 #31
#32 #33 #34 #35 #36 #37 u=4 $ Basket above PFE
C Cells - PWR Canister Cavity vl.5
40 0 -23 fill=6 trcl = ( -23.5331 70.5993 0.0000 ) u=3 $ Assy loc 1
41 like 40 but fill=6 trcl = ( 0.0000 70.5993 0.0000 ) u=3 $ Assy loc 2
42 like 40 but fill=6 trcl = ( 23.5331 70.5993 0.0000 ) u=3 $ Assy loc 3
43 like 40 but fill=6 trcl = ( -47.0662 47.0662 0.0000 ) u=3 $ Assy loc 4
44 like 40 but fill=6 trcl = ( -23.5331 47.0662 0.0000 ) u=3 $ Assy loc 5
45 like 40 but fill=6 trcl = ( 0.0000 47.0662 0.0000 ) u=3 $ Assy loc 6
46 like 40 but fill=6 trcl = ( 23.5331 47.0662 0.0000 ) u=3 $ Assy loc 7
47 like 40 but fill=6 trcl = ( 47.0662 47.0662 0.0000 ) u=3 $ Assy loc 8
48 like 40 but fill=6 trcl = ( -70.5993 23.5331 0.0000 ) u=3 $ Assy loc 9
49 like 40 but fill=6 trcl = ( -47.0662 23.5331 0.0000 ) u=3 $ Assy loc 10
50 like 40 but fill=6 trcl = ( -23.5331 23.5331 0.0000 ) u=3 $ Assy loc 11
51 like 40 but fill=6 trcl = ( 0.0000 23.5331 0.0000 ) u=3 $ Assy loc 12
52 like 40 but fill=6 trcl = ( 23.5331 23.5331 0.0000 ) u=3 $ Assy loc 13
53 like 40 but fill=6 trcl = ( 47.0662 23.5331 0.0000 ) u=3 $ Assy loc 14
54 like 40 but fill=6 trcl = ( 70.5993 23.5331 0.0000 ) u=3 $ Assy loc 15
55 like 40 but fill=6 trcl = ( -70.5993 0.0000 0.0000 ) u=3 $ Assy loc 16
56 like 40 but fill=6 trcl = ( -47.0662 0.0000 0.0000 ) u=3 $ Assy loc 17

```

```
57 like 40 but fill=6 trcl = ( -23.5331 0.0000 0.0000 )      u=3 $ Assy loc 18
58 like 40 but fill=6 trcl = ( 0.0000 0.0000 0.0000 )      u=3 $ Assy loc 19
59 like 40 but fill=6 trcl = ( 23.5331 0.0000 0.0000 )      u=3 $ Assy loc 20
60 like 40 but fill=6 trcl = ( 47.0662 0.0000 0.0000 )      u=3 $ Assy loc 21
61 like 40 but fill=6 trcl = ( 70.5993 0.0000 0.0000 )      u=3 $ Assy loc 22
62 like 40 but fill=6 trcl = ( -70.5993 -23.5331 0.0000 )    u=3 $ Assy loc 23
63 like 40 but fill=6 trcl = ( -47.0662 -23.5331 0.0000 )    u=3 $ Assy loc 24
64 like 40 but fill=6 trcl = ( -23.5331 -23.5331 0.0000 )    u=3 $ Assy loc 25
65 like 40 but fill=6 trcl = ( 0.0000 -23.5331 0.0000 )      u=3 $ Assy loc 26
66 like 40 but fill=6 trcl = ( 23.5331 -23.5331 0.0000 )      u=3 $ Assy loc 27
67 like 40 but fill=6 trcl = ( 47.0662 -23.5331 0.0000 )      u=3 $ Assy loc 28
68 like 40 but fill=6 trcl = ( 70.5993 -23.5331 0.0000 )      u=3 $ Assy loc 29
69 like 40 but fill=6 trcl = ( -47.0662 -47.0662 0.0000 )    u=3 $ Assy loc 30
70 like 40 but fill=6 trcl = ( -23.5331 -47.0662 0.0000 )    u=3 $ Assy loc 31
71 like 40 but fill=6 trcl = ( 0.0000 -47.0662 0.0000 )      u=3 $ Assy loc 32
72 like 40 but fill=6 trcl = ( 23.5331 -47.0662 0.0000 )      u=3 $ Assy loc 33
73 like 40 but fill=6 trcl = ( 47.0662 -47.0662 0.0000 )      u=3 $ Assy loc 34
74 like 40 but fill=6 trcl = ( -23.5331 -70.5993 0.0000 )    u=3 $ Assy loc 35
75 like 40 but fill=6 trcl = ( 0.0000 -70.5993 0.0000 )      u=3 $ Assy loc 36
76 like 40 but fill=6 trcl = ( 23.5331 -70.5993 0.0000 )      u=3 $ Assy loc 37
77 0      #40 #41 #42 #43 #44 #45 #46 #47 #48 #49 #50 #51 #52
          #53 #54 #55 #56 #57 #58 #59 #60 #61 #62 #63 #64 #65
          #66 #67 #68 #69 #70 #71 #72 #73 #74 #75 #76      fill=4 u=3 $ Cavity
C Cells - Canister vl.3
78 0      -24 fill=3      u=2 $ Cavity
79 7 -7.9400 -31 +24.3      u=2 $ Canister Bottom
80 7 -7.9400 -25 +24.2 -28 trcl = ( 61.7220 44.7040 0.0000 )    u=2 $ Bottom Drain Port
81 7 -7.9400 -26 +28 -30 trcl = ( 61.7220 44.7040 0.0000 )    u=2 $ Middle Drain Port
82 7 -7.9400 -27 +30 -31.2 trcl = ( 61.7220 44.7040 0.0000 )    u=2 $ Top Drain Port
83 like 80 but trcl = ( -61.7220 -44.7040 0.0000 )      u=2 $ Bottom Vent Port
84 like 81 but trcl = ( -61.7220 -44.7040 0.0000 )      u=2 $ Middle Vent Port
85 like 82 but trcl = ( -61.7220 -44.7040 0.0000 )      u=2 $ Top Vent Port
86 7 -7.9400 -31 -24.3 +24.1      u=2 $ Canister Shell
87 8 -7.8212 -31 -24.1 +24.2 -29 #80 #81 #83 #84      u=2 $ Lower lid
88 7 -7.9400 -31 -24.1 +29 #81 #82 #84 #85      u=2 $ Upper lid
89 0      +31      u=2 $ Outside
C VCC Cells - vl.3.1_ngl4b
90 8 -7.8212 -32      u=1 $ Pedestal plate
91 8 -7.8212 -33 +34      u=1 $ Stand
92 8 -7.8212 -39 +40 +46 +47      u=1 $ Bottom plate outer
93 8 -7.8212 (-40 +41 -35) : (-40 +41 -36)      u=1 $ Bottom plate connector
94 8 -7.8212 -41      u=1 $ Bottom plate inner
95 8 -7.8212 (-34 -60 +61 -43) : (-34 -58 +59 +60 -43)      u=1 $ Support rail inside stand
96 8 -7.8212 (+33 -60 +61 -43) : (+33 -58 +59 +60 -43)      u=1 $ Support rail outside stand
97 8 -7.8212 (-51 +53 +35 +36 -44) :
          (-52 +53 +35 +36 -44 +51)      u=1 $ Air inlet top
98 8 -7.8212 (-48 +46 +50 -44 +35 +36 +39) :
          (-49 +47 +50 -44 +35 +36 +39)      u=1 $ Air inlet wall
99 8 -7.8212 (-35 +37 +33 -44 +39) : (-36 +38 +33 -44 +39)      u=1 $ Air inlet angular wall
100 8 -7.8212 (-50 -48 +46 +35 +36 +47 +39) :
          (-50 -49 +47 +35 +36 +46 +39)      u=1 $ Air inlet remaining wall
101 8 -7.8212 -54 +56 +43 -44      u=1 $ Air outlet steel X
102 8 -7.8212 -55 +57 +43 -44      u=1 $ Air outlet steel Y
103 13 -2.3234 -44 +42 +35 +36 +39 +51 +52 +48 +49 +45 +54 +55 +62
          fill=7 u=1 $ Concrete
104 13 -2.3234 -45      u=1 $ Concrete pad
105 8 -7.8212 -42 +43 +54 +55      u=1 $ Liner
106 8 -7.8212 -62 +42      u=1 $ Top flange
107 8 -7.8212 -63      u=1 $ Lid top
108 13 -2.2432 -64      u=1 $ Lid concrete
109 8 -7.8212 -65 +64      u=1 $ Lid shell
110 8 -7.8212 (-66 +78 -43) :
          (-67 +79 -43) :
          (-68 +80 -43) :
          (-69 +81 -43) :
          (-70 +82 -43) :
          (-71 +83 -43) :
          (-72 +84 -43) :
          (-73 +85 -43) :
```

```
(-74 +86 -43) :  
(-75 +87 -43) :  
(-76 +88 -43) :  
(-77 +89 -43)      u=1 $ Standoffs  
111 8 -7.8212 -90    u=1 $ -x inlet pipe 1  
112 8 -7.8212 -91    u=1 $ -x inlet pipe 2  
113 8 -7.8212 -92    u=1 $ -x inlet pipe 3  
114 8 -7.8212 -93    u=1 $ -x inlet pipe 4  
115 8 -7.8212 -94    u=1 $ -x inlet pipe 5  
116 8 -7.8212 -95    u=1 $ -x inlet pipe 6  
117 8 -7.8212 -96    u=1 $ -x inlet pipe 7  
118 8 -7.8212 -97    u=1 $ -x inlet pipe 8  
119 8 -7.8212 -98    u=1 $ -x inlet pipe 9  
120 8 -7.8212 -99    u=1 $ -x inlet pipe 10  
121 8 -7.8212 -100   u=1 $ -x inlet pipe 11  
122 8 -7.8212 -101   u=1 $ -x inlet pipe 12  
123 8 -7.8212 -102   u=1 $ -x inlet pipe 13  
124 8 -7.8212 -103   u=1 $ -x inlet pipe 14  
125 8 -7.8212 -104   u=1 $ -x inlet pipe 15  
126 8 -7.8212 -105   u=1 $ -x inlet pipe 16  
127 8 -7.8212 -106   u=1 $ -x inlet pipe 17  
128 8 -7.8212 -107   u=1 $ +x inlet pipe 1  
129 8 -7.8212 -108   u=1 $ +x inlet pipe 2  
130 8 -7.8212 -109   u=1 $ +x inlet pipe 3  
131 8 -7.8212 -110   u=1 $ +x inlet pipe 4  
132 8 -7.8212 -111   u=1 $ +x inlet pipe 5  
133 8 -7.8212 -112   u=1 $ +x inlet pipe 6  
134 8 -7.8212 -113   u=1 $ +x inlet pipe 7  
135 8 -7.8212 -114   u=1 $ +x inlet pipe 8  
136 8 -7.8212 -115   u=1 $ +x inlet pipe 9  
137 8 -7.8212 -116   u=1 $ +x inlet pipe 10  
138 8 -7.8212 -117   u=1 $ +x inlet pipe 11  
139 8 -7.8212 -118   u=1 $ +x inlet pipe 12  
140 8 -7.8212 -119   u=1 $ +x inlet pipe 13  
141 8 -7.8212 -120   u=1 $ +x inlet pipe 14  
142 8 -7.8212 -121   u=1 $ +x inlet pipe 15  
143 8 -7.8212 -122   u=1 $ +x inlet pipe 16  
144 8 -7.8212 -123   u=1 $ +x inlet pipe 17  
145 8 -7.8212 -124   u=1 $ -y inlet pipe 1  
146 8 -7.8212 -125   u=1 $ -y inlet pipe 2  
147 8 -7.8212 -126   u=1 $ -y inlet pipe 3  
148 8 -7.8212 -127   u=1 $ -y inlet pipe 4  
149 8 -7.8212 -128   u=1 $ -y inlet pipe 5  
150 8 -7.8212 -129   u=1 $ -y inlet pipe 6  
151 8 -7.8212 -130   u=1 $ -y inlet pipe 7  
152 8 -7.8212 -131   u=1 $ -y inlet pipe 8  
153 8 -7.8212 -132   u=1 $ -y inlet pipe 9  
154 8 -7.8212 -133   u=1 $ -y inlet pipe 10  
155 8 -7.8212 -134   u=1 $ -y inlet pipe 11  
156 8 -7.8212 -135   u=1 $ -y inlet pipe 12  
157 8 -7.8212 -136   u=1 $ -y inlet pipe 13  
158 8 -7.8212 -137   u=1 $ -y inlet pipe 14  
159 8 -7.8212 -138   u=1 $ -y inlet pipe 15  
160 8 -7.8212 -139   u=1 $ -y inlet pipe 16  
161 8 -7.8212 -140   u=1 $ -y inlet pipe 17  
162 8 -7.8212 -141   u=1 $ +y inlet pipe 1  
163 8 -7.8212 -142   u=1 $ +y inlet pipe 2  
164 8 -7.8212 -143   u=1 $ +y inlet pipe 3  
165 8 -7.8212 -144   u=1 $ +y inlet pipe 4  
166 8 -7.8212 -145   u=1 $ +y inlet pipe 5  
167 8 -7.8212 -146   u=1 $ +y inlet pipe 6  
168 8 -7.8212 -147   u=1 $ +y inlet pipe 7  
169 8 -7.8212 -148   u=1 $ +y inlet pipe 8  
170 8 -7.8212 -149   u=1 $ +y inlet pipe 9  
171 8 -7.8212 -150   u=1 $ +y inlet pipe 10  
172 8 -7.8212 -151   u=1 $ +y inlet pipe 11  
173 8 -7.8212 -152   u=1 $ +y inlet pipe 12  
174 8 -7.8212 -153   u=1 $ +y inlet pipe 13  
175 8 -7.8212 -154   u=1 $ +y inlet pipe 14
```

```
176 8 -7.8212 -155      u=1 $ +y inlet pipe 15
177 8 -7.8212 -156      u=1 $ +y inlet pipe 16
178 8 -7.8212 -157      u=1 $ +y inlet pipe 17
179 0      -39 +40 -46
      +90 +91 +92 +93 +94 +95 +96
      +97 +98 +99 +100 +101 +102 +103
      +104 +105 +106 +107 +108 +109 +110
      +111 +112 +113 +114 +115 +116 +117
      +118 +119 +120 +121 +122 +123      u=1 $ Bottom plate outer void x
180 0      -39 +40 -47
      +124 +125 +126 +127 +128 +129 +130
      +131 +132 +133 +134 +135 +136 +137
      +138 +139 +140 +141 +142 +143 +144
      +145 +146 +147 +148 +149 +150 +151
      +152 +153 +154 +155 +156 +157      u=1 $ Bottom plate outer void y
181 0      -40 +41 +35 +36      u=1 $ Bottom plate connector void
182 0      (-34 -61 -43) : (-34 -59 +60 -43)      u=1 $ Support rail inside stand void
183 0      (+33 -61 -43) : (+33 -59 +60 -43)      u=1 $ Support rail outside stand void
184 0      -46 +33 +35 +36 -44 +39
      +90 +91 +92 +93 +94 +95 +96
      +97 +98 +99 +100 +101 +102 +103
      +104 +105 +106 +107 +108 +109 +110
      +111 +112 +113 +114 +115 +116 +117
      +118 +119 +120 +121 +122 +123      u=1 $ Air inlet void x
185 0      -47 +33 +35 +36 -44 +39 +46
      +124 +125 +126 +127 +128 +129 +130
      +131 +132 +133 +134 +135 +136 +137
      +138 +139 +140 +141 +142 +143 +144
      +145 +146 +147 +148 +149 +150 +151
      +152 +153 +154 +155 +156 +157      u=1 $ Air inlet void y
186 0      -53 +33 +35 +36      u=1 $ Air inlet top void
187 0      (-37 +39 +33) : (-38 +39 +33)      u=1 $ Connector void
188 0      -34 +58 +60      u=1 $ Stand void
189 0      -56 +43 -44      u=1 $ Air outlet void X
190 0      -57 +43 -44      u=1 $ Air outlet void Y
191 0      -43 +32 +33 +58 +60 +65 #110
      fill=2 ( 0.0000 0.0000 6.9850 )      u=1 $ Cavity
192 0      +44 +42 +62 63      u=1 $ Outside
C VCC Rebar Cells - vl.3.1_ngl4b
193 8 -7.8212 -158      u=7 $ Outer hoop 1
194 8 -7.8212 -159      u=7 $ Outer hoop 2
195 8 -7.8212 -160      u=7 $ Outer hoop 3
196 8 -7.8212 -161      u=7 $ Outer hoop 4
197 8 -7.8212 -162      u=7 $ Outer hoop 5
198 8 -7.8212 -163      u=7 $ Outer hoop 6
199 8 -7.8212 -164      u=7 $ Outer hoop 7
200 8 -7.8212 -165      u=7 $ Outer hoop 8
201 8 -7.8212 -166      u=7 $ Outer hoop 9
202 8 -7.8212 -167      u=7 $ Outer hoop 10
203 8 -7.8212 -168      u=7 $ Outer hoop 11
204 8 -7.8212 -169      u=7 $ Outer hoop 12
205 8 -7.8212 -170      u=7 $ Outer hoop 13
206 8 -7.8212 -171      u=7 $ Outer hoop 14
207 8 -7.8212 -172      u=7 $ Outer hoop 15
208 8 -7.8212 -173      u=7 $ Outer hoop 16
209 8 -7.8212 -174      u=7 $ Outer hoop 17
210 8 -7.8212 -175      u=7 $ Outer hoop 18
211 8 -7.8212 -176      u=7 $ Outer hoop 19
212 8 -7.8212 -177      u=7 $ Outer hoop 20
213 8 -7.8212 -178      u=7 $ Outer hoop 21
214 8 -7.8212 -179      u=7 $ Outer hoop 22
215 8 -7.8212 -180      u=7 $ Outer hoop 23
216 8 -7.8212 -181      u=7 $ Outer hoop 24
217 8 -7.8212 -182      u=7 $ Outer hoop 25
218 8 -7.8212 -183      u=7 $ Outer hoop 26
219 8 -7.8212 -184      u=7 $ Outer hoop 27
220 8 -7.8212 -185      u=7 $ Outer hoop 28
221 8 -7.8212 -186      u=7 $ Outer hoop 29
222 8 -7.8212 -187      u=7 $ Outer hoop 30
```

```
223 8 -7.8212 -188      u=7 $ Outer hoop 31
224 8 -7.8212 -189      u=7 $ Outer hoop 32
225 8 -7.8212 -190      u=7 $ Outer hoop 33
226 8 -7.8212 -191      u=7 $ Outer hoop 34
227 8 -7.8212 -192      u=7 $ Outer hoop 35
228 8 -7.8212 -193      u=7 $ Outer hoop 36
229 8 -7.8212 -194      u=7 $ Outer hoop 37
230 8 -7.8212 -195      u=7 $ Outer hoop 38
231 8 -7.8212 -196      u=7 $ Outer hoop 39
232 8 -7.8212 -197      u=7 $ Outer hoop 40
233 8 -7.8212 -198      u=7 $ Outer hoop 41
234 8 -7.8212 -199      u=7 $ Outer hoop 42
235 8 -7.8212 -200      u=7 $ Outer hoop 43
236 8 -7.8212 -201      u=7 $ Outer hoop 44
237 8 -7.8212 -202      u=7 $ Outer hoop 45
238 8 -7.8212 -203      u=7 $ Outer hoop 46
239 8 -7.8212 -204      u=7 $ Outer hoop 47
240 8 -7.8212 -205      u=7 $ Outer hoop 48
241 8 -7.8212 -206      u=7 $ Outer hoop 49
242 8 -7.8212 -207      u=7 $ Outer hoop 50
243 13 -2.3234 #193 #194 #195 #196 #197 #198 #199
      #200 #201 #202 #203 #204 #205 #206 #207 #208 #209
      #210 #211 #212 #213 #214 #215 #216 #217 #218 #219
      #220 #221 #222 #223 #224 #225 #226 #227 #228 #229
      #230 #231 #232 #233 #234 #235 #236 #237 #238 #239
      #240 #241 #242      fill=8 u=7
244 8 -7.8212 -208      trcl = ( 160.3375 0.0000 0.0000 )      u=8 $ Outer bar 1
245 like 244 but      trcl = ( 159.3293 17.9521 0.0000 )      u=8 $ Outer bar 2
246 like 244 but      trcl = ( 156.3175 35.6785 0.0000 )      u=8 $ Outer bar 3
247 like 244 but      trcl = ( 151.3399 52.9561 0.0000 )      u=8 $ Outer bar 4
248 like 244 but      trcl = ( 144.4591 69.5678 0.0000 )      u=8 $ Outer bar 5
249 like 244 but      trcl = ( 135.7616 85.3047 0.0000 )      u=8 $ Outer bar 6
250 like 244 but      trcl = ( 125.3569 99.9688 0.0000 )      u=8 $ Outer bar 7
251 like 244 but      trcl = ( 113.3757 113.3757 0.0000 )      u=8 $ Outer bar 8
252 like 244 but      trcl = ( 99.9688 125.3569 0.0000 )      u=8 $ Outer bar 9
253 like 244 but      trcl = ( 85.3047 135.7616 0.0000 )      u=8 $ Outer bar 10
254 like 244 but      trcl = ( 69.5678 144.4591 0.0000 )      u=8 $ Outer bar 11
255 like 244 but      trcl = ( 52.9561 151.3399 0.0000 )      u=8 $ Outer bar 12
256 like 244 but      trcl = ( 35.6785 156.3175 0.0000 )      u=8 $ Outer bar 13
257 like 244 but      trcl = ( 17.9521 159.3293 0.0000 )      u=8 $ Outer bar 14
258 like 244 but      trcl = ( 0.0000 160.3375 0.0000 )      u=8 $ Outer bar 15
259 like 244 but      trcl = ( -17.9521 159.3293 0.0000 )      u=8 $ Outer bar 16
260 like 244 but      trcl = ( -35.6785 156.3175 0.0000 )      u=8 $ Outer bar 17
261 like 244 but      trcl = ( -52.9561 151.3399 0.0000 )      u=8 $ Outer bar 18
262 like 244 but      trcl = ( -69.5678 144.4591 0.0000 )      u=8 $ Outer bar 19
263 like 244 but      trcl = ( -85.3047 135.7616 0.0000 )      u=8 $ Outer bar 20
264 like 244 but      trcl = ( -99.9688 125.3569 0.0000 )      u=8 $ Outer bar 21
265 like 244 but      trcl = ( -113.3757 113.3757 0.0000 )      u=8 $ Outer bar 22
266 like 244 but      trcl = ( -125.3569 99.9688 0.0000 )      u=8 $ Outer bar 23
267 like 244 but      trcl = ( -135.7616 85.3047 0.0000 )      u=8 $ Outer bar 24
268 like 244 but      trcl = ( -144.4591 69.5678 0.0000 )      u=8 $ Outer bar 25
269 like 244 but      trcl = ( -151.3399 52.9561 0.0000 )      u=8 $ Outer bar 26
270 like 244 but      trcl = ( -156.3175 35.6785 0.0000 )      u=8 $ Outer bar 27
271 like 244 but      trcl = ( -159.3293 17.9521 0.0000 )      u=8 $ Outer bar 28
272 like 244 but      trcl = ( -160.3375 0.0000 0.0000 )      u=8 $ Outer bar 29
273 like 244 but      trcl = ( -159.3293 -17.9521 0.0000 )      u=8 $ Outer bar 30
274 like 244 but      trcl = ( -156.3175 -35.6785 0.0000 )      u=8 $ Outer bar 31
275 like 244 but      trcl = ( -151.3399 -52.9561 0.0000 )      u=8 $ Outer bar 32
276 like 244 but      trcl = ( -144.4591 -69.5678 0.0000 )      u=8 $ Outer bar 33
277 like 244 but      trcl = ( -135.7616 -85.3047 0.0000 )      u=8 $ Outer bar 34
278 like 244 but      trcl = ( -125.3569 -99.9688 0.0000 )      u=8 $ Outer bar 35
279 like 244 but      trcl = ( -113.3757 -113.3757 0.0000 )      u=8 $ Outer bar 36
280 like 244 but      trcl = ( -99.9688 -125.3569 0.0000 )      u=8 $ Outer bar 37
281 like 244 but      trcl = ( -85.3047 -135.7616 0.0000 )      u=8 $ Outer bar 38
282 like 244 but      trcl = ( -69.5678 -144.4591 0.0000 )      u=8 $ Outer bar 39
283 like 244 but      trcl = ( -52.9561 -151.3399 0.0000 )      u=8 $ Outer bar 40
284 like 244 but      trcl = ( -35.6785 -156.3175 0.0000 )      u=8 $ Outer bar 41
285 like 244 but      trcl = ( -17.9521 -159.3293 0.0000 )      u=8 $ Outer bar 42
286 like 244 but      trcl = ( 0.0000 -160.3375 0.0000 )      u=8 $ Outer bar 43
```



287 like 244 but trcl = ( 17.9521 -159.3293 0.0000 ) u=8 \$ Outer bar 44  
288 like 244 but trcl = ( 35.6785 -156.3175 0.0000 ) u=8 \$ Outer bar 45  
289 like 244 but trcl = ( 52.9561 -151.3399 0.0000 ) u=8 \$ Outer bar 46  
290 like 244 but trcl = ( 69.5678 -144.4591 0.0000 ) u=8 \$ Outer bar 47  
291 like 244 but trcl = ( 85.3047 -135.7616 0.0000 ) u=8 \$ Outer bar 48  
292 like 244 but trcl = ( 99.9688 -125.3569 0.0000 ) u=8 \$ Outer bar 49  
293 like 244 but trcl = ( 113.3757 -113.3757 0.0000 ) u=8 \$ Outer bar 50  
294 like 244 but trcl = ( 125.3569 -99.9688 0.0000 ) u=8 \$ Outer bar 51  
295 like 244 but trcl = ( 135.7616 -85.3047 0.0000 ) u=8 \$ Outer bar 52  
296 like 244 but trcl = ( 144.4591 -69.5678 0.0000 ) u=8 \$ Outer bar 53  
297 like 244 but trcl = ( 151.3399 -52.9561 0.0000 ) u=8 \$ Outer bar 54  
298 like 244 but trcl = ( 156.3175 -35.6785 0.0000 ) u=8 \$ Outer bar 55  
299 like 244 but trcl = ( 159.3293 -17.9521 0.0000 ) u=8 \$ Outer bar 56

300 13 -2.3234 #244 #245 #246  
#247 #248 #249 #250 #251 #252 #253 #254 #255 #256  
#257 #258 #259 #260 #261 #262 #263 #264 #265 #266  
#267 #268 #269 #270 #271 #272 #273 #274 #275 #276  
#277 #278 #279 #280 #281 #282 #283 #284 #285 #286  
#287 #288 #289 #290 #291 #292 #293 #294 #295 #296  
#297 #298 #299 u=8

C Detector Cells - Radial Biasing

399 0 -399 fill=1 \$ Cask  
400 0 -400 +399 \$ Surface  
450 0 -450 +399 +400 \$ SurfAzi  
500 0 -500 +399 +400 +450 \$ 1ft  
600 0 -600 +399 +400 +450 +500 \$ 1m  
700 0 -700 +399 +400 +450 +500 +600 \$ 2m  
800 0 -800 +399 +400 +450 +500 +600 +700 \$ 4m  
900 0 +399 +400 +450 +500 +600 +700 +800 \$ Exterior

C Fuel Assembly Surfaces - ngl4b - vl.1

1 RPP -9.8590 9.8590 -9.8590 9.8590 0.0000 8.0975 \$ Lower Nozzle  
2 RPP -9.8590 9.8590 -9.8590 9.8590 0.0000 9.8374 \$ Lower Plenum  
3 RPP -9.8590 9.8590 -9.8590 9.8590 0.0000 378.6454 \$ Fuel  
4 RPP -9.8590 9.8590 -9.8590 9.8590 0.0000 400.3040 \$ Upper Plenum  
5 RPP -9.8590 9.8590 -9.8590 9.8590 0.0000 409.1940 \$ Upper Nozzle  
6 PZ 255.7094 \$ Flood elevation

C Surfaces - Fuel Tube vl.3

7 RPP -11.6015 11.6015 -11.6015 11.6015 7.6200 439.4962 \$ Tube void  
8 RPP -12.3952 12.3952 -12.3952 12.3952 7.6200 430.5300 \$ Tube  
9 RPP -11.6015 -11.2840 -10.2362 10.2362 9.2075 428.9425 \$ Poison left  
10 RPP 11.2840 11.6015 -10.2362 10.2362 9.2075 428.9425 \$ Poison right  
11 RPP -10.2362 10.2362 11.2840 11.6015 9.2075 428.9425 \$ Poison top  
12 RPP -10.2362 10.2362 -11.6015 -11.2840 9.2075 428.9425 \$ Poison bottom

C Surfaces - PWR Basket vl.5

13 RPP -12.3952 12.3952 -12.3952 12.3952 0.0000 439.4962 \$ Tube opening  
14 9 RPP -16.6370 16.6370 -16.6370 16.6370 0.0000 439.4962 \$ Tube radius  
15 RPP 81.8833 83.7883 -33.1851 33.1851 7.6200 430.5300 \$ Side support +x  
16 RPP -83.7883 -81.8833 -33.1851 33.1851 7.6200 430.5300 \$ Side support -x  
17 RPP -33.1851 33.1851 81.8833 83.7883 7.6200 430.5300 \$ Side support +y  
18 RPP -33.1851 33.1851 -83.7883 -81.8833 7.6200 430.5300 \$ Side support -y  
19 RPP -60.2552 60.2552 -60.2552 60.2552 7.6200 430.5300 \$ Corner outer  
20 RPP -59.4614 59.4614 -59.4614 59.4614 7.6200 430.5300 \$ Corner inner  
21 9 RPP -78.6267 78.6267 -78.6267 78.6267 7.6200 430.5300 \$ Corner dia. outer  
22 9 RPP -77.8329 77.8329 -77.8329 77.8329 7.6200 430.5300 \$ Corner dia. inner

C Surfaces - PWR Canister Cavity vl.5

23 RPP -9.8595 9.8595 -9.8595 9.8595 0.0000 409.1941 \$ Assy opening

C Surfaces - Canister vl.3

24 RCC 0.0000 0.0000 0.0000 0.0000 0.0000 439.4962 90.1700 \$ Cavity  
25 CZ 2.6924 \$ Bot Cylinder Radius  
26 CZ 6.7691 \$ Mid Cylinder Radius  
27 CZ 7.4041 \$ Top Cylinder Radius  
28 PZ 450.8500 \$ Port plane bot/mid  
29 PZ 452.1962 \$ Lower/upper lid  
30 PZ 459.5114 \$ Port plane mid/top  
31 RCC 0.0000 0.0000 -6.9850 0.0000 0.0000 469.3412 91.4400 \$ Canister

C VCC Surfaces - vl.3.1\_ngl4b

32 RCC 0.0000 0.0000 -5.0800 0.0000 0.0000 5.0800 91.4401 \$ Pedestal plate  
33 RCC 0.0000 0.0000 -30.4800 0.0000 0.0000 25.4000 63.4999 \$ Stand outer

34 RCC 0.0000 0.0000 -30.4800 0.0000 0.0000 25.4000 62.3888 \$ Stand inner  
35 9 RPP -100.3300 100.3300 -10.4775 10.4775 -33.0200 -16.5100 \$ Connector plate A  
36 10 RPP -100.3300 100.3300 -10.4775 10.4775 -33.0200 -16.5100 \$ Connector plate B  
37 9 RPP -99.0600 99.0600 -9.2075 9.2075 -33.0200 -16.5100 \$ Air inlet angled wall A  
38 10 RPP -99.0600 99.0600 -9.2075 9.2075 -33.0200 -16.5100 \$ Air inlet angled wall B  
39 RCC 0.0000 0.0000 -33.0200 0.0000 0.0000 2.5400 172.7200 \$ Bottom plate outer  
40 RCC 0.0000 0.0000 -33.0200 0.0000 0.0000 2.5400 100.3300 \$ Connector radius  
41 RCC 0.0000 0.0000 -33.0200 0.0000 0.0000 2.5400 63.5000 \$ Bottom plate inner  
42 RCC 0.0000 0.0000 -16.5100 0.0000 0.0000 538.0228 105.41 \$ VCC liner outer  
43 RCC 0.0000 0.0000 -16.5100 0.0000 0.0000 538.0228 100.965 \$ VCC liner inner  
44 RCC 0.0000 0.0000 -133.0200 0.0000 0.0000 654.5328 172.7200 \$ Concrete  
45 RCC 0.0000 0.0000 -133.0200 0.0000 0.0000 100.0000 172.7200 \$ Concrete pad  
46 RPP -172.7200 172.7200 -63.5000 63.5000 -33.0200 -21.5900 \$ Air inlet void X  
47 RPP -63.5000 63.5000 -172.7200 172.7200 -33.0200 -21.5900 \$ Air inlet void Y  
48 RPP -172.7200 172.7200 -64.7700 64.7700 -33.0200 -21.5900 \$ Air inlet wall X  
49 RPP -64.7700 64.7700 -172.7200 172.7200 -33.0200 -21.5900 \$ Air inlet wall Y  
50 RCC 0.0000 0.0000 -33.0200 0.0000 0.0000 11.4300 100.3300 \$ Air inlet divider  
51 RPP -172.7200 172.7200 -64.7700 64.7700 -21.5900 -16.5100 \$ Air inlet top X  
52 RPP -64.7700 64.7700 -172.7200 172.7200 -21.5900 -16.5100 \$ Air inlet top Y  
53 RCC 0.0000 0.0000 -21.5900 0.0000 0.0000 5.0800 93.9800 \$ Air inlet top plate radius  
54 RPP -172.7200 172.7200 -64.7700 64.7700 494.0808 505.0028 \$ Air outlet steel X  
55 RPP -64.7700 64.7700 -172.7200 172.7200 494.0808 505.0028 \$ Air outlet steel Y  
56 RPP -172.7200 172.7200 -64.1350 64.1350 494.7158 504.3678 \$ Air outlet void X  
57 RPP -64.1350 64.1350 -172.7200 172.7200 494.7158 504.3678 \$ Air outlet void Y  
58 RPP -106.6800 106.6800 -5.7150 5.7150 -16.5100 -5.0800 \$ Support rail exterior X  
59 RPP -106.6800 106.6800 -4.4450 4.4450 -16.5100 -5.0800 \$ Support rail interior X  
60 RPP -5.7150 5.7150 -106.6800 106.6800 -16.5100 -5.0800 \$ Support rail exterior Y  
61 RPP -4.4450 4.4450 -106.6800 106.6800 -16.5100 -5.0800 \$ Support rail interior Y  
62 RCC 0.0000 0.0000 518.9728 0.0000 0.0000 2.5400 118.7450 \$ Top flange  
63 RCC 0.0000 0.0000 521.5128 0.0000 0.0000 1.9050 116.2050 \$ Lid top  
64 RCC 0.0000 0.0000 506.7808 0.0000 0.0000 14.7320 99.6950 \$ Lid concrete  
65 RCC 0.0000 0.0000 506.1458 0.0000 0.0000 15.3670 100.3300 \$ Lid shell  
66 RPP -100.9650 100.9650 -0.4432 0.4432 174.8028 479.6028 \$ Standoff outer 1  
67 11 RPP -100.9650 100.9650 -0.4432 0.4432 174.8028 479.6028 \$ Standoff outer 2  
68 12 RPP -100.9650 100.9650 -0.4432 0.4432 174.8028 479.6028 \$ Standoff outer 3  
69 9 RPP -100.9650 100.9650 -0.4432 0.4432 174.8028 479.6028 \$ Standoff outer 4  
70 13 RPP -100.9650 100.9650 -0.4432 0.4432 174.8028 479.6028 \$ Standoff outer 5  
71 14 RPP -100.9650 100.9650 -0.4432 0.4432 174.8028 479.6028 \$ Standoff outer 6  
72 RPP -0.4432 0.4432 -100.9650 100.9650 174.8028 479.6028 \$ Standoff outer 7  
73 11 RPP -0.4432 0.4432 -100.9650 100.9650 174.8028 479.6028 \$ Standoff outer 8  
74 12 RPP -0.4432 0.4432 -100.9650 100.9650 174.8028 479.6028 \$ Standoff outer 9  
75 9 RPP -0.4432 0.4432 -100.9650 100.9650 174.8028 479.6028 \$ Standoff outer 10  
76 13 RPP -0.4432 0.4432 -100.9650 100.9650 174.8028 479.6028 \$ Standoff outer 11  
77 14 RPP -0.4432 0.4432 -100.9650 100.9650 174.8028 479.6028 \$ Standoff outer 12  
78 RPP -93.3450 93.3450 -0.4432 0.4432 174.8028 479.6028 \$ Standoff inner 1  
79 11 RPP -93.3450 93.3450 -0.4432 0.4432 174.8028 479.6028 \$ Standoff inner 2  
80 12 RPP -93.3450 93.3450 -0.4432 0.4432 174.8028 479.6028 \$ Standoff inner 3  
81 9 RPP -93.3450 93.3450 -0.4432 0.4432 174.8028 479.6028 \$ Standoff inner 4  
82 13 RPP -93.3450 93.3450 -0.4432 0.4432 174.8028 479.6028 \$ Standoff inner 5  
83 14 RPP -93.3450 93.3450 -0.4432 0.4432 174.8028 479.6028 \$ Standoff inner 6  
84 RPP -0.4432 0.4432 -93.3450 93.3450 174.8028 479.6028 \$ Standoff inner 7  
85 11 RPP -0.4432 0.4432 -93.3450 93.3450 174.8028 479.6028 \$ Standoff inner 8  
86 12 RPP -0.4432 0.4432 -93.3450 93.3450 174.8028 479.6028 \$ Standoff inner 9  
87 9 RPP -0.4432 0.4432 -93.3450 93.3450 174.8028 479.6028 \$ Standoff inner 10  
88 13 RPP -0.4432 0.4432 -93.3450 93.3450 174.8028 479.6028 \$ Standoff inner 11  
89 14 RPP -0.4432 0.4432 -93.3450 93.3450 174.8028 479.6028 \$ Standoff inner 12  
90 RCC -146.0500 58.4200 -33.0200 0.0000 0.0000 11.4300 3.8100 \$ -x inlet pipe 1  
91 RCC -146.0500 36.5760 -33.0200 0.0000 0.0000 11.4300 3.8100 \$ -x inlet pipe 2  
92 RCC -146.0500 14.7320 -33.0200 0.0000 0.0000 11.4300 3.8100 \$ -x inlet pipe 3  
93 RCC -146.0500 -7.1120 -33.0200 0.0000 0.0000 11.4300 3.8100 \$ -x inlet pipe 4  
94 RCC -146.0500 -28.9560 -33.0200 0.0000 0.0000 11.4300 3.8100 \$ -x inlet pipe 5  
95 RCC -146.0500 -50.8000 -33.0200 0.0000 0.0000 11.4300 3.8100 \$ -x inlet pipe 6  
96 RCC -133.3500 50.8000 -33.0200 0.0000 0.0000 11.4300 3.8100 \$ -x inlet pipe 7  
97 RCC -133.3500 28.9560 -33.0200 0.0000 0.0000 11.4300 3.8100 \$ -x inlet pipe 8  
98 RCC -133.3500 7.1120 -33.0200 0.0000 0.0000 11.4300 3.8100 \$ -x inlet pipe 9  
99 RCC -133.3500 -14.7320 -33.0200 0.0000 0.0000 11.4300 3.8100 \$ -x inlet pipe 10  
100 RCC -133.3500 -36.5760 -33.0200 0.0000 0.0000 11.4300 3.8100 \$ -x inlet pipe 11  
101 RCC -133.3500 -58.4200 -33.0200 0.0000 0.0000 11.4300 3.8100 \$ -x inlet pipe 12  
102 RCC -120.6500 43.1800 -33.0200 0.0000 0.0000 11.4300 3.8100 \$ -x inlet pipe 13

```
103 RCC -120.6500 21.3360 -33.0200 0.0000 0.0000 11.4300 3.8100 $ -x inlet pipe 14
104 RCC -120.6500 -0.5080 -33.0200 0.0000 0.0000 11.4300 3.8100 $ -x inlet pipe 15
105 RCC -120.6500 -22.3520 -33.0200 0.0000 0.0000 11.4300 3.8100 $ -x inlet pipe 16
106 RCC -120.6500 -44.1960 -33.0200 0.0000 0.0000 11.4300 3.8100 $ -x inlet pipe 17
107 RCC 146.0500 -58.4200 -33.0200 0.0000 0.0000 11.4300 3.8100 $ +x inlet pipe 1
108 RCC 146.0500 -36.5760 -33.0200 0.0000 0.0000 11.4300 3.8100 $ +x inlet pipe 2
109 RCC 146.0500 -14.7320 -33.0200 0.0000 0.0000 11.4300 3.8100 $ +x inlet pipe 3
110 RCC 146.0500 7.1120 -33.0200 0.0000 0.0000 11.4300 3.8100 $ +x inlet pipe 4
111 RCC 146.0500 28.9560 -33.0200 0.0000 0.0000 11.4300 3.8100 $ +x inlet pipe 5
112 RCC 146.0500 50.8000 -33.0200 0.0000 0.0000 11.4300 3.8100 $ +x inlet pipe 6
113 RCC 133.3500 -50.8000 -33.0200 0.0000 0.0000 11.4300 3.8100 $ +x inlet pipe 7
114 RCC 133.3500 -28.9560 -33.0200 0.0000 0.0000 11.4300 3.8100 $ +x inlet pipe 8
115 RCC 133.3500 -7.1120 -33.0200 0.0000 0.0000 11.4300 3.8100 $ +x inlet pipe 9
116 RCC 133.3500 14.7320 -33.0200 0.0000 0.0000 11.4300 3.8100 $ +x inlet pipe 10
117 RCC 133.3500 36.5760 -33.0200 0.0000 0.0000 11.4300 3.8100 $ +x inlet pipe 11
118 RCC 133.3500 58.4200 -33.0200 0.0000 0.0000 11.4300 3.8100 $ +x inlet pipe 12
119 RCC 120.6500 -43.1800 -33.0200 0.0000 0.0000 11.4300 3.8100 $ +x inlet pipe 13
120 RCC 120.6500 -21.3360 -33.0200 0.0000 0.0000 11.4300 3.8100 $ +x inlet pipe 14
121 RCC 120.6500 0.5080 -33.0200 0.0000 0.0000 11.4300 3.8100 $ +x inlet pipe 15
122 RCC 120.6500 22.3520 -33.0200 0.0000 0.0000 11.4300 3.8100 $ +x inlet pipe 16
123 RCC 120.6500 44.1960 -33.0200 0.0000 0.0000 11.4300 3.8100 $ +x inlet pipe 17
124 RCC -58.4200 -146.0500 -33.0200 0.0000 0.0000 11.4300 3.8100 $ -y inlet pipe 1
125 RCC -36.5760 -146.0500 -33.0200 0.0000 0.0000 11.4300 3.8100 $ -y inlet pipe 2
126 RCC -14.7320 -146.0500 -33.0200 0.0000 0.0000 11.4300 3.8100 $ -y inlet pipe 3
127 RCC 7.1120 -146.0500 -33.0200 0.0000 0.0000 11.4300 3.8100 $ -y inlet pipe 4
128 RCC 28.9560 -146.0500 -33.0200 0.0000 0.0000 11.4300 3.8100 $ -y inlet pipe 5
129 RCC 50.8000 -146.0500 -33.0200 0.0000 0.0000 11.4300 3.8100 $ -y inlet pipe 6
130 RCC -50.8000 -133.3500 -33.0200 0.0000 0.0000 11.4300 3.8100 $ -y inlet pipe 7
131 RCC -28.9560 -133.3500 -33.0200 0.0000 0.0000 11.4300 3.8100 $ -y inlet pipe 8
132 RCC -7.1120 -133.3500 -33.0200 0.0000 0.0000 11.4300 3.8100 $ -y inlet pipe 9
133 RCC -14.7320 -133.3500 -33.0200 0.0000 0.0000 11.4300 3.8100 $ -y inlet pipe 10
134 RCC 36.5760 -133.3500 -33.0200 0.0000 0.0000 11.4300 3.8100 $ -y inlet pipe 11
135 RCC 58.4200 -133.3500 -33.0200 0.0000 0.0000 11.4300 3.8100 $ -y inlet pipe 12
136 RCC -43.1800 -120.6500 -33.0200 0.0000 0.0000 11.4300 3.8100 $ -y inlet pipe 13
137 RCC -21.3360 -120.6500 -33.0200 0.0000 0.0000 11.4300 3.8100 $ -y inlet pipe 14
138 RCC 0.5080 -120.6500 -33.0200 0.0000 0.0000 11.4300 3.8100 $ -y inlet pipe 15
139 RCC 22.3520 -120.6500 -33.0200 0.0000 0.0000 11.4300 3.8100 $ -y inlet pipe 16
140 RCC 44.1960 -120.6500 -33.0200 0.0000 0.0000 11.4300 3.8100 $ -y inlet pipe 17
141 RCC 58.4200 146.0500 -33.0200 0.0000 0.0000 11.4300 3.8100 $ +y inlet pipe 1
142 RCC 36.5760 146.0500 -33.0200 0.0000 0.0000 11.4300 3.8100 $ +y inlet pipe 2
143 RCC 14.7320 146.0500 -33.0200 0.0000 0.0000 11.4300 3.8100 $ +y inlet pipe 3
144 RCC -7.1120 146.0500 -33.0200 0.0000 0.0000 11.4300 3.8100 $ +y inlet pipe 4
145 RCC -28.9560 146.0500 -33.0200 0.0000 0.0000 11.4300 3.8100 $ +y inlet pipe 5
146 RCC -50.8000 146.0500 -33.0200 0.0000 0.0000 11.4300 3.8100 $ +y inlet pipe 6
147 RCC 50.8000 133.3500 -33.0200 0.0000 0.0000 11.4300 3.8100 $ +y inlet pipe 7
148 RCC 28.9560 133.3500 -33.0200 0.0000 0.0000 11.4300 3.8100 $ +y inlet pipe 8
149 RCC 7.1120 133.3500 -33.0200 0.0000 0.0000 11.4300 3.8100 $ +y inlet pipe 9
150 RCC -14.7320 133.3500 -33.0200 0.0000 0.0000 11.4300 3.8100 $ +y inlet pipe 10
151 RCC -36.5760 133.3500 -33.0200 0.0000 0.0000 11.4300 3.8100 $ +y inlet pipe 11
152 RCC -58.4200 133.3500 -33.0200 0.0000 0.0000 11.4300 3.8100 $ +y inlet pipe 12
153 RCC 43.1800 120.6500 -33.0200 0.0000 0.0000 11.4300 3.8100 $ +y inlet pipe 13
154 RCC 21.3360 120.6500 -33.0200 0.0000 0.0000 11.4300 3.8100 $ +y inlet pipe 14
155 RCC -0.5080 120.6500 -33.0200 0.0000 0.0000 11.4300 3.8100 $ +y inlet pipe 15
156 RCC -22.3520 120.6500 -33.0200 0.0000 0.0000 11.4300 3.8100 $ +y inlet pipe 16
157 RCC -44.1960 120.6500 -33.0200 0.0000 0.0000 11.4300 3.8100 $ +y inlet pipe 17
C VCC Rebar Surfaces - v1.3.1_ngl4b
158 TZ 0.0000 0.0000 -1.7182 162.2425 0.9525 0.9525 $ Outer hoop 1
159 TZ 0.0000 0.0000 7.9935 162.2425 0.9525 0.9525 $ Outer hoop 2
160 TZ 0.0000 0.0000 17.7053 162.2425 0.9525 0.9525 $ Outer hoop 3
161 TZ 0.0000 0.0000 27.4171 162.2425 0.9525 0.9525 $ Outer hoop 4
162 TZ 0.0000 0.0000 37.1288 162.2425 0.9525 0.9525 $ Outer hoop 5
163 TZ 0.0000 0.0000 46.8406 162.2425 0.9525 0.9525 $ Outer hoop 6
164 TZ 0.0000 0.0000 56.5524 162.2425 0.9525 0.9525 $ Outer hoop 7
165 TZ 0.0000 0.0000 66.2641 162.2425 0.9525 0.9525 $ Outer hoop 8
166 TZ 0.0000 0.0000 75.9759 162.2425 0.9525 0.9525 $ Outer hoop 9
167 TZ 0.0000 0.0000 85.6876 162.2425 0.9525 0.9525 $ Outer hoop 10
168 TZ 0.0000 0.0000 95.3994 162.2425 0.9525 0.9525 $ Outer hoop 11
169 TZ 0.0000 0.0000 105.1112 162.2425 0.9525 0.9525 $ Outer hoop 12
170 TZ 0.0000 0.0000 114.8229 162.2425 0.9525 0.9525 $ Outer hoop 13
```

171	TZ	0.0000	0.0000	124.5347	162.2425	0.9525	0.9525	\$	Outer hoop 14
172	TZ	0.0000	0.0000	134.2465	162.2425	0.9525	0.9525	\$	Outer hoop 15
173	TZ	0.0000	0.0000	143.9582	162.2425	0.9525	0.9525	\$	Outer hoop 16
174	TZ	0.0000	0.0000	153.6700	162.2425	0.9525	0.9525	\$	Outer hoop 17
175	TZ	0.0000	0.0000	163.3818	162.2425	0.9525	0.9525	\$	Outer hoop 18
176	TZ	0.0000	0.0000	173.0935	162.2425	0.9525	0.9525	\$	Outer hoop 19
177	TZ	0.0000	0.0000	182.8053	162.2425	0.9525	0.9525	\$	Outer hoop 20
178	TZ	0.0000	0.0000	192.5171	162.2425	0.9525	0.9525	\$	Outer hoop 21
179	TZ	0.0000	0.0000	202.2288	162.2425	0.9525	0.9525	\$	Outer hoop 22
180	TZ	0.0000	0.0000	211.9406	162.2425	0.9525	0.9525	\$	Outer hoop 23
181	TZ	0.0000	0.0000	221.6524	162.2425	0.9525	0.9525	\$	Outer hoop 24
182	TZ	0.0000	0.0000	231.3641	162.2425	0.9525	0.9525	\$	Outer hoop 25
183	TZ	0.0000	0.0000	241.0759	162.2425	0.9525	0.9525	\$	Outer hoop 26
184	TZ	0.0000	0.0000	250.7876	162.2425	0.9525	0.9525	\$	Outer hoop 27
185	TZ	0.0000	0.0000	260.4994	162.2425	0.9525	0.9525	\$	Outer hoop 28
186	TZ	0.0000	0.0000	270.2112	162.2425	0.9525	0.9525	\$	Outer hoop 29
187	TZ	0.0000	0.0000	279.9229	162.2425	0.9525	0.9525	\$	Outer hoop 30
188	TZ	0.0000	0.0000	289.6347	162.2425	0.9525	0.9525	\$	Outer hoop 31
189	TZ	0.0000	0.0000	299.3465	162.2425	0.9525	0.9525	\$	Outer hoop 32
190	TZ	0.0000	0.0000	309.0582	162.2425	0.9525	0.9525	\$	Outer hoop 33
191	TZ	0.0000	0.0000	318.7700	162.2425	0.9525	0.9525	\$	Outer hoop 34
192	TZ	0.0000	0.0000	328.4818	162.2425	0.9525	0.9525	\$	Outer hoop 35
193	TZ	0.0000	0.0000	338.1935	162.2425	0.9525	0.9525	\$	Outer hoop 36
194	TZ	0.0000	0.0000	347.9053	162.2425	0.9525	0.9525	\$	Outer hoop 37
195	TZ	0.0000	0.0000	357.6171	162.2425	0.9525	0.9525	\$	Outer hoop 38
196	TZ	0.0000	0.0000	367.3288	162.2425	0.9525	0.9525	\$	Outer hoop 39
197	TZ	0.0000	0.0000	377.0406	162.2425	0.9525	0.9525	\$	Outer hoop 40
198	TZ	0.0000	0.0000	386.7524	162.2425	0.9525	0.9525	\$	Outer hoop 41
199	TZ	0.0000	0.0000	396.4641	162.2425	0.9525	0.9525	\$	Outer hoop 42
200	TZ	0.0000	0.0000	406.1759	162.2425	0.9525	0.9525	\$	Outer hoop 43
201	TZ	0.0000	0.0000	415.8876	162.2425	0.9525	0.9525	\$	Outer hoop 44
202	TZ	0.0000	0.0000	425.5994	162.2425	0.9525	0.9525	\$	Outer hoop 45
203	TZ	0.0000	0.0000	435.3112	162.2425	0.9525	0.9525	\$	Outer hoop 46
204	TZ	0.0000	0.0000	445.0229	162.2425	0.9525	0.9525	\$	Outer hoop 47
205	TZ	0.0000	0.0000	454.7347	162.2425	0.9525	0.9525	\$	Outer hoop 48
206	TZ	0.0000	0.0000	464.4465	162.2425	0.9525	0.9525	\$	Outer hoop 49
207	TZ	0.0000	0.0000	474.1582	162.2425	0.9525	0.9525	\$	Outer hoop 50
208	RCC	0.0000	0.0000	-11.4300	0.0000	0.0000	495.3000	0.9525	\$ Bar
C Storage Cask & Pad Container									
399	RCC	0.0000	0.0000	-133.0200	0.0000	0.0000	656.4378	172.7201	
C Radial Detector DRA (Surface)									
400	RCC	0.0000	0.0000	-33.0200	0.0000	0.0000	556.5378	172.8201	
401	PZ	13.3582							
402	PZ	59.7363							
403	PZ	106.1145							
404	PZ	152.4926							
405	PZ	198.8708							
406	PZ	245.2489							
407	PZ	291.6271							
408	PZ	338.0052							
409	PZ	384.3834							
410	PZ	430.7615							
411	PZ	477.1357							
C Radial Detector DRAA (SurfAzi)									
450	RCC	0.0000	0.0000	16.8224	0.0000	0.0000	368.8080	172.9201	
451	PX	0.0000							
452	1	PX	0.0000						
453	2	PX	0.0000						
454	3	PX	0.0000						
455	4	PX	0.0000						
456	5	PY	0.0000						
457	6	PX	0.0000						
458	7	PX	0.0000						
459	8	PX	0.0000						
460	9	PX	0.0000						
C Radial Detector DRB (1ft)									
500	RCC	0.0000	0.0000	-33.0200	0.0000	0.0000	587.0178	203.3001	
501	PZ	15.8982							
502	PZ	64.8163							

503 PZ 113.7345  
504 PZ 162.6526  
505 PZ 211.5708  
506 PZ 260.4889  
507 PZ 309.4071  
508 PZ 358.3252  
509 PZ 407.2434  
510 PZ 456.1615  
511 PZ 505.0797  
C Radial Detector DRC (1m)  
600 RCC 0.0000 0.0000 -33.0200 0.0000 0.0000 656.5378 272.8201  
601 PZ 10.7492  
602 PZ 54.5184  
603 PZ 98.2876  
604 PZ 142.0567  
605 PZ 185.8259  
606 PZ 229.5951  
607 PZ 273.3643  
608 PZ 317.1335  
609 PZ 360.9027  
610 PZ 404.6719  
611 PZ 448.4411  
612 PZ 492.2102  
613 PZ 535.9794  
614 PZ 579.7486  
C Radial Detector DRD (2m)  
700 RCC 0.0000 0.0000 -33.0200 0.0000 0.0000 756.5378 372.8201  
701 PZ 4.8069  
702 PZ 42.6338  
703 PZ 80.4607  
704 PZ 118.2876  
705 PZ 156.1145  
706 PZ 193.9413  
707 PZ 231.7682  
708 PZ 269.5951  
709 PZ 307.4220  
710 PZ 345.2489  
711 PZ 383.0758  
712 PZ 420.9027  
713 PZ 458.7296  
714 PZ 496.5565  
715 PZ 534.3834  
716 PZ 572.2102  
717 PZ 610.0371  
718 PZ 647.8640  
719 PZ 685.6909  
C Radial Detector DRE (4m)  
800 RCC 0.0000 0.0000 -33.0200 0.0000 0.0000 956.5378 572.8201  
801 PZ 14.8069  
802 PZ 62.6338  
803 PZ 110.4607  
804 PZ 158.2876  
805 PZ 206.1145  
806 PZ 253.9413  
807 PZ 301.7682  
808 PZ 349.5951  
809 PZ 397.4220  
810 PZ 445.2489  
811 PZ 493.0758  
812 PZ 540.9027  
813 PZ 588.7296  
814 PZ 636.5565  
815 PZ 684.3834  
816 PZ 732.2102  
817 PZ 780.0371  
818 PZ 827.8640  
819 PZ 875.6909

C

C Materials List - Common Materials - v1.7  
C  
C Homogenized Lower Nozzle  
m1 24000 -1.9000E-01 25055 -2.0000E-02 26000 -6.9500E-01  
28000 -9.5000E-02  
C Homogenized Lower Plenum  
m2 24000 -1.0000E-03 50000 -1.5000E-02  
26000 -1.2500E-03 7014 -5.0000E-04  
40000 -9.8225E-01  
C Homogenized UO2 Fuel - Dry  
m3 92235 -3.6891E-02 40000 -1.6011E-01 24000 -1.6300E-04  
92238 -7.0092E-01 50000 -2.4450E-03 7014 -8.1499E-05  
8016 -9.9186E-02 26000 -2.0375E-04  
C Homogenized Upper Plenum  
m4 24000 -1.4890E-01 50000 -3.2622E-03 25055 -1.5650E-02  
26000 -5.4413E-01 7014 -1.0874E-04 28000 -7.4340E-02  
40000 -2.1362E-01  
C Homogenized Upper Nozzle  
m5 24000 -1.9000E-01 25055 -2.0000E-02 26000 -6.9500E-01  
28000 -9.5000E-02  
C Water  
m6 1001 2 8016 1  
C Stainless Steel  
m7 24000 -0.190 25055 -0.020 26000 -0.695  
28000 -0.095  
C Carbon Steel  
m8 26000 -0.99 6012 -0.01  
C Neutron Poison  
m9 13027 -0.6605 5010 -0.0478 5011 -0.2179  
6012 -0.0737  
C Aluminum  
m10 13027 -1.0  
C Lead  
m11 82000 -1.0  
C NS-4-FR  
m12 5010 -9.3127E-04 13027 -2.1420E-01 6000 -2.7627E-01  
5011 -3.7721E-03 1001 -6.0012E-02 7014 -1.9815E-02  
8016 -4.2500E-01  
C Concrete  
m13 26000 -0.014 20000 -0.044 14000 -0.337  
1001 -0.010 8016 -0.532 11023 -0.029  
13027 -0.034  
C Vent Port Middle Cylinder  
m14 24000 -0.190 25055 -0.020 26000 -0.695  
28000 -0.095  
C Balsa  
m15 6012 6 1001 10 8016 5  
C NS-4-FR (Accident)  
m16 5010 -1.7596E-03 13027 -4.3257E-01 6012 -5.5793E-01  
5011 -7.7389E-03  
C Copper  
m17 29063 -6.8499E-01 29065 -3.1501E-01  
C Damaged Fuel  
m18 92235 -4.1222E-02  
92238 -7.8321E-01  
8016 -1.1083E-01  
40000 -6.3583E-02  
50000 -9.7099E-04  
26000 -8.0916E-05  
24000 -6.4732E-05  
7014 -3.2366E-05  
C Damaged Lower Nozzle  
m19 92235 -3.2602E-02  
92238 -6.1944E-01  
8016 -8.7656E-02  
24000 -4.9457E-02  
25055 -5.2060E-03  
26000 -1.8091E-01  
28000 -2.4728E-02

```
C Damaged Lower Plenum
m20  92235 -3.0443E-02
      92238 -5.7843E-01
      8016 -8.1852E-02
      24000 -3.0928E-04
      26000 -3.8660E-04
      40000 -3.0379E-01
      50000 -4.6392E-03
      7014 -1.5464E-04
C Damaged Upper Plenum
m21  92235 -3.9655E-02
      92238 -7.5344E-01
      8016 -1.0662E-01
      24000 -1.4932E-02
      26000 -5.4568E-02
      40000 -2.1423E-02
      50000 -3.2715E-04
      7014 -1.0905E-05
      25055 -1.5695E-03
      28000 -7.4552E-03
C Damaged upper Nozzle
m22  92235 -3.0832E-02
      92238 -5.8581E-01
      8016 -8.2897E-02
      24000 -5.7087E-02
      25055 -6.0091E-03
      26000 -2.0882E-01
      28000 -2.8543E-02
phys:p 100 0 0 0 1    $ Disable Doppler energy broadening
C
C Cell Importances
C
imp:p 1 306r 0
C
C Source Definition - Fuel Gamma Response to Group 7 - Symmetric Position B2
C
sdef x=d1 y=d2 z=d3 erg=d4 cell=399:191:78:d5:3
si1  -9.85901 9.85901
spl  0 1
si2  -9.85901 9.85901
sp2  0 1
si3  a 9.8374 19.0576 28.2778 37.4980 46.7182 55.9384 65.1586
      323.3242 332.5444 341.7646 350.9848 360.2050 369.4252 378.6454
sp3  d 0.5470 0.6358 0.7247 0.8135 0.9023 0.9912 1.0800
      1.0800 0.9912 0.9023 0.8135 0.7247 0.6358 0.5470
sb3  d 1.00E+00 1.00E+00 1.00E+00 1.00E+00 1.00E+00 1.00E+00 1.00E+00
      1.00E+00 1.00E+00 1.00E+00 1.00E+00 1.00E+00 1.00E+00
si4  3.000E+00 4.000E+00
sp4  0 1
C Source Information
si5  l 40 41 42
      43 44 45 46 47
      48 49 50 51 52 53 54
      55 56 57 58 59 60 61
      62 63 64 65 66 67 68
      69 70 71 72 73
      74 75 76
C Source Probability
sp5  0.0 0.0 0.0
      0.0000 0.0 1.0 0.0 0.0000
      0.0 0.0 0.0 0.0 0.0 0.0 0.0
      0.0 1.0 0.0 0.0 0.0 1.0 0.0
      0.0 0.0 0.0 0.0 0.0 0.0 0.0
      0.0000 0.0 1.0 0.0 0.0000
      0.0 0.0 0.0
mode p
nps 40000000
C
C ANSI/ANS-6.1.1-1977 - Gamma Flux-to-Dose Conversion Factors
```

```
C (mrem/hr)/(photons/cm2-sec)
C
de0  0.01 0.03 0.05 0.07 0.1 0.15 0.2
      0.25 0.3 0.35 0.4 0.45 0.5 0.55
      0.6 0.65 0.7 0.8 1 1.4 1.8
      2.2 2.6 2.8 3.25 3.75 4.25 4.75
      5 5.25 5.75 6.25 6.75 7.5 9
      11 13 15
df0  3.96E-03 5.82E-04 2.90E-04 2.58E-04 2.83E-04 3.79E-04 5.01E-04
      6.31E-04 7.59E-04 8.78E-04 9.85E-04 1.08E-03 1.17E-03 1.27E-03
      1.36E-03 1.44E-03 1.52E-03 1.68E-03 1.98E-03 2.51E-03 2.99E-03
      3.42E-03 3.82E-03 4.01E-03 4.41E-03 4.83E-03 5.23E-03 5.60E-03
      5.80E-03 6.01E-03 6.37E-03 6.74E-03 7.11E-03 7.66E-03 8.77E-03
      1.03E-02 1.18E-02 1.33E-02
C
C Weight Window Generation - Radial
C
wwg 2 0 0 0 0
wvp:p 5 3 5 0 -1 0
mesh geom=cyl ref=57 0 201 origin=0.1 0.1 -134
      imesh 90.2 91.4 101.0 105.4 172.7 672.7
      iints 5 1 1 1 5 1
      jmesh 101 104 112 118 129 141 151 520 550 581 603 640 656 1156
      jint 1 1 1 1 1 1 1 1 1 1 1 1 1
      kmesh 1
      kints 1
C wwge:p 1e-3 1 20
fc2 Radial Surface Tally
f2:p +400.1
fm2 4.0000E+00
fs2 -401 -402 -403 -404 -405 -406
      -407 -408 -409 -410 -411 T
tf2
fc12 Radial SurfAzi Tally Q1 (+x+y)
f12:p +450.1
fm12 4.0000E+00
fs12 -451 -456
      +455 +454 +453 +452 T
sd12 2.0035E+05 1.0018E+05 2.0035E+04 4r 4.0071E+05
tf12
fc22 Radial SurfAzi Tally Q2 (-x+y)
f22:p +450.1
fm22 4.0000E+00
fs22 +451 -456
      -460 -459 -458 -457 T
sd22 2.0035E+05 1.0018E+05 2.0035E+04 4r 4.0071E+05
tf22
fc32 Radial SurfAzi Tally Q3 (-x-y)
f32:p +450.1
fm32 4.0000E+00
fs32 +451 +456
      -455 -454 -453 -452 T
sd32 2.0035E+05 1.0018E+05 2.0035E+04 4r 4.0071E+05
tf32
fc42 Radial SurfAzi Tally Q4 (+x-y)
f42:p +450.1
fm42 4.0000E+00
fs42 -451 +456
      +460 +459 +458 +457 T
sd42 2.0035E+05 1.0018E+05 2.0035E+04 4r 4.0071E+05
tf42
fc52 Radial 1ft Tally
f52:p +500.1
fm52 4.0000E+00
fs52 -501 -502 -503 -504 -505 -506
      -507 -508 -509 -510 -511 T
tf52
fc62 Radial 1m Tally
f62:p +600.1
```



```
fm62 4.0000E+00
fs62 -601 -602 -603 -604 -605 -606
      -607 -608 -609 -610 -611 -612
      -613 -614 T
tf62
fc72 Radial 2m Tally
f72:p +700.1
fm72 4.0000E+00
fs72 -701 -702 -703 -704 -705 -706
      -707 -708 -709 -710 -711 -712
      -713 -714 -715 -716 -717 -718
      -719 T
tf72
fc82 Radial 4m Tally
f82:p +800.1
fm82 4.0000E+00
fs82 -801 -802 -803 -804 -805 -806
      -807 -808 -809 -810 -811 -812
      -813 -814 -815 -816 -817 -818
      -819 T
tf82
C
C
C Print Control
C
prdump -30 -60 1 2
print
C
C Random Number Generator
C
rand gen=2 seed=19073486328125 stride=152917 hist=1
C
C Rotation Matrix
C
C 18 degree rotation around z-axis
*TR1 0.0 0.0 0.0 18 108 90 -72 18 90 90 90 0
C 36 degree rotation around z-axis
*TR2 0.0 0.0 0.0 36 126 90 -54 36 90 90 90 0
C 54 degree rotation around z-axis
*TR3 0.0 0.0 0.0 54 144 90 -36 54 90 90 90 0
C 72 degree rotation around z-axis
*TR4 0.0 0.0 0.0 72 162 90 -18 72 90 90 90 0
C 108 degree rotation around z-axis
*TR5 0.0 0.0 0.0 108 198 90 18 108 90 90 90 0
C 126 degree rotation around z-axis
*TR6 0.0 0.0 0.0 126 216 90 36 126 90 90 90 0
C 144 degree rotation around z-axis
*TR7 0.0 0.0 0.0 144 234 90 54 144 90 90 90 0
C 162 degree rotation around z-axis
*TR8 0.0 0.0 0.0 162 252 90 72 162 90 90 90 0
C 45 degree rotation around z-axis
*TR9 0.0 0.0 0.0 45 135 90 -45 45 90 90 90 0
C 135 degree rotation around z-axis
*TR10 0.0 0.0 0.0 135 225 90 45 135 90 90 90 0
C 15 degree rotation around z-axis
*TR11 0.0 0.0 0.0 15 105 90 -75 15 90 90 90 0
C 30 degree rotation around z-axis
*TR12 0.0 0.0 0.0 30 120 90 -60 30 90 90 90 0
C 60 degree rotation around z-axis
*TR13 0.0 0.0 0.0 60 150 90 -30 60 90 90 90 0
C 75 degree rotation around z-axis
*TR14 0.0 0.0 0.0 75 165 90 -15 75 90 90 90 0
```

### 5.9.8 Cool-Time Tables

PWR system performance is evaluated for a cask heat load of 35.5 kW with preferential (1.8 kW max) and uniform (959 W/assy) heat load patterns. Minimum cool times are summarized for the uniform and preferential heat load patterns.

Allowed low burnup (up to 30,000 MWd/MTU) fuel loadings are shown in Table 5.8.9-1. Note that the listed minimum cool times at each burnup step are bounding for all fuel types and initial enrichments above the minimum enrichment specified. Collapsing the fuel type and initial enrichment-dependent minimum cool time matrix to a single value may result in a minimum cool time longer than individual values presented for higher burnups in the detailed tables that follow.

The minimum cool time tables account for potential uncertainties in the source generation abilities of SAS2H at burnups greater than 45 GWd/MTU by reducing allowed heat loads by 5 percent. Fuel assembly loading tables at greater than 45 GWd/MTU are, therefore, generated for a cask heat load of 33.725 kW with preferential (1.71 kW max) and uniform (911 W/assy) heat load patterns.

The 5% penalty adjusted four-zone preferential loading pattern is as follows.

Zone Description	Designator	Heat Load [W/assy]	Adjusted Heat Load [W/assy]	# Assemblies
Inner Ring	A	513	487	9
Middle Ring	B1	1300	1235	8
	B2	1800	1710	4
Outer Ring	C	830	788	16

Table 5.9.8-1 contains the minimum cool times for a uniform heat load of 959 W/assy ( $\leq 45$  GWd/MTU) PWR fuel. Greater than 45 GWd/MTU uniform heat load minimum cool times are listed in Section 5.8.9. Table 5.9.8-2 through Table 5.9.8-5 contain the minimum cool times for the preferential loading of  $\leq 45$  GWd/MTU with higher burnup fuel cool times listed in Table 5.9.8-6 through Table 5.9.8-9.

Decay heat associated with loading nonfuel components requires an increase in the minimum fuel assembly cool time. The incremental cool time increase is documented in Table 5.9.4-1 for the BPRAs and TPs. The incremental cool time increase to allow loading of the Westinghouse 14x14 CEAs with a minimum cool time of 2.5 years is shown in Table 5.9.5-4.

Table 5.9.8-1 Loading Table for PWR Fuel – 959 W/Assembly

Minimum Initial Assembly Avg. Enrichment wt % <sup>235</sup> U (E)	Assembly Average Burnup (B) GWd/MTU					
	B ≤10	10< B ≤15	15< B ≤20	20< B ≤25	25< B ≤30	30< B ≤32.5
1.3 ≤ E < 1.5	2.5	-	-	-	-	-
1.5 ≤ E < 1.7	2.5	2.5	-	-	-	-
1.7 ≤ E < 1.9	2.5	2.5	2.9	-	-	-
1.9 ≤ E < 2.1	2.5	2.5	2.9	3.4	-	-
2.1 ≤ E < 2.3	2.5	2.5	2.8	3.3	3.9	4.1
2.3 ≤ E < 2.5	2.5	2.5	2.8	3.3	3.8	4.1
2.5 ≤ E < 2.7	2.5	2.5	2.8	3.3	3.8	4.0
2.7 ≤ E < 2.9	2.5	2.5	2.8	3.2	3.7	4.0
2.9 ≤ E < 3.1	2.5	2.5	2.7	3.2	3.7	3.9
3.1 ≤ E < 3.3	2.5	2.5	2.7	3.2	3.7	3.9
3.3 ≤ E < 3.5	2.5	2.5	2.7	3.2	3.6	3.9
3.5 ≤ E < 3.7	2.5	2.5	2.7	3.1	3.6	3.8
3.7 ≤ E < 3.9	2.5	2.5	2.7	3.1	3.6	3.8
3.9 ≤ E < 4.1	2.5	2.5	2.6	3.1	3.6	3.8
4.1 ≤ E < 4.3	2.5	2.5	2.6	3.1	3.5	3.8
4.3 ≤ E < 4.5	2.5	2.5	2.6	3.0	3.5	3.7
4.5 ≤ E < 4.7	2.5	2.5	2.6	3.0	3.5	3.7
4.7 ≤ E < 4.9	2.5	2.5	2.6	3.0	3.5	3.7
E ≥ 4.9	2.5	2.5	2.6	3.0	3.5	3.7

Table 5.9.8-1 Loading Table for PWR Fuel – 959 W/Assembly (Continued)

Minimum Initial Assembly Avg. Enrichment wt % <sup>235</sup> U (E)	Assembly Average Burnup (B) GWd/MTU					
	32.5< B ≤35	35< B ≤37.5	37.5< B ≤40	40< B ≤41	41< B ≤42	42< B ≤43
1.3 ≤ E < 1.5	-	-	-	-	-	-
1.5 ≤ E < 1.7	-	-	-	-	-	-
1.7 ≤ E < 1.9	-	-	-	-	-	-
1.9 ≤ E < 2.1	-	-	-	-	-	-
2.1 ≤ E < 2.3	-	-	-	-	-	-
2.3 ≤ E < 2.5	4.4	4.8	-	-	-	-
2.5 ≤ E < 2.7	4.4	4.7	5.2	5.4	5.6	5.8
2.7 ≤ E < 2.9	4.3	4.7	5.1	5.3	5.5	5.7
2.9 ≤ E < 3.1	4.3	4.6	5.0	5.2	5.4	5.6
3.1 ≤ E < 3.3	4.2	4.5	4.9	5.1	5.3	5.6
3.3 ≤ E < 3.5	4.2	4.5	4.9	5.1	5.3	5.5
3.5 ≤ E < 3.7	4.1	4.5	4.8	5.0	5.2	5.4
3.7 ≤ E < 3.9	4.1	4.4	4.8	4.9	5.1	5.3
3.9 ≤ E < 4.1	4.1	4.4	4.8	4.9	5.1	5.3
4.1 ≤ E < 4.3	4.0	4.4	4.7	4.9	5.0	5.2
4.3 ≤ E < 4.5	4.0	4.3	4.7	4.8	5.0	5.2
4.5 ≤ E < 4.7	4.0	4.3	4.6	4.8	4.9	5.1
4.7 ≤ E < 4.9	4.0	4.3	4.6	4.7	4.9	5.0
E ≥ 4.9	3.9	4.2	4.5	4.7	4.9	5.0

Table 5.9.8-1 Loading Table for PWR Fuel – 959 W/Assembly (Continued)

Minimum Initial Assembly Avg. Enrichment wt % <sup>235</sup> U (E)	Assembly Average Burnup (B) GWd/MTU	
	43< B ≤44	44< B ≤45
1.3 ≤ E < 1.5	-	-
1.5 ≤ E < 1.7	-	-
1.7 ≤ E < 1.9	-	-
1.9 ≤ E < 2.1	-	-
2.1 ≤ E < 2.3	-	-
2.3 ≤ E < 2.5	-	-
2.5 ≤ E < 2.7	6.0	-
2.7 ≤ E < 2.9	5.9	6.2
2.9 ≤ E < 3.1	5.8	6.0
3.1 ≤ E < 3.3	5.8	6.0
3.3 ≤ E < 3.5	5.7	5.9
3.5 ≤ E < 3.7	5.6	5.8
3.7 ≤ E < 3.9	5.6	5.8
3.9 ≤ E < 4.1	5.5	5.7
4.1 ≤ E < 4.3	5.4	5.6
4.3 ≤ E < 4.5	5.4	5.6
4.5 ≤ E < 4.7	5.3	5.5
4.7 ≤ E < 4.9	5.3	5.5
E ≥ 4.9	5.2	5.4

Table 5.9.8-2 Loading Table for PWR Fuel – 513 W/Assembly

Minimum Initial Assembly Avg. Enrichment wt % <sup>235</sup> U (E)	Assembly Average Burnup (B) GWd/MTU					
	B ≤10	10< B ≤15	15< B ≤20	20< B ≤25	25< B ≤30	30< B ≤32.5
1.3 ≤ E < 1.5	2.9	-	-	-	-	-
1.5 ≤ E < 1.7	2.9	3.8	-	-	-	-
1.7 ≤ E < 1.9	2.9	3.7	4.5	-	-	-
1.9 ≤ E < 2.1	2.9	3.7	4.5	5.7	-	-
2.1 ≤ E < 2.3	2.8	3.7	4.5	5.7	7.5	8.9
2.3 ≤ E < 2.5	2.8	3.6	4.4	5.6	7.4	8.8
2.5 ≤ E < 2.7	2.8	3.6	4.4	5.6	7.3	8.6
2.7 ≤ E < 2.9	2.8	3.6	4.4	5.5	7.2	8.5
2.9 ≤ E < 3.1	2.8	3.5	4.4	5.5	7.1	8.5
3.1 ≤ E < 3.3	2.8	3.5	4.3	5.5	7.1	8.4
3.3 ≤ E < 3.5	2.8	3.5	4.3	5.4	7.0	8.3
3.5 ≤ E < 3.7	2.7	3.5	4.3	5.4	7.0	8.2
3.7 ≤ E < 3.9	2.7	3.5	4.3	5.4	7.0	8.1
3.9 ≤ E < 4.1	2.7	3.5	4.3	5.3	6.9	8.1
4.1 ≤ E < 4.3	2.7	3.5	4.2	5.3	6.9	8.0
4.3 ≤ E < 4.5	2.7	3.5	4.2	5.3	6.8	8.0
4.5 ≤ E < 4.7	2.7	3.5	4.2	5.2	6.8	7.9
4.7 ≤ E < 4.9	2.7	3.4	4.2	5.2	6.8	7.9
E ≥ 4.9	2.7	3.4	4.2	5.2	6.8	7.9

Table 5.9.8-2 Loading Table for PWR Fuel – 513 W/Assembly (continued)

Minimum Initial Assembly Avg. Enrichment wt % <sup>235</sup> U (E)	Assembly Average Burnup (B) GWd/MTU					
	32.5< B ≤35	35< B ≤37.5	37.5< B ≤40	40< B ≤41	41< B ≤42	42< B ≤43
1.3 ≤ E < 1.5	-	-	-	-	-	-
1.5 ≤ E < 1.7	-	-	-	-	-	-
1.7 ≤ E < 1.9	-	-	-	-	-	-
1.9 ≤ E < 2.1	-	-	-	-	-	-
2.1 ≤ E < 2.3	-	-	-	-	-	-
2.3 ≤ E < 2.5	10.9	13.7	-	-	-	-
2.5 ≤ E < 2.7	10.7	13.5	16.9	18.2	19.7	21.2
2.7 ≤ E < 2.9	10.5	13.3	16.5	18.0	19.4	20.8
2.9 ≤ E < 3.1	10.4	13.1	16.3	17.7	19.2	20.6
3.1 ≤ E < 3.3	10.2	12.8	16.0	17.5	18.9	20.4
3.3 ≤ E < 3.5	10.1	12.7	15.9	17.2	18.7	20.1
3.5 ≤ E < 3.7	10.0	12.5	15.6	17.0	18.4	19.9
3.7 ≤ E < 3.9	9.9	12.4	15.5	16.8	18.2	19.6
3.9 ≤ E < 4.1	9.8	12.3	15.3	16.7	18.0	19.5
4.1 ≤ E < 4.3	9.8	12.1	15.2	16.5	17.9	19.3
4.3 ≤ E < 4.5	9.7	12.0	15.1	16.3	17.7	19.2
4.5 ≤ E < 4.7	9.7	11.9	15.0	16.2	17.6	19.0
4.7 ≤ E < 4.9	9.6	11.9	14.9	16.1	17.5	18.8
E ≥ 4.9	9.5	11.8	14.8	16.0	17.3	18.7

Table 5.9.8-2 Loading Table for PWR Fuel – 513 W/Assembly (continued)

Minimum Initial Assembly Avg. Enrichment wt % <sup>235</sup> U (E)	Assembly Average Burnup (B) GWd/MTU	
	43< B ≤44	44< B ≤45
1.3 ≤ E < 1.5	-	-
1.5 ≤ E < 1.7	-	-
1.7 ≤ E < 1.9	-	-
1.9 ≤ E < 2.1	-	-
2.1 ≤ E < 2.3	-	-
2.3 ≤ E < 2.5	-	-
2.5 ≤ E < 2.7	22.7	-
2.7 ≤ E < 2.9	22.3	23.8
2.9 ≤ E < 3.1	22.1	23.5
3.1 ≤ E < 3.3	21.8	23.2
3.3 ≤ E < 3.5	21.6	22.9
3.5 ≤ E < 3.7	21.3	22.7
3.7 ≤ E < 3.9	21.1	22.5
3.9 ≤ E < 4.1	20.9	22.3
4.1 ≤ E < 4.3	20.8	22.1
4.3 ≤ E < 4.5	20.6	21.9
4.5 ≤ E < 4.7	20.4	21.8
4.7 ≤ E < 4.9	20.3	21.6
E ≥ 4.9	20.1	21.5



Table 5.9.8-3 Loading Table for PWR Fuel – 1,300 W/Assembly

Minimum Initial Assembly Avg. Enrichment wt % <sup>235</sup> U (E)	Assembly Average Burnup (B) GWd/MTU					
	B ≤10	10< B ≤15	15< B ≤20	20< B ≤25	25< B ≤30	30< B ≤32.5
1.3 ≤ E < 1.5	2.5	-	-	-	-	-
1.5 ≤ E < 1.7	2.5	2.5	-	-	-	-
1.7 ≤ E < 1.9	2.5	2.5	2.5	-	-	-
1.9 ≤ E < 2.1	2.5	2.5	2.5	2.7	-	-
2.1 ≤ E < 2.3	2.5	2.5	2.5	2.6	3.0	3.2
2.3 ≤ E < 2.5	2.5	2.5	2.5	2.6	3.0	3.2
2.5 ≤ E < 2.7	2.5	2.5	2.5	2.6	3.0	3.1
2.7 ≤ E < 2.9	2.5	2.5	2.5	2.6	2.9	3.1
2.9 ≤ E < 3.1	2.5	2.5	2.5	2.5	2.9	3.0
3.1 ≤ E < 3.3	2.5	2.5	2.5	2.5	2.9	3.0
3.3 ≤ E < 3.5	2.5	2.5	2.5	2.5	2.9	3.0
3.5 ≤ E < 3.7	2.5	2.5	2.5	2.5	2.8	3.0
3.7 ≤ E < 3.9	2.5	2.5	2.5	2.5	2.8	3.0
3.9 ≤ E < 4.1	2.5	2.5	2.5	2.5	2.8	2.9
4.1 ≤ E < 4.3	2.5	2.5	2.5	2.5	2.8	2.9
4.3 ≤ E < 4.5	2.5	2.5	2.5	2.5	2.8	2.9
4.5 ≤ E < 4.7	2.5	2.5	2.5	2.5	2.7	2.9
4.7 ≤ E < 4.9	2.5	2.5	2.5	2.5	2.7	2.9
E ≥ 4.9	2.5	2.5	2.5	2.5	2.7	2.8

Table 5.9.8-3 Loading Table for PWR Fuel – 1,300 W/Assembly (continued)

Minimum Initial Assembly Avg. Enrichment wt % <sup>235</sup> U (E)	Assembly Average Burnup (B) GWd/MTU					
	32.5< B ≤35	35< B ≤37.5	37.5< B ≤40	40< B ≤41	41< B ≤42	42< B ≤43
1.3 ≤ E < 1.5	-	-	-	-	-	-
1.5 ≤ E < 1.7	-	-	-	-	-	-
1.7 ≤ E < 1.9	-	-	-	-	-	-
1.9 ≤ E < 2.1	-	-	-	-	-	-
2.1 ≤ E < 2.3	-	-	-	-	-	-
2.3 ≤ E < 2.5	3.4	3.6	-	-	-	-
2.5 ≤ E < 2.7	3.3	3.6	3.8	3.9	4.0	4.1
2.7 ≤ E < 2.9	3.3	3.5	3.8	3.9	4.0	4.1
2.9 ≤ E < 3.1	3.3	3.5	3.7	3.8	3.9	4.0
3.1 ≤ E < 3.3	3.2	3.4	3.7	3.8	3.9	4.0
3.3 ≤ E < 3.5	3.2	3.4	3.6	3.7	3.8	3.9
3.5 ≤ E < 3.7	3.2	3.4	3.6	3.7	3.8	3.9
3.7 ≤ E < 3.9	3.1	3.4	3.6	3.6	3.8	3.9
3.9 ≤ E < 4.1	3.1	3.3	3.5	3.6	3.7	3.8
4.1 ≤ E < 4.3	3.1	3.3	3.5	3.6	3.7	3.8
4.3 ≤ E < 4.5	3.0	3.3	3.5	3.6	3.6	3.8
4.5 ≤ E < 4.7	3.0	3.2	3.4	3.5	3.6	3.7
4.7 ≤ E < 4.9	3.0	3.2	3.4	3.5	3.6	3.7
E ≥ 4.9	3.0	3.2	3.4	3.5	3.5	3.7

Table 5.9.8-3 Loading Table for PWR Fuel – 1,300 W/Assembly (continued)

Minimum Initial Assembly Avg. Enrichment wt % <sup>235</sup> U (E)	Assembly Average Burnup (B) GWd/MTU	
	43< B ≤44	44< B ≤45
1.3 ≤ E < 1.5	-	-
1.5 ≤ E < 1.7	-	-
1.7 ≤ E < 1.9	-	-
1.9 ≤ E < 2.1	-	-
2.1 ≤ E < 2.3	-	-
2.3 ≤ E < 2.5	-	-
2.5 ≤ E < 2.7	4.3	-
2.7 ≤ E < 2.9	4.2	4.3
2.9 ≤ E < 3.1	4.2	4.3
3.1 ≤ E < 3.3	4.1	4.2
3.3 ≤ E < 3.5	4.0	4.2
3.5 ≤ E < 3.7	4.0	4.1
3.7 ≤ E < 3.9	4.0	4.0
3.9 ≤ E < 4.1	3.9	4.0
4.1 ≤ E < 4.3	3.9	4.0
4.3 ≤ E < 4.5	3.8	3.9
4.5 ≤ E < 4.7	3.9	3.9
4.7 ≤ E < 4.9	3.8	3.9
E ≥ 4.9	3.8	3.8

Table 5.9.8-4 Loading Table for PWR Fuel – 1,800 W/Assembly

Minimum Initial Assembly Avg. Enrichment wt % <sup>235</sup> U (E)	Assembly Average Burnup (B) GWd/MTU					
	B ≤10	10< B ≤15	15< B ≤20	20< B ≤25	25< B ≤30	30< B ≤32.5
1.3 ≤ E < 1.5	2.5	-	-	-	-	-
1.5 ≤ E < 1.7	2.5	2.5	-	-	-	-
1.7 ≤ E < 1.9	2.5	2.5	2.5	-	-	-
1.9 ≤ E < 2.1	2.5	2.5	2.5	2.5	-	-
2.1 ≤ E < 2.3	2.5	2.5	2.5	2.5	2.5	2.5
2.3 ≤ E < 2.5	2.5	2.5	2.5	2.5	2.5	2.5
2.5 ≤ E < 2.7	2.5	2.5	2.5	2.5	2.5	2.5
2.7 ≤ E < 2.9	2.5	2.5	2.5	2.5	2.5	2.5
2.9 ≤ E < 3.1	2.5	2.5	2.5	2.5	2.5	2.5
3.1 ≤ E < 3.3	2.5	2.5	2.5	2.5	2.5	2.5
3.3 ≤ E < 3.5	2.5	2.5	2.5	2.5	2.5	2.5
3.5 ≤ E < 3.7	2.5	2.5	2.5	2.5	2.5	2.5
3.7 ≤ E < 3.9	2.5	2.5	2.5	2.5	2.5	2.5
3.9 ≤ E < 4.1	2.5	2.5	2.5	2.5	2.5	2.5
4.1 ≤ E < 4.3	2.5	2.5	2.5	2.5	2.5	2.5
4.3 ≤ E < 4.5	2.5	2.5	2.5	2.5	2.5	2.5
4.5 ≤ E < 4.7	2.5	2.5	2.5	2.5	2.5	2.5
4.7 ≤ E < 4.9	2.5	2.5	2.5	2.5	2.5	2.5
E ≥ 4.9	2.5	2.5	2.5	2.5	2.5	2.5

Table 5.9.8-4 Loading Table for PWR Fuel – 1,800 W/Assembly (continued)

Minimum Initial Assembly Avg. Enrichment wt % <sup>235</sup> U (E)	Assembly Average Burnup (B) GWd/MTU					
	32.5< B ≤35	35< B ≤37.5	37.5< B ≤40	40< B ≤41	41< B ≤42	42< B ≤43
1.3 ≤ E < 1.5	-	-	-	-	-	-
1.5 ≤ E < 1.7	-	-	-	-	-	-
1.7 ≤ E < 1.9	-	-	-	-	-	-
1.9 ≤ E < 2.1	-	-	-	-	-	-
2.1 ≤ E < 2.3	-	-	-	-	-	-
2.3 ≤ E < 2.5	2.6	2.7	-	-	-	-
2.5 ≤ E < 2.7	2.5	2.7	2.9	2.9	3.0	3.1
2.7 ≤ E < 2.9	2.5	2.7	2.8	2.9	3.0	3.0
2.9 ≤ E < 3.1	2.5	2.6	2.8	2.9	2.9	3.0
3.1 ≤ E < 3.3	2.5	2.6	2.8	2.8	2.9	3.0
3.3 ≤ E < 3.5	2.5	2.6	2.7	2.8	2.9	2.9
3.5 ≤ E < 3.7	2.5	2.5	2.7	2.8	2.8	2.9
3.7 ≤ E < 3.9	2.5	2.5	2.7	2.7	2.8	2.9
3.9 ≤ E < 4.1	2.5	2.5	2.6	2.7	2.8	2.8
4.1 ≤ E < 4.3	2.5	2.5	2.6	2.7	2.8	2.8
4.3 ≤ E < 4.5	2.5	2.5	2.6	2.7	2.7	2.8
4.5 ≤ E < 4.7	2.5	2.5	2.6	2.6	2.7	2.8
4.7 ≤ E < 4.9	2.5	2.5	2.5	2.6	2.7	2.7
E ≥ 4.9	2.5	2.5	2.5	2.6	2.6	2.7

Table 5.9.8-4 Loading Table for PWR Fuel – 1,800 W/Assembly (continued)

Minimum Initial Assembly Avg. Enrichment wt % <sup>235</sup> U (E)	Assembly Average Burnup (B) GWd/MTU	
	43< B ≤44	44< B ≤45
1.3 ≤ E < 1.5	-	-
1.5 ≤ E < 1.7	-	-
1.7 ≤ E < 1.9	-	-
1.9 ≤ E < 2.1	-	-
2.1 ≤ E < 2.3	-	-
2.3 ≤ E < 2.5	-	-
2.5 ≤ E < 2.7	3.1	-
2.7 ≤ E < 2.9	3.1	3.2
2.9 ≤ E < 3.1	3.1	3.1
3.1 ≤ E < 3.3	3.0	3.1
3.3 ≤ E < 3.5	3.0	3.1
3.5 ≤ E < 3.7	3.0	3.0
3.7 ≤ E < 3.9	2.9	3.0
3.9 ≤ E < 4.1	2.9	3.0
4.1 ≤ E < 4.3	2.9	2.9
4.3 ≤ E < 4.5	2.8	2.9
4.5 ≤ E < 4.7	2.9	2.9
4.7 ≤ E < 4.9	2.8	2.9
E ≥ 4.9	2.8	2.8

Table 5.9.8-5 Loading Table for PWR Fuel – 830 W/Assembly

Minimum Initial Assembly Avg. Enrichment wt % <sup>235</sup> U (E)	Assembly Average Burnup (B) GWd/MTU					
	B ≤10	10< B ≤15	15< B ≤20	20< B ≤25	25< B ≤30	30< B ≤32.5
1.3 ≤ E < 1.5	2.5	-	-	-	-	-
1.5 ≤ E < 1.7	2.5	2.7	-	-	-	-
1.7 ≤ E < 1.9	2.5	2.7	3.2	-	-	-
1.9 ≤ E < 2.1	2.5	2.7	3.2	3.8	-	-
2.1 ≤ E < 2.3	2.5	2.6	3.1	3.7	4.4	4.7
2.3 ≤ E < 2.5	2.5	2.6	3.1	3.7	4.3	4.6
2.5 ≤ E < 2.7	2.5	2.6	3.1	3.6	4.3	4.6
2.7 ≤ E < 2.9	2.5	2.6	3.0	3.6	4.2	4.5
2.9 ≤ E < 3.1	2.5	2.5	3.0	3.6	4.2	4.5
3.1 ≤ E < 3.3	2.5	2.5	3.0	3.5	4.2	4.5
3.3 ≤ E < 3.5	2.5	2.5	3.0	3.5	4.1	4.4
3.5 ≤ E < 3.7	2.5	2.5	3.0	3.5	4.1	4.4
3.7 ≤ E < 3.9	2.5	2.5	3.0	3.5	4.0	4.4
3.9 ≤ E < 4.1	2.5	2.5	2.9	3.5	4.0	4.3
4.1 ≤ E < 4.3	2.5	2.5	2.9	3.4	4.0	4.3
4.3 ≤ E < 4.5	2.5	2.5	2.9	3.4	4.0	4.3
4.5 ≤ E < 4.7	2.5	2.5	2.9	3.4	4.0	4.2
4.7 ≤ E < 4.9	2.5	2.5	2.9	3.4	3.9	4.2
E ≥ 4.9	2.5	2.5	2.9	3.4	3.9	4.2

Table 5.9.8-5 Loading Table for PWR Fuel – 830 W/Assembly (continued)

Minimum Initial Assembly Avg. Enrichment wt % <sup>235</sup> U (E)	Assembly Average Burnup (B) GWd/MTU					
	32.5< B ≤35	35< B ≤37.5	37.5< B ≤40	40< B ≤41	41< B ≤42	42< B ≤43
1.3 ≤ E < 1.5	-	-	-	-	-	-
1.5 ≤ E < 1.7	-	-	-	-	-	-
1.7 ≤ E < 1.9	-	-	-	-	-	-
1.9 ≤ E < 2.1	-	-	-	-	-	-
2.1 ≤ E < 2.3	-	-	-	-	-	-
2.3 ≤ E < 2.5	5.1	5.6	-	-	-	-
2.5 ≤ E < 2.7	5.0	5.6	6.1	6.4	6.8	7.1
2.7 ≤ E < 2.9	5.0	5.5	6.0	6.3	6.6	6.9
2.9 ≤ E < 3.1	4.9	5.4	6.0	6.2	6.5	6.8
3.1 ≤ E < 3.3	4.9	5.4	5.9	6.1	6.4	6.7
3.3 ≤ E < 3.5	4.8	5.3	5.8	6.0	6.3	6.6
3.5 ≤ E < 3.7	4.8	5.2	5.8	6.0	6.3	6.6
3.7 ≤ E < 3.9	4.7	5.2	5.7	5.9	6.2	6.5
3.9 ≤ E < 4.1	4.7	5.1	5.7	5.9	6.1	6.4
4.1 ≤ E < 4.3	4.6	5.1	5.6	5.8	6.0	6.3
4.3 ≤ E < 4.5	4.6	5.0	5.6	5.8	6.0	6.2
4.5 ≤ E < 4.7	4.6	5.0	5.5	5.7	5.9	6.2
4.7 ≤ E < 4.9	4.5	5.0	5.5	5.7	5.9	6.1
E ≥ 4.9	4.5	4.9	5.4	5.6	5.9	6.0



Table 5.9.8-5 Loading Table for PWR Fuel – 830 W/Assembly (continued)

Minimum Initial Assembly Avg. Enrichment wt % <sup>235</sup> U (E)	Assembly Average Burnup (B) GWd/MTU	
	43< B ≤44	44< B ≤45
1.3 ≤ E < 1.5	-	-
1.5 ≤ E < 1.7	-	-
1.7 ≤ E < 1.9	-	-
1.9 ≤ E < 2.1	-	-
2.1 ≤ E < 2.3	-	-
2.3 ≤ E < 2.5	-	-
2.5 ≤ E < 2.7	7.5	-
2.7 ≤ E < 2.9	7.3	7.7
2.9 ≤ E < 3.1	7.2	7.6
3.1 ≤ E < 3.3	7.0	7.5
3.3 ≤ E < 3.5	6.9	7.3
3.5 ≤ E < 3.7	6.8	7.2
3.7 ≤ E < 3.9	6.8	7.1
3.9 ≤ E < 4.1	6.7	7.0
4.1 ≤ E < 4.3	6.6	6.9
4.3 ≤ E < 4.5	6.6	6.8
4.5 ≤ E < 4.7	6.5	6.8
4.7 ≤ E < 4.9	6.4	6.7
E ≥ 4.9	6.4	6.7

Table 5.9.8-6 Loading Table for PWR Fuel – 487 W/Assembly

Minimum Initial Assembly Avg. Enrichment wt % <sup>235</sup> U (E)	Assembly Average Burnup (B) GWd/MTU					
	45< B ≤46	46< B ≤47	47< B ≤48	48< B ≤49	49< B ≤50	50< B ≤51
1.3 ≤ E < 1.5	-	-	-	-	-	-
1.5 ≤ E < 1.7	-	-	-	-	-	-
1.7 ≤ E < 1.9	-	-	-	-	-	-
1.9 ≤ E < 2.1	-	-	-	-	-	-
2.1 ≤ E < 2.3	-	-	-	-	-	-
2.3 ≤ E < 2.5	-	-	-	-	-	-
2.5 ≤ E < 2.7	-	-	-	-	-	-
2.7 ≤ E < 2.9	27.9	29.3	30.7	32.0	-	-
2.9 ≤ E < 3.1	27.6	29.0	30.4	31.8	32.7	33.9
3.1 ≤ E < 3.3	27.4	28.8	30.2	31.6	32.4	33.7
3.3 ≤ E < 3.5	27.1	28.5	30.0	31.4	32.2	33.6
3.5 ≤ E < 3.7	26.9	28.3	29.7	31.1	32.0	33.3
3.7 ≤ E < 3.9	26.7	28.1	29.5	30.9	31.8	33.1
3.9 ≤ E < 4.1	26.6	27.9	29.4	30.8	31.6	32.9
4.1 ≤ E < 4.3	26.3	27.8	29.2	30.6	31.4	33.5
4.3 ≤ E < 4.5	26.1	27.5	29.0	30.3	31.2	32.6
4.5 ≤ E < 4.7	26.0	27.4	28.8	30.2	31.1	32.4
4.7 ≤ E < 4.9	25.9	27.3	28.6	30.1	30.9	32.3
E ≥ 4.9	25.8	27.1	28.5	30.0	30.8	32.1

Table 5.9.8-6 Loading Table for PWR Fuel – 487 W/Assembly (continued)

Minimum Initial Assembly Avg. Enrichment wt % <sup>235</sup> U (E)	Assembly Average Burnup (B) GWd/MTU					
	51< B ≤52	52< B ≤53	53< B ≤54	54< B ≤55	55< B ≤56	56< B ≤57
1.3 ≤ E < 1.5	-	-	-	-	-	-
1.5 ≤ E < 1.7	-	-	-	-	-	-
1.7 ≤ E < 1.9	-	-	-	-	-	-
1.9 ≤ E < 2.1	-	-	-	-	-	-
2.1 ≤ E < 2.3	-	-	-	-	-	-
2.3 ≤ E < 2.5	-	-	-	-	-	-
2.5 ≤ E < 2.7	-	-	-	-	-	-
2.7 ≤ E < 2.9	-	-	-	-	-	-
2.9 ≤ E < 3.1	35.2	36.4	37.7	-	-	-
3.1 ≤ E < 3.3	35.0	36.2	37.4	38.8	39.8	41.0
3.3 ≤ E < 3.5	34.8	36.0	37.2	38.5	39.6	40.9
3.5 ≤ E < 3.7	34.5	35.9	37.1	38.4	39.5	40.7
3.7 ≤ E < 3.9	34.3	35.6	36.9	38.2	39.4	40.5
3.9 ≤ E < 4.1	34.2	35.4	36.7	38.1	39.2	40.4
4.1 ≤ E < 4.3	34.1	35.2	36.6	37.9	39.2	40.2
4.3 ≤ E < 4.5	33.9	35.2	36.4	37.7	39.0	40.2
4.5 ≤ E < 4.7	33.7	35.0	36.3	37.6	38.8	40.0
4.7 ≤ E < 4.9	33.5	34.8	36.1	37.4	38.7	39.8
E ≥ 4.9	33.4	34.7	35.9	37.3	38.6	39.7

Table 5.9.8-6 Loading Table for PWR Fuel – 487 W/Assembly (continued)

Minimum Initial Assembly Avg. Enrichment wt % <sup>235</sup> U (E)	Assembly Average Burnup (B) GWd/MTU		
	57< B ≤58	58< B ≤59	59< B ≤60
1.3 ≤ E < 1.5	-	-	-
1.5 ≤ E < 1.7	-	-	-
1.7 ≤ E < 1.9	-	-	-
1.9 ≤ E < 2.1	-	-	-
2.1 ≤ E < 2.3	-	-	-
2.3 ≤ E < 2.5	-	-	-
2.5 ≤ E < 2.7	-	-	-
2.7 ≤ E < 2.9	-	-	-
2.9 ≤ E < 3.1	-	-	-
3.1 ≤ E < 3.3	42.1	43.3	-
3.3 ≤ E < 3.5	42.0	43.1	44.1
3.5 ≤ E < 3.7	41.9	43.0	44.1
3.7 ≤ E < 3.9	41.7	42.9	43.9
3.9 ≤ E < 4.1	41.6	42.7	43.8
4.1 ≤ E < 4.3	41.5	42.6	43.7
4.3 ≤ E < 4.5	41.3	42.5	43.6
4.5 ≤ E < 4.7	41.2	42.4	43.5
4.7 ≤ E < 4.9	41.0	42.3	43.4
E ≥ 4.9	40.9	42.1	43.3

Table 5.9.8-7 Loading Table for PWR Fuel – 1235 W/Assembly

Minimum Initial Assembly Avg. Enrichment wt % <sup>235</sup> U (E)	Assembly Average Burnup (B) GWd/MTU					
	45< B ≤46	46< B ≤47	47< B ≤48	48< B ≤49	49< B ≤50	50< B ≤51
1.3 ≤ E < 1.5	-	-	-	-	-	-
1.5 ≤ E < 1.7	-	-	-	-	-	-
1.7 ≤ E < 1.9	-	-	-	-	-	-
1.9 ≤ E < 2.1	-	-	-	-	-	-
2.1 ≤ E < 2.3	-	-	-	-	-	-
2.3 ≤ E < 2.5	-	-	-	-	-	-
2.5 ≤ E < 2.7	-	-	-	-	-	-
2.7 ≤ E < 2.9	4.7	4.9	5.0	5.2	-	-
2.9 ≤ E < 3.1	4.6	4.8	4.9	5.1	5.2	5.4
3.1 ≤ E < 3.3	4.6	4.7	4.9	5.0	5.1	5.3
3.3 ≤ E < 3.5	4.5	4.6	4.8	4.9	5.0	5.2
3.5 ≤ E < 3.7	4.5	4.6	4.7	4.9	5.0	5.2
3.7 ≤ E < 3.9	4.4	4.5	4.7	4.8	4.9	5.1
3.9 ≤ E < 4.1	4.4	4.5	4.6	4.8	4.9	5.0
4.1 ≤ E < 4.3	4.3	4.4	4.5	4.7	4.8	4.9
4.3 ≤ E < 4.5	4.3	4.4	4.5	4.6	4.8	4.9
4.5 ≤ E < 4.7	4.2	4.3	4.5	4.6	4.7	4.8
4.7 ≤ E < 4.9	4.2	4.3	4.4	4.6	4.7	4.8
E ≥ 4.9	4.1	4.3	4.4	4.5	4.6	4.7

Table 5.9.8-7 Loading Table for PWR Fuel – 1235 W/Assembly (continued)

Minimum Initial Assembly Avg. Enrichment wt % <sup>235</sup> U (E)	Assembly Average Burnup (B) GWd/MTU					
	51< B ≤52	52< B ≤53	53< B ≤54	54< B ≤55	55< B ≤56	56< B ≤57
1.3 ≤ E < 1.5	-	-	-	-	-	-
1.5 ≤ E < 1.7	-	-	-	-	-	-
1.7 ≤ E < 1.9	-	-	-	-	-	-
1.9 ≤ E < 2.1	-	-	-	-	-	-
2.1 ≤ E < 2.3	-	-	-	-	-	-
2.3 ≤ E < 2.5	-	-	-	-	-	-
2.5 ≤ E < 2.7	-	-	-	-	-	-
2.7 ≤ E < 2.9	-	-	-	-	-	-
2.9 ≤ E < 3.1	5.6	5.8	6.0	-	-	-
3.1 ≤ E < 3.3	5.5	5.7	5.9	6.1	6.4	6.7
3.3 ≤ E < 3.5	5.4	5.6	5.8	6.0	6.3	6.5
3.5 ≤ E < 3.7	5.4	5.5	5.7	5.9	6.1	6.4
3.7 ≤ E < 3.9	5.3	5.5	5.6	5.8	6.0	6.3
3.9 ≤ E < 4.1	5.2	5.4	5.6	5.8	5.9	6.1
4.1 ≤ E < 4.3	5.1	5.3	5.5	5.7	5.9	6.0
4.3 ≤ E < 4.5	5.0	5.2	5.4	5.6	5.8	6.0
4.5 ≤ E < 4.7	5.0	5.1	5.3	5.5	5.7	5.9
4.7 ≤ E < 4.9	4.9	5.1	5.3	5.5	5.6	5.8
E ≥ 4.9	4.9	5.0	5.3	5.4	5.6	5.7

Table 5.9.8-7 Loading Table for PWR Fuel – 1235 W/Assembly (continued)

Minimum Initial Assembly Avg. Enrichment wt % <sup>235</sup> U (E)	Assembly Average Burnup (B) GWd/MTU		
	57< B ≤58	58< B ≤59	59< B ≤60
1.3 ≤ E < 1.5	-	-	-
1.5 ≤ E < 1.7	-	-	-
1.7 ≤ E < 1.9	-	-	-
1.9 ≤ E < 2.1	-	-	-
2.1 ≤ E < 2.3	-	-	-
2.3 ≤ E < 2.5	-	-	-
2.5 ≤ E < 2.7	-	-	-
2.7 ≤ E < 2.9	-	-	-
2.9 ≤ E < 3.1	-	-	-
3.1 ≤ E < 3.3	6.9	7.2	-
3.3 ≤ E < 3.5	6.8	7.0	7.4
3.5 ≤ E < 3.7	6.7	6.9	7.2
3.7 ≤ E < 3.9	6.5	6.8	7.0
3.9 ≤ E < 4.1	6.4	6.7	6.9
4.1 ≤ E < 4.3	6.3	6.5	6.8
4.3 ≤ E < 4.5	6.2	6.4	6.7
4.5 ≤ E < 4.7	6.1	6.3	6.6
4.7 ≤ E < 4.9	6.0	6.2	6.5
E ≥ 4.9	5.9	6.1	6.4

Table 5.9.8-8 Loading Table for PWR Fuel – 1710 W/Assembly

Minimum Initial Assembly Avg. Enrichment wt % <sup>235</sup> U (E)	Assembly Average Burnup (B) GWd/MTU					
	45< B ≤46	46< B ≤47	47< B ≤48	48< B ≤49	49< B ≤50	50< B ≤51
1.3 ≤ E < 1.5	-	-	-	-	-	-
1.5 ≤ E < 1.7	-	-	-	-	-	-
1.7 ≤ E < 1.9	-	-	-	-	-	-
1.9 ≤ E < 2.1	-	-	-	-	-	-
2.1 ≤ E < 2.3	-	-	-	-	-	-
2.3 ≤ E < 2.5	-	-	-	-	-	-
2.5 ≤ E < 2.7	-	-	-	-	-	-
2.7 ≤ E < 2.9	3.4	3.5	3.6	3.7	-	-
2.9 ≤ E < 3.1	3.4	3.5	3.5	3.6	3.7	3.8
3.1 ≤ E < 3.3	3.3	3.4	3.5	3.6	3.6	3.7
3.3 ≤ E < 3.5	3.3	3.4	3.4	3.5	3.6	3.7
3.5 ≤ E < 3.7	3.3	3.3	3.4	3.5	3.5	3.6
3.7 ≤ E < 3.9	3.2	3.3	3.4	3.4	3.5	3.6
3.9 ≤ E < 4.1	3.2	3.3	3.3	3.4	3.5	3.5
4.1 ≤ E < 4.3	3.1	3.2	3.3	3.4	3.4	3.5
4.3 ≤ E < 4.5	3.1	3.2	3.3	3.3	3.4	3.5
4.5 ≤ E < 4.7	3.1	3.2	3.2	3.3	3.4	3.4
4.7 ≤ E < 4.9	3.0	3.1	3.2	3.3	3.4	3.4
E ≥ 4.9	3.0	3.1	3.2	3.2	3.3	3.4



Table 5.9.8-8 Loading Table for PWR Fuel – 1710 W/Assembly (continued)

Minimum Initial Assembly Avg. Enrichment wt % <sup>235</sup> U (E)	Assembly Average Burnup (B) GWd/MTU					
	51< B ≤52	52< B ≤53	53< B ≤54	54< B ≤55	55< B ≤56	56< B ≤57
1.3 ≤ E < 1.5	-	-	-	-	-	-
1.5 ≤ E < 1.7	-	-	-	-	-	-
1.7 ≤ E < 1.9	-	-	-	-	-	-
1.9 ≤ E < 2.1	-	-	-	-	-	-
2.1 ≤ E < 2.3	-	-	-	-	-	-
2.3 ≤ E < 2.5	-	-	-	-	-	-
2.5 ≤ E < 2.7	-	-	-	-	-	-
2.7 ≤ E < 2.9	-	-	-	-	-	-
2.9 ≤ E < 3.1	3.9	4.0	4.0	-	-	-
3.1 ≤ E < 3.3	3.8	3.9	4.0	4.1	4.2	4.3
3.3 ≤ E < 3.5	3.8	3.9	4.0	4.0	4.2	4.3
3.5 ≤ E < 3.7	3.7	3.8	3.9	4.0	4.1	4.2
3.7 ≤ E < 3.9	3.7	3.8	3.8	3.9	4.0	4.2
3.9 ≤ E < 4.1	3.6	3.7	3.8	3.9	4.0	4.1
4.1 ≤ E < 4.3	3.6	3.7	3.8	3.8	3.9	4.0
4.3 ≤ E < 4.5	3.5	3.6	3.7	3.8	3.9	4.0
4.5 ≤ E < 4.7	3.5	3.6	3.7	3.8	3.9	3.9
4.7 ≤ E < 4.9	3.5	3.5	3.6	3.7	3.8	3.9
E ≥ 4.9	3.4	3.5	3.6	3.7	3.8	3.9

Table 5.9.8-8 Loading Table for PWR Fuel – 1710 W/Assembly (continued)

Minimum Initial Assembly Avg. Enrichment wt % <sup>235</sup> U (E)	Assembly Average Burnup (B) GWd/MTU		
	57< B	58< B	59< B
	≤58	≤59	≤60
1.3 ≤ E < 1.5	-	-	-
1.5 ≤ E < 1.7	-	-	-
1.7 ≤ E < 1.9	-	-	-
1.9 ≤ E < 2.1	-	-	-
2.1 ≤ E < 2.3	-	-	-
2.3 ≤ E < 2.5	-	-	-
2.5 ≤ E < 2.7	-	-	-
2.7 ≤ E < 2.9	-	-	-
2.9 ≤ E < 3.1	-	-	-
3.1 ≤ E < 3.3	4.4	4.6	-
3.3 ≤ E < 3.5	4.4	4.5	4.6
3.5 ≤ E < 3.7	4.3	4.4	4.5
3.7 ≤ E < 3.9	4.3	4.4	4.5
3.9 ≤ E < 4.1	4.2	4.3	4.4
4.1 ≤ E < 4.3	4.1	4.2	4.3
4.3 ≤ E < 4.5	4.1	4.2	4.3
4.5 ≤ E < 4.7	4.0	4.1	4.2
4.7 ≤ E < 4.9	4.0	4.1	4.2
E ≥ 4.9	3.9	4.0	4.1

Table 5.9.8-9 Loading Table for PWR Fuel – 788 W/Assembly

Minimum Initial Assembly Avg. Enrichment wt % <sup>235</sup> U (E)	Assembly Average Burnup (B) GWd/MTU					
	45< B ≤46	46< B ≤47	47< B ≤48	48< B ≤49	49< B ≤50	50< B ≤51
1.3 ≤ E < 1.5	-	-	-	-	-	-
1.5 ≤ E < 1.7	-	-	-	-	-	-
1.7 ≤ E < 1.9	-	-	-	-	-	-
1.9 ≤ E < 2.1	-	-	-	-	-	-
2.1 ≤ E < 2.3	-	-	-	-	-	-
2.3 ≤ E < 2.5	-	-	-	-	-	-
2.5 ≤ E < 2.7	-	-	-	-	-	-
2.7 ≤ E < 2.9	9.0	9.7	10.4	11.2	-	-
2.9 ≤ E < 3.1	8.9	9.5	10.1	10.9	11.4	12.2
3.1 ≤ E < 3.3	8.7	9.2	9.9	10.6	11.1	11.9
3.3 ≤ E < 3.5	8.5	9.0	9.7	10.3	10.9	11.6
3.5 ≤ E < 3.7	8.4	8.9	9.5	10.1	10.6	11.4
3.7 ≤ E < 3.9	8.2	8.7	9.3	9.9	10.4	11.1
3.9 ≤ E < 4.1	8.1	8.6	9.1	9.7	10.2	10.9
4.1 ≤ E < 4.3	8.0	8.5	9.0	9.5	10.0	10.7
4.3 ≤ E < 4.5	7.9	8.4	8.8	9.4	9.8	10.5
4.5 ≤ E < 4.7	7.8	8.2	8.7	9.3	9.7	10.3
4.7 ≤ E < 4.9	7.7	8.1	8.6	9.1	9.5	10.2
E ≥ 4.9	7.6	8.0	8.5	9.0	9.4	10.0

Table 5.9.8-9 Loading Table for PWR Fuel – 788 W/Assembly (continued)

Minimum Initial Assembly Avg. Enrichment wt % <sup>235</sup> U (E)	Assembly Average Burnup (B) GWd/MTU					
	51< B ≤52	52< B ≤53	53< B ≤54	54< B ≤55	55< B ≤56	56< B ≤57
1.3 ≤ E < 1.5	-	-	-	-	-	-
1.5 ≤ E < 1.7	-	-	-	-	-	-
1.7 ≤ E < 1.9	-	-	-	-	-	-
1.9 ≤ E < 2.1	-	-	-	-	-	-
2.1 ≤ E < 2.3	-	-	-	-	-	-
2.3 ≤ E < 2.5	-	-	-	-	-	-
2.5 ≤ E < 2.7	-	-	-	-	-	-
2.7 ≤ E < 2.9	-	-	-	-	-	-
2.9 ≤ E < 3.1	13.1	14.0	15.0	-	-	-
3.1 ≤ E < 3.3	12.8	13.6	14.6	15.6	16.6	17.7
3.3 ≤ E < 3.5	12.4	13.3	14.2	15.3	16.2	17.3
3.5 ≤ E < 3.7	12.1	13.0	13.9	14.9	15.9	16.9
3.7 ≤ E < 3.9	11.9	13.0	13.6	14.6	15.5	16.5
3.9 ≤ E < 4.1	11.6	12.5	13.3	14.2	15.2	16.2
4.1 ≤ E < 4.3	11.4	12.2	13.1	13.9	14.9	15.9
4.3 ≤ E < 4.5	11.3	11.9	12.8	13.7	14.7	15.6
4.5 ≤ E < 4.7	11.1	11.8	12.6	13.5	14.4	15.3
4.7 ≤ E < 4.9	10.9	11.6	12.4	13.3	14.1	15.1
E ≥ 4.9	10.7	11.5	12.6	13.1	13.9	14.8

Table 5.9.8-9 Loading Table for PWR Fuel – 788 W/Assembly (continued)

Minimum Initial Assembly Avg. Enrichment wt % <sup>235</sup> U (E)	Assembly Average Burnup (B) GWd/MTU		
	57< B ≤58	58< B ≤59	59< B ≤60
1.3 ≤ E < 1.5	-	-	-
1.5 ≤ E < 1.7	-	-	-
1.7 ≤ E < 1.9	-	-	-
1.9 ≤ E < 2.1	-	-	-
2.1 ≤ E < 2.3	-	-	-
2.3 ≤ E < 2.5	-	-	-
2.5 ≤ E < 2.7	-	-	-
2.7 ≤ E < 2.9	-	-	-
2.9 ≤ E < 3.1	-	-	-
3.1 ≤ E < 3.3	18.7	19.7	-
3.3 ≤ E < 3.5	18.2	19.3	20.4
3.5 ≤ E < 3.7	17.9	18.9	19.9
3.7 ≤ E < 3.9	17.5	18.6	19.6
3.9 ≤ E < 4.1	17.2	18.2	19.2
4.1 ≤ E < 4.3	16.9	17.9	18.9
4.3 ≤ E < 4.5	16.6	17.6	18.6
4.5 ≤ E < 4.7	16.3	17.3	18.3
4.7 ≤ E < 4.9	16.0	17.0	18.0
E ≥ 4.9	15.8	16.8	17.8

### **5.9.9      Damaged Fuel**

Damaged PWR fuel assemblies may be loaded in damaged fuel cans in the four corner assembly locations of the PWR damaged fuel basket. DFC slots are locations 4, 8, 30 and 34 in Figure 5.9.9-1. To ensure that the worst case configuration is considered, two damaged fuel scenarios are evaluated. Damaged fuel includes fuel debris.

The first scenario assumes the damaged fuel collects over the active fuel length of the fuel assembly. This scenario is modeled by filling the fuel assembly interstitial volume with  $\text{UO}_2$  and increasing the fuel neutron, gamma and n-gamma source consistent with this increase in mass.

In the second scenario, damaged fuel is assumed to migrate from the active fuel into the lower end fitting region of the fuel assembly, filling all the modeled void space. However, no credit is taken for the reduction in lower end fitting hardware dose rate due to the added  $\text{UO}_2$  mass and self-shielding nor for the reduction in fuel mass migrated from the active fuel region.

The resulting material compositions are shown in Table 5.9.9-1 for WE 14×14 (14b) PWR fuel.

In the model, no credit is taken for the thicker plates in the corner locations of the damaged fuel basket or the thickness of the damaged fuel cans themselves.

The 1.8 kW preferential loading is also evaluated under both damaged fuel scenarios. Only zone C, where the damaged fuel is located, needs to be evaluated under the damaged fuel scenarios.

The four-zone preferential loading damaged fuel dose rates are statistically unchanged or less than the uniform loading damaged fuel dose rates.

#### **5.9.9.1      Transfer Cask Dose Rates**

As the reduction in minimum cool time has no impact on the bounding source terms of the stainless steel MTC, no additional uniform loading damaged fuel evaluations are run for the MTC. See Section 5.8.12 for the uniformly loaded MTC damaged fuel evaluation.

##### **5.9.9.1.1      Preferential Loading Active Fuel Scenario - MTC**

Transfer cask dose rates are computed using the bounding fuel assembly source terms from Section 5.9.6 for the first scenario (fuel material filling void space at the active fuel region elevation).

On the radial and bottom surfaces of the cask, the damaged PWR fuel results are greater than those in Section 5.9.6. In order to compare the radial and bottom results to the lower nozzle scenario, the remaining source regions and BPRA results are added to the surface dose rates resulting in maximum dose rates of 1,029 mrem/hr and 5,740 mrem/hr, respectively. The radial

surface dose rate is greater than the lower nozzle scenario maximum dose rate of 952 mrem/hr. The bottom surface dose rate is less than the lower nozzle scenario maximum dose rate of 5,969 mrem/hr.

#### **5.9.9.1.2 Preferential Loading Lower End Fitting Scenario - MTC**

Transfer cask dose rates are computed using the bounding fuel assemblies from Section 5.9.6 for the second scenario.

Damaged fuel maximum dose rates are greater than those in Section 5.9.6. Dose rates are summarized in Table 5.9.9-2.

#### **5.9.9.2 CC4 Dose Rates**

As only the CC4 radial bounding source term was affected by the decrease in minimum cool time, only the uniformly loaded CC4 radial detector is evaluated with damaged fuel in this section. Section 5.8.12 contains the damaged fuel results for the remaining detectors. The 1.8 kW four zone preferential pattern is evaluated under both damaged fuel scenarios.

##### **5.9.9.2.1 Uniform Loading Active Fuel Scenario – CC4**

Uniformly loaded CC4 dose rates are computed using the bounding fuel assembly source terms from Section 5.9.3 for the first scenario. At the radial surface of the cask, maximum and average dose rates for the damaged PWR fuel model are statistically equivalent to those of the undamaged fuel model.

##### **5.9.9.2.2 Uniform Loading Lower End Fitting Scenario – CC4**

Uniformly loaded CC4 dose rates are computed using the bounding fuel assemblies from Section 5.9.3 for the second scenario. Damaged fuel maximum radial dose rates are statistically unchanged from those in Section 5.9.4.1. Dose rates are summarized in Table 5.9.9-3.

##### **5.9.9.2.3 Preferential Loading Active Fuel Scenario – CC4**

Preferentially loaded CC4 dose rates are computed using the bounding fuel assembly source terms from Section 5.9.6 for the first scenario. At the radial and inlet surfaces of the cask, maximum and average dose rates for the damaged PWR fuel model are slightly higher than those of the undamaged fuel model. All preferentially loaded CC4 damaged fuel dose rates remain below the dose rates of the uniformly loaded CC4 damaged fuel dose rates.

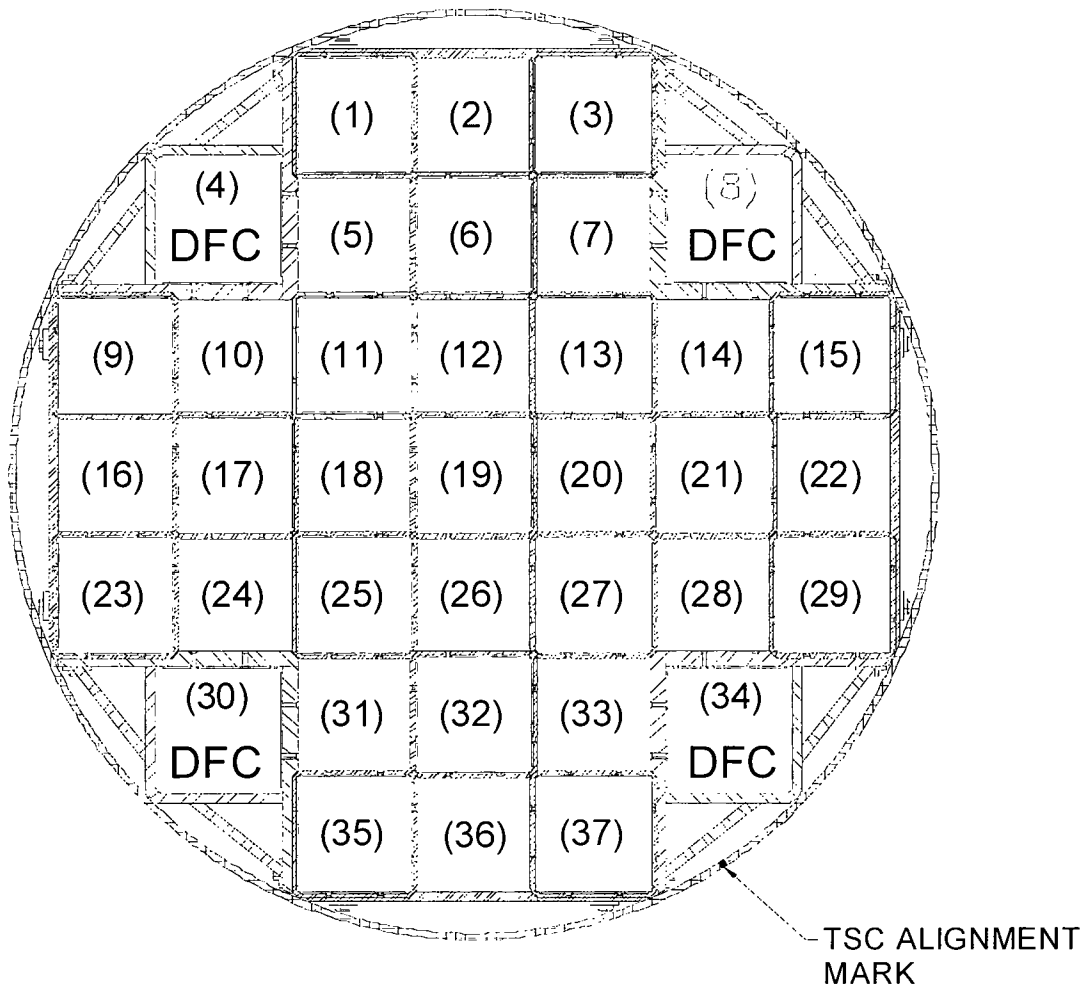
##### **5.9.9.2.4 Preferential Loading Lower End Fitting Scenario – CC4**

CC4 dose rates are computed using the bounding fuel assemblies from Section 5.9.6 for the second scenario. There is no change in radial dose rates from the damaged fuel in the lower end fitting region. There is an 8.5 mrem/hr increase in inlet dose rate from damaged fuel in the lower end fitting region of the four damaged fuel can basket. Inlet dose rates are increased for the

preferentially loaded CC4 damaged fuel but are bounded by the uniformly loaded CC4 damaged fuel dose rates. Dose rates are summarized in Table 5.9.9-4.



Figure 5.9.9-1 Schematic of DF Basket Assembly Configuration for PWR SNF with DFCs



DFC designated locations may contain a loaded DFC or a PWR UNDAMAGED SNF ASSEMBLY.

Table 5.9.9-1 Damaged Fuel Material Summary – 14b PWR Fuel

Material	Element/ Isotope	Density [atom/-b-cm]	Density [g/cm <sup>3</sup> ]
Damaged Fuel (Lower Nozzle)	Chromium	5.5169E-03	9.6315
	Manganese	5.4963E-04	
	Iron	1.8789E-02	
	Nickel	2.4436E-03	
	Uranium 235	8.0452E-04	
	Uranium 238	1.5093E-02	
	Oxygen	3.1786E-02	
Damaged Fuel (Active Fuel)	Zirconium	3.6954E-03	9.8635
	Chromium	6.6005E-06	
	Tin	4.3366E-05	
	Nitrogen	1.2255E-05	
	Iron	7.6817E-06	
	Uranium 235	1.0495E-03	
	Uranium 238	1.9688E-02	
	Oxygen	4.1462E-02	

Table 5.9.9-2 Preferentially Loaded Stainless Steel MTC Maximum Damaged Fuel Dose Rates

Detector	Source	Surface		1 meter	
		mrem/hr	FSD <sup>a</sup>	mrem/hr	FSD
Radial	Neutron	231	0.2%	82	0.2%
	Gamma	734	2.2%	318	1.2%
	BPRA	64	2.2%	29	1.2%
	Total	1029	1.6%	429	0.9%
Bottom	Undamaged	5630	0.6%	2402	0.9%
	BPRA	79	1.8%	43	1.9%
	Damaged Neutron	85	0.2%	25	0.3%
	Damaged Gamma	175	9.7%	95	8.3%
	Total	5969	0.6%	2565	0.9%

<sup>a</sup> Fractional standard deviation.

Table 5.9.9-3 Uniformly Loaded CC4 Maximum Damaged PWR Fuel Dose Rates

Detector	Source	Surface		1 meter	
		mrem/hr	FSD	mrem/hr	FSD
Radial	Undamaged	107.2	1.9%	55.2	1.4%
	BPRA	6.6	0.8%	3.30	0.53%
	Damaged Neutron	< 0.1	3.0%	< 0.1	0.9%
	Damaged Gamma	< 0.1	14.8%	0.1	3.9%
	Total	113.9	1.8%	58.6	1.3%

Table 5.9.9-4 Preferentially Loaded CC4 Maximum Damaged PWR Fuel Dose Rates

Detector	Source	Surface		1 meter	
		mrem/hr	FSD	mrem/hr	FSD
Radial	Neutron	0.4	2.0%	0.2	1.3%
	Gamma	105.8	2.2%	55.0	1.5%
	BPRA	6.5	1.1%	3.3	0.7%
	Total	112.7	2.1%	58.5	1.4%
Inlet	Undamaged	103.7	1.0%	14.1	2.1%
	BPRA	8.7	3.5%	1.3	5.7%
	Damaged Neutron	2.5	0.5%	0.3	1.2%
	Damaged Gamma	6.0	5.3%	0.5	12.7%
	Total	120.9	0.9%	16.2	1.9%

#### 5.10 CE16 Four-Zone Preferential Heat Load Pattern Shielding Evaluation Detail

This section contains evaluation detail for Combustion Engineering 16x16 fuel assemblies with a minimum cool time of 4 years loaded in the CC and carbon steel MTC. The carbon steel MTC evaluation bounds the stainless steel MTC configuration as stainless steel has a higher density and therefore has more shielding. The CC model is that of the standard shielded concrete cask detailed in Section 5.5. This section includes four-zone preferential heat load pattern with a maximum assembly heat load of 1.8 kW. Evaluations are documented for undamaged and damaged fuel. The minimum cool time for the CE 16x16 CEAs was reduced to 5 years from the previous minimum cool time of 10 years.

Evaluation methods and models are based on those described in Section 5.9

Uniform heat load evaluations at a minimum cool time of 4 years are included in Section 5.8.3. Preferential loading for heat load is discussed in Section 5.10.3. The effects of nonfuel hardware components to dose rates and heat load are discussed in Section 5.10.4. Model differences, dose rates, and minimum loading time impacts resulting from the damaged fuel basket configuration are discussed in Section 5.10.5.

**5.10.1      Contents Description**

As described in Section 5.2, PWR fuel assemblies were surveyed to construct hybrids containing maximum fuel and hardware masses. Section 5.8.1 contains geometry data of the CE 16x16 hybrid used in this evaluation. Sample in-core characteristics are also contained in Section 5.8.1.

#### **5.10.2      Response Function Method**

The evaluation of CE 16x16 fuel in the four-zone preferential loading in the CC and MTC use the response function method described in Section 5.8.2.

Section 5.8.2 demonstrates the applicability of the response method to determine the dose rates of the MAGNASTOR concrete cask and transfer cask systems.

### 5.10.3 Preferential Loading of CE 16x16 Fuel at a Minimum Cool time of 4 Years

The four-zone preferential loading pattern and method from Section 5.9 is used here to evaluate CE 16x16 fuel with a minimum cool time of 4 years. The four-zone preferential loading pattern is as follows.

Zone Description	Designator	Heat Load [W/assy]	# Assemblies
Inner Ring	A	513	9
Middle Ring	B1	1,300	8
	B2	1,800	4
Outer Ring	C	830	16

A sketch of the PWR basket and loading pattern is shown in Figure 5.10.3-1.

Preferential and uniform loading patterns limit total cask heat load to 35.5 kW. With the exception of the CC outlet, the maximum dose rates for the preferential loading pattern are less than those calculated for a uniform pattern.

Minimum cool time tables for CE 16x16 in the preferential heat load pattern are included in Section 5.10.6. The method used for the preferential loading pattern shielding evaluations is identical to those in Section 5.9 with the exception of the reduction in minimum cool time.

#### 5.10.3.1 MTC and CC Dose Rates

Maximum and average surface dose rates for the preferential pattern are shown in Table 5.10.3-1, with the corresponding limiting results for the uniform pattern. The maximum dose rates for the analyzed preferential loading pattern are less than or statistically unchanged from those calculated for a uniform pattern at each detector surface for both casks with the exception of CC outlet dose rates. Maximum CC outlet dose rates are increased minimally (7%).

The concrete cask radial and top axial average dose rates are less than or statistically unchanged in the preferential pattern. Therefore, using the uniform pattern to characterize the restricted area and controlled area boundaries is acceptable.

Table 5.10.3-1 Preferential Pattern Dose Rate Results

Cask / Dose Location	Uniform <sup>a</sup>		Preferential	
	Avg. Dose Rate (mrem/hr)	Max. Dose Rate (mrem/hr)	Avg. Dose Rate (mrem/hr)	Max. Dose Rate (mrem/hr)
Carbon Steel MTC Radial	650	939	574.5	899.1
Carbon Steel MTC Top	172	451	190	430.0
Carbon Steel MTC Bottom	2,953	5,824	2,717	5,747
Standard Shield CC Radial	54.4	76.7	49.1	65.1
Standard Shield CC Top	82.3	378	75.7	366.3
Standard Shield CC Inlet	--	425	--	377.1
Standard Shield CC Outlet	--	38.3	--	41.1

<sup>a</sup> Bounding uniform dose rates from Section 5.8.3.3.1 and Section 5.8.3.4.1



#### 5.10.4 Nonfuel Hardware Component – Reactor Control Elements

Reactor control elements (e.g., CEAs and RCCAs) are evaluated using methods from Section 5.8.6 with the minimum cool time of the CEA reduced to 5 years.

Results are shown in Table 5.10.4-1. On the sides of the concrete and transfer casks, the additive dose rate does not affect the maximum dose rates. At the concrete cask inlets and transfer cask bottom, loading of CEAs statistically significantly increases the maximum dose rates. Dose rate increases are significantly below those listed in Section 5.8.6.

The maximum decay heat produced by loading a single CEA is 6.8 W. An increase in assembly cool time to accommodate loading a CEA is shown in Table 5.10.4-2 for each assembly heat load limit. As an increase in cool time will also decrease the fuel source term, the strict application of increased cool time without a recalculation of fuel dose rates is conservative.

**Table 5.10.4-1 CEA Dose Rate Contributions – CE 16x16**

Cask / Dose Location	Maximum Dose (mrem/hr)	Average Dose (mrem/hr)
Carbon Steel Transfer Cask Radial	0.4	< 0.1
Carbon Steel Transfer Cask Bottom	396.6	131.3
CC Radial	0.5	< 0.1
CC Inlet	3.7	--

**Table 5.10.4-2 Additional Assembly Cool Time (Years) Required to Load CEA**

Zone:	A	B1	B2	C	Uniform
Additional Assy Cool Time:	0.8	0.1	0.1	0.4	0.3

#### 5.10.5 Damaged Fuel

CE 16x16 damaged fuel in the four-zone preferentially loaded CC and MTC systems are evaluated in this section using the methods described in Section 5.9.9. Damaged PWR fuel assemblies may be loaded in damaged fuel cans in the four corner assembly locations of the PWR damaged fuel basket. DFC slots are locations 4, 8, 30 and 34 in Figure 5.10.5-1. The damaged fuel scenarios evaluated for the CE16x16 preferential heat load pattern evaluated are those described in Section 5.8.12.

The first scenario assumes the damaged fuel collects over the active fuel length of the fuel assembly. In the second scenario, damaged fuel is assumed to migrate from the active fuel into the lower end fitting region of the fuel assembly, filling all the modeled void space. For the preferentially loaded CE 16x16 fuel the second scenario produces bounding dose rates for all detectors.

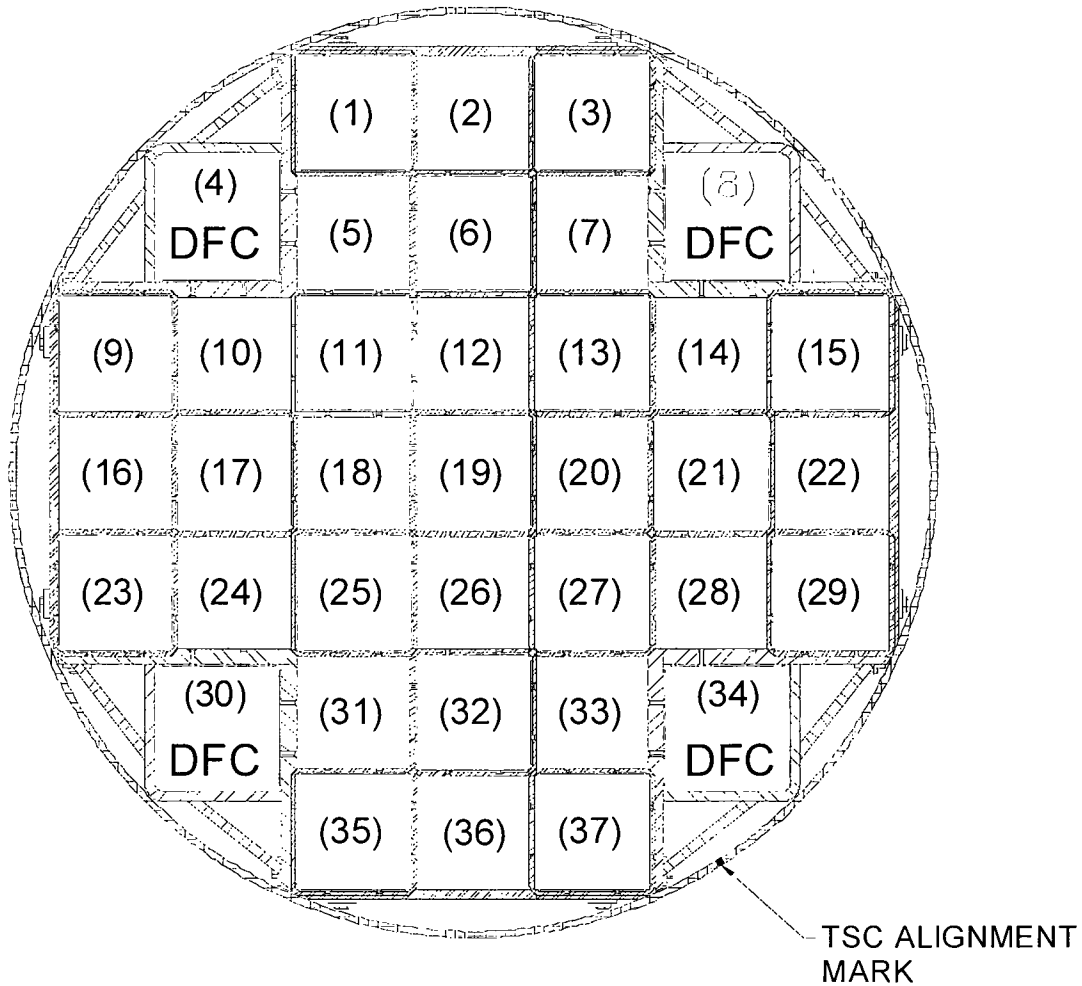
In the model, no credit is taken for the thicker plates in the corner locations of the damaged fuel basket or the thickness of the damaged fuel cans themselves.

Only zone C, where the damaged fuel is located, needs to be reevaluated under the damaged fuel scenarios. Heat load allowed in the peripheral basket locations, including DFC locations, of the preferential heat load configuration is less than that of the uniform pattern. The incremental effect of the damaged fuel in the preferential loaded pattern will therefore be less than that of the uniformly loaded basket.

The results for the preferentially loaded carbon steel MTC with damaged fuel are listed in Table 5.10.5-1. The results for the preferentially loaded CC with damaged fuel are listed in Table 5.10.5-2.

The CE 16x16 four-zone preferential loading damaged fuel dose rates are statistically unchanged or less than the bounding damaged fuel dose rates in Section 5.8.12.

Figure 5.10.5-1 Schematic of DF Basket Assembly Configuration for PWR SNF with DFCs



DFC designated locations may contain a loaded DFC or a PWR UNDAMAGED SNF ASSEMBLY.

**Table 5.10.5-1 Preferentially Loaded Carbon Steel MTC Maximum Damaged CE16  
Fuel Dose Rates**

Detector	Source	Surface		1 meter	
		mrem/hr	FSD <sup>a</sup>	mrem/hr	FSD
Radial	Undamaged	899.1	0.8%	275.7	0.2%
	Damaged Neutron	11.2	1.3%	0.1	4.7%
	Damaged Gamma	63.4	6.9%	0.5	18.9%
	Total	973.7	0.8%	276.3	0.2%
Bottom	Undamaged	5,745	0.8%	2,407	1.0 %
	Damaged Neutron	118	2.2%	35	4.4%
	Damaged Gamma	183	8.7%	90	7.4%
	Total	6,046	0.8%	2,532	1.0%

<sup>a</sup> Fractional standard deviation.

Table 5.10.5-2 Preferentially Loaded CC Maximum Damaged CE16 Fuel Dose Rates

Detector	Source	Surface		1 meter	
		mrem/hr	FSD	mrem/hr	FSD
Radial	Undamaged	65.1	1.5%	32.1	1.6%
	Damaged Neutron	0.2	0.2%	0.1	0.3%
	Damaged Gamma	5.4	4.7%	2.1	5.6%
	Total	70.7	1.4%	34.3	1.5%
Inlet	Undamaged	379.2	0.8%	64.01	1.3%
	Damaged Neutron	4.3	0.7%	0.61	1.7%
	Damaged Gamma	36.8	2.5%	6.44	3.9%
	Total	420.3	0.8%	7.05	3.6%

### 5.10.6 Cool-Time Tables

PWR system performance is evaluated for a cask heat load of 35.5 kW with a four-zone preferential (1.8 kW max) heat load pattern. Minimum cool times are summarized for the preferential heat load pattern.

Allowed low burnup (up to 30,000 MWd/MTU) fuel loadings are shown in Table 5.8.9-1. Note that the listed minimum cool times at each burnup step are bounding for all fuel types and initial enrichments above the minimum enrichment specified. Collapsing the fuel type and initial enrichment-dependent minimum cool time matrix to a single value may result in a minimum cool time longer than individual values presented for higher burnups in the detailed tables that follow.

The minimum cool time tables account for potential uncertainties in the source generation abilities of SAS2H at burnups greater than 45 GWd/MTU by reducing allowed heat loads by 5 percent. Fuel assembly loading tables at greater than 45 GWd/MTU are, therefore, generated for a cask heat load of 33.725 kW with preferential (1.71 kW max) heat load patterns.

The 5% penalty adjusted four-zone preferential loading pattern is as follows.

Zone Description	Designator	Heat Load [W/assy]	Adjusted Heat Load [W/assy]	# Assemblies
Inner Ring	A	513	487	9
Middle Ring	B1	1300	1235	8
	B2	1800	1710	4
Outer Ring	C	830	788	16

Table 5.10.6-1 through Table 5.10.6-4 contain the minimum cool times for the preferential loading of  $\leq 45$  GWd/MTU with higher burnup fuel cool times listed in Table 5.10.6-5 through Table 5.10.6-8. Section 5.8.9 contains the minimum cool times for a uniform heat load of 959 W/assy.

Decay heat associated with loading nonfuel components requires an increase in the minimum fuel assembly cool time. The incremental cool time increase to allow loading of the CE 16x16 CEAs with a minimum cool time of 5 years is shown in Table 5.10.4-2.

Table 5.10.6-1 Loading Table for CE 16x16 Fuel – 513 W/Assembly

Minimum Initial Assembly Avg. Enrichment wt % <sup>235</sup> U (E)	Assembly Average Burnup (B) GWd/MTU					
	B ≤10	10< B ≤15	15< B ≤20	20< B ≤25	25< B ≤30	30< B ≤32.5
1.3 ≤ E < 1.5	4.0	-	-	-	-	-
1.5 ≤ E < 1.7	4.0	4.0	-	-	-	-
1.7 ≤ E < 1.9	4.0	4.0	4.9	-	-	-
1.9 ≤ E < 2.1	4.0	4.0	4.8	6.1	-	-
2.1 ≤ E < 2.3	4.0	4.0	4.8	6.0	8.2	10.0
2.3 ≤ E < 2.5	4.0	4.0	4.7	6.0	8.1	9.9
2.5 ≤ E < 2.7	4.0	4.0	4.7	6.0	8.1	9.8
2.7 ≤ E < 2.9	4.0	4.0	4.7	5.9	8.0	9.7
2.9 ≤ E < 3.1	4.0	4.0	4.6	5.9	7.9	9.6
3.1 ≤ E < 3.3	4.0	4.0	4.6	5.9	7.9	9.5
3.3 ≤ E < 3.5	4.0	4.0	4.6	5.8	7.9	9.4
3.5 ≤ E < 3.7	4.0	4.0	4.6	5.8	7.8	9.4
3.7 ≤ E < 3.9	4.0	4.0	4.5	5.8	7.8	9.3
3.9 ≤ E < 4.1	4.0	4.0	4.5	5.8	7.7	9.2
4.1 ≤ E < 4.3	4.0	4.0	4.5	5.8	7.7	9.2
4.3 ≤ E < 4.5	4.0	4.0	4.5	5.7	7.7	9.2
4.5 ≤ E < 4.7	4.0	4.0	4.5	5.7	7.6	9.1
4.7 ≤ E < 4.9	4.0	4.0	4.5	5.7	7.6	9.1
E ≥ 4.9	4.0	4.0	4.5	5.7	7.6	9.0

Table 5.10.6-1 Loading Table for CE 16x16 Fuel – 513 W/Assembly (continued)

Minimum Initial Assembly Avg. Enrichment wt % <sup>235</sup> U (E)	Assembly Average Burnup (B) GWd/MTU					
	32.5< B ≤35	35< B ≤37.5	37.5< B ≤40	40< B ≤41	41< B ≤42	42< B ≤43
1.3 ≤ E < 1.5	-	-	-	-	-	-
1.5 ≤ E < 1.7	-	-	-	-	-	-
1.7 ≤ E < 1.9	-	-	-	-	-	-
1.9 ≤ E < 2.1	-	-	-	-	-	-
2.1 ≤ E < 2.3	-	-	-	-	-	-
2.3 ≤ E < 2.5	12.5	15.8	-	-	-	-
2.5 ≤ E < 2.7	12.3	15.6	19.2	20.7	22.2	23.7
2.7 ≤ E < 2.9	12.1	15.4	19.0	20.5	22.0	23.4
2.9 ≤ E < 3.1	12.0	15.2	18.8	20.2	21.7	23.2
3.1 ≤ E < 3.3	11.9	15.0	18.5	19.9	21.5	23.0
3.3 ≤ E < 3.5	11.8	14.8	18.4	19.8	21.3	22.8
3.5 ≤ E < 3.7	11.7	14.7	18.2	19.7	21.1	22.5
3.7 ≤ E < 3.9	11.7	14.6	18.0	19.5	20.9	22.3
3.9 ≤ E < 4.1	11.6	14.5	17.9	19.3	20.8	22.2
4.1 ≤ E < 4.3	11.5	14.4	17.8	19.2	20.7	22.1
4.3 ≤ E < 4.5	11.4	14.3	17.7	19.1	20.5	21.9
4.5 ≤ E < 4.7	11.4	14.3	17.6	19.0	20.4	21.8
4.7 ≤ E < 4.9	11.4	14.2	17.5	18.9	20.3	21.7
E ≥ 4.9	11.3	14.1	17.4	18.8	20.2	21.6



Table 5.10.6-1 Loading Table for CE 16x16 Fuel – 513 W/Assembly (continued)

Minimum Initial Assembly Avg. Enrichment wt % <sup>235</sup> U (E)	Assembly Average Burnup (B) GWd/MTU	
	43< B ≤44	44< B ≤45
1.3 ≤ E < 1.5	-	-
1.5 ≤ E < 1.7	-	-
1.7 ≤ E < 1.9	-	-
1.9 ≤ E < 2.1	-	-
2.1 ≤ E < 2.3	-	-
2.3 ≤ E < 2.5	-	-
2.5 ≤ E < 2.7	25.1	-
2.7 ≤ E < 2.9	24.8	26.3
2.9 ≤ E < 3.1	24.6	26.1
3.1 ≤ E < 3.3	24.4	25.8
3.3 ≤ E < 3.5	24.2	25.6
3.5 ≤ E < 3.7	24.0	25.4
3.7 ≤ E < 3.9	23.8	25.3
3.9 ≤ E < 4.1	23.7	25.0
4.1 ≤ E < 4.3	23.6	24.9
4.3 ≤ E < 4.5	23.4	24.8
4.5 ≤ E < 4.7	23.2	24.6
4.7 ≤ E < 4.9	23.1	24.5
E ≥ 4.9	23.0	24.4

Table 5.10.6-2 Loading Table for CE 16x16 Fuel – 1,300 W/Assembly

Minimum Initial Assembly Avg. Enrichment wt % <sup>235</sup> U (E)	Assembly Average Burnup (B) GWd/MTU					
	B ≤10	10< B ≤15	15< B ≤20	20< B ≤25	25< B ≤30	30< B ≤32.5
1.3 ≤ E < 1.5	4.0	-	-	-	-	-
1.5 ≤ E < 1.7	4.0	4.0	-	-	-	-
1.7 ≤ E < 1.9	4.0	4.0	4.0	-	-	-
1.9 ≤ E < 2.1	4.0	4.0	4.0	4.0	-	-
2.1 ≤ E < 2.3	4.0	4.0	4.0	4.0	4.0	4.0
2.3 ≤ E < 2.5	4.0	4.0	4.0	4.0	4.0	4.0
2.5 ≤ E < 2.7	4.0	4.0	4.0	4.0	4.0	4.0
2.7 ≤ E < 2.9	4.0	4.0	4.0	4.0	4.0	4.0
2.9 ≤ E < 3.1	4.0	4.0	4.0	4.0	4.0	4.0
3.1 ≤ E < 3.3	4.0	4.0	4.0	4.0	4.0	4.0
3.3 ≤ E < 3.5	4.0	4.0	4.0	4.0	4.0	4.0
3.5 ≤ E < 3.7	4.0	4.0	4.0	4.0	4.0	4.0
3.7 ≤ E < 3.9	4.0	4.0	4.0	4.0	4.0	4.0
3.9 ≤ E < 4.1	4.0	4.0	4.0	4.0	4.0	4.0
4.1 ≤ E < 4.3	4.0	4.0	4.0	4.0	4.0	4.0
4.3 ≤ E < 4.5	4.0	4.0	4.0	4.0	4.0	4.0
4.5 ≤ E < 4.7	4.0	4.0	4.0	4.0	4.0	4.0
4.7 ≤ E < 4.9	4.0	4.0	4.0	4.0	4.0	4.0
E ≥ 4.9	4.0	4.0	4.0	4.0	4.0	4.0

Table 5.10.6-2 Loading Table for CE 16x16 Fuel – 1,300 W/Assembly (continued)

Minimum Initial Assembly Avg. Enrichment wt % <sup>235</sup> U (E)	Assembly Average Burnup (B) GWd/MTU					
	32.5< B ≤35	35< B ≤37.5	37.5< B ≤40	40< B ≤41	41< B ≤42	42< B ≤43
1.3 ≤ E < 1.5	-	-	-	-	-	-
1.5 ≤ E < 1.7	-	-	-	-	-	-
1.7 ≤ E < 1.9	-	-	-	-	-	-
1.9 ≤ E < 2.1	-	-	-	-	-	-
2.1 ≤ E < 2.3	-	-	-	-	-	-
2.3 ≤ E < 2.5	4.0	4.0	-	-	-	-
2.5 ≤ E < 2.7	4.0	4.0	4.1	4.2	4.3	4.5
2.7 ≤ E < 2.9	4.0	4.0	4.1	4.2	4.3	4.4
2.9 ≤ E < 3.1	4.0	4.0	4.0	4.1	4.2	4.4
3.1 ≤ E < 3.3	4.0	4.0	4.0	4.1	4.2	4.3
3.3 ≤ E < 3.5	4.0	4.0	4.0	4.0	4.1	4.3
3.5 ≤ E < 3.7	4.0	4.0	4.0	4.0	4.1	4.2
3.7 ≤ E < 3.9	4.0	4.0	4.0	4.0	4.0	4.2
3.9 ≤ E < 4.1	4.0	4.0	4.0	4.0	4.0	4.1
4.1 ≤ E < 4.3	4.0	4.0	4.0	4.0	4.0	4.1
4.3 ≤ E < 4.5	4.0	4.0	4.0	4.0	4.0	4.0
4.5 ≤ E < 4.7	4.0	4.0	4.0	4.0	4.0	4.0
4.7 ≤ E < 4.9	4.0	4.0	4.0	4.0	4.0	4.0
E ≥ 4.9	4.0	4.0	4.0	4.0	4.0	4.0

Table 5.10.6-2 Loading Table for CE 16x16 Fuel – 1,300 W/Assembly (continued)

Minimum Initial Assembly Avg. Enrichment wt % <sup>235</sup> U (E)	Assembly Average Burnup (B) GWd/MTU	
	43< B ≤44	44< B ≤45
1.3 ≤ E < 1.5	-	-
1.5 ≤ E < 1.7	-	-
1.7 ≤ E < 1.9	-	-
1.9 ≤ E < 2.1	-	-
2.1 ≤ E < 2.3	-	-
2.3 ≤ E < 2.5	-	-
2.5 ≤ E < 2.7	4.6	-
2.7 ≤ E < 2.9	4.5	4.7
2.9 ≤ E < 3.1	4.5	4.6
3.1 ≤ E < 3.3	4.4	4.5
3.3 ≤ E < 3.5	4.4	4.5
3.5 ≤ E < 3.7	4.3	4.4
3.7 ≤ E < 3.9	4.3	4.4
3.9 ≤ E < 4.1	4.2	4.3
4.1 ≤ E < 4.3	4.2	4.3
4.3 ≤ E < 4.5	4.2	4.3
4.5 ≤ E < 4.7	4.1	4.2
4.7 ≤ E < 4.9	4.1	4.2
E ≥ 4.9	4.0	4.2

Table 5.10.6-3 Loading Table for CE 16x16 Fuel – 1,800 W/Assembly

Minimum Initial Assembly Avg. Enrichment wt % <sup>235</sup> U (E)	Assembly Average Burnup (B) GWd/MTU					
	B ≤10	10< B ≤15	15< B ≤20	20< B ≤25	25< B ≤30	30< B ≤32.5
1.3 ≤ E < 1.5	4.0	-	-	-	-	-
1.5 ≤ E < 1.7	4.0	4.0	-	-	-	-
1.7 ≤ E < 1.9	4.0	4.0	4.0	-	-	-
1.9 ≤ E < 2.1	4.0	4.0	4.0	4.0	-	-
2.1 ≤ E < 2.3	4.0	4.0	4.0	4.0	4.0	4.0
2.3 ≤ E < 2.5	4.0	4.0	4.0	4.0	4.0	4.0
2.5 ≤ E < 2.7	4.0	4.0	4.0	4.0	4.0	4.0
2.7 ≤ E < 2.9	4.0	4.0	4.0	4.0	4.0	4.0
2.9 ≤ E < 3.1	4.0	4.0	4.0	4.0	4.0	4.0
3.1 ≤ E < 3.3	4.0	4.0	4.0	4.0	4.0	4.0
3.3 ≤ E < 3.5	4.0	4.0	4.0	4.0	4.0	4.0
3.5 ≤ E < 3.7	4.0	4.0	4.0	4.0	4.0	4.0
3.7 ≤ E < 3.9	4.0	4.0	4.0	4.0	4.0	4.0
3.9 ≤ E < 4.1	4.0	4.0	4.0	4.0	4.0	4.0
4.1 ≤ E < 4.3	4.0	4.0	4.0	4.0	4.0	4.0
4.3 ≤ E < 4.5	4.0	4.0	4.0	4.0	4.0	4.0
4.5 ≤ E < 4.7	4.0	4.0	4.0	4.0	4.0	4.0
4.7 ≤ E < 4.9	4.0	4.0	4.0	4.0	4.0	4.0
E ≥ 4.9	4.0	4.0	4.0	4.0	4.0	4.0

Table 5.10.6-3 Loading Table for CE 16x16 Fuel – 1,800 W/Assembly (continued)

Minimum Initial Assembly Avg. Enrichment wt % <sup>235</sup> U (E)	Assembly Average Burnup (B) GWd/MTU					
	32.5< B ≤35	35< B ≤37.5	37.5< B ≤40	40< B ≤41	41< B ≤42	42< B ≤43
1.3 ≤ E < 1.5	-	-	-	-	-	-
1.5 ≤ E < 1.7	-	-	-	-	-	-
1.7 ≤ E < 1.9	-	-	-	-	-	-
1.9 ≤ E < 2.1	-	-	-	-	-	-
2.1 ≤ E < 2.3	-	-	-	-	-	-
2.3 ≤ E < 2.5	4.0	4.0	-	-	-	-
2.5 ≤ E < 2.7	4.0	4.0	4.0	4.0	4.0	4.0
2.7 ≤ E < 2.9	4.0	4.0	4.0	4.0	4.0	4.0
2.9 ≤ E < 3.1	4.0	4.0	4.0	4.0	4.0	4.0
3.1 ≤ E < 3.3	4.0	4.0	4.0	4.0	4.0	4.0
3.3 ≤ E < 3.5	4.0	4.0	4.0	4.0	4.0	4.0
3.5 ≤ E < 3.7	4.0	4.0	4.0	4.0	4.0	4.0
3.7 ≤ E < 3.9	4.0	4.0	4.0	4.0	4.0	4.0
3.9 ≤ E < 4.1	4.0	4.0	4.0	4.0	4.0	4.0
4.1 ≤ E < 4.3	4.0	4.0	4.0	4.0	4.0	4.0
4.3 ≤ E < 4.5	4.0	4.0	4.0	4.0	4.0	4.0
4.5 ≤ E < 4.7	4.0	4.0	4.0	4.0	4.0	4.0
4.7 ≤ E < 4.9	4.0	4.0	4.0	4.0	4.0	4.0
E ≥ 4.9	4.0	4.0	4.0	4.0	4.0	4.0

Table 5.10.6-3 Loading Table for CE 16x16 Fuel – 1,800 W/Assembly (continued)

Minimum Initial Assembly Avg. Enrichment wt % <sup>235</sup> U (E)	Assembly Average Burnup (B) GWd/MTU	
	43< B ≤44	44< B ≤45
1.3 ≤ E < 1.5	-	-
1.5 ≤ E < 1.7	-	-
1.7 ≤ E < 1.9	-	-
1.9 ≤ E < 2.1	-	-
2.1 ≤ E < 2.3	-	-
2.3 ≤ E < 2.5	-	-
2.5 ≤ E < 2.7	4.0	-
2.7 ≤ E < 2.9	4.0	4.0
2.9 ≤ E < 3.1	4.0	4.0
3.1 ≤ E < 3.3	4.0	4.0
3.3 ≤ E < 3.5	4.0	4.0
3.5 ≤ E < 3.7	4.0	4.0
3.7 ≤ E < 3.9	4.0	4.0
3.9 ≤ E < 4.1	4.0	4.0
4.1 ≤ E < 4.3	4.0	4.0
4.3 ≤ E < 4.5	4.0	4.0
4.5 ≤ E < 4.7	4.0	4.0
4.7 ≤ E < 4.9	4.0	4.0
E ≥ 4.9	4.0	4.0

Table 5.10.6-4 Loading Table for CE 16x16 Fuel – 830 W/Assembly

Minimum Initial Assembly Avg. Enrichment wt % <sup>235</sup> U (E)	Assembly Average Burnup (B) GWd/MTU					
	B ≤10	10< B ≤15	15< B ≤20	20< B ≤25	25< B ≤30	30< B ≤32.5
1.3 ≤ E < 1.5	4.0	-	-	-	-	-
1.5 ≤ E < 1.7	4.0	4.0	-	-	-	-
1.7 ≤ E < 1.9	4.0	4.0	4.0	-	-	-
1.9 ≤ E < 2.1	4.0	4.0	4.0	4.0	-	-
2.1 ≤ E < 2.3	4.0	4.0	4.0	4.0	4.7	5.0
2.3 ≤ E < 2.5	4.0	4.0	4.0	4.0	4.6	5.0
2.5 ≤ E < 2.7	4.0	4.0	4.0	4.0	4.6	4.9
2.7 ≤ E < 2.9	4.0	4.0	4.0	4.0	4.5	4.9
2.9 ≤ E < 3.1	4.0	4.0	4.0	4.0	4.5	4.8
3.1 ≤ E < 3.3	4.0	4.0	4.0	4.0	4.4	4.8
3.3 ≤ E < 3.5	4.0	4.0	4.0	4.0	4.4	4.7
3.5 ≤ E < 3.7	4.0	4.0	4.0	4.0	4.4	4.7
3.7 ≤ E < 3.9	4.0	4.0	4.0	4.0	4.4	4.7
3.9 ≤ E < 4.1	4.0	4.0	4.0	4.0	4.3	4.6
4.1 ≤ E < 4.3	4.0	4.0	4.0	4.0	4.3	4.6
4.3 ≤ E < 4.5	4.0	4.0	4.0	4.0	4.3	4.6
4.5 ≤ E < 4.7	4.0	4.0	4.0	4.0	4.3	4.5
4.7 ≤ E < 4.9	4.0	4.0	4.0	4.0	4.2	4.5
E ≥ 4.9	4.0	4.0	4.0	4.0	4.2	4.5



Table 5.10.6-4 Loading Table for CE 16x16 Fuel – 830 W/Assembly (continued)

Minimum Initial Assembly Avg. Enrichment wt % <sup>235</sup> U (E)	Assembly Average Burnup (B) GWd/MTU					
	32.5< B ≤35	35< B ≤37.5	37.5< B ≤40	40< B ≤41	41< B ≤42	42< B ≤43
1.3 ≤ E < 1.5	-	-	-	-	-	-
1.5 ≤ E < 1.7	-	-	-	-	-	-
1.7 ≤ E < 1.9	-	-	-	-	-	-
1.9 ≤ E < 2.1	-	-	-	-	-	-
2.1 ≤ E < 2.3	-	-	-	-	-	-
2.3 ≤ E < 2.5	5.5	6.0	-	-	-	-
2.5 ≤ E < 2.7	5.4	6.0	6.7	7.0	7.4	7.8
2.7 ≤ E < 2.9	5.4	5.9	6.6	6.9	7.2	7.7
2.9 ≤ E < 3.1	5.3	5.8	6.5	6.8	7.1	7.5
3.1 ≤ E < 3.3	5.2	5.8	6.4	6.7	7.0	7.4
3.3 ≤ E < 3.5	5.2	5.7	6.3	6.6	6.9	7.3
3.5 ≤ E < 3.7	5.1	5.7	6.3	6.6	6.8	7.2
3.7 ≤ E < 3.9	5.1	5.6	6.2	6.5	6.8	7.1
3.9 ≤ E < 4.1	5.0	5.6	6.1	6.4	6.7	7.0
4.1 ≤ E < 4.3	5.0	5.5	6.0	6.4	6.7	6.9
4.3 ≤ E < 4.5	5.0	5.5	6.0	6.3	6.6	6.9
4.5 ≤ E < 4.7	4.9	5.5	6.0	6.2	6.5	6.8
4.7 ≤ E < 4.9	4.9	5.4	5.9	6.2	6.5	6.8
E ≥ 4.9	4.9	5.4	5.9	6.1	6.4	6.7

Table 5.10.6-4 Loading Table for CE 16x16 Fuel – 830 W/Assembly (continued)

Minimum Initial Assembly Avg. Enrichment wt % <sup>235</sup> U (E)	Assembly Average Burnup (B) GWd/MTU	
	43< B ≤44	44< B ≤45
1.3 ≤ E < 1.5	-	-
1.5 ≤ E < 1.7	-	-
1.7 ≤ E < 1.9	-	-
1.9 ≤ E < 2.1	-	-
2.1 ≤ E < 2.3	-	-
2.3 ≤ E < 2.5	-	-
2.5 ≤ E < 2.7	8.2	-
2.7 ≤ E < 2.9	8.0	8.6
2.9 ≤ E < 3.1	7.9	8.4
3.1 ≤ E < 3.3	7.8	8.2
3.3 ≤ E < 3.5	7.7	8.1
3.5 ≤ E < 3.7	7.6	8.0
3.7 ≤ E < 3.9	7.5	7.9
3.9 ≤ E < 4.1	7.4	7.8
4.1 ≤ E < 4.3	7.3	7.7
4.3 ≤ E < 4.5	7.2	7.6
4.5 ≤ E < 4.7	7.1	7.5
4.7 ≤ E < 4.9	7.0	7.4
E ≥ 4.9	7.0	7.4

Table 5.10.6-5 Loading Table for CE 16x16 Fuel – 487 W/Assembly

Minimum Initial Assembly Avg. Enrichment wt % <sup>235</sup> U (E)	Assembly Average Burnup (B) GWd/MTU					
	45< B ≤46	46< B ≤47	47< B ≤48	48< B ≤49	49< B ≤50	50< B ≤51
1.3 ≤ E < 1.5	-	-	-	-	-	-
1.5 ≤ E < 1.7	-	-	-	-	-	-
1.7 ≤ E < 1.9	-	-	-	-	-	-
1.9 ≤ E < 2.1	-	-	-	-	-	-
2.1 ≤ E < 2.3	-	-	-	-	-	-
2.3 ≤ E < 2.5	-	-	-	-	-	-
2.5 ≤ E < 2.7	-	-	-	-	-	-
2.7 ≤ E < 2.9	30.4	31.8	33.2	34.5	-	-
2.9 ≤ E < 3.1	30.1	31.6	32.9	34.3	35.5	36.8
3.1 ≤ E < 3.3	30.0	31.4	32.7	34.1	35.4	36.7
3.3 ≤ E < 3.5	29.8	31.2	32.6	33.9	35.2	36.6
3.5 ≤ E < 3.7	29.6	31.1	32.5	33.8	35.1	36.3
3.7 ≤ E < 3.9	29.4	30.8	32.3	33.6	34.9	36.3
3.9 ≤ E < 4.1	29.3	30.7	32.1	33.5	34.7	36.1
4.1 ≤ E < 4.3	29.1	30.6	32.0	33.4	34.6	35.9
4.3 ≤ E < 4.5	29.0	30.4	31.9	33.2	34.5	35.9
4.5 ≤ E < 4.7	28.9	30.2	31.7	33.1	34.4	35.7
4.7 ≤ E < 4.9	28.8	30.2	31.5	33.0	34.3	35.6
E ≥ 4.9	28.7	30.1	31.4	32.8	34.2	35.4

Table 5.10.6-5 Loading Table for CE 16x16 Fuel – 487 W/Assembly (continued)

Minimum Initial Assembly Avg. Enrichment wt % <sup>235</sup> U (E)	Assembly Average Burnup (B) GWd/MTU					
	51< B ≤52	52< B ≤53	53< B ≤54	54< B ≤55	55< B ≤56	56< B ≤57
1.3 ≤ E < 1.5	-	-	-	-	-	-
1.5 ≤ E < 1.7	-	-	-	-	-	-
1.7 ≤ E < 1.9	-	-	-	-	-	-
1.9 ≤ E < 2.1	-	-	-	-	-	-
2.1 ≤ E < 2.3	-	-	-	-	-	-
2.3 ≤ E < 2.5	-	-	-	-	-	-
2.5 ≤ E < 2.7	-	-	-	-	-	-
2.7 ≤ E < 2.9	-	-	-	-	-	-
2.9 ≤ E < 3.1	38.1	39.3	40.5	-	-	-
3.1 ≤ E < 3.3	38.0	39.2	40.3	41.5	42.1	43.1
3.3 ≤ E < 3.5	37.8	39.1	40.2	41.4	41.9	43.1
3.5 ≤ E < 3.7	37.6	38.9	40.0	41.2	41.8	42.9
3.7 ≤ E < 3.9	37.6	38.7	39.9	41.1	41.7	42.8
3.9 ≤ E < 4.1	37.4	38.7	39.8	41.1	41.6	42.7
4.1 ≤ E < 4.3	37.3	38.6	39.7	40.9	41.4	42.6
4.3 ≤ E < 4.5	37.2	38.4	39.6	40.9	41.3	42.5
4.5 ≤ E < 4.7	37.0	38.2	39.4	40.8	41.2	42.4
4.7 ≤ E < 4.9	36.9	38.2	39.5	40.7	41.0	42.3
E ≥ 4.9	36.8	38.0	39.3	40.5	40.9	42.1

Table 5.10.6-5 Loading Table for CE 16x16 Fuel – 487 W/Assembly (continued)

Minimum Initial Assembly Avg. Enrichment wt % <sup>235</sup> U (E)	Assembly Average Burnup (B) GWd/MTU		
	57< B ≤58	58< B ≤59	59< B ≤60
1.3 ≤ E < 1.5	-	-	-
1.5 ≤ E < 1.7	-	-	-
1.7 ≤ E < 1.9	-	-	-
1.9 ≤ E < 2.1	-	-	-
2.1 ≤ E < 2.3	-	-	-
2.3 ≤ E < 2.5	-	-	-
2.5 ≤ E < 2.7	-	-	-
2.7 ≤ E < 2.9	-	-	-
2.9 ≤ E < 3.1	-	-	-
3.1 ≤ E < 3.3	44.3	45.3	-
3.3 ≤ E < 3.5	44.1	45.2	46.2
3.5 ≤ E < 3.7	44.0	45.1	46.2
3.7 ≤ E < 3.9	43.9	44.9	46.1
3.9 ≤ E < 4.1	43.8	44.9	46.0
4.1 ≤ E < 4.3	43.7	44.8	45.8
4.3 ≤ E < 4.5	43.7	44.7	45.8
4.5 ≤ E < 4.7	43.5	44.6	45.7
4.7 ≤ E < 4.9	43.4	44.5	45.7
E ≥ 4.9	43.4	44.4	45.6

Table 5.10.6-6 Loading Table for CE 16x16 Fuel – 1235 W/Assembly

Minimum Initial Assembly Avg. Enrichment wt % <sup>235</sup> U (E)	Assembly Average Burnup (B) GWd/MTU					
	45< B ≤46	46< B ≤47	47< B ≤48	48< B ≤49	49< B ≤50	50< B ≤51
1.3 ≤ E < 1.5	-	-	-	-	-	-
1.5 ≤ E < 1.7	-	-	-	-	-	-
1.7 ≤ E < 1.9	-	-	-	-	-	-
1.9 ≤ E < 2.1	-	-	-	-	-	-
2.1 ≤ E < 2.3	-	-	-	-	-	-
2.3 ≤ E < 2.5	-	-	-	-	-	-
2.5 ≤ E < 2.7	-	-	-	-	-	-
2.7 ≤ E < 2.9	5.1	5.3	5.5	5.7	-	-
2.9 ≤ E < 3.1	5.0	5.2	5.4	5.6	5.8	6.0
3.1 ≤ E < 3.3	4.9	5.1	5.3	5.5	5.7	5.9
3.3 ≤ E < 3.5	4.9	5.0	5.2	5.4	5.6	5.8
3.5 ≤ E < 3.7	4.8	5.0	5.1	5.3	5.5	5.7
3.7 ≤ E < 3.9	4.8	4.9	5.0	5.2	5.4	5.6
3.9 ≤ E < 4.1	4.7	4.9	5.0	5.2	5.4	5.6
4.1 ≤ E < 4.3	4.7	4.8	4.9	5.1	5.3	5.5
4.3 ≤ E < 4.5	4.6	4.8	4.9	5.0	5.2	5.4
4.5 ≤ E < 4.7	4.5	4.7	4.8	5.0	5.1	5.3
4.7 ≤ E < 4.9	4.5	4.7	4.8	4.9	5.1	5.3
E ≥ 4.9	4.5	4.6	4.8	4.9	5.0	5.2

Table 5.10.6-6 Loading Table for CE 16x16 Fuel – 1235 W/Assembly (continued)

Minimum Initial Assembly Avg. Enrichment wt % <sup>235</sup> U (E)	Assembly Average Burnup (B) GWd/MTU					
	51< B ≤52	52< B ≤53	53< B ≤54	54< B ≤55	55< B ≤56	56< B ≤57
1.3 ≤ E < 1.5	-	-	-	-	-	-
1.5 ≤ E < 1.7	-	-	-	-	-	-
1.7 ≤ E < 1.9	-	-	-	-	-	-
1.9 ≤ E < 2.1	-	-	-	-	-	-
2.1 ≤ E < 2.3	-	-	-	-	-	-
2.3 ≤ E < 2.5	-	-	-	-	-	-
2.5 ≤ E < 2.7	-	-	-	-	-	-
2.7 ≤ E < 2.9	-	-	-	-	-	-
2.9 ≤ E < 3.1	6.2	6.5	6.7	-	-	-
3.1 ≤ E < 3.3	6.1	6.3	6.6	6.8	7.0	7.3
3.3 ≤ E < 3.5	6.0	6.2	6.5	6.7	6.9	7.1
3.5 ≤ E < 3.7	5.9	6.1	6.3	6.6	6.7	7.0
3.7 ≤ E < 3.9	5.8	6.0	6.2	6.5	6.6	6.9
3.9 ≤ E < 4.1	5.7	5.9	6.1	6.4	6.5	6.8
4.1 ≤ E < 4.3	5.7	5.8	6.0	6.3	6.4	6.7
4.3 ≤ E < 4.5	5.6	5.8	5.9	6.2	6.3	6.6
4.5 ≤ E < 4.7	5.5	5.7	5.9	6.0	6.2	6.4
4.7 ≤ E < 4.9	5.5	5.6	5.8	6.0	6.1	6.4
E ≥ 4.9	5.4	5.6	5.8	5.9	6.0	6.3

Table 5.10.6-6 Loading Table for CE 16x16 Fuel – 1235 W/Assembly (continued)

Minimum Initial Assembly Avg. Enrichment wt % <sup>235</sup> U (E)	Assembly Average Burnup (B) GWd/MTU		
	57< B ≤58	58< B ≤59	59< B ≤60
1.3 ≤ E < 1.5	-	-	-
1.5 ≤ E < 1.7	-	-	-
1.7 ≤ E < 1.9	-	-	-
1.9 ≤ E < 2.1	-	-	-
2.1 ≤ E < 2.3	-	-	-
2.3 ≤ E < 2.5	-	-	-
2.5 ≤ E < 2.7	-	-	-
2.7 ≤ E < 2.9	-	-	-
2.9 ≤ E < 3.1	-	-	-
3.1 ≤ E < 3.3	7.7	8.0	-
3.3 ≤ E < 3.5	7.5	7.8	8.2
3.5 ≤ E < 3.7	7.3	7.6	8.0
3.7 ≤ E < 3.9	7.1	7.5	7.8
3.9 ≤ E < 4.1	7.0	7.3	7.7
4.1 ≤ E < 4.3	6.9	7.2	7.5
4.3 ≤ E < 4.5	6.8	7.0	7.4
4.5 ≤ E < 4.7	6.7	6.9	7.2
4.7 ≤ E < 4.9	6.6	6.9	7.1
E ≥ 4.9	6.5	6.8	7.0



Table 5.10.6-7 Loading Table for CE 16x16 Fuel – 1710 W/Assembly

Minimum Initial Assembly Avg. Enrichment wt % <sup>235</sup> U (E)	Assembly Average Burnup (B) GWd/MTU					
	45< B ≤46	46< B ≤47	47< B ≤48	48< B ≤49	49< B ≤50	50< B ≤51
1.3 ≤ E < 1.5	-	-	-	-	-	-
1.5 ≤ E < 1.7	-	-	-	-	-	-
1.7 ≤ E < 1.9	-	-	-	-	-	-
1.9 ≤ E < 2.1	-	-	-	-	-	-
2.1 ≤ E < 2.3	-	-	-	-	-	-
2.3 ≤ E < 2.5	-	-	-	-	-	-
2.5 ≤ E < 2.7	-	-	-	-	-	-
2.7 ≤ E < 2.9	4.0	4.0	4.0	4.0	-	-
2.9 ≤ E < 3.1	4.0	4.0	4.0	4.0	4.0	4.1
3.1 ≤ E < 3.3	4.0	4.0	4.0	4.0	4.0	4.1
3.3 ≤ E < 3.5	4.0	4.0	4.0	4.0	4.0	4.0
3.5 ≤ E < 3.7	4.0	4.0	4.0	4.0	4.0	4.0
3.7 ≤ E < 3.9	4.0	4.0	4.0	4.0	4.0	4.0
3.9 ≤ E < 4.1	4.0	4.0	4.0	4.0	4.0	4.0
4.1 ≤ E < 4.3	4.0	4.0	4.0	4.0	4.0	4.0
4.3 ≤ E < 4.5	4.0	4.0	4.0	4.0	4.0	4.0
4.5 ≤ E < 4.7	4.0	4.0	4.0	4.0	4.0	4.0
4.7 ≤ E < 4.9	4.0	4.0	4.0	4.0	4.0	4.0
E ≥ 4.9	4.0	4.0	4.0	4.0	4.0	4.0

Table 5.10.6-7 Loading Table for CE 16x16 Fuel – 1710 W/Assembly (continued)

Minimum Initial Assembly Avg. Enrichment wt % <sup>235</sup> U (E)	Assembly Average Burnup (B) GWd/MTU					
	51< B ≤52	52< B ≤53	53< B ≤54	54< B ≤55	55< B ≤56	56< B ≤57
1.3 ≤ E < 1.5	-	-	-	-	-	-
1.5 ≤ E < 1.7	-	-	-	-	-	-
1.7 ≤ E < 1.9	-	-	-	-	-	-
1.9 ≤ E < 2.1	-	-	-	-	-	-
2.1 ≤ E < 2.3	-	-	-	-	-	-
2.3 ≤ E < 2.5	-	-	-	-	-	-
2.5 ≤ E < 2.7	-	-	-	-	-	-
2.7 ≤ E < 2.9	-	-	-	-	-	-
2.9 ≤ E < 3.1	4.2	4.4	4.5	-	-	-
3.1 ≤ E < 3.3	4.2	4.3	4.4	4.5	4.6	4.7
3.3 ≤ E < 3.5	4.1	4.2	4.3	4.4	4.5	4.6
3.5 ≤ E < 3.7	4.0	4.2	4.3	4.4	4.5	4.6
3.7 ≤ E < 3.9	4.0	4.1	4.2	4.3	4.4	4.5
3.9 ≤ E < 4.1	4.0	4.1	4.2	4.3	4.3	4.4
4.1 ≤ E < 4.3	4.0	4.0	4.1	4.2	4.3	4.4
4.3 ≤ E < 4.5	4.0	4.0	4.1	4.2	4.2	4.3
4.5 ≤ E < 4.7	4.0	4.0	4.0	4.1	4.2	4.3
4.7 ≤ E < 4.9	4.0	4.0	4.0	4.0	4.1	4.2
E ≥ 4.9	4.0	4.0	4.0	4.0	4.1	4.2

Table 5.10.6-7 Loading Table for CE 16x16 Fuel – 1710 W/Assembly (continued)

Minimum Initial Assembly Avg. Enrichment wt % <sup>235</sup> U (E)	Assembly Average Burnup (B) GWd/MTU		
	57< B ≤58	58< B ≤59	59< B ≤60
1.3 ≤ E < 1.5	-	-	-
1.5 ≤ E < 1.7	-	-	-
1.7 ≤ E < 1.9	-	-	-
1.9 ≤ E < 2.1	-	-	-
2.1 ≤ E < 2.3	-	-	-
2.3 ≤ E < 2.5	-	-	-
2.5 ≤ E < 2.7	-	-	-
2.7 ≤ E < 2.9	-	-	-
2.9 ≤ E < 3.1	-	-	-
3.1 ≤ E < 3.3	4.9	5.0	-
3.3 ≤ E < 3.5	4.8	4.9	5.0
3.5 ≤ E < 3.7	4.7	4.8	5.0
3.7 ≤ E < 3.9	4.6	4.8	4.9
3.9 ≤ E < 4.1	4.5	4.7	4.8
4.1 ≤ E < 4.3	4.5	4.6	4.7
4.3 ≤ E < 4.5	4.4	4.5	4.7
4.5 ≤ E < 4.7	4.4	4.5	4.6
4.7 ≤ E < 4.9	4.3	4.4	4.5
E ≥ 4.9	4.3	4.4	4.5

Table 5.10.6-8 Loading Table for CE 16x16 Fuel – 788 W/Assembly

Minimum Initial Assembly Avg. Enrichment wt % <sup>235</sup> U (E)	Assembly Average Burnup (B) GWd/MTU					
	45< B ≤46	46< B ≤47	47< B ≤48	48< B ≤49	49< B ≤50	50< B ≤51
1.3 ≤ E < 1.5	-	-	-	-	-	-
1.5 ≤ E < 1.7	-	-	-	-	-	-
1.7 ≤ E < 1.9	-	-	-	-	-	-
1.9 ≤ E < 2.1	-	-	-	-	-	-
2.1 ≤ E < 2.3	-	-	-	-	-	-
2.3 ≤ E < 2.5	-	-	-	-	-	-
2.5 ≤ E < 2.7	-	-	-	-	-	-
2.7 ≤ E < 2.9	10.2	11.0	11.8	12.7	-	-
2.9 ≤ E < 3.1	9.9	10.7	11.5	12.3	13.3	14.2
3.1 ≤ E < 3.3	9.8	10.5	11.2	12.0	12.9	13.9
3.3 ≤ E < 3.5	9.6	10.2	11.0	11.8	12.6	13.6
3.5 ≤ E < 3.7	9.4	10.0	10.8	11.6	12.4	13.3
3.7 ≤ E < 3.9	9.2	9.8	10.6	11.3	12.0	13.0
3.9 ≤ E < 4.1	9.1	9.7	10.4	11.1	11.9	12.8
4.1 ≤ E < 4.3	9.0	9.5	10.2	11.0	11.7	12.5
4.3 ≤ E < 4.5	8.9	9.4	10.0	10.8	11.5	12.3
4.5 ≤ E < 4.7	8.8	9.3	9.9	10.6	11.4	12.1
4.7 ≤ E < 4.9	8.7	9.2	9.8	10.5	11.2	12.0
E ≥ 4.9	8.6	9.1	9.7	10.3	11.1	11.8

Table 5.10.6-8 Loading Table for CE 16x16 Fuel – 788 W/Assembly (continued)

Minimum Initial Assembly Avg. Enrichment wt % <sup>235</sup> U (E)	Assembly Average Burnup (B) GWd/MTU					
	51< B ≤52	52< B ≤53	53< B ≤54	54< B ≤55	55< B ≤56	56< B ≤57
1.3 ≤ E < 1.5	-	-	-	-	-	-
1.5 ≤ E < 1.7	-	-	-	-	-	-
1.7 ≤ E < 1.9	-	-	-	-	-	-
1.9 ≤ E < 2.1	-	-	-	-	-	-
2.1 ≤ E < 2.3	-	-	-	-	-	-
2.3 ≤ E < 2.5	-	-	-	-	-	-
2.5 ≤ E < 2.7	-	-	-	-	-	-
2.7 ≤ E < 2.9	-	-	-	-	-	-
2.9 ≤ E < 3.1	15.2	16.3	17.4	-	-	-
3.1 ≤ E < 3.3	14.9	15.9	17.0	18.0	18.7	19.7
3.3 ≤ E < 3.5	14.6	15.6	16.6	17.7	18.2	19.3
3.5 ≤ E < 3.7	14.2	15.2	16.3	17.3	17.9	19.0
3.7 ≤ E < 3.9	13.9	14.9	15.9	17.0	17.5	18.6
3.9 ≤ E < 4.1	13.7	14.6	15.6	16.7	17.2	18.2
4.1 ≤ E < 4.3	13.4	14.3	15.4	16.4	16.9	18.0
4.3 ≤ E < 4.5	13.2	14.1	15.1	16.1	16.7	17.7
4.5 ≤ E < 4.7	13.0	13.9	14.9	15.8	16.4	17.4
4.7 ≤ E < 4.9	12.8	13.7	14.7	15.7	16.1	17.2
E ≥ 4.9	12.7	13.5	14.5	15.4	16.0	17.0

Table 5.10.6-8 Loading Table for CE 16x16 Fuel – 788 W/Assembly (continued)

Minimum Initial Assembly Avg. Enrichment wt % <sup>235</sup> U (E)	Assembly Average Burnup (B) GWd/MTU		
	57< B ≤58	58< B ≤59	59< B ≤60
1.3 ≤ E < 1.5	-	-	-
1.5 ≤ E < 1.7	-	-	-
1.7 ≤ E < 1.9	-	-	-
1.9 ≤ E < 2.1	-	-	-
2.1 ≤ E < 2.3	-	-	-
2.3 ≤ E < 2.5	-	-	-
2.5 ≤ E < 2.7	-	-	-
2.7 ≤ E < 2.9	-	-	-
2.9 ≤ E < 3.1	-	-	-
3.1 ≤ E < 3.3	20.8	21.8	-
3.3 ≤ E < 3.5	20.4	21.4	22.5
3.5 ≤ E < 3.7	20.0	21.1	22.1
3.7 ≤ E < 3.9	19.7	20.7	21.7
3.9 ≤ E < 4.1	19.3	20.3	21.4
4.1 ≤ E < 4.3	19.0	20.0	21.1
4.3 ≤ E < 4.5	18.7	19.7	20.8
4.5 ≤ E < 4.7	18.4	19.5	20.5
4.7 ≤ E < 4.9	18.2	19.2	20.2
E ≥ 4.9	17.9	19.0	20.0

## 6.1 Discussion and Results

### 6.1.1 MAGNASTOR System Criticality Evaluation

MAGNASTOR consists of a TSC (Transportable Storage Canister), a transfer cask, and a concrete cask. The system is designed to safely store up to 37 undamaged PWR fuel assemblies in the 37 PWR basket assembly or up to 87 undamaged BWR fuel assemblies in the 87 BWR basket assembly. The system is also designed to store up to four damaged fuel cans (DFCs) in the DF Basket Assembly. The DF Basket Assembly has a capacity of up to 37 undamaged PWR fuel assemblies, including 4 DFC locations. DFCs may be placed in up to four of the DFC locations. Each DFC may contain an undamaged PWR fuel assembly, a damaged PWR fuel assembly, or PWR fuel debris equivalent to one PWR fuel assembly. Undamaged PWR fuel assemblies may be placed directly in the DFC locations of a DF Basket Assembly.

The TSC is comprised of a stainless steel canister and a basket within which fuel is loaded. The PWR and BWR system each includes two TSC lengths to store fuel assemblies without the requirement of spacers. Spacers may be employed to simplify loading or unloading operations. The TSC is loaded into the concrete cask for storage. A transfer cask is used for handling the TSC during loading of spent fuel. Fuel is loaded into the TSC contained within the transfer cask underwater in the spent fuel pool. Once loaded with fuel, the TSC closure lid is welded and the TSC is drained, dried and backfilled with helium. The transfer cask is then used to move the TSC into or out of the concrete cask. The transfer cask provides shielding during the TSC loading and transfer operations. Multiple-size concrete and transfer casks accommodate all of the PWR and BWR TSCs.

Under normal conditions, such as loading in a spent fuel pool, moderator (water) is present in the TSC during the initial stages of fuel transfer. During draining and drying operations, moderator with varying density is present. Thus, the criticality evaluation of the transfer cask includes a variation in moderator density and a determination of optimum moderator density. Cask accident conditions are bounded by inclusion in the analysis of the most reactive mechanical basket configuration as well as moderator intrusion into the fuel cladding. The PWR TSC is evaluated at minimum soluble boron levels during flooded conditions.

Structural analyses demonstrate that the TSC confinement boundary remains intact through all storage operating conditions. Therefore, moderator is not present in the TSC while it is in the concrete cask. However, access to the concrete cask interior environment is possible via the air inlets and outlets and the heat transfer annulus between the TSC and the cask steel liner. This access provides paths for moderator intrusion during a flood. Under off-normal and accident conditions, moderator intrusion into the convective heat transfer annulus is evaluated.

PWR system criticality control is achieved through a combination of neutron absorber sheets on the interior faces of the fuel tubes/developed cells and soluble boron. BWR system criticality control relies solely on the absorber sheets. Individual fuel assemblies are held in place by the fuel tubes, by developed cells formed from fuel tubes, or by a combination of fuel tubes and side or corner weldments. The neutron absorber modeled is a borated aluminum sheet. Any material meeting the physical dimension requirements specified on the License Drawings and the effective  $^{10}\text{B}$  areal density specified in Table 6.1.1-5 will produce similar reactivity results. A combination of steel cover sheets and weld posts holds the neutron absorber sheets in place. The PWR undamaged fuel basket design includes 21 fuel tubes forming 37 fuel-assembly-sized openings while the PWR damaged fuel basket design includes 17 fuel tubes and four corner weldments forming 37 openings. A sketch of a cross-section of the damaged fuel basket is shown in figure 6.1.1-2. The BWR basket contains 45 fuel tubes forming 89 fuel-assembly-sized openings.

The combination of 45 BWR fuel tubes with four corner and four side weldments form 89 fuel-assembly-sized openings; however, two openings are below the vent and drain ports and are not loaded. For simplicity and cask symmetry, all 89 slots are modeled as filled with fuel.

An optional “86-assembly” configuration of the BWR basket is evaluated where the center basket location is left unoccupied. An optional “82-assembly” configuration of the BWR basket is evaluated, where five center openings in an “X” pattern are left unoccupied (the basket model fills the openings below the port cover and, therefore, contains 84 assemblies). An alternate 82-assembly configuration is also evaluated with the empty basket locations moved further out from the center of the basket. See Figure 6.1.1-1 for the loadable basket locations in the 82-assembly basket configuration.

Initial criticality evaluations rely on neutron absorber sheet effective  $^{10}\text{B}$  loadings of  $0.036 \text{ g/cm}^2$  and  $0.027 \text{ g/cm}^2$  for the PWR and BWR system, respectively. The system is also evaluated for effective  $^{10}\text{B}$  loading of  $0.030$  and  $0.027 \text{ g/cm}^2$  for PWR baskets and  $0.0225$  and  $0.020 \text{ g/cm}^2$  for BWR baskets. Depending on the PWR payload, variable soluble boron concentrations in the pool water are necessary to achieve sufficient neutron absorber content in the system. The soluble boron absorbs thermal neutrons inside the assembly, in addition to the neutrons removed by the absorber sheets on the tubes.

The minimum as-manufactured loading of the neutron absorber sheets depends on the effectiveness of the absorber and the minimum effective absorber areal density. Effectiveness of the absorber is influenced by the uniformity and quantity of the  $^{10}\text{B}$  nuclide within the absorber base material. Table 6.1.1-5 translates the effective absorber content to absorber materials at 75% and 90% credit.



MCNP, a three-dimensional Monte Carlo code, is used in the system criticality analysis. Evaluations are primarily based on the ENDF/B-VI continuous energy neutron cross-section library [4] available in the MCNP distribution. Nuclides for which no ENDF/B-VI data is available are set to the latest cross-section sets available in the code distribution. The code and cross-section libraries are benchmarked by comparison to a range of critical experiments relevant to light water reactor fuel in storage and transport casks. An upper subcritical limit (USL) for the system is determined based on guidance given in NUREG/CR-6361 [10].

Key assembly physical characteristics, maximum initial enrichment, and soluble boron requirements (PWR only) for each PWR and BWR fuel assembly type are shown in Table 6.1.1-1, Table 6.1.1-2 and Table 6.1.1-6 for the PWR system and Table 6.1.1-3 and Table 6.1.1-4 for the BWR system. PWR results represent the bounding values for fuel assemblies with and without nonfuel inserts in the guide tubes. Maximum enrichment is defined as peak rod enrichment for PWR assemblies and the maximum peak planar-average enrichment for BWR assemblies. The maximum initial peak planar-average enrichment is the maximum planar-average enrichment at any height along the axis of the fuel assembly.

Assemblies are evaluated with a full, nominal set of fuel rods. Fuel rod (lattice) locations may contain filler rods. A filler rod must occupy, at a minimum, a volume equivalent to the fuel rod it displaces. Filler rods may be placed into the lattice after assembly in-core use or be designed to replace fuel rods prior to use, such as integral burnable absorber rods.

The assembly must contain its nominal set of guide and instrument tubes (PWR), and water rods (BWR). Analysis demonstrated that variations in the guide/instrument tube and water rod thickness and diameter have no significant effect on system reactivity.

#### **6.1.1.1      Undamaged Fuel Criticality Results**

The maximum multiplication factors ( $k_{eff} + 2\sigma$ ) are calculated, using conservative assumptions, for the transfer and concrete cask. The USL applied to the analysis results is 0.9376 per Section 6.5.2. The results of the analyses are presented in detail in Sections 6.4.3 and 6.7, and are summarized as follows.

Cask Body	Gap Condition	Operating Condition	Water Density (g/cc)		PWR	BWR
			Interior	Exterior	$k_{eff} + 2\sigma$	$k_{eff} + 2\sigma$
Transfer	Dry	Normal	0.9982	0.0001	0.93183	0.92900
Transfer	Wet	Normal	0.9982	0.0001	0.93712	0.93679
Transfer	Dry	Normal	0.9982	0.9982	0.92975	0.92839
Transfer	Wet	Normal	0.9982	0.9982	0.93615	0.93674
Storage	Dry	Normal	0.0001	0.0001	0.48145	0.43685
Storage	Dry	Accident	0.0001	0.9982	0.47104	0.42991

Analysis of simultaneous moderator density variation inside and outside either the transfer or concrete cask shows a monotonic decrease in reactivity with decreasing moderator density. For the BWR system, there is a statistically significant increase in reactivity when moving from void to full moderator density. In the PWR system, reactivity increases as moderator density rises from void conditions, but there is no significant reactivity difference at water densities above 0.9 g/cm<sup>3</sup>. The use of soluble boron in PWR systems, specified in parts per million of moderator, flattens out the reactivity curve by increasing absorber quantity in conjunction with increasing moderator. The full moderator density TSC interior condition bounds any off-normal or accident condition. Analysis of moderator intrusion into the concrete cask heat transfer annulus with the dry TSC shows a slight decrease in reactivity from the completely dry condition.

#### 6.1.1.2 Damaged PWR Fuel Criticality Results

The PWR system is designed to safely store up to 37 PWR fuel assemblies of which up to 4 may be classified as damaged and be placed into damaged fuel cans (DFCs) in the four corner basket locations. The DFC provides a screened container to prevent gross fissile material release into the TSC cavity from failed fuel rod cladding. The results of the analyses are presented in detail in Section 6.7.8 and are summarized as follows. All results are below the USL of 0.9376.

Cask Body	Gap Condition	Operating Condition	Water Density (g/cc)		PWR
			Interior	Exterior	$k_{eff} + 2\sigma$
Transfer	Wet	Normal	0.9982	N/A <sup>a</sup>	0.93757
Storage	Dry	Normal	0.0001	0.0001	0.49142
Storage	Dry	Accident	0.0001	0.9982	0.48211

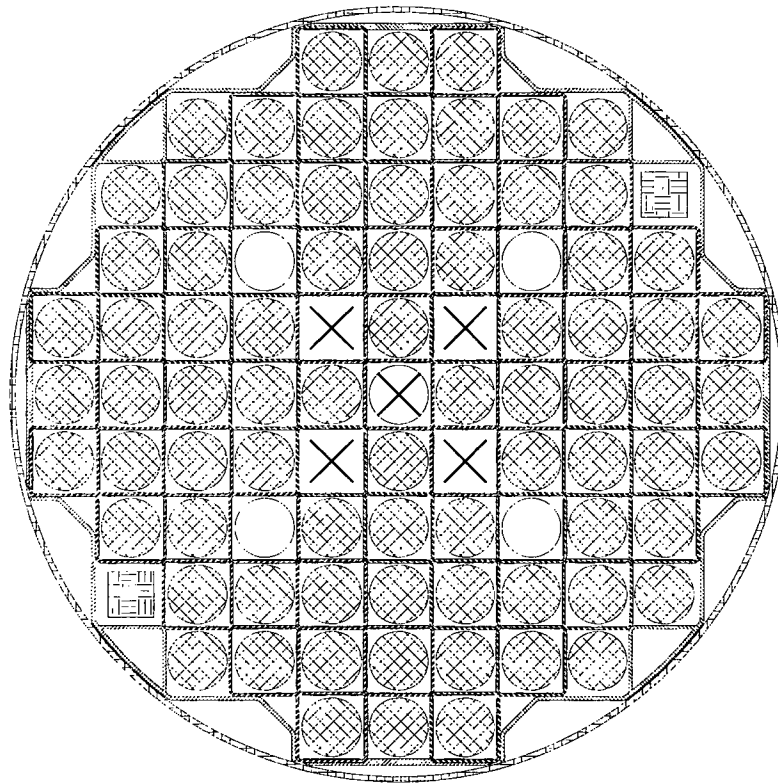
<sup>a</sup> Exterior moderator has been demonstrated in Section 6.7.3 to not affect system reactivity for a fully flooded TSC.

Three damaged fuel configurations are evaluated. Damaged fuel includes fuel debris. In the first configuration, undamaged fuel is loaded into a DFC to demonstrate the effect of the additional stainless steel from the DFC and the DFC corner weldments. In the second configuration, damaged fuel is postulated to lose its cladding and the array is modeled at an increased pitch. In the third configuration, mixtures of fuel and water simulate small fuel rubble inside the DFC.

Three moderator configurations are evaluated. Moderator density studies are performed on the preferentially flooded DFC, partially flooded cask, and mixture moderator density. In the preferentially flooded DFC scenario, the DFC is assumed to vary in moderator density with a wet and dry canister. A partial draindown of the TSC to the top of the active fuel is referred to as partial flooding. A study on the mixture moderator density is performed to ensure that the homogenized mixture remains undermoderated.


For each of the fuel types, with and without nonfuel inserts in the active fuel region of the undamaged assemblies, several combinations of minimum soluble boron and maximum initial enrichments are determined. The allowable loadings are documented in Table 6.1.1-6.

Figure 6.1.1-1 82-Assembly BWR Basket Configuration



 = Fuel Assembly Locations

 = Vent/Drain Port Locations

 -- Designated Nonfuel Locations for Standard 82-Assembly Config


 -- Designated Nonfuel Locations for Alternate 82-Assembly Config

Table 6.1.1-4 BWR Fuel Assembly Loading Criteria  
(Enrichment Limits)

	Max. Initial Enrichment <sup>a</sup> (wt % <sup>235</sup> U)					
	Absorber <sup>b</sup> 0.027 <sup>10</sup> B g/cm <sup>2</sup>		Absorber 0.0225 <sup>10</sup> B g/cm <sup>2</sup>		Absorber 0.02 <sup>10</sup> B g/cm <sup>2</sup>	
	87-Assy Basket	82-Assy Basket	87-Assy Basket	82-Assy Basket	87-Assy Basket	82-Assy Basket
B7_48A	4.0%	4.5%	3.7%	4.5%	3.6%	4.4%
B7_49A	3.8%	4.5%	3.6%	4.4%	3.5%	4.3%
B7_49B	3.8%	4.5%	3.6%	4.4%	3.5%	4.2%
B8_59A	3.9%	4.5%	3.7%	4.5%	3.6%	4.3%
B8_60A	3.8%	4.5%	3.7%	4.4%	3.5%	4.2%
B8_60B	3.8%	4.5%	3.6%	4.3%	3.5%	4.2%
B8_61B	3.8%	4.5%	3.6%	4.3%	3.5%	4.2%
B8_62A	3.8%	4.5%	3.6%	4.3%	3.5%	4.1%
B8_63A	3.8%	4.5%	3.6%	4.3%	3.4%	4.2%
B8_64A	3.8%	4.5%	3.6%	4.3%	3.5%	4.2%
B8_64B	3.6%	4.3%	3.4%	4.1%	3.3%	4.0%
B9_72A	3.8%	4.5%	3.6%	4.3%	3.4%	4.1%
B9_74A	3.7% <sup>c</sup>	4.3%	3.4%	4.1%	3.4%	4.0%
B9_76A	3.5%	4.2%	3.4%	4.0%	3.3%	3.9%
B9_79A	3.7%	4.4%	3.4%	4.2%	3.3%	4.0%
B9_80A	3.8%	4.5%	3.6%	4.3%	3.5%	4.2%
B10_91A	3.7%	4.5% <sup>d</sup>	3.6%	4.3%	3.5%	4.1%
B10_92A	3.8%	4.5% <sup>d</sup>	3.6%	4.3%	3.5%	4.1%
B10_96A	3.7%	4.3%	3.5%	4.1%	3.4%	4.0%
B10_100A	3.6%	4.4%	3.5%	4.1%	3.4%	4.0%

<sup>a</sup> Maximum planar average.

<sup>b</sup> Borated aluminum neutron absorber sheet effective areal <sup>10</sup>B density.

<sup>c</sup> 3.85% in the 86-assembly basket configuration.

<sup>d</sup> 4.55% in the alternate 82-assembly basket configuration.

Table 6.1.1-5 Effective Areal Density as a Function of Absorber Credit

	Effective <sup>a</sup> g <sup>10</sup> B/cm <sup>2</sup>	75% Credit g <sup>10</sup> B/cm <sup>2</sup>	90% Credit g <sup>10</sup> B/cm <sup>2</sup>
PWR	0.036	0.048	0.040
	0.030	0.040	0.0334
	0.027	0.036	0.30
BWR	0.027	0.036	0.030
	0.0225	0.030	0.025
	0.020	0.0267	0.0223

Note: The effective column contains the <sup>10</sup>B content modeled in the criticality evaluations. The 75% and 90% credit columns contain the minimum as manufactured <sup>10</sup>B content requirements. Effective contents equals as manufactured content times the percent credit permitted (also termed percent effectiveness).

<sup>a</sup> The effective areal density represents the value input into the criticality model and is, therefore, the "100% credit" value.

Table 6.1.1-6 Damaged Fuel Basket Bounding PWR Fuel Assembly Loading Criteria  
(Enrichment/Soluble Boron Limits)

Max. Initial Enrichment (wt % <sup>235</sup> U)															
Soluble Boron	Absorber <sup>a</sup> 0.036 <sup>10</sup> B g/cm <sup>2</sup>					Absorber <sup>a</sup> 0.030 <sup>10</sup> B g/cm <sup>2</sup>					Absorber <sup>a</sup> 0.027 <sup>10</sup> B g/cm <sup>2</sup>				
	1500 (ppm)	1750 (ppm)	2000 (ppm)	2250 (ppm)	2500 (ppm)	1500 (ppm)	1750 (ppm)	2000 (ppm)	2250 (ppm)	2500 (ppm)	1500 (ppm)	1750 (ppm)	2000 (ppm)	2250 (ppm)	2500 (ppm)
BW15H1	3.7%	4.0%	4.3%	4.6%	4.9%	3.6%	3.9%	4.2%	4.5%	4.7%	3.6%	3.8%	4.1%	4.4%	4.7%
BW15H2	3.6%	3.9%	4.2%	4.5%	4.8%	3.6%	3.8%	4.1%	4.4%	4.7%	3.5%	3.8%	4.1%	4.3%	4.6%
BW15H3	3.6%	3.9%	4.2%	4.5%	4.8%	3.5%	3.8%	4.1%	4.4%	4.6%	3.5%	3.8%	4.0%	4.3%	4.6%
BW15H4	3.8%	4.1%	4.4%	4.7%	5.0%	3.7%	4.0%	4.3%	4.6%	4.9%	3.6%	3.9%	4.2%	4.5%	4.8%
BW17H1	3.6%	3.9%	4.2%	4.5%	4.8%	3.6%	3.9%	4.1%	4.4%	4.7%	3.5%	3.8%	4.1%	4.4%	4.6%
CE14H1	4.4%	4.8%	5.0%	5.0%	5.0%	4.3%	4.7%	5.0%	5.0%	5.0%	4.3%	4.6%	4.9%	5.0%	5.0%
CE16H1	4.4%	4.7%	5.0%	5.0%	5.0%	4.2%	4.6%	5.0%	5.0%	5.0%	4.2%	4.5%	4.9%	5.0%	5.0%
WE14H1	4.6%	5.0%	5.0%	5.0%	5.0%	4.5%	5.0%	5.0%	5.0%	5.0%	4.5%	4.9%	5.0%	5.0%	5.0%
WE15H1	3.8%	4.1%	4.4%	4.7%	5.0%	3.7%	4.0%	4.3%	4.6%	4.9%	3.6%	4.0%	4.3%	4.6%	4.8%
WE15H2	3.9%	4.3%	4.6%	4.9%	5.0%	3.8%	4.2%	4.5%	4.8%	5.0%	3.8%	4.1%	4.4%	4.7%	5.0%
WE17H1	3.7%	4.0%	4.3%	4.6%	4.9%	3.6%	3.9%	4.2%	4.5%	4.8%	3.6%	3.9%	4.2%	4.5%	4.8%
WE17H2	3.9%	4.3%	4.6%	5.0%	5.0%	3.9%	4.2%	4.5%	4.9%	5.0%	3.8%	4.1%	4.5%	4.8%	5.0%

<sup>a</sup> Borated aluminum neutron absorber sheet effective areal <sup>10</sup>B density.

**Table 6.4.3-4 BWR Fuel Basket Allowable Loading  
(Enrichment Limits)**

	Max. Initial Enrichment <sup>a</sup> ( wt % <sup>235</sup> U)					
	Absorber <sup>b</sup> 0.027 <sup>10</sup> B g/cm <sup>2</sup>		Absorber 0.0225 <sup>10</sup> B g/cm <sup>2</sup>		Absorber 0.02 <sup>10</sup> B g/cm <sup>2</sup>	
	87-Assy Basket	82-Assy Basket	87-Assy Basket	82-Assy Basket	87-Assy Basket	82-Assy Basket
B7_48A	4.0%	4.5%	3.7%	4.5%	3.6%	4.4%
B7_49A	3.8%	4.5%	3.6%	4.4%	3.5%	4.3%
B7_49B	3.8%	4.5%	3.6%	4.4%	3.5%	4.2%
B8_59A	3.9%	4.5%	3.7%	4.5%	3.6%	4.3%
B8_60A	3.8%	4.5%	3.7%	4.4%	3.5%	4.2%
B8_60B	3.8%	4.5%	3.6%	4.3%	3.5%	4.2%
B8_61B	3.8%	4.5%	3.6%	4.3%	3.5%	4.2%
B8_62A	3.8%	4.5%	3.6%	4.3%	3.5%	4.1%
B8_63A	3.8%	4.5%	3.6%	4.3%	3.4%	4.2%
B8_64A	3.8%	4.5%	3.6%	4.3%	3.5%	4.2%
B8_64B	3.6%	4.3%	3.4%	4.1%	3.3%	4.0%
B9_72A	3.8%	4.5%	3.6%	4.3%	3.4%	4.1%
B9_74A	3.7% <sup>c</sup>	4.3%	3.4%	4.1%	3.4%	4.0%
B9_76A	3.5%	4.2%	3.4%	4.0%	3.3%	3.9%
B9_79A	3.7%	4.4%	3.4%	4.2%	3.3%	4.0%
B9_80A	3.8%	4.5%	3.6%	4.3%	3.5%	4.2%
B10_91A	3.7%	4.5% <sup>d</sup>	3.6%	4.3%	3.5%	4.1%
B10_92A	3.8%	4.5% <sup>d</sup>	3.6%	4.3%	3.5%	4.1%
B10_96A	3.7%	4.3%	3.5%	4.1%	3.4%	4.0%
B10_100A	3.6%	4.4%	3.5%	4.1%	3.4%	4.0%

<sup>a</sup> Maximum planar average.

<sup>b</sup> Borated aluminum neutron absorber sheet effective areal <sup>10</sup>B density.

<sup>c</sup> 3.85% in the 86-assembly basket configuration.

<sup>d</sup> 4.55% in the alternate 82-assembly basket configuration.



**Table 6.4.3-5 Damaged Fuel Basket PWR Fuel Assembly Loading Criteria  
(Enrichment/Soluble Boron Limits)**

Soluble Boron	Max. Initial Enrichment ( wt % <sup>235</sup> U)														
	Absorber <sup>a</sup> 0.036 <sup>10</sup> B g/cm <sup>2</sup>					Absorber <sup>a</sup> 0.030 <sup>10</sup> B g/cm <sup>2</sup>					Absorber <sup>a</sup> 0.027 <sup>10</sup> B g/cm <sup>2</sup>				
	1500 (ppm)	1750 (ppm)	2000 (ppm)	2250 (ppm)	2500 (ppm)	1500 (ppm)	1750 (ppm)	2000 (ppm)	2250 (ppm)	2500 (ppm)	1500 (ppm)	1750 (ppm)	2000 (ppm)	2250 (ppm)	2500 (ppm)
BW15H1	3.7%	4.0%	4.3%	4.6%	4.9%	3.6%	3.9%	4.2%	4.5%	4.7%	3.6%	3.8%	4.1%	4.4%	4.7%
BW15H2	3.6%	3.9%	4.2%	4.5%	4.8%	3.6%	3.8%	4.1%	4.4%	4.7%	3.5%	3.8%	4.1%	4.3%	4.6%
BW15H3	3.6%	3.9%	4.2%	4.5%	4.8%	3.5%	3.8%	4.1%	4.4%	4.6%	3.5%	3.8%	4.0%	4.3%	4.6%
BW15H4	3.8%	4.1%	4.4%	4.7%	5.0%	3.7%	4.0%	4.3%	4.6%	4.9%	3.6%	3.9%	4.2%	4.5%	4.8%
BW17H1	3.6%	3.9%	4.2%	4.5%	4.8%	3.6%	3.9%	4.1%	4.4%	4.7%	3.5%	3.8%	4.1%	4.4%	4.6%
CE14H1	4.4%	4.8%	5.0%	5.0%	5.0%	4.3%	4.7%	5.0%	5.0%	5.0%	4.3%	4.6%	4.9%	5.0%	5.0%
CE16H1	4.4%	4.7%	5.0%	5.0%	5.0%	4.2%	4.6%	5.0%	5.0%	5.0%	4.2%	4.5%	4.9%	5.0%	5.0%
WE14H1	4.6%	5.0%	5.0%	5.0%	5.0%	4.5%	5.0%	5.0%	5.0%	5.0%	4.5%	4.9%	5.0%	5.0%	5.0%
WE15H1	3.8%	4.1%	4.4%	4.7%	5.0%	3.7%	4.0%	4.3%	4.6%	4.9%	3.6%	4.0%	4.3%	4.6%	4.8%
WE15H2	3.9%	4.3%	4.6%	4.9%	5.0%	3.8%	4.2%	4.5%	4.8%	5.0%	3.8%	4.1%	4.4%	4.7%	5.0%
WE17H1	3.7%	4.0%	4.3%	4.6%	4.9%	3.6%	3.9%	4.2%	4.5%	4.8%	3.6%	3.9%	4.2%	4.5%	4.8%
WE17H2	3.9%	4.3%	4.6%	5.0%	5.0%	3.9%	4.2%	4.5%	4.9%	5.0%	3.8%	4.1%	4.5%	4.8%	5.0%

<sup>a</sup> Borated aluminum neutron absorber sheet effective areal <sup>10</sup>B density.

#### 6.7.4 BWR Model Details

The BWR system payload consists of 87 fuel assemblies that are placed into 87 of 89 openings formed by a combination of 45 fuel tubes, and 4 side and corner weldments. Two of the basket opening are located on the basket periphery below the vent and drain port opening and are not designed to contain fuel assemblies. All 89-fuel assembly openings are filled in the “87-Assembly” basket model.

Additional configurations are evaluated with assemblies removed from the basket. An 86 assembly configuration is evaluated with the center basket location without a fuel assembly. An “82-Assembly” configuration is evaluated with five assemblies removed in an x-pattern from the basket center. The alternate 82-assembly configuration moves the four empty basket locations out from the center of the basket. A sketch of the basket configuration is shown in Figure 6.1.1-1. The 86 and 82-assembly configurations removes a significant quantity of fissile material from the basket center in addition to providing flux traps for neutrons from the adjacent assemblies to thermalize and be absorbed by the absorber sheets. These effects combine to allow a significant enrichment increase over the 87-assembly configuration.

The BWR basket model is similar in structure to the PWR model documented in Section 6.7.1, with differences being limited to the addition of an optional zirconium-based alloy channel and the option to model sub-channeled type assemblies. Sub-channeled assemblies are comprised of four fuel rod sub-bundles. Dimensioned fuel tubes forming the base configuration of the basket are shown in Figure 6.7.4-1. The assembled BWR basket is shown in Figure 6.7.4-2.

All fuel tubes are initially modeled as containing four neutron absorber sheets with weld post locations along the tube face for the criticality evaluations associated with maximum reactivity payload and basket configuration and optimum moderation. Final system configuration increases the number of weld posts and allows the removal of the neutron absorber sheets or replacement by aluminum sheets at up to 24 basket peripheral locations for the 87-assembly basket and up to 16 locations for the 82-assembly basket. The reduction in the number of absorber sheets does not affect system reactivity, as demonstrated in Section 6.7.6.1. Similarly, an additional column of weld posts has no significant effect on system reactivity as shown in Section 6.7.6.1. Since the combination of a reduced number of absorber sheets and an increase in the number of weld posts has the potential for increasing  $k_{eff}$  slightly above the statistically significant level threshold, the maximum enrichments and  $k_{eff}$  in Section 6.7.6.2 are calculated using a model incorporating both design attributes.

Sample input files for the BWR transfer cask 87-assembly configuration and 82-assembly configuration are shown in Figure 6.7.4-3 and Figure 6.7.4-4, respectively. Only the transfer

cask model is shown since PWR and BWR concrete cask models are identical with the exception of the TSC contents. The inputs provided represent the maximum reactivity configuration and include the minimum cell spacing, replacement of the optional peripheral absorbers by aluminum sheets, and the full number of weld posts illustrated in the licensing drawings.

### 6.7.5 BWR Fuel Characterization

Fuel definitions listed in Section 6.4 are the result of grouping the large range of commercial fuel types by core type, number of fuel rods, and key criticality characteristics. These characteristics are primarily associated with the assembly moderator ratio and fuel mass and include pellet diameter, active fuel length, fuel rod diameter and clad thickness, and water rod configuration. Another variable for BWR assemblies is the presence, and thickness, of the channel.

Characterization studies are based on the 87-assembly basket configuration. For assemblies exceeding the USL at the enrichment specified in the studies either the 86-assembly basket, the 82-assembly basket configurations or reduced maximum enrichments are required. Enrichment limits for the basket configurations are provided in Section 6.7.6.

#### Lattice Configuration and Channel Studies

BWR fuel assemblies are typically undermoderated in the basket structure (H/U ratio below optimum levels). Therefore, initial criticality analysis extracts from each assembly type the following characteristics.

- Minimum fuel rod outer diameter
- Minimum clad thickness (only relevant to flooded pellet-to-clad gap scenarios)
- Minimum water rod outer diameter and thickness
- Maximum rod pitch (assemblies are grouped by core type and, therefore, typically have single nominal pitch)

Based on the maximum H/U set of characteristics, the reactivity of each assembly is determined under various conditions. Evaluated is a dry and flooded pellet-to-clad gap. Since relative reactivity for the assembly design and flood conditions are evaluated, the models are based on nominal basket characteristics with the assemblies centered in the tube and developed cell. Comparisons are performed at a 4 wt.% enrichment level.

Results of the analysis at various clad-to-gap conditions are shown in Table 6.7.5-1. Flooding the pellet-to-clad gap raised system reactivity across the majority of fuel types, indicating that the fuel assemblies are significantly undermoderated in the basket. No statistically significant reactivity decrease occurs as a result of flooding the gap for any of the fuel types. The channel thickness study documented in Table 6.7.5-2 demonstrates that modeling the maximum channel thickness is conservative and that it is permissible to load assemblies without channel.

The evaluation presented previously assumed that the assemblies are undermoderated and that choosing the corresponding set of parameters maximizes system reactivity. This assumption is supported by the pellet-to-clad gap flood evaluation, which clearly demonstrates that providing

additional moderator to the lattice increases reactivity. This assumption is further validated by evaluating a subset of the fuel assembly types for a variation in the lattice parameters. As typical assemblies loaded into the cask are expected to be intact (no leak), the pellet-to-clad gap is specified to be dry for these analyses. Fuel assemblies are evaluated in a nominal configuration basket with fuel assemblies centered in the tube. As this evaluation is concerned with relative reactivity differences due to lattice parameter changes, the results of this analysis may be applied to the maximum reactivity basket configuration. Each assembly hybrid is evaluated over its range of nominal lattice parameters.

Rather than evaluating individual parameter effects separately, the fuel characteristics analysis is divided into distinct regions.

Fuel rod lattice unit cell

- H/U ratio controlled by rod pitch, rod diameter, and clad thickness

Water rod unit cell (note that not all BWR assemblies contain water rods)

- H/U controlled by water rod diameter and thickness

Pellet diameter (NUREG-6716 [9] indicates the possibility of a minimum pellet diameter increasing system reactivity)

Monte Carlo evaluation results of the nominal assembly parameter ranges provided limited useful information, as the majority of reactivity changes were not resolvable within a two or three sigma uncertainty band. Statistically significant results were obtained from an additional calculation set applying increased variances to each of the parameters. The results of the increased variance evaluation for 4.0 wt.% enriched cases are shown in Table 6.7.5-3. As shown, the cases containing maximum H/U ratio in the fuel rod lattice location, maximum H/U in the water rod location (minimum water rod diameter and thickness), and maximum pellet diameter produce a maximum reactivity configuration system. The result set also demonstrates that water rod dimensions are not a crucial to system criticality control. Critical assemblies characteristics are listed below.

Number of fuel rods

Minimum fuel rod outer diameter

Minimum clad thickness

Maximum rod pitch

Maximum active fuel length (not evaluated but based on neutron leakage maximum active fuel length results in a bounding payload definition)

### **Homogeneous versus Heterogeneous Assembly Enrichment Evaluation**

BWR fuel assemblies are typically loaded with a heterogeneous enrichment scheme of multiple fuel pin enrichments in one assembly. For the criticality analysis presented previously, an initial peak planar-average enrichment is used. The initial peak planar-average enrichment is the

## 6.7.6 BWR Undamaged Fuel Criticality Evaluation

### 6.7.6.1 Optimum System Configuration

Enrichment limits are based on a maximum reactivity configuration system. To determine the maximum reactivity system, the following system perturbations are evaluated:

- TSC interior moderator elevation variations (partial flooding)
- Moderator density changes from void to full density (inside and outside the TSC)
- Basket fabrication tolerance
- Component shift scenarios

All system perturbation analyses are based on fuel assemblies at the maximum lattice moderator (H/U) ratio. Justification for this fuel assembly configuration is provided in Section 6.7.5. Only transfer cask cases are used in these evaluations since the transfer cask is the only cask body in which TSC flooding occurs. In the dry concrete cask, the TSC has a low reactivity,  $k_{eff} < 0.5$ .

All elevations in this section are based on full-length rods in all assemblies. Partial length rods are addressed in the loading tables. Optimum system configuration studies are based on the 87-assembly basket configuration and a 4.0 wt %  $^{235}\text{U}$  initial enrichment, unless otherwise stated. Certain assembly types and configurations exceed the USL at the 4.0 wt %  $^{235}\text{U}$  in the 87-assembly basket configuration. These assemblies require the use of either the 86-assembly basket, the 82-assembly basket configurations, or reduced maximum enrichments.

Initial reactivity analysis is based on a basket and neutron absorber configuration with the following characteristics:

- a.) Neutron absorbers on all four sides of each tube.
- b.) A single column of weld posts connecting neutron absorber to tube.
- c.) A neutron absorber thickness tolerance of  $\pm 0.005$  inch.
- d.) A neutron absorber width tolerance of  $\pm 0.02$  inch.
- e.) Neutron absorber sheet effective areal density of  $0.027^{10}\text{B g/cm}^2$ .

Differences in reactivity due to system configuration and tolerance changes from these characteristics are evaluated in the subsection titled "Neutron Absorber Modifications."

Changes in neutron absorber areal density are addressed in Section 6.7.6.2.

### **Partial Flooding**

Partial flood cases drain the TSC to the top of the active fuel region. The partial flood reactivity cases investigate reactivity difference between a water reflector over the active fuel region and reflection from the steel lid. The results of the partial flooding study, documented in Table 6.7.6-1, demonstrate that BWR system reactivity is independent of TSC moderator elevations.

### **Moderator Density Variations**

Moderator density variation cases are based on a cask array model generated by surrounding a single cask body with a cylindrical reflecting enclosure. The reflecting body is spaced 20 cm from the cask body to allow exterior moderator density conditions to affect the results. Reactivities calculated for various moderator densities are graphically illustrated in Figure 6.7.6-1 and Figure 6.7.6-2 for the 87-assembly and 82-assembly basket configurations, respectively. Moderator density curves are based on the B9\_79A assembly hybrid at an initial enrichment of 4.0 wt %  $^{235}\text{U}$  and a flooded pellet-to-clad gap. Reactivity increases in the system as TSC interior moderator density rises. Exterior moderator conditions have no significant effect on system reactivity for a flooded TSC. The  $k_{\text{eff}}$  of the dry TSC is less than 0.5 under all exterior conditions.

### **Fabrication Tolerances and Component Shift**

Fabrication tolerances and shift effects are evaluated using representative fuel types from the major core configurations. Nominal fuel assembly characteristics are employed in the tolerance and shifting evaluations.

### **Fabrication Tolerance**

The basket is composed of a set of fuel tubes, pinned together in the tube corners, and located in the TSC cavity with side and corner weldments. Tube location in the basket is controlled by the diagonal dimension across the exterior face of the fuel tube corners. This value is a key dimension for tube array and developed cell size. The tube diagonal is referred to as tube “interface width” in the analysis discussions. Similar to the PWR model, neutron absorber and tube tolerances are evaluated. Neutron absorber thickness studies are based on the minimum  $^{10}\text{B}$  areal density allowed for the design. As such, variations in absorber thickness require adjustments in the sheet composition. The results of the tolerance evaluation for centered fuel assemblies and basket components are included in Table 6.7.6-2. As indicated in the table, little statistically significant information ( $>3\sigma$ ) is available from this study. None of the fabrication-related tolerances, with the exception of maximum tube wall thickness, produce significant reactivity increases when taken independently.

Further evaluations of the component tolerances, including combinations of tolerances, are performed in conjunction with the shifted component configuration.

### **Component Shift**

In addition to the component tolerances, a reactivity study on component shifts is required. Based on the pinned tube arrangement, the only radial shift to be evaluated is the shift of the fuel assembly within the tubes. The tubes are restrained in the corner by pins, minimizing tube shift potential. Evaluations on tube shift are included within the Phase 3 Design Modifications subsection (pages 6.7.6-5 through 6.7.6-7). The results of shift evaluations are shown in Table 6.7.6-2, indicating that shifting the fuel assembly towards the basket center clearly increases system reactivity.

### **Combined Shift and Tolerance Study**

This section evaluates the effect of combining various basket tolerances with the maximum reactivity shift configuration (radial in). The results for this evaluation are shown in Table 6.7.6-3. Similar to the results of the independent basket tolerance evaluation, only fuel tube thickness affects system reactivity to a statistically significant level.

While no statistically significant reactivity difference is found between the cases with and without tolerances applied, the maximum reactivity configuration chosen for the evaluations of all fuel hybrids is as follows.

- Minimum tube width and interface width
- Maximum tube thickness
- Minimum absorber width and maximum thickness
- Fuel assemblies shifted to basket center

This configuration produced reactivities within a  $3\sigma$  uncertainty band of the maximum reported value for all fuel types evaluated, and provides for the minimum separation between adjacent assemblies. The minimum separation reduces the amount of moderation and the corresponding effectiveness of the absorber sheet, which depend on the  $^{10}\text{B}$  neutron capture cross-section in the thermal energy range.

Shift and tolerance evaluations were based on a full, 87-assembly, basket loading. While fabrication tolerance impacts relate to tube and developed cell unit behavior, a limited set of evaluations is performed to verify that the radial shifting in a fuel assembly pattern remains bounding for the 82-assembly basket configuration. The results of this evaluation are shown in Table 6.7.6-4 and demonstrate that the radial shifting in a fuel assembly pattern is limiting.



## Neutron Absorber Modifications

### Phase I Design Modifications

Design options permit the replacement or removal of up to 24 neutron absorber sheets in the 87-assembly and 86-assembly basket peripheral fuel tubes or up to 16 neutron absorber sheets in the 82-assembly baskets. Locations for the optional absorber sheets are shown in Figure 6.7.6-3 and Figure 6.7.6-4, respectively. Replacement sheets for the neutron absorber in the peripheral basket locations are composed of unborated aluminum. Using the most reactive basket and fuel assembly shifting specified in Section 6.7.6.1, each BWR fuel type specified in Section 6.7.5 was analyzed at 4.0 wt %  $^{235}\text{U}$  for the 87-assembly basket and 4.5 wt %  $^{235}\text{U}$  for the 82-assembly basket. As shown in Table 6.7.6-5 and Table 6.7.6-6, no statistically significant reactivity changes are associated with the absorber sheet removal or replacement in the model. Results were calculated using unborated water in the pellet-to-clad gap. Results for the 87-assembly basket may exceed the USL at 4.0 wt%  $^{235}\text{U}$ . For assemblies exceeding the USL, a lower enrichment or the use of either the 86 or 82-assembly basket configuration is required.

Design enhancements introduced after completion of the primary criticality evaluations replaced the single column of weld posts down the tube face centerline with a two-column weld post configuration. The weld post columns are located 1.8 in from the tube centerline. As demonstrated in Table 6.7.6-7, the increased number of weld posts does not significantly change system reactivity. Results were calculated using unborated water in the pellet-to-clad gap.

As the combined reactivity effect of a reduced number of absorber sheets and an increased number of weld posts may exceed the statistically significant threshold ( $> 3\sigma$ ) or potentially result in a  $k_{\text{eff}} + 2\sigma > \text{USL}$  if added as a  $\Delta k$ , the maximum allowed enrichments are calculated with a model containing the reduced number of absorber sheets and the increased number of weld posts.

### Phase 2 Design Modifications

Neutron absorbers may be manufactured at an increased tolerance band. Rather than the  $\pm 0.005$ -inch thickness and  $\pm 0.02$ -inch width tolerance evaluated in the previous calculations, a thickness tolerance of  $\pm 0.006$  inch and a width tolerance of  $\pm 0.08$  inch may be applied. Changes in the absorber thickness tolerance do not result in changes in the areal density of the  $^{10}\text{B}$  absorber material as it is defined at its minimum value regardless of absorber thickness. The focus of the revised analysis is maximum tolerance sheet thickness and minimum width, as the maximum thickness change displaces moderator between fuel and absorber (i.e., potentially decreases absorber efficiency) and the minimum width removes absorber from the system.

Based on the studies described in the previous section, the interface (tube grind flat-to-flat) width controls the critical tube spacing and, therefore, assembly spacing and system reactivity.

#### 6.7.6.2 Allowable Loading Definitions and Maximum System Reactivities

Based on the most reactive basket configuration, each of the fuel assembly types is evaluated at various enrichment levels to determine the maximum enrichment at which  $k_{eff} + 2\sigma$  remains below the USL. Physical limitation on the assemblies allowed for loading are listed in Table 6.7.6-9. The maximum allowed planar average initial enrichment are listed in Table 6.7.6-8 for assemblies with and without partial length rods, where applicable, for a  $0.027^{10}\text{B g/cm}^2$  absorber basket configuration. Table 6.7.6-13 summarizes the enrichment limits for 87-assembly, 86-assembly, 82-assembly, and alternate 82-assembly basket configurations at neutron absorber sheet effective areal densities of 0.027, 0.0225, and  $0.020^{10}\text{B g/cm}^2$ . The 86-assembly and alternate 82-assembly configurations are only applicable to the  $0.027^{10}\text{B/cm}^2$  absorber. In all evaluations, the pellet-to-clad gap is flooded.

Maximum system reactivities are summarized as follows. Analysis results represent maximum reactivity basket and fuel geometry. There are no design basis off-normal or accident transfer cask conditions affecting system reactivity. Therefore, only normal condition results are presented. An accident condition for the concrete cask represents a flooding of the concrete cask to canister annulus. Concrete cask results are based on the maximum fuel mass assembly at the highest allowed enrichment (4.5 wt %  $^{235}\text{U}$ ).

Condition	Pellet to Clad Gap Condition	Maximum Multiplication Factors ( $k_{eff} + 2\sigma$ )	
		Transfer Cask	Concrete Cask
Normal	Dry	0.92900	0.43685
Normal	Wet	0.93679	N/A
Accident / Off-Normal	Dry	N/A	0.42991

Note that there is no statistical difference between normal and accident condition cases, which differ only by the flooding of the pellet-to-clad gap under the “accident condition.”



Figure 6.7.6-1 87-Assembly Basket BWR Water Density Variations

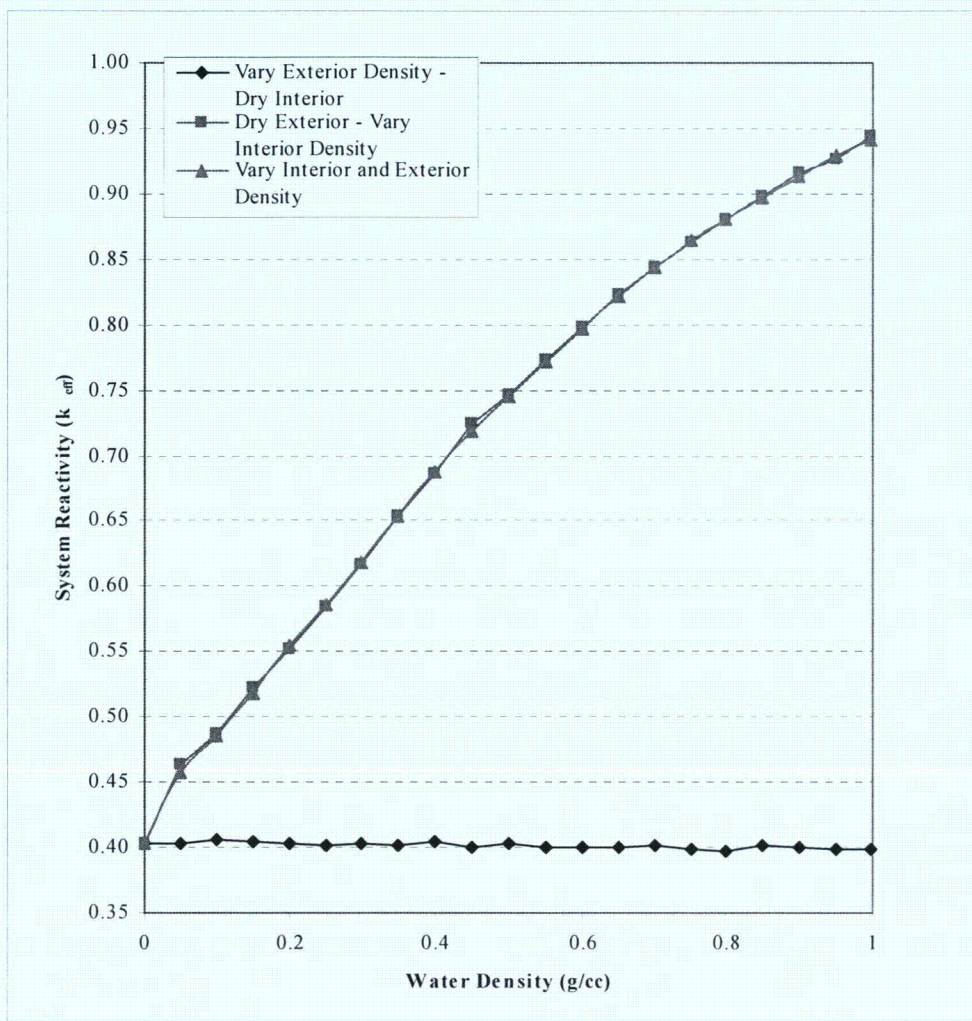


Table 6.7.6-8 BWR System Maximum Reactivity Summary

Assembly Type	Number of Fuel Rods	87-Assembly Basket		82-Assembly Basket	
		Max Initial Enrich. (wt % <sup>235</sup> U)	Reactivity $k_{eff} + 2\sigma$	Max Initial Enrich. (wt % <sup>235</sup> U)	Reactivity $k_{eff} + 2\sigma$
B7_48A	48	4.00%	0.93601	4.50%	0.91816
B7_49A	49	3.80%	0.93206	4.50%	0.92623
B7_49B	49	3.80%	0.93335	4.50%	0.92750
B8_59A	59	3.90%	0.93132	4.50%	0.92395
B8_60A	60	3.80%	0.93167	4.50%	0.92748
B8_60B	60	3.80%	0.93143	4.50%	0.93014
B8_61B	61	3.80%	0.93322	4.50%	0.92787
B8_62A	62	3.80%	0.93469	4.50%	0.93102
B8_63A	63	3.80%	0.93679	4.50%	0.93126
B8_64A	64	3.80%	0.93298	4.50%	0.92949
B8_64B	64	3.60%	0.93222	4.30%	0.93539
B9_72A	72	3.80%	0.93632	4.50%	0.93408
B9_74A	74	3.70%	0.93578	4.40%	0.93440
B9_76A	76	3.50%	0.92937	4.20%	0.93158
B9_79A	79	3.70%	0.93665	4.40%	0.93406
B9_80A	80	3.80%	0.93143	4.50%	0.92882
B10_91A	91	3.80%	0.93566	4.50%	0.93093
B10_92A	92	3.90%	0.93620	4.50%	0.92773
B10_96A	96	3.70%	0.93534	4.40%	0.93498
B10_100A	100	3.60%	0.93295	4.40%	0.93505
B9_74A <sup>a</sup>	74	3.70%	0.93575	4.30%	0.93223
B10_91A <sup>a</sup>	91	3.70%	0.92844	4.50%	0.93477
B10_92A <sup>a</sup>	92	3.80%	0.93488	4.50%	0.93570
B10_96A <sup>a</sup>	96	3.70%	0.93368	4.30%	0.93310
		86-Assembly Basket		Alternate 82-Assembly Basket	
B9_74A <sup>b</sup>	74	3.85%	0.93380	--	--
B10_91A <sup>b</sup>	91	--	--	4.55%	0.93220
B10_92A <sup>b</sup>	92	--	--	4.55%	0.93216

<sup>a</sup> Assemblies contain partial length fuel rods. Partial length rod assemblies are evaluated by removing partial length rods from the lattice. This configuration bounds an assembly with full length rods and combinations of full and partial length rods.

<sup>b</sup> Evaluation results for the bounding case of full length and partial length rods.

Table 6.7.6-9 BWR System Generic Load Limits

Assembly Type	Number of Fuel Rods	Number of Partial Length Rods	Max Pitch (inch)	Min Clad OD (inch)	Min Clad Thick. (inch)	Max Pellet OD (inch)	Max Active Length (inch)	Max Loading (MTU)	87-Assy. Max Enrichment (wt % <sup>235</sup> U)	82-Assy Max Enrichment (wt % <sup>235</sup> U)
B7_48A	48	N/A	0.7380	0.5700	0.03600	0.4900	144.0	0.1981	4.00%	4.50%
B7_49A	49	N/A	0.7380	0.5630	0.03200	0.4880	146.0	0.2034	3.80%	4.50%
B7_49B	49	N/A	0.7380	0.5630	0.03200	0.4910	150.0	0.2115	3.80%	4.50%
B8_59A	59	N/A	0.6400	0.4930	0.03400	0.4160	150.0	0.1828	3.90%	4.50%
B8_60A	60	N/A	0.6417	0.4840	0.03150	0.4110	150.0	0.1815	3.80%	4.50%
B8_60B	60	N/A	0.6400	0.4830	0.03000	0.4140	150.0	0.1841	3.80%	4.50%
B8_61B	61	N/A	0.6400	0.4830	0.03000	0.4140	150.0	0.1872	3.80%	4.50%
B8_62A	62	N/A	0.6417	0.4830	0.02900	0.4160	150.0	0.1921	3.80%	4.50%
B8_63A	63	N/A	0.6420	0.4840	0.02725	0.4195	150.0	0.1985	3.80%	4.50%
B8_64A	64	N/A	0.6420	0.4840	0.02725	0.4195	150.0	0.2017	3.80%	4.50%
B8_64B	64	N/A	0.6090	0.4576	0.02900	0.3913	150.0	0.1755	3.60%	4.30%
B9_72A	72	N/A	0.5720	0.4330	0.02600	0.3740	150.0	0.1803	3.80%	4.50%
B9_74A	74 <sup>a</sup>	8	0.5720	0.4240	0.02390	0.3760	150.0	0.1873	3.70% <sup>b</sup>	4.30%
B9_76A	76	N/A	0.5720	0.4170	0.02090	0.3750	150.0	0.1914	3.50%	4.20%
B9_79A	79	N/A	0.5720	0.4240	0.02390	0.3760	150.0	0.2000	3.70%	4.40%
B9_80A	80	N/A	0.5720	0.4230	0.02950	0.3565	150.0	0.1821	3.80%	4.50%
B10_91A	91 <sup>a</sup>	8	0.5100	0.3957	0.02385	0.3420	150.0	0.1906	3.70%	4.50% <sup>c</sup>
B10_92A	92 <sup>a</sup>	14	0.5100	0.4040	0.02600	0.3455	150.0	0.1966	3.80%	4.50% <sup>c</sup>
B10_96A	96 <sup>a</sup>	12	0.4880	0.3780	0.02430	0.3224	150.0	0.1787	3.70%	4.30%
B10_100A	100	N/A	0.4880	0.3780	0.02430	0.3224	150.0	0.1861	3.60%	4.40%

Note: Assembly characteristics represent cold, unirradiated, nominal configurations.

<sup>a</sup> Assemblies contain partial length fuel rods. Partial length rod assemblies are evaluated by removing partial length rods from the lattice. This configuration bounds an assembly with full length rods and combinations of full and partial length rods.

<sup>b</sup> 3.85% in the 86-assembly basket configuration.

<sup>c</sup> 4.55% in the alternate 82-assembly basket configuration.

Table 6.7.6-12 BWR System Tube Location Study Detail – Baseline to Square  
Tube/Biased Grind/45° Alignment

Assembly Type	87 Assy	$\Delta k/\sigma$	82 Assy	$\Delta k/\sigma$
	(wt% <sup>235</sup> U)		(wt% <sup>235</sup> U)	
B7_48A	4.00%	1.2	4.50%	0.6
B7_49A	3.80%	2.0	4.50%	2.7
B7_49B	3.80%	1.7	4.50%	1.2
B8_59A	3.90%	2.3	4.50%	0.2
B8_60A	3.80%	-0.6	4.50%	1.5
B8_60B	3.80%	2.5	4.50%	-0.5
B8_61B	3.80%	1.4	4.50%	2.9
B8_62A	3.80%	2.0	4.50%	3.0
B8_63A	3.80%	1.2	4.50%	0.2
B8_64A	3.80%	1.5	4.50%	0.7
B8_64B	3.60%	1.2	4.30%	0.6
B9_72A	3.80%	-0.4	4.50%	2.3
B9_74A	3.70%	1.7	4.40%	1.1
B9_76A	3.50%	1.9	4.20%	2.9
B9_79A	3.70%	0.1	4.40%	0.8
B9_80A	3.80%	2.7	4.50%	0.7
B10_91A	3.80%	1.2	4.50%	0.1
B10_92A	3.90%	2.9	4.50%	-0.8
B10_96A	3.70%	1.2	4.40%	0.8
B10_100A	3.60%	-1.1	4.40%	1.8
B9_74A	3.70%	1.1	4.30%	2.0
B10_91A	3.70%	2.2	4.50%	1.7
B10_92A	3.80%	2.0	4.50%	0.7
B10_96A	3.70%	1.3	4.30%	-0.2

**Table 6.7.6-13 BWR Fuel Assembly Loading Criteria  
(Enrichment Limits)**

	Max. Initial Enrichment <sup>a</sup> ( wt % <sup>235</sup> U)					
	Absorber <sup>b</sup> 0.027 <sup>10</sup> B g/cm <sup>2</sup>		Absorber 0.0225 <sup>10</sup> B g/cm <sup>2</sup>		Absorber 0.02 <sup>10</sup> B g/cm <sup>2</sup>	
	87-Assy Basket	82-Assy Basket	87-Assy Basket	82-Assy Basket	87-Assy Basket	82-Assy Basket
B7_48A	4.0%	4.5%	3.7%	4.5%	3.6%	4.4%
B7_49A	3.8%	4.5%	3.6%	4.4%	3.5%	4.3%
B7_49B	3.8%	4.5%	3.6%	4.4%	3.5%	4.2%
B8_59A	3.9%	4.5%	3.7%	4.5%	3.6%	4.3%
B8_60A	3.8%	4.5%	3.7%	4.4%	3.5%	4.2%
B8_60B	3.8%	4.5%	3.6%	4.3%	3.5%	4.2%
B8_61B	3.8%	4.5%	3.6%	4.3%	3.5%	4.2%
B8_62A	3.8%	4.5%	3.6%	4.3%	3.5%	4.1%
B8_63A	3.8%	4.5%	3.6%	4.3%	3.4%	4.2%
B8_64A	3.8%	4.5%	3.6%	4.3%	3.5%	4.2%
B8_64B	3.6%	4.3%	3.4%	4.1%	3.3%	4.0%
B9_72A	3.8%	4.5%	3.6%	4.3%	3.4%	4.1%
B9_74A	3.7% <sup>c</sup>	4.3%	3.4%	4.1%	3.4%	4.0%
B9_76A	3.5%	4.2%	3.4%	4.0%	3.3%	3.9%
B9_79A	3.7%	4.4%	3.4%	4.2%	3.3%	4.0%
B9_80A	3.8%	4.5%	3.6%	4.3%	3.5%	4.2%
B10_91A	3.7%	4.5% <sup>d</sup>	3.6%	4.3%	3.5%	4.1%
B10_92A	3.8%	4.5% <sup>d</sup>	3.6%	4.3%	3.5%	4.1%
B10_96A	3.7%	4.3%	3.5%	4.1%	3.4%	4.0%
B10_100A	3.6%	4.4%	3.5%	4.1%	3.4%	4.0%

<sup>a</sup> Maximum planar average.

<sup>b</sup> Borated aluminum neutron absorber sheet effective areal <sup>10</sup>B density.

<sup>c</sup> 3.85% in the 86-assembly basket configuration.

<sup>d</sup> 4.55% in the alternate 82-assembly basket configuration.

significantly affect system reactivity. Increased plate thickness would add parasitic absorber to the system, while further separating fissile material masses and, therefore, does not represent a criticality concern.

#### **6.7.8.3      Sample Input Files**

Three sample damaged fuel basket input files are provided. Figure 6.7.8-2 contains an input file for an undamaged assembly loaded into the four DFCs. Figure 6.7.8-3 contains an input file for an unclad rod array input file without inserts. Figure 6.7.8-4 contains a mixture input file that is also partially flooded. In this input file, the flooded mixture elevation is at the top of the active fuel in the DFC.

#### **6.7.8.4      Damaged Fuel Characterization**

Starting with the most reactive basket configuration determined for undamaged fuel, various damaged fuel configurations are evaluated. Each DFC configuration is evaluated at 0.036, 0.030 and 0.027 g  $^{10}\text{B}/\text{cm}^2$  effective absorber densities with and without inserts in the fuel assembly guide tubes. Use of the maximum reactivity configuration for undamaged fuel as the baseline is appropriate because it maintains the most reactive configuration of the 33 undamaged fuel assemblies and minimizes the separation between the damaged fuel assemblies and the rest of the payload.

#### **Clad Rods – Grid Undamaged**

DFC evaluations are initiated by placing undamaged fuel assemblies into the DFC to demonstrate the effect of the additional stainless steel shell and thicker corner weldment. Undamaged rods within a nominal lattice/pitch configuration are identified by the acronym “IAA” in the DFC content description.

With all 37 assemblies modeled as undamaged at their limiting enrichments (see Section 6.7.3.2), the DFC and corner weldment material has no statistically significant effect on system reactivity with average reactivity changes of 0.44, 0.55 and 0.48  $\Delta k/\sigma$  for the 0.036, 0.030 and 0.027 g  $^{10}\text{B}/\text{cm}^2$  absorbers, respectively. Sample results for the 0.036 g  $^{10}\text{B}/\text{cm}^2$  without inserts are presented in Table 6.7.8-1. Similar to results of the undamaged fuel basket evaluations, the presence or absence of the inserts has no statistically significant effect on system performance.

As the undamaged fuel basket enrichment limits resulted in reactivities (eigenvalues) within a very small margin to the USL, the statistical nature of the Monte Carlo evaluation resulted in a limited number of enrichment/soluble boron/fuel type combinations exceeding the USL. The



maximum required reduction in enrichment for all combinations to remain below the USL is 0.1 wt %  $^{235}\text{U}$  under the undamaged fuel basket limits.

The system is designed to allow loading of undamaged fuel assemblies into the four designated DFC locations in the DF basket assembly without the use of a DFC. The difference between this configuration and undamaged fuel in the DFC evaluated previously in this section is the presence of the 0.048-inch thick DFC wall. Given that the 1.125-inch inner wall plate separates DFC content from adjoining assemblies in both models, there is no expectation of statistically resolvable reactivity differences between models with and without a DFC. Evaluating each primary array type at 0.036 and 0.027 g/cm<sup>2</sup>  $^{10}\text{B}$  concentration in the absorber sheets, with minimum (1500 ppm) and maximum (2500ppm) borated water concentrations, resulted in an absolute average change in reactivity of 0.30  $\Delta\text{k}/\sigma$ . All cases remain under the USL of 0.9376. Loading of undamaged fuel into the four designated DFC locations in the DF basket assembly without a DFC is, therefore, acceptable.

#### **Unclad Rods – Loose Pellet Stack**

In this stage of the DFC evaluations, damaged fuel is postulated to lose its cladding and pellets are allowed to separate. As PWR assemblies are typically undermoderated, the removal of cladding, in conjunctions with pitch variations, has the potential to increase system reactivity. Pellet array pitch is allowed to increase until it fills the DFC opening. Clad removal and pitch modification affects system reactivity by varying moderator between fuel rods, therefore, changing neutron thermalization and utilization, while simultaneously varying the neutron absorber quantity in the form of soluble boron in the moderator. These are offsetting phenomena (i.e., increasing pitch increases the borated moderator quantity between fuel rods, which improves thermalization of fast fission neutron for absorption in the fuel, while also increasing the  $^{10}\text{B}$  absorber quantity between rods and thereby reducing thermal neutron flux). As shown in Table 6.7.8-2, a sample analysis using the 0.036 g  $\text{B}^{10}/\text{cm}^2$  absorber at a 2250 ppm soluble boron content, the result of the offsetting phenomena is that there is no statistically resolvable trend of pellet pitch to system reactivity (pitch indicated is either the nominal, as assembly design pitch, the maximum pitch allowed by the DFC opening, or the average pitch between nominal and maximum). As lower soluble boron shifts the trend towards increasing system reactivity as a function of increasing pitch, maximum pitch is applied to the remaining pellet evaluations.

Similar to the undamaged fuel assembly in the DFC evaluation, the loose pellets study results in no statistically significant change in system reactivity, with average reactivity changes of 0.57, 0.52, and 0.49  $\Delta\text{k}/\sigma$  for the 0.036, 0.030, and 0.027 g  $^{10}\text{B}/\text{cm}^2$  absorbers, respectively. Sample results for the 0.036 g  $^{10}\text{B}/\text{cm}^2$  without inserts are presented in Table 6.7.8-3.

Table 6.7.8-1 Sample Results for Undamaged Fuel in DFC (Damaged Fuel Basket)

Assembly Type	Minimum 1500 ppm B Max. Initial Enrichment	Reactivity			Minimum 2000 ppm B Max. Initial Enrichment	Reactivity			Minimum 2500 ppm B Max. Initial Enrichment	Reactivity		
		(wt% <sup>235</sup> U)	σ	k <sub>eff</sub> + 2σ		Δk/σ	(wt% <sup>235</sup> U)	σ		k <sub>eff</sub> + 2σ	Δk/σ	(wt% <sup>235</sup> U)
BW15H1	3.7%	0.00073	0.92965		4.4%	0.00073	0.93538		5.0%	0.00070	0.93416	
	3.7%	0.00073	0.93240	2.66	4.4%	0.00072	0.93503	-0.34	5.0%	0.00073	0.93594	1.76
BW15H2	3.7%	0.00068	0.93581		4.3%	0.00071	0.93498		4.9%	0.00072	0.93317	
	3.7%	0.00073	0.93607		4.3%	0.00073	0.93763	2.60	4.9%	0.00077	0.93435	
BW15H3					4.2%	0.00076	0.92842					
	3.7%	0.00071	0.93700		4.3%	0.00074	0.93514		4.9%	0.00072	0.93415	
	3.7%	0.00070	0.93818	1.18	4.3%	0.00074	0.93697	1.75	4.9%	0.00074	0.93686	2.62
BW15H4	3.6%	0.00070	0.93066									
	3.8%	0.00071	0.93146		4.5%	0.00073	0.93364		5.0%	0.00073	0.92368	
BW17H1	3.8%	0.00074	0.93284		4.5%	0.00078	0.93488	1.16	5.0%	0.00075	0.92548	
	3.7%	0.00073	0.93296		4.3%	0.00070	0.93382		5.0%	0.00072	0.93716	
	3.7%	0.00071	0.93589	2.88	4.3%	0.00072	0.93432	0.50	5.0%	0.00072	0.94043	3.21
CE14H1									4.9%	0.00072	0.93171	
	4.5%	0.00073	0.93518		5.0%	0.00078	0.91583		5.0%	0.00078	0.87766	
CE16H1	4.5%	0.00081	0.93353		5.0%	0.00074	0.91808	2.09	5.0%	0.00071	0.87934	
	4.4%	0.00075	0.93329		5.0%	0.00077	0.92515		5.0%	0.00080	0.88644	
WE14H1	4.4%	0.00074	0.93299	-0.28	5.0%	0.00073	0.92359	-1.47	5.0%	0.00079	0.88529	-1.02
	4.7%	0.00073	0.93682		5.0%	0.00073	0.90625		5.0%	0.00077	0.86657	
WE15H1	4.7%	0.00077	0.93520	-1.53	5.0%	0.00075	0.90620	-0.05	5.0%	0.00074	0.86864	1.94
	3.8%	0.00072	0.93295		4.5%	0.00078	0.93614		5.0%	0.00074	0.92470	
WE15H2	3.8%	0.00079	0.93092		4.5%	0.00074	0.93534	-0.74	5.0%	0.00075	0.92747	
	4.0%	0.00077	0.93454		4.7%	0.00072	0.93520		5.0%	0.00071	0.91355	
WE17H1	4.0%	0.00071	0.93602	1.41	4.7%	0.00074	0.93494	-0.25	5.0%	0.00073	0.91313	-0.41
	3.7%	0.00074	0.92921		4.4%	0.00076	0.93628		5.0%	0.00070	0.93402	
	3.7%	0.00070	0.93064		4.4%	0.00074	0.93712	0.79	5.0%	0.00073	0.93419	
WE17H2	4.0%	0.00073	0.93415		4.7%	0.00071	0.93342		5.0%	0.00071	0.91309	
	4.0%	0.00076	0.93355	-0.57	4.7%	0.00072	0.93507	1.63	5.0%	0.00070	0.91196	-1.13

Table 6.7.8-2 DFC Unclad Rod Array Pitch Study Results

Assembly	Enrichment (wt% <sup>235</sup> U)	Reactivity with Maximum Pitch		Reactivity with Average Pitch			Reactivity with Nominal Pitch		
		$\sigma$	$k_{eff} + 2\sigma$	$\sigma$	$k_{eff} + 2\sigma$	$\Delta k/\sigma$	$\sigma$	$k_{eff} + 2\sigma$	$\Delta k/\sigma$
BW15H1	4.7%	0.00071	0.93472	0.00072	0.93607	1.34	0.00075	0.93646	1.68
BW15H2	4.6%	0.00073	0.93589	0.00075	0.93641	0.50	0.00076	0.93473	-1.10
BW15H3	4.6%	0.00066	0.93711	0.00073	0.93765	0.55	0.00078	0.93778	0.66
BW15H4	4.8%	0.00071	0.93398	0.00077	0.93390	-0.08	0.00075	0.93433	0.34
BW17H1	4.6%	0.00073	0.93383	0.00072	0.93446	0.61	0.00073	0.93466	0.80
CE14H1	5.0%	0.00079	0.89735	0.00077	0.89484	-2.28	0.00074	0.89522	-1.97
CE16H1	5.0%	0.00075	0.90438	0.00074	0.90395	-0.41	0.00077	0.90557	1.11
WE14H1	5.0%	0.00077	0.88574	0.00078	0.88600	0.24	0.00079	0.88591	0.15
WE15H1	4.8%	0.00074	0.93410	0.00075	0.93307	-0.98	0.00075	0.93368	-0.40
WE15H2	5.0%	0.00079	0.93251	0.00075	0.93201	-0.46	0.00073	0.93239	-0.11
WE17H1	4.7%	0.00073	0.93349	0.00075	0.93626	2.65	0.00074	0.93546	1.90
WE17H2	5.0%	0.00073	0.93227	0.00071	0.93048	-1.76	0.00077	0.93145	-0.77

Table 6.7.8-3 Sample Results for Unclad Rod/Loose Pellet Fuel in DFC (Damaged Fuel Basket)

Assembly Type	Minimum 1500 ppm B					Minimum 2000 ppm B					Minimum 2500 ppm B				
	Max. Initial					Max. Initial					Max. Initial				
	Enrichment	Reactivity				Enrichment	Reactivity				Enrichment	Reactivity			
	(wt% <sup>235</sup> U)	$\sigma$	$k_{eff} + 2\sigma$	$\Delta k/\sigma$	(wt% <sup>235</sup> U)	$\sigma$	$k_{eff} + 2\sigma$	$\Delta k/\sigma$	(wt% <sup>235</sup> U)	$\sigma$	$k_{eff} + 2\sigma$	$\Delta k/\sigma$			
BW15H1	3.7%	0.00073	0.92965		4.4%	0.00073	0.93538		5.0%	0.00070	0.93416				
	3.7%	0.00072	0.93127	1.58	4.4%	0.00073	0.93700	1.57	5.0%	0.00075	0.93608	1.87			
BW15H2	3.7%	0.00068	0.93581		4.3%	0.00071	0.93498		4.9%	0.00072	0.93317				
	3.7%	0.00070	0.93704	1.26	4.3%	0.00075	0.93589	0.88	4.9%	0.00073	0.93554	2.31			
BW15H3	3.7%	0.00071	0.93700		4.3%	0.00074	0.93514		4.9%	0.00072	0.93415				
	3.7%	0.00069	0.93818	1.19	4.3%	0.00069	0.93668	1.52	4.9%	0.00071	0.93579	1.62			
	3.6%	0.00072	0.93134												
BW15H4	3.8%	0.00071	0.93146		4.5%	0.00073	0.93364		5.0%	0.00073	0.92368				
	3.8%	0.00072	0.93393	2.44	4.5%	0.00073	0.93438	0.72	5.0%	0.00074	0.92418	0.48			
BW17H1	3.7%	0.00073	0.93296		4.3%	0.00070	0.93382		5.0%	0.00072	0.93716				
	3.7%	0.00072	0.93545	2.43	4.3%	0.00071	0.93443	0.61	5.0%	0.00069	0.93818	1.02			
									4.9%	0.00072	0.93174				
CE14H1	4.5%	0.00073	0.93518		5.0%	0.00078	0.91583		5.0%	0.00078	0.87766				
	4.5%	0.00077	0.93387	-1.23	5.0%	0.00079	0.91801	1.96	5.0%	0.00081	0.87926	1.42			
CE16H1	4.4%	0.00075	0.93329		5.0%	0.00077	0.92515		5.0%	0.00080	0.88644				
	4.4%	0.00076	0.93404	0.70	5.0%	0.00076	0.92362	-1.41	5.0%	0.00073	0.88414	-2.12			
WE14H1	4.7%	0.00073	0.93682		5.0%	0.00073	0.90625		5.0%	0.00077	0.86657				
	4.7%	0.00074	0.93777	0.91	5.0%	0.00077	0.90693	0.64	5.0%	0.00074	0.86736	0.74			
	4.6%	0.00074	0.93090												
WE15H1	3.8%	0.00072	0.93295		4.5%	0.00078	0.93614		5.0%	0.00074	0.92470				
	3.8%	0.00070	0.93213	-0.82	4.5%	0.00075	0.93689	0.69	5.0%	0.00072	0.92569	0.96			
WE15H2	4.0%	0.00077	0.93454		4.7%	0.00072	0.93520		5.0%	0.00071	0.91355				
	4.0%	0.00074	0.93465	0.10	4.7%	0.00070	0.93439	-0.81	5.0%	0.00076	0.91163	-1.85			
WE17H1	3.7%	0.00074	0.92921		4.4%	0.00076	0.93628		5.0%	0.00070	0.93402				
	3.7%	0.00075	0.92991	0.66	4.4%	0.00070	0.93500	-1.24	5.0%	0.00072	0.93484	0.82			
WE17H2	4.0%	0.00073	0.93415		4.7%	0.00071	0.93342		5.0%	0.00071	0.91309				
	4.0%	0.00072	0.93379	-0.35	4.7%	0.00074	0.93522	1.76	5.0%	0.00072	0.91258	-0.50			

Table 6.7.8-4 DFC Missing Rod Study

# Missing Rods	Reactivity			
	$k_{eff}$	$\sigma$	$k_{eff} + 2\sigma$	$\Delta k/\sigma$
0	0.93574	0.00072	0.93718	-
1	0.9357	0.0007	0.93710	-0.08
4	0.93565	0.00075	0.93715	-0.03
8	0.93526	0.00072	0.93670	-0.47
12	0.93574	0.00071	0.93716	-0.02
16	0.93492	0.00075	0.93642	-0.73
20	0.93544	0.0007	0.93684	-0.34
32	0.93535	0.00075	0.93685	-0.32
50	0.93334	0.00067	0.93468	-2.54

Table 6.7.8-5 Sample DFC Fuel Mixture Height Study Results

Assembly Type	Mixture Height Percent DFC Cavity	Minimum 1500 ppm B Max. Initial Enrichment (wt% <sup>235</sup> U)	Reactivity $k_{eff} + 2\sigma$	Minimum 2000 ppm B Max. Initial Enrichment (wt% <sup>235</sup> U)	Reactivity $k_{eff} + 2\sigma$	Minimum 2500 ppm B Max. Initial Enrichment (wt% <sup>235</sup> U)	Reactivity $k_{eff} + 2\sigma$
BW15H1	50	3.7%	0.93203	4.4%	0.93744	5.0%	0.93465
	60	3.7%	0.93267	4.3%	0.93287	4.9%	0.93410
	70	3.7%	0.93273	4.3%	0.93553	4.9%	0.93356
	80	3.7%	0.93300	4.3%	0.93461	4.9%	0.93303
	90	3.7%	0.93323	4.3%	0.93335	4.9%	0.93382
	100	3.7%	0.93212	4.3%	0.93387	4.9%	0.93372
BW17H1	50	3.7%	0.93527	4.3%	0.93451	4.9%	0.93511
	60	3.7%	0.93596	4.3%	0.93658	4.9%	0.93623
	70	3.6%	0.92912	4.3%	0.93688	4.9%	0.93675
	80	3.7%	0.93683	4.2%	0.93055	4.9%	0.93691
	90	3.7%	0.93517	4.2%	0.92919	4.9%	0.93694
	100	3.7%	0.93737	4.3%	0.93706	4.9%	0.93686
CE14H1	50	4.5%	0.93318	5.0%	0.91737	5.0%	0.88014
	60	4.5%	0.93691	5.0%	0.91876	5.0%	0.88041
	70	4.5%	0.93728	5.0%	0.91941	5.0%	0.88169
	80	4.5%	0.93586	5.0%	0.91827	5.0%	0.88088
	90	4.5%	0.93320	5.0%	0.91968	5.0%	0.88176
	100	4.5%	0.93383	5.0%	0.91738	5.0%	0.88101
CE16H1	50	4.4%	0.93480	5.0%	0.92518	5.0%	0.88682
	60	4.4%	0.93399	5.0%	0.92902	5.0%	0.88868
	70	4.4%	0.93472	5.0%	0.92689	5.0%	0.88974
	80	4.4%	0.93575	5.0%	0.92611	5.0%	0.88962
	90	4.4%	0.93515	5.0%	0.92598	5.0%	0.88946
	100	4.4%	0.93395	5.0%	0.92705	5.0%	0.89002
WE14H1	50	4.7%	0.93751	5.0%	0.90583	5.0%	0.86685
	60	4.7%	0.93750	5.0%	0.90787	5.0%	0.87013
	70	4.7%	0.93733	5.0%	0.90738	5.0%	0.87007
	80	4.7%	0.93717	5.0%	0.90915	5.0%	0.86996
	90	4.7%	0.93660	5.0%	0.90841	5.0%	0.86892
	100	4.7%	0.93717	5.0%	0.90721	5.0%	0.86698
WE15H1	50	3.8%	0.93095	4.5%	0.93691	5.0%	0.92753
	60	3.8%	0.93313	4.5%	0.93737	5.0%	0.93028
	70	3.8%	0.93436	4.5%	0.93735	5.0%	0.93016
	80	3.8%	0.93408	4.4%	0.93060	5.0%	0.92991
	90	3.8%	0.93436	4.4%	0.93150	5.0%	0.92964
	100	3.8%	0.93538	4.5%	0.93697	5.0%	0.92849
WE17H2	50	4.0%	0.93462	4.7%	0.93661	5.0%	0.91502
	60	3.9%	0.92899	4.6%	0.93299	5.0%	0.91658
	70	3.9%	0.92934	4.6%	0.93247	5.0%	0.91559
	80	4.0%	0.93563	4.6%	0.93343	5.0%	0.91805
	90	4.0%	0.93669	4.6%	0.93159	5.0%	0.91537
	100	3.9%	0.92870	4.7%	0.93653	5.0%	0.91664

**Table 6.7.8-6 DFC Fuel Mixture Maximum Reactivity Height for 0.036 g/cm<sup>2</sup> <sup>10</sup>B – No Inserts**

Assembly	Parameter	Minimum 1500 ppm	Minimum 1750 ppm	Minimum 2000 ppm	Minimum 2250 ppm	Minimum 2500 ppm
BW15H1	Enrichment	3.7%	4.0%	4.3%	4.6%	4.9%
	k <sub>eff</sub> +2σ	0.93323	0.93439	0.93553	0.93571	0.93410
	Configuration	MIX90	MIX70	MIX70	MIX70	MIX60
BW15H2	Enrichment	3.6%	3.9%	4.2%	4.5%	4.8%
	k <sub>eff</sub> +2σ	0.93147	0.93234	0.93312	0.93368	0.93355
	Configuration	MIX80	MIX80	MIX90	MIX80	MIX70
BW15H3	Enrichment	3.6%	3.9%	4.2%	4.5%	4.8%
	k <sub>eff</sub> +2σ	0.93380	0.93398	0.93450	0.93518	0.93674
	Configuration	MIX80	MIX100	MIX90	MIX80	MIX80
BW15H4	Enrichment	3.8%	4.1%	4.4%	4.7%	5.0%
	k <sub>eff</sub> +2σ	0.93650	0.93692	0.93368	0.93302	0.93165
	Configuration	MIX80	MIX90	MIX70	MIX70	MIX70
BW17H1	Enrichment	3.6%	3.9%	4.2%	4.5%	4.9%
	k <sub>eff</sub> +2σ	0.92912	0.92805	0.93055	0.93166	0.93694
	Configuration	MIX70	MIX60	MIX80	MIX90	MIX90
CE14H1	Enrichment	4.5%	4.9%	5.0%	5.0%	5.0%
	k <sub>eff</sub> +2σ	0.93728	0.93616	0.91968	0.90123	0.88176
	Configuration	MIX70	MIX70	MIX90	MIX60	MIX90
CE16H1	Enrichment	4.4%	4.7%	5.0%	5.0%	5.0%
	k <sub>eff</sub> +2σ	0.93575	0.93022	0.92902	0.90938	0.89002
	Configuration	MIX80	MIX70	MIX60	MIX80	MIX100
WE14H1	Enrichment	4.7%	5.0%	5.0%	5.0%	5.0%
	k <sub>eff</sub> +2σ	0.93751	0.92989	0.90915	0.88872	0.87013
	Configuration	MIX50	MIX60	MIX80	MIX80	MIX60
WE15H1	Enrichment	3.8%	4.1%	4.4%	4.7%	5.0%
	k <sub>eff</sub> +2σ	0.93538	0.93541	0.93150	0.93075	0.93028
	Configuration	MIX100	MIX70	MIX90	MIX80	MIX60
WE15H2	Enrichment	3.9%	4.3%	4.6%	5.0%	5.0%
	k <sub>eff</sub> +2σ	0.93365	0.93581	0.93464	0.93720	0.91729
	Configuration	MIX70	MIX70	MIX70	MIX60	MIX70
WE17H1	Enrichment	3.7%	4.0%	4.3%	4.6%	4.9%
	k <sub>eff</sub> +2σ	0.93327	0.93385	0.93517	0.93304	0.93417
	Configuration	MIX80	MIX90	MIX70	MIX90	MIX90
WE17H2	Enrichment	3.9%	4.3%	4.6%	5.0%	5.0%
	k <sub>eff</sub> +2σ	0.92934	0.93490	0.93343	0.93722	0.91805
	Configuration	MIX70	MIX70	MIX80	MIX70	MIX80

Table 6.7.8-7 DFC Fuel Mixture Maximum Reactivity Height for 0.036 g/cm<sup>2</sup> <sup>10</sup>B – Inserts

Assembly	Parameter	Minimum 1500 ppm	Minimum 1750 ppm	Minimum 2000 ppm	Minimum 2250 ppm	Minimum 2500 ppm
BW15H1	Enrichment	3.7%	4.0%	4.3%	4.6%	4.9%
	k <sub>eff</sub> +2σ	0.93185	0.93353	0.93536	0.93570	0.93666
	Configuration	MIX70	MIX90	MIX80	MIX70	MIX100
BW15H2	Enrichment	3.7%	3.9%	4.2%	4.5%	4.8%
	k <sub>eff</sub> +2σ	0.93732	0.92857	0.93295	0.93446	0.93579
	Configuration	MIX80	MIX100	MIX80	MIX80	MIX70
BW15H3	Enrichment	3.6%	3.9%	4.2%	4.5%	4.8%
	k <sub>eff</sub> +2σ	0.92862	0.93150	0.93343	0.93497	0.93723
	Configuration	MIX80	MIX70	MIX80	MIX100	MIX80
BW15H4	Enrichment	3.8%	4.1%	4.4%	4.7%	5.0%
	k <sub>eff</sub> +2σ	0.93574	0.93435	0.93620	0.93567	0.93522
	Configuration	MIX70	MIX70	MIX80	MIX70	MIX70
BW17H1	Enrichment	3.7%	4.0%	4.3%	4.5%	4.8%
	k <sub>eff</sub> +2σ	0.93562	0.93574	0.93608	0.93184	0.93432
	Configuration	MIX70	MIX70	MIX80	MIX80	MIX70
CE14H1	Enrichment	4.4%	4.8%	5.0%	5.0%	5.0%
	k <sub>eff</sub> +2σ	0.93160	0.93612	0.92831	0.91230	0.89638
	Configuration	MIX80	MIX70	MIX70	MIX60	MIX80
CE16H1	Enrichment	4.4%	4.7%	5.0%	5.0%	5.0%
	k <sub>eff</sub> +2σ	0.93572	0.93177	0.93160	0.91441	0.89748
	Configuration	MIX80	MIX80	MIX70	MIX70	MIX90
WE14H1	Enrichment	4.8%	5.0%	5.0%	5.0%	5.0%
	k <sub>eff</sub> +2σ	0.93667	0.92601	0.90543	0.88775	0.86940
	Configuration	MIX90	MIX60	MIX80	MIX70	MIX70
WE15H1	Enrichment	3.8%	4.1%	4.4%	4.7%	5.0%
	k <sub>eff</sub> +2σ	0.93169	0.93364	0.93274	0.93291	0.93317
	Configuration	MIX70	MIX80	MIX70	MIX70	MIX100
WE15H2	Enrichment	4.0%	4.3%	4.6%	4.9%	5.0%
	k <sub>eff</sub> +2σ	0.93503	0.93522	0.93350	0.93434	0.92239
	Configuration	MIX90	MIX80	MIX90	MIX80	MIX90
WE17H1	Enrichment	3.8%	4.1%	4.4%	4.7%	4.9%
	k <sub>eff</sub> +2σ	0.93430	0.93452	0.93541	0.93710	0.93099
	Configuration	MIX90	MIX70	MIX70	MIX80	MIX90
WE17H2	Enrichment	4.0%	4.3%	4.7%	5.0%	5.0%
	k <sub>eff</sub> +2σ	0.93202	0.93278	0.93680	0.93721	0.91961
	Configuration	MIX60	MIX80	MIX80	MIX90	MIX70



Table 6.7.8-8 DFC Partial Flooding Mixture Moderator Density Study  
(BW Fuel 3.7 wt %  $^{235}\text{U}$ , 1500 ppm B)

Mixture Fraction of DFC Cavity	Water Density in Fuel/Water Mixture							
	0.9982 g/cm <sup>3</sup>		0.9 g/cm <sup>3</sup>		$\Delta$ to 0.9982 g/cm <sup>3</sup>	0.8 g/cm <sup>3</sup>		$\Delta$ to 0.9982 g/cm <sup>3</sup>
	$k_{\text{eff}}+2\sigma$	$\sigma$	$k_{\text{eff}}+2\sigma$	$\sigma$	$\Delta k/\sigma$	$k_{\text{eff}}+2\sigma$	$\sigma$	$\Delta k/\sigma$
25%	0.92697	0.00071	0.92642	0.00070	-0.6	0.92611	0.00072	-0.9
30%	0.92726	0.00070	0.92584	0.00074	-1.4	0.92685	0.00071	-0.4
40%	0.92924	0.00074	0.92973	0.00075	0.5	0.92986	0.00074	0.6
50%	0.93155	0.00072	0.93056	0.00070	-1.0	0.92967	0.00071	-1.9
60%	0.93286	0.00073	0.93171	0.00069	-1.1	0.93009	0.00072	-2.7
70%	0.93492	0.00074	0.93173	0.00072	-3.1	0.93192	0.00069	-3.0
80%	0.93351	0.00074	0.93300	0.00072	-0.5	0.93167	0.00073	-1.8
90%	0.93485	0.00071	0.93417	0.00073	-0.7	0.93347	0.00071	-1.4
100%	0.93212	0.00075	0.93181	0.00073	-0.3	0.93161	0.00075	-0.5

Table 6.7.8-9 PWR Damaged Fuel Storage Cask Analyses Results (BW Fuel 5.0 wt % <sup>235</sup>U)

Water Density (g/cm <sup>3</sup> )			DFC Configuration	0 ppm B	Reactivity
Interior	Exterior	Inside DFC		Max. Initial Enrichment	
				(wt% <sup>235</sup> U)	k <sub>eff</sub> + 2σ
0.0001	0.0001	0.0001	IAA	5.0%	0.48727
0.0001	0.0001	0.0001	URA	5.0%	0.48578
0.0001	0.0001	0.0001	MIX50	5.0%	0.49142
0.0001	0.0001	0.0001	MIX60	5.0%	0.49042
0.0001	0.0001	0.0001	MIX70	5.0%	0.48882
0.0001	0.0001	0.0001	MIX80	5.0%	0.48578
0.0001	0.0001	0.0001	MIX90	5.0%	0.48614
0.0001	0.0001	0.0001	MIX100	5.0%	0.48210
0.0001	0.9982	0.0001	IAA	5.0%	0.48064
0.0001	0.9982	0.0001	URA	5.0%	0.48140
0.0001	0.9982	0.0001	MIX50	5.0%	0.48211
0.0001	0.9982	0.0001	MIX60	5.0%	0.48014
0.0001	0.9982	0.0001	MIX70	5.0%	0.48015
0.0001	0.9982	0.0001	MIX80	5.0%	0.48030
0.0001	0.9982	0.0001	MIX90	5.0%	0.47815
0.0001	0.9982	0.0001	MIX100	5.0%	0.47796

Notes:

IAA - undamaged assembly

URA - unclad rod array

MIX - fuel mixture cases (in the context of storage analysis various fissile material heights; no moderator)

**Table 6.7.8-10 PWR Damaged Fuel Assembly Allowable Loading  
(Enrichment/Soluble Boron Limits)**

Soluble Boron	Max. Initial Enrichment (wt % <sup>235</sup> U)														
	Absorber <sup>a</sup> 0.036 <sup>10</sup> B g/cm <sup>2</sup>					Absorber <sup>a</sup> 0.030 <sup>10</sup> B g/cm <sup>2</sup>					Absorber <sup>a</sup> 0.027 <sup>10</sup> B g/cm <sup>2</sup>				
	1500 (ppm)	1750 (ppm)	2000 (ppm)	2250 (ppm)	2500 (ppm)	1500 (ppm)	1750 (ppm)	2000 (ppm)	2250 (ppm)	2500 (ppm)	1500 (ppm)	1750 (ppm)	2000 (ppm)	2250 (ppm)	2500 (ppm)
BW15H1	3.7%	4.0%	4.3%	4.6%	4.9%	3.6%	3.9%	4.2%	4.5%	4.7%	3.6%	3.8%	4.1%	4.4%	4.7%
BW15H2	3.6%	3.9%	4.2%	4.5%	4.8%	3.6%	3.8%	4.1%	4.4%	4.7%	3.5%	3.8%	4.1%	4.3%	4.6%
BW15H3	3.6%	3.9%	4.2%	4.5%	4.8%	3.5%	3.8%	4.1%	4.4%	4.6%	3.5%	3.8%	4.0%	4.3%	4.6%
BW15H4	3.8%	4.1%	4.4%	4.7%	5.0%	3.7%	4.0%	4.3%	4.6%	4.9%	3.6%	3.9%	4.2%	4.5%	4.8%
BW17H1	3.6%	3.9%	4.2%	4.5%	4.8%	3.6%	3.9%	4.1%	4.4%	4.7%	3.5%	3.8%	4.1%	4.4%	4.6%
CE14H1	4.4%	4.8%	5.0%	5.0%	5.0%	4.3%	4.7%	5.0%	5.0%	5.0%	4.3%	4.6%	4.9%	5.0%	5.0%
CE16H1	4.4%	4.7%	5.0%	5.0%	5.0%	4.2%	4.6%	5.0%	5.0%	5.0%	4.2%	4.5%	4.9%	5.0%	5.0%
WE14H1	4.6%	5.0%	5.0%	5.0%	5.0%	4.5%	5.0%	5.0%	5.0%	5.0%	4.5%	4.9%	5.0%	5.0%	5.0%
WE15H1	3.8%	4.1%	4.4%	4.7%	5.0%	3.7%	4.0%	4.3%	4.6%	4.9%	3.6%	4.0%	4.3%	4.6%	4.8%
WE15H2	3.9%	4.3%	4.6%	4.9%	5.0%	3.8%	4.2%	4.5%	4.8%	5.0%	3.8%	4.1%	4.4%	4.7%	5.0%
WE17H1	3.7%	4.0%	4.3%	4.6%	4.9%	3.6%	3.9%	4.2%	4.5%	4.8%	3.6%	3.9%	4.2%	4.5%	4.8%
WE17H2	3.9%	4.3%	4.6%	5.0%	5.0%	3.9%	4.2%	4.5%	4.9%	5.0%	3.8%	4.1%	4.5%	4.8%	5.0%

<sup>a</sup> Borated aluminum neutron absorber sheet effective areal <sup>10</sup>B density.

welds joining the closure ring to the closure lid and shell, and joining the redundant port covers to the closure lid are PT examined. The inner port cover welds are helium leakage tested as defined in Chapter 10.

During fabrication, the TSC shell and bottom plate welds are volumetrically inspected and the shell assembly is shop helium leakage tested to the leaktight criteria of  $2 \times 10^{-7}$  cm<sup>3</sup>/sec (helium) in accordance with the requirements and approved methods of ASME Code, Section V, Article 10, and ANSI N14.5 [8]. A minimum test sensitivity of  $1 \times 10^{-7}$  cm<sup>3</sup>/sec (helium) is required. In addition, the 9-inch stainless steel closure lid assembly (TSC1 and TSC2) are volumetrically inspected in accordance with ASME Code, Section III, Subsection NB-2500 requirements. The 4-inch stainless steel closure lid that is part of the composite closure lid assembly (TSC3 and TSC4) is shop helium leakage tested due to its reduced thickness and shield plate bolt holes. The closure lid is tested in accordance with the requirements and approved methods of ASME Code, Section V, Article 10, and ANSI N14.5 [8] to the leak tight criteria of  $2 \times 10^{-7}$  cm<sup>3</sup>/sec (helium). A minimum test sensitivity of  $1 \times 10^{-7}$  cm<sup>3</sup>/sec (helium) is required.

Based on the shop helium leakage testing of the 4-inch thick closure lid, the TSC shell, bottom plate and the joining welds; the design analyses and qualifications of the closure lid and inner port cover welds; the performance of a TSC field hydrostatic pressure test of the closure lid assembly-to-TSC shell weld; the helium leakage test performed on the inner vent and drain port covers; and the multiple NDE performed on all of the confinement boundary welds, the loaded TSC is considered and analyzed as having no credible leakage.

The confinement boundary details at the top of the TSC are shown in Figure 7.1-1. The closure is welded by qualified welders using weld procedures qualified in accordance with ASME Code, Section IX. Over its 50-year design life, the TSC precludes the release of radioactive contents to the environment and the entry of air or water that could potentially damage the cladding of the stored spent fuel.

### **7.1.2      Confinement Penetrations**

Two penetrations fitted with quick-disconnect fittings are provided in the TSC closure lid for operational functions during system loading and sealing operations. The drain port accesses a drain tube that extends into a sump located in the bottom plate. The vent port extends to the underside of the closure lid and accesses the top of the TSC cavity.

After the completion of the closure lid-to-TSC shell weld, TSC pressure test and cavity draining, the vent and drain penetrations are utilized for drying the TSC internals and contents, and for helium backfilling and pressurizing the TSC. After backfilling to a specific helium density, both

penetrations are closed with redundant port covers welded to the closure lid. As presented for storage, the TSC has no exposed or accessible penetrations, has no mechanical closures, and does not employ seals to maintain confinement.

### **7.1.3      Seals and Welds**

The confinement boundary welds consist of the field-installed welds that close and seal the TSC, and the shop welds that join the bottom plate to the TSC and that join the rolled plates that form the TSC shell. The TSC shell may incorporate both longitudinal and circumferential weld seams in joining the rolled plates. No elastomer or metallic seals are used in the confinement boundary of the TSC. All cutting, machining, welding, and forming of the TSC vessel are performed in accordance with Section III, Article NB-4000 of the ASME Code, unless otherwise specified in the approved fabrication drawings and specifications. Code alternatives are listed in Table 2.1-2.

Weld procedures, welders, and welding machine operators shall be qualified in accordance with ASME Code, Section IX. Refer to Chapter 10 for the acceptance criteria for the TSC weld visual inspections and nondestructive examinations (NDE).

The loaded TSC is closed using field-installed welds. The closure lid to TSC shell weld is liquid penetrant examined at the root, at the midplane level and the final surface. After the completion of TSC hydrostatic pressure testing or helium backfilling, the closure ring is installed and welded to the TSC shell and closure lid. The final surface of each of the closure ring welds is liquid penetrant examined. Following draining, drying, and helium backfilling operations, the vent and drain ports are closed with redundant port covers that are welded in place. The inner port cover welds are helium leakage tested. The final surface of each port cover to closure lid weld is liquid penetrant examined.

Shop and field examinations of TSC confinement boundary welds are performed by personnel qualified in accordance with American Society of Nondestructive Testing Recommended Practice No. SNT-TC-1A [9]. Weld examinations are documented in written reports.

### **7.1.4      Closure**

The closure of the TSC consists of the welded closure lid, the welded closure ring, and the welded redundant vent and drain port covers. There are no bolted closures or mechanical seals in the confinement boundary.

Table 8.3-27 Neutron Absorber Material Minimum Effective Thermal Conductivity -  
BTU/(hr-in-°F)

Fuel Basket Type	Radial		Axial	
	100°F	500°F	100°F	500°F
BWR	1.503	1.972	3.295	3.669

**Table 8.3-28 Thermal Properties of Carbon Steel**

Property (units)	Value at Temperature (°F)						
	-40	100	200	400	500	700	800
Conductivity (Btu/hr-in-°F) <sup>a</sup>	2.28	2.30	2.30	2.22	2.16	2.0	1.92
Specific Heat (Btu/lbm-°F) <sup>b</sup>	0.113						
Emissivity <sup>c</sup>	0.80						
Density (lb/in <sup>3</sup> ) <sup>d</sup>	0.284						

**Table 8.3-29 Thermal Properties of Chemical Copper Grade Lead**

Property (units)	Value at Temperature (°F)					
	-40	70	200	400	600	800
Conductivity (Btu/hr-in-°F) <sup>e</sup>	1.767	1.707	1.636	1.526	1.131	0.309
Specific Heat (Btu/lbm-°F) <sup>e</sup>	0.03 (68°F)					
Emissivity <sup>c</sup>	0.28 (75°F)					
Density (lb/in <sup>3</sup> ) <sup>e</sup>	0.411 (68°F)					

**Table 8.3-30 Thermal Properties of SA240, Type 304/304L, Stainless Steel**

Property (units)	Value at Temperature (°F)							
	-40	100	200	400	550	750	800	900
Conductivity (Btu/hr-in-°F) <sup>a</sup>	0.686	0.725	0.775	0.867	0.925	1.0	1.017	1.058
Specific Heat (Btu/lbm-°F) <sup>f</sup>	0.10 <sup>g</sup>	0.116	0.12	0.127	0.131	0.136	0.136	0.138
Emissivity <sup>g,h</sup>	0.36 (300°F)							
Density (lb/in <sup>3</sup> ) <sup>h</sup>	0.29	0.29	0.289	0.287	0.286	0.284	0.283	0.283

Note: The SA240 stainless steel is dual certified as Type 304 and 304L.

<sup>a</sup> ASME Boiler and Pressure Vessel Code, Table TCD [5]

<sup>b</sup> Principles of Heat Transfer, Kreith, Fifth Edition [15]

<sup>c</sup> Standard Handbook for Mechanical Engineers [13]

<sup>d</sup> Metallic Materials Specification Handbook [6]

<sup>e</sup> TRUMP, A Computer Program for Transient and Steady State Temperature Distributions in Multidimensional Systems [16]

<sup>f</sup> Nuclear Systems Materials Handbook [14]

<sup>g</sup> Metallic Materials and Elements for Aerospace Vehicle Structures [7]

<sup>h</sup> Metals Handbook Desk Edition [23]

6. Fill the TSC with clean or pool water. For PWR spent fuel contents, the soluble boron concentration in the TSC shall be verified and monitored in accordance with the LCO 3.2.1.
7. Attach the lift yoke to a crane suitable for handling the loaded TSC, transfer cask and yoke. Position the lift yoke over the transfer cask and engage it with the two transfer cask trunnions.  
Note: The temperature of the transfer cask (surrounding ambient air temperature) must be verified to be at or above the minimum operating temperature of 0°F, per Section 4.3.1.f. of the Technical Specifications (not applicable to the stainless steel MTC2 design).
8. Lift the transfer cask containing the empty TSC and move it to the spent fuel pool following the prescribed load path.  
Note: An optional protective cover, attached to the bottom of the transfer cask, may be used to prevent imbedding contaminated particles in the shield doors and door rails.
9. Connect the clean water lines to the lower annulus fill ports of the transfer cask. Ensure that the unused ports are closed or capped to prevent pool water in-leakage.
10. Lower the transfer cask to the pool surface and turn on the clean water supply lines to the lower annulus fill ports to fill the transfer cask/TSC annulus.  
Note: Sequence on connection and filling/draining transfer cask/TSC annulus is at the discretion of the user based on approved site-specific procedures.
11. Spray the transfer cask and lift yoke with clean water to wet the exposed surfaces.  
Note: Wetting the components that enter the spent fuel pool and spraying the components leaving the pool will reduce the effort required to decontaminate the components.
12. Lower the transfer cask as the annulus fills with clean water until the upper annulus fill ports are accessible. Hold this position and connect the clean water annulus fill lines to the upper fill ports. Ensure the unused ports are closed or capped to prevent pool water in-leakage.
13. Lower the transfer cask to the bottom of the pool in the cask loading area.
14. Disengage the lift yoke and visually verify that the lift yoke is fully disengaged. Remove the lift yoke from the spent fuel pool while spraying the yoke and crane cables with clean water.
15. Load the previously selected fuel assemblies into the TSC basket.  
Note: The fuel assemblies shall be selected in compliance with the requirements of the approved contents specified in Appendix B of the Technical Specifications and the boron concentration limits of the Technical Specifications, including limitations on fuel assembly positions within the basket. Specific fuel assembly positions for preferential and zoned loading patterns shall be in full compliance with the requirements of Appendix B of the Technical Specifications. Assembly selection, placement and compliance with preferential zone loading patterns within the basket shall be independently verified.



Note: Up to four DFCs containing authorized PWR contents may be loaded in a TSC with a DF Basket Assembly. A DFC spacer is required to be positioned in the Designated DF Basket Assembly corner locations for the shorter length DFCs. Independently, visually verify proper placement and correct orientation of each required DFC spacer.

Note: At the option of the user, install fuel assembly spacers for the axial positioning of the PWR fuel assembly types to be loaded. Verify spacer identification and install fuel spacers in each intended fuel loading location based on the fuel spacer plan prepared, which is based on the fuel assembly inventory and nonfuel hardware to be loaded. Independently, visually verify proper placement and correct orientation of each required fuel spacer.

16. Visually verify the fuel assembly (and DFC, as applicable) identifications to confirm the serial numbers match the approved fuel-loading pattern.

17. Install three swivel hoist rings hand tight in the three closure lid lifting holes or in three of the six TSC lift holes. Install a three-legged sling set to the hoist rings and connect the sling set to the crane hook or the attachment point on the lift yoke.

Note: At the discretion of the user, the closure lid can be attached to the lift yoke and the lid installed during the lowering of the lift yoke.

18. Raise the closure lid. Adjust closure lid rigging to level the closure lid.

19. Move the closure lid over the spent fuel pool and align the lift yoke (if used) to the transfer cask trunnions and align the closure lid to the match marks of the TSC.

20. Lower the closure lid until it enters the TSC and seats in the top of the TSC. Visually verify closure lid alignment using the match marks ( $\pm \frac{1}{2}$  inch).

Caution: Following closure lid installation, there is a thermal time limit of 18 hours to begin the Annulus Circulating Water System (ACWS), or approved alternative annulus flow system operation, and to begin temperature measurement of the MTC annulus outlet flow to verify MTC outlet temperature is maintained  $< 113^{\circ}\text{F}$ . If ACWS flow cannot be initiated in the time allowed, return the MTC to the spent fuel pool and remove the closure lid to allow cooling by the spent fuel pool water.

21. Allow sling cables to go slack and move the lift yoke into position to engage the transfer cask trunnions. Engage the lift yoke to the trunnions, apply a slight tension, and visually verify engagement.

22. Raise the transfer cask until its top clears the pool surface. Visually verify that the closure lid is properly seated. If necessary, lower the transfer cask and reinstall the closure lid. Rinse the lift yoke and transfer cask with clean water as the equipment is removed from the pool.

23. Rinse and flush the top of the transfer cask and TSC with clean water as necessary to remove any radioactive particles. Survey the top of the TSC closure lid and the top of the transfer cask to check for radioactive particles.

#### **10.1.2.3      Pressure Testing of the TSC**

Following completion of the closure lid-to-TSC shell weld during the TSC preparation operations after fuel loading, the TSC shall be hydrostatically pressure tested at not less than 125% of the design pressure of 110 psig in accordance with ASME Code, Section III, Subsection NB, NB-6200 requirements as described and defined in Section 9.1.1. A bounding minimum test pressure of 150 psig shall be applied to the drain port connection for a minimum 10-minute hold period. There shall be no visible water leakage from the closure lid-to-TSC shell weld based on visual examination of the weld after a minimum 10-minute hold period, while maintaining the test pressure. Test pressure shall be maintained until the completion of the visual weld examination. The design pressure and minimum test pressure are identical for both PWR and BWR TSCs. The minimum test pressure conservatively exceeds the hydrostatic test pressure commitment stated in Table 2.1-2 (125% of MNOP).

#### **10.1.2.4      Load Testing of Damaged Fuel Can (DFC)**

To qualify the design of the MAGNASTOR DFC, the first DFC to be provided to a user shall be load tested to 150% of the total weight of the DFC plus the heaviest contents to be loaded in the DFC. The test load on the DFC shall be applied and held for a minimum of 10 minutes. Following completion of the load test, all load bearing welds and surfaces shall be visually inspected for permanent deformation, galling or cracking. Load bearing welds shall be inspected using liquid penetrant examination in accordance with ASME Code, Section V, Article 6. Acceptance criteria shall be in accordance with ASME Code, Section III, NG-5350.

Any evidence of permanent deformation, cracking or galling of load bearing surfaces, or unacceptable liquid penetrant examination results shall be cause for rejection, repair, reperformance of the load test and reexamination of the DFC.

#### **10.1.3      Leakage Tests**

The confinement boundary is defined as the TSC shell weldment, closure lid assembly, and vent and drain port covers. As described in Section 10.1.1, the confinement boundary is designed, fabricated, examined, and tested in accordance with the requirements of the ASME Code, Section III, Subsection NB, except for the code alternatives listed in Table 2.1-2.

At the completion of the TSC shell weldment confinement boundary welds (e.g., TSC shell seam and shell to bottom plate), the TSC shell weldment shall be leakage tested. The leakage test shall be performed in accordance with the requirements and approved methods of ASME Code, Section V, Article 10, and ANSI N14.5-1997 [20] to confirm the total leakage rate is less than, or equal to,  $1 \times 10^{-7}$  ref. cm<sup>3</sup>/s (i.e., leaktight). The sensitivity of the test shall be one-half of the acceptance test criteria as specified in ANSI N14.5-1997.

The TSC shell weldment will be closed using a test lid installed over the top of the shell and the cavity evacuated. A test envelope will be installed around the TSC enclosing all of the TSC shell confinement welds and base metal plates, and filled with 99.995% (minimum) pure helium to an acceptable test concentration. The percentage of helium gas in the test envelope shall be accounted for in the determination of the test sensitivity. A mass spectrometer leak detector (MSLD) will be used to sample the evacuated volume for helium.

If helium leakage is detected, the area of leakage shall be identified, repaired and re-examined in accordance with the ASME Code, Section III, Subsection NB, NB-4450 or NB-4130, as appropriate. Following repair, the complete helium leakage test shall be re-performed to the original test acceptance criteria.

Leakage testing of the TSC shell weldment shall be performed in accordance with written and approved procedures, and the test results documented.

Based on the confinement system materials, welding requirements and inspection methods, shop helium leakage testing of the 9-inch thick closure lid is not required. However, due to the reduced thickness of the stainless steel closure lid (4-inch thick base material) of the composite closure lid assembly, and the presence of extended bolt holes for attachment of the shield plate assembly, a shop helium leakage test of the composite closure lid stainless steel plate shall be performed following fabrication. The leakage test shall be performed in accordance with the requirements and approved methods of ASME Code, Section V, Article 10, and ANSI N14.5-1997 to confirm the total leakage rate is less than, or equal to,  $2 \times 10^{-7}$  cm<sup>3</sup>/s (helium). The sensitivity of the test shall be one-half of the acceptance test criteria as specified in ANSI N14.5-1997.

If leakage is detected, the area of leakage shall be identified, repaired and re-examined in accordance with ASME Code, Section III, Subsection NB, NB-4130. Following repair and completion of required NDE, the helium leak test shall be re-performed to the original test acceptance criteria.

Leakage testing of the composite closure lid shall be performed in accordance with written and approved procedures, and the test results documented.

In order to ensure the integrity of the vent and drain inner port cover welds, a helium leakage test of each weld is performed following welding of the inner port covers to the closure lid assembly using the evacuated envelope method, as described in ASME Code, Section V, Article 10, and ANSI N14.5. The leakage test is to confirm that the leakage rate for each port cover is  $\leq 2 \times 10^{-7}$  cm<sup>3</sup>/s helium. Following inner port cover welding, a test bell is installed over the top of the port cover and the test bell volume is evacuated to a low pressure by a helium MSLD system. The

and/or widespread rough surface conditions such as die chatter or porosity shall be identified as nonconforming. Nonconforming items are segregated and evaluated within the NAC International Quality Assurance Program, and assigned one of the following dispositions: "Use-As-Is," "Rework/Repair" or "Reject." Only material that is determined to meet all applicable conditions of the license will be accepted. Local or cosmetic conditions such as scratches, nicks, die lines, inclusions, abrasion, isolated pores or discoloration are acceptable based on material neutron attenuation and thermal performance not being impacted by minor fabrication anomalies.

#### **10.1.6.4.4 Thermal Conductivity and Yield Strength Testing of Metal Matrix and Borated Aluminum Neutron Absorber Material**

##### **Thermal Conductivity Testing**

Thermal conductivity qualification testing of the neutron absorber materials shall conform to ASTM E1225 [15], ASTM E1461 [16], or an equivalent method. The testing shall be performed on test coupons taken from production material. Note that thermal conductivity increases slightly with temperature increases.

- Sampling will initially be one test per lot and may be reduced if the first five tests meet the specified minimum thermal conductivity. Additional tests may be performed on the material from a lot whose test result does not meet the required minimum value, but the lot will be rejected if the mean value of the tests does not meet the required minimum value.
- Upon completion of 25 tests of a single type of neutron absorber material having the same aluminum alloy matrix and boron content (in the same compound), further testing may be terminated if the mean value of all of the test results minus two standard deviations meets the specified minimum thermal conductivity. Similarly, testing may be terminated if the matrix of the material changes to an alloy with a larger coefficient of thermal conductivity, or if the boron compound remains the same, but the boron content is reduced.

In the Chapter 4 thermal analyses, the neutron absorber is conservatively evaluated as a 0.125-in nominal thickness sheet for the PWR fuel basket and a 0.10-in nominal thickness sheet for the BWR fuel basket. The required minimum thermal conductivities for the MAGNASTOR absorbers are as follows.

Fuel Basket Type	Minimum Effective Thermal Conductivity - BTU/(hr-in-°F)			
	Radial		Axial	
	100°F	500°F	100°F	500°F
BWR	1.503	1.972	3.295	3.669

The neutron absorber thermal acceptance criterion will be based on the nominal sheet thickness. Surface anomalies increase radiation heat transfer and have insignificant influence on thermal conductivity, permitting acceptance of minor surface defects without additional material testing.

Additional thermal conductivity qualification testing of neutron absorber material is not required if certified quality-controlled test results (from an NAC approved supplier) that meet the specified minimum thermal conductivity are available as referenced documentation.

#### **Yield Strength Testing**

Yield strength qualification testing of the neutron absorber shall conform to ASTM Test Method B 557/B 557M, E 8 or E 21 [17, 18, 19].

Neutron absorber material yield strength must be equal to or greater than 1.6 ksi at 700°F. Per Section 8.3, a yield strength of 1.6 ksi is the material strength of the neutron absorber at 700°F and is applied as a temperature-independent value in the structural evaluations of the absorber. This yield strength assures that the material will maintain its form when subjected to normal, off-normal and accident condition loads.

The neutron absorber yield strength acceptance criterion will be based on the absorber meeting the specified nominal sheet thickness. Control and limitations on the neutron absorber boron content (primary driver to material structural performance) permits acceptance without additional material yield strength acceptance testing.

Additional yield strength qualification testing of neutron absorber material is not required if certified quality-controlled test results (from an NAC approved supplier) that meet the specified minimum yield strength are available as referenced documentation.

BASES (continued)

---

SR 3.0.4 (continued) The provisions of this Specification should not be interpreted as endorsing the failure to exercise the good practice of restoring systems or components before entering an associated specified condition in the Applicability.

However, in certain circumstances, failing to meet an SR will not result in SR 3.0.4 restricting a change in specified condition. When a system, subsystem, division, component, device, or variable is outside the specified limits, the associated SR(s) are not required to be performed per SR 3.0.1, which states that Surveillances do not have to be performed on equipment that has been determined to not meet the LCO. When equipment does not meet the LCO, SR 3.0.4 does not apply to the associated SR(s) since the requirement for the SR(s) to be performed is removed. Therefore, failing to perform the Surveillance(s) within the specified conditions of the Applicability. However, since the LCO is not met in this instance, LCO 3.0.4 will govern any restrictions that may (or may not) apply to specified condition changes.

The provisions of SR 3.0.4 shall not prevent changes in specified conditions in the Applicability that is required to comply with ACTIONS.

In addition, the provisions of LCO 3.0.4 shall not prevent changes in specified conditions in the Applicability that is related to the unloading of the MAGNASTOR SYSTEM.

The precise requirements of performance of SRs are specified such that exceptions to SR 3.0.4 are not necessary. The specific time frames and conditions necessary for meeting the SRs are specified in the Frequency, in the Surveillance, or both. This allows performance of Surveillances when the prerequisite condition(s) specified in a Surveillance procedure require entry into the specified condition in the Applicability of the associated LCO prior to the performance or completion of Surveillance. A Surveillance that could not be performed until after entering the LCO Applicability would have its Frequency specified such that it is not "due" until the specific conditions needed are met.

Alternately, the Surveillance may be stated in the form of a Note as not required (to be met or performed) until a particular event, condition, or time has been reached. Further, discussion of the specific formats of SRs annotation is found in Technical Specification Section 1.4, Frequency.

---

3.1 MAGNASTOR SYSTEM Integrity

---

3.1.1 Transportable Storage Canister (TSC)

BASES

---

BACKGROUND

A TRANSFER CASK with an empty TSC is placed into the spent fuel pool and loaded with SNF assemblies and other approved contents meeting the requirements of Appendix B, Approved Contents. A closure lid is then placed on the TSC, and the TRANSFER CASK containing the TSC is removed from the pool and placed in the cask preparation area or prepared in a partially submerged condition. Cooling water flow to the TRANSFER CASK annulus shall be provided to assist in limiting the MAGNASTOR SYSTEM component temperatures during TSC preparation and closure activities. The closure lid is welded to the TSC shell and the weld is examined by dye penetrant examination methods (i.e., root, mid-plane and final surface). A hydrostatic pressure test of the weld is performed at a minimum of 125% of the TSC maximum normal operating pressure. The TSC cavity water is removed by pumping and/or blow down while backfilling the cavity with helium, and the free volume of the TSC is determined by measuring the volume of water removed.

TSC cavity moisture removal is performed using vacuum drying methods following draining of the bulk cavity water. TSC cavity dryness is confirmed by ensuring that any pressure rise in the isolated TSC cavity with the vacuum pump turned off and isolated is less than the acceptance criteria.

Upon verification of the dryness of the TSC cavity following vacuum drying operations, the TSC is further evacuated using the vacuum pumping system to a vacuum pressure that excludes significant quantity of oxidizing gases (i.e.,  $< 1$  mole). The TSC cavity is then backfilled with high purity helium ( $\geq 99.995\%$  purity) until the required helium mass density is established. Drying and backfilling the TSC cavity with helium provides the capability to remove the contents decay heat by convective and conductive heat transfer and minimizes any oxidizing gases to below a significant value. Establishment of the inert helium atmosphere protects the fuel cladding from degradation. The backfilling and resulting pressurization of the cavity with helium to an established helium mass density will provide the required helium mass and pressure to ensure the operation of the heat transfer design of the MAGNASTOR SYSTEM, and will eliminate the possibility of air in-leakage over the storage period.

The closure ring is installed in the closure lid-to-TSC shell weld groove, welded to the shell and to the closure lid, and the final weld surface examined by dye penetrant methods. The inner port covers of the vent and drain openings are installed, welded and the final weld surface examined by final surface dye penetrant methods. The vent and drain inner port covers are then helium leak tested to verify the absence of helium leakage to a minimum sensitivity of  $1.0 \times 10^{-7} \text{ cm}^3 / \text{sec}$  (helium).

(continued)

BASES (continued)

---

BACKGROUND  
(cont.)

The outer port covers are then installed, welded and the final weld surface examined by dye penetrant methods.

The TSC weldment is designed, analyzed, and tested to meet the leaktight criteria of ANSI N14.5. In addition, the closure lid-to-TSC shell weld is hydrostatically pressure tested and examined by multi-pass dye penetrant examination following fuel loading. The closure lid, closure ring and inner and outer port covers provide redundant closures to ensure confinement boundary integrity. Therefore, leakage of radioactive materials from the TSC and loss of helium and possible in-leakage of air are not considered credible.

APPLICABLE  
SAFETY ANALYSIS

The confinement of the radioactive materials contents in the TSC is ensured by the multiple confinement boundaries, including the fuel pellet matrix, the fuel rod cladding, and the pressure boundary provided by the TSC. Long-term integrity of the spent fuel contents is ensured by the inert helium atmosphere of the TSC, which is accomplished by the removal of free water, elimination of residual oxidizing gases, and backfilling with a measured mass of high purity helium. The pressurized helium atmosphere in the TSC ensures that the MAGNASTOR SYSTEM convective heat transfer thermal design will perform as analyzed. The measurement of the helium backfill mass ensures that the TSC internal pressure does not exceed the TSC's design pressure under design storage operating conditions.

LCO

A dry pressurized, helium filled and sealed TSC establishes the inert environment that will ensure the integrity of the fuel cladding and proper performance of the MAGNASTOR SYSTEM thermal design, while precluding air in-leakage and out-leakage of radioactive materials.

The Section 1 Tables of the LCO specify the limits for both PWR and BWR SNF contents (based on the decay heat load of the TSC contents) for Maximum Vacuum Drying Times; Minimum Helium Backfill Time (i.e., minimum time period the TSC is allowed to soak with annulus cooling system in operation following completion of the helium mass backfill prior to the initiation of the TSC transfer to the CONCRETE CASK in the TRANSFER CASK); and the Maximum TSC Transfer Time available to complete the transfer of the TSC to the CONCRETE CASK.

The Section 2 Table in the LCO provides the Maximum Drying Time Limit for the second and subsequent vacuum drying cycles following a minimum of 24 hours of either in-pool cooling or annulus circulating water system (ACWS) cooling with the TSC backfilled to 75 psig (+10, -0) with high purity helium, if the TSC dryness criteria were not met on the first vacuum drying cycle (this Table is not applicable to PWR contents with decay heat loads of  $\leq 20$  kW, which has unlimited vacuum drying time, no minimum helium backfill time and 600-hour TSC transfer time).

---

(continued)



BASES (continued)

LCO  
(cont.)

The Section 2 Table in the LCO provides the Maximum Drying Time Limit for the second and subsequent vacuum drying cycles following a minimum of 24 hours of either in-pool cooling or annulus circulating water system (ACWS) cooling with the TSC backfilled to 75 psig (+10, -0) with high purity helium, if the TSC dryness criteria were not met on the first vacuum drying cycle.

A Note in Section 2 refers the Licensee to use Table 1.B and 1.D following the additional drying cycle(s) to determine the Minimum Helium Backfill Time and Maximum TSC Transfer Time applicable for the second TSC transfer cycle. Note that the helium backfill (soak) and transfer times in Tables 1.B and 1.D would also be applicable for a second cycle of TSC transfer to the CONCRETE CASK if the first transfer cycle was not completed in the allowed time. The minimum 24-hour helium soak would lower and reset the TSC and SNF content temperatures to a value corresponding to the temperatures used in the determination of the Table 1.B and 1.D values for maximum transfer time limits.

Each temperature transient, either resulting from additional water cooling and vacuum drying cycles, or from additional helium soak and TSC transfer cycles, would need to be accounted for in the 10 allowable thermal transients for SNF assemblies with burnups exceeding 45,000 MWd/MTU.

APPLICABILITY

The sealed TSC with a dry measured helium mass cavity atmosphere is required to be established prior to TRANSPORT OPERATIONS to ensure integrity of the fuel contents and the effectiveness of the heat dissipation capability during LOADING OPERATIONS and STORAGE OPERATIONS.

ACTIONS

A note has been added to the ACTIONS, which states that, for this LCO, separate Condition entry is allowed for each TSC. This is acceptable as the Required Actions for each Condition provide appropriate compensatory measures for each TSC not meeting the LCO. Subsequent TSCs that do not meet the LCO are governed by subsequent Condition entry and application of associated Required Actions.

A.1

If the cavity vacuum drying pressure with the vacuum pump isolated and turned off is not met prior to TRANSPORT OPERATIONS, an engineering evaluation is necessary to determine the potential quantity of moisture left in the TSC. Since moisture remaining in the cavity during TRANSPORT and STORAGE OPERATIONS may represent a long-term degradation issue, immediate action is not required. The Completion Time is sufficient to complete an engineering evaluation of the safety significance of the Condition.

(continued)

3.1 MAGNASTOR SYSTEM Integrity

3.1.2 CONCRETE CASK Heat Removal System

BASES

---

BACKGROUND	<p>The heat removal system for the CONCRETE CASK containing a loaded TSC is a passive, convective air-cooled heat transfer system that ensures that the decay heat emitted from the TSC is transferred to the environment by the upward flow of air through the CONCRETE CASK annulus. During STORAGE OPERATIONS, ambient air is drawn into the CONCRETE CASK annulus through the four air inlets located at the base of the CONCRETE CASK. The heat from the TSC surfaces is transferred to the air flow via natural circulation. The buoyancy of the heated air creates a chimney effect forcing the heated air upward and drawing additional ambient air into the annulus through the air inlets. The heated air flows back to the ambient environment through the four air outlets located in the CONCRETE CASK lid.</p>
APPLICABLE SAFETY ANALYSIS	<p>The thermal analyses of the MAGNASTOR SYSTEM take credit for the decay heat from the TSC contents being transferred to the ambient environment surrounding the CONCRETE CASK. Transfer of heat from the TSC contents ensures that the fuel cladding and TSC component temperatures do not exceed established limits. During normal STORAGE OPERATIONS, the four air inlets and four air outlets are unobstructed and full natural convection heat transfer occurs (i.e., maximum heat transfer for a given ambient temperature and decay heat load). Vent obstruction can be any type of accumulation within the vent that restricts airflow.</p> <p>Analyses have been performed for two scenarios corresponding to the complete obstruction of what is equivalent to two and four air inlets. Blockage of the equivalent area of two air inlets reduces the convective air flow through the CONCRETE CASK/TSC annulus and decreases the heat transfer from the TSC surfaces to the ambient environment. Under this off-normal event, no CONCRETE CASK or TSC components or fuel cladding exceed established short-term temperature limits, and the TSC internal pressure does not exceed the analyzed maximum pressure.</p> <p>The complete blockage of all four air inlets effectively stops the transfer of the decay heat from the TSC due to the elimination of the convective air flow. The TSC will continue to radiate heat to the liner of the CONCRETE CASK. Upon loss of air cooling, the MAGNASTOR SYSTEM component temperatures will increase toward their respective established accident temperature limits. The spent fuel cladding and fuel basket and CONCRETE CASK structural component temperatures do not reach their accident limits for a time period of approximately 72</p>

---

(continued)

BASES (continued)

---

APPLICABLE  
SAFETY ANALYSIS  
(cont.)

hours. The internal pressure in the TSC cavity will not reach the analyzed maximum pressure condition for approximately 58 hours after a complete blockage condition occurs.

Therefore, following the identification of a reduction in the heat dissipation capabilities of the CONCRETE CASK by the temperature-monitoring program or the visual inspection of the air inlet and outlet screens, actions are to be taken immediately to restore at least partial convective airflow (i.e., a minimum area of what is equivalent of two air inlet and all four air outlets are unobstructed). Once partial airflow is established, the fuel cladding and the TSC and component temperatures will not exceed normal STORAGE OPERATIONS limits. Efforts to reestablish full OPERABLE status for the CONCRETE CASK can then be undertaken in a controlled manner. If necessary, the TSC may be transferred into the TRANSFER CASK to permit full access to the base of the CONCRETE CASK for repairs with minimal radiological effects.

LCO

The CONCRETE CASK heat removal system is to be verified to be OPERABLE to preserve the applicability of the design bases thermal analyses. The continued operability of the heat removal system ensures that the decay heat generated by the TSC contents is transferred to the ambient environment to maintain the fuel cladding and CONCRETE CASK and TSC temperatures within established limits.

APPLICABILITY

The LCO is applicable during STORAGE OPERATIONS. Once the CONCRETE CASK lid is installed following transfer of a loaded TSC, the heat removal system is required to be OPERABLE to ensure adequate heat transfer.

ACTIONS

A Note has been added to the Actions that states for this LCO, separate condition entry is allowed for each CONCRETE CASK. This is acceptable, as the Required Actions for each Condition provide appropriate compensatory measures for each CONCRETE CASK not meeting the LCO. Other CONCRETE CASKs that do not meet the LCO are addressed by independent Condition entry and application of the associated Required Actions.

A.1

If the CONCRETE CASK heat removal system has been determined to be inoperable, full operability is to be restored, or at a minimum, adequate heat removal must be restored or verified to prevent exceeding fuel cladding and critical component temperatures for accident events. Adequate heat removal capability is ensured by

---

(continued)

BASES (continued)

---

ACTIONS (cont.)

having at least the equivalent area of two CONCRETE CASK air inlets and all four air outlets unobstructed, which is consistent with the analyzed off-normal event. Alternatively, adequate heat removal can be verified by measuring the exit air temperature from the four air outlets and determining the temperature rise over the ISFSI ambient air temperature.

This verification must be completed immediately where "immediately" is defined as "the required action should be pursued without delay in a controlled manner". Restoration of adequate heat removal must be completed within 58 hours of the last operability determination to ensure the TSC internal pressure limit is not exceeded per the analysis in FSAR Section 12.2.13.3, which is the most restrictive time limit.

Thermal analyses of a fully blocked CONCRETE CASK air inlet condition show that fuel cladding and critical basket material accident temperatures and internal pressure limits could be exceeded over time. As a result, requiring immediate verification, or restoration, of adequate heat removal capability will ensure that accident temperature and pressure limits are not exceeded. Once adequate heat removal has been reestablished or verified, the additional actions required to restore the CONCRETE CASK to OPERABLE status can be completed under A.2.

AND

A.2

In addition to Required Action A.1, efforts are required to be continued to restore the CONCRETE CASK heat removal system to OPERABLE.

As long as adequate heat removal capability has been verified to exist, restoring the CONCRETE CASK heat removal system to fully OPERABLE is not an immediate concern. Therefore, restoring it to OPERABLE within 30 days is a reasonable Completion Time.

---

SURVEILLANCE  
REQUIREMENTS

SR 3.1.2.1

The long-term integrity of the stored spent fuel is dependent on the continuing ability of the CONCRETE CASK to reject decay heat from the TSC to the ambient environment. Routine verification that the four air inlets and four air outlets are unobstructed and intact ensures that convective airflow through the CONCRETE CASK/TSC annulus is occurring and performing effective heat transfer. Alternatively, the Surveillance Requirement can be fulfilled by measuring the exit air temperature from the four air outlets and determining the temperature rise over the ISFSI ambient air temperature. As long as the temperature increase of the convective airflow is less than the surveillance limits, adequate heat transfer is occurring to maintain

(continued)

BASES (continued)

---

SURVEILLANCE  
REQUIREMENTS  
(continued)

SR 3.1.2.1 (continued)

CONCRETE CASK, TSC, and spent fuel cladding temperatures below long-term limits.

If partial or complete blockage of the CONCRETE CASK air inlets occurs, the heat rejection system will be rendered inoperable and this LCO is not met. Immediate corrective actions are to be taken to remove the obstructions from at least two air inlets and all four air outlets, or equivalent area, to restore partial air flow, and additional corrective actions are to be taken to remove all air inlet and outlet obstructions and return the CONCRETE CASK to a fully OPERABLE status.

The Frequency of 24 hours is reasonable based on the time necessary for the spent fuel cladding and CONCRETE CASK and TSC component temperatures to reach their short-term temperature limits and the internal pressure to increase to the accident condition pressure limit. The Frequency will allow appropriate corrective actions to be completed in a timely manner.

---

REFERENCES

FSAR Section 4.4.

---